

**Factors underpinning plant megadiversity in the extremely
phosphorus-impooverished Southwest Australian biodiversity hotspot**

Clément E. Gille

BSc, MSc



THE UNIVERSITY OF
**WESTERN
AUSTRALIA**

This thesis is presented for the degree of Doctor of Philosophy of
The University of Western Australia

School of Biological Sciences

2024

THESIS DECLARATION

I, Clément E. Gille, certify that:

This thesis has been substantially accomplished during enrolment in this degree.

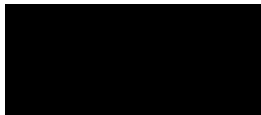
This thesis is my own work and does not contain any material previously published or written by another person, except where due reference has been made in the text or authorship declaration. All photographs and artwork are my own.

This thesis does not contain material which has been submitted for the award of any other degree or diploma in my name, in any university or other tertiary institution.

In the future, no part of this thesis will be used in a submission in my name, for any other degree or diploma in any university or other tertiary institution without the prior approval of The University of Western Australia and where applicable, any partner institution responsible for the joint-award of this degree.

This thesis does not violate or infringe any copyright, trademark, patent, or other rights whatsoever of any person.

This thesis is in agreement with the University of Western Australia Doctor of Philosophy Rules for the content and format of a thesis and is presented as a series of papers. This thesis contains published, submitted and/or work prepared for publication, some of which has been co-authored. All chapter are formatted per the requirements of *New Phytologist*.



Clément E. Gille
29 February 2024

ABSTRACT

The Southwest Australian biodiversity hotspot is home to exceptional plant species diversity. Soils are severely nutrient impoverished, particularly in phosphorus (P), and adaptations have evolved in plant species that allow them to acquire and use scarce nutrients efficiently. Most Proteaceae, an emblematic and ecologically-important family in south-western Australia, form cluster roots, which are ephemeral non-mycorrhizal root structures composed of hundreds to thousands of hairy rootlets that effectively ‘mine’ P bound to soil particles by releasing large amounts of carboxylates. Carboxylates mobilise P and other elements, including manganese (Mn). Manganese uptake is poorly regulated in plants and accumulates in leaves, allowing Mn concentration ([Mn]) to be used as a proxy for carboxylate concentration in the rhizosphere. Mycorrhizal species (including Myrtaceae and most Fabaceae) acquire P through their ‘scavenging’ symbionts. While these plants are less efficient than non-mycorrhizal Proteaceae at acquiring P on extremely P-impooverished soils, they still co-occur with Proteaceae, contributing to the remarkable species diversity within the severely P-impooverished south-western Australian landscapes. Phosphorus-economising adaptations have also evolved in leaves, allowing plants in P-impooverished environments to function at low foliar P concentrations. For example, Proteaceae replace phospholipids by other non-P-containing lipids during leaf development, function at low ribosomal RNA levels, and preferentially allocate P to photosynthetically-active mesophyll cells, rather than epidermal cells. By doing so, Proteaceae achieve a very high photosynthetic-P use efficiency (PPUE).

This thesis investigated factors contributing to plant diversity in extremely P-impooverished habitats in south-western Australia through a series of physiological studies on the below- and aboveground functioning of P-efficient Proteaceae and co-occurring species.

The first study investigated the association of leaf Mn accumulation with the ability of a species to release carboxylates. Some *Hakea* species (Proteaceae) produce functional cluster roots and release large amounts of carboxylates, but have low leaf [Mn], challenging the previously established model linking carboxylate release to leaf [Mn]. My physiological assessment of *Hakea* species with contrasting leaf [Mn] revealed that Mn accumulation was tightly associated with the capacity of a species to release protons to balance the negative charges of the carboxylates released. Species with low leaf [Mn] released greater amounts of

other cations such as potassium and magnesium. The release of cations other than protons increases soil pH, rendering Mn less available. I provide a comprehensive alternative conceptual model relating root carboxylate exudation with leaf Mn accumulation.

I also examined the interaction between *Banksia menziesii*, a non-mycorrhizal cluster-rooted Proteaceae, and *Eucalyptus todtiana*, a co-occurring mycorrhizal Myrtaceae, in a glasshouse experiment. As expected in extremely P-limiting environments, facilitation of P acquisition was a key process in the success of the two species with contrasting nutrient-acquisition strategies. Cluster roots of *B. menziesii* enhanced the P acquisition of mycorrhizal *E. todtiana*, which strongly competed for mobilised P. In turn, the presence of a mycorrhizal fungus and its host increased phytohormone concentrations in the roots of non-mycorrhizal *B. menziesii* challenged by native oomycete *Phytophthora* pathogens. I suggest that mycorrhizal *E. todtiana* and ectomycorrhizal fungi contribute to inducing and priming the defence of *B. menziesii* against soilborne pathogens. I highlight the complex interplay between non-mycorrhizal species, mycorrhizal species and their fungal partners, and native oomycete pathogens. For the first time, I demonstrate how intricate interactions shape species coexistence in an extremely P-impooverished environment.

Finally, I investigated the P-allocation patterns in leaves of five *Banksia* and five *Hakea* species, two species-rich Proteaceae genera in south-western Australia, in relation to their high PPUE. Within each genus, PPUE varied among species. Phosphorus-allocation patterns to different biochemical fractions explained the high PPUE of the studied species. Within each genus, species with higher PPUE allocated more P to small metabolites and less P to phospholipids than species with lower PPUE. However, correlations between PPUE and inorganic phosphate or residual P concentrations (likely containing phosphorylated proteins), were not consistent for the two genera. For *Banksia* species, PPUE was positively and negatively correlated with P allocation to small metabolites and to the residual P fraction, respectively. Accordingly, I suggest a trade-off exists between allocation to P-containing substrates and to ribosomal RNA to achieve high PPUE.

In conclusion, the physiological assessment of below- and aboveground functioning of highly P-efficient Proteaceae and co-existing species highlights complementarity in functional diversity. From P-acquisition and belowground interactions to resource partitioning in leaves, this functional diversity underpins the species diversity in extremely P-impooverished environments in south-western Australia.

TABLE OF CONTENTS

Thesis Declaration	iii
Abstract.....	iv
Table of Contents	vi
Acknowledgements.....	x
Authorship Declaration.....	xii
Chapter One — General Introduction.....	1
Southwest Australia, a global biodiversity hotspot.....	2
Phosphorus-acquisition strategies	2
Plant interactions: facilitation rather than competition.....	5
Phosphorus-utilisation efficiency.....	9
Thesis outline.....	11
References.....	13
Chapter Two — Cluster-root physiology of carboxylate-releasing <i>Hakea</i> (Proteaceae) species determines manganese accumulation in leaves	30
Summary.....	32
Introduction.....	33
Materials and Methods.....	35
Species and site selection.....	35
Leaf sampling and analyses of field plants.....	36
Soil sampling and analyses	37
Solution ³¹ P-NMR spectroscopy.....	38
Rhizobox-growth of plants and analyses	40
Hydroponically-grown plants and analyses	41
Statistical analyses	42
Results.....	43
Soil and leaf chemical properties.....	43
Non-cluster and cluster roots physiology	46
Correlation between leaf [Mn], edaphic conditions and root physiology.....	48
Discussion.....	52

Cations co-exuded with carboxylates explain leaf Mn accumulation	52
A more highly-expressed phosphorus-acquisition strategy in <i>Hakea</i> species with low leaf Mn	54
Carboxylate-exudation physiology: a strategy beyond P acquisition	55
Concluding remarks	56
References	58
Supporting Information.....	65

Chapter Three — Facilitative and competitive interactions between mycorrhizal and non-mycorrhizal plants in an extremely phosphorus-impooverished environment: role of ectomycorrhizal fungi and oomycete pathogens in shaping species coexistence..... 78

Summary	80
Introduction.....	81
Materials and Methods.....	83
Species selection and experimental design	83
Soil preparation.....	85
Inoculation of seeds with ectomycorrhizal fungi and growth conditions	85
Inoculation of seedlings with <i>Phytophthora</i> spp.	86
Harvest and growth-related measurements.....	87
Microbial colonisation	87
Root phytohormones.....	89
Statistical analyses	90
Results.....	91
Growth-related parameters of plants.....	91
Defence-related compounds in fine roots	94
Discussion	99
Facilitative and competitive dynamics between a mycorrhizal and a non-mycorrhizal species	99
Phytochemical responses and pathways of defence against <i>Phytophthora</i> spp.....	101
Interactions between ectomycorrhizal fungi and <i>Phytophthora</i> spp. alter defence responses in the non-mycorrhizal <i>Banksia menziesii</i>	103
Conclusions.....	103
References.....	105
Supporting Information.....	114

Chapter Four — Proteaceae with high photosynthesis phosphorus-use efficiency on the conservative end of the leaf economics spectrum allocate phosphorus to biochemical fractions differently	126
Summary	128
Introduction.....	129
Materials and Methods.....	131
Species selection and study area	131
Leaf characteristics and nutrient analyses.....	132
Analysis of leaf P fractions	133
Gas exchange measurements	134
Soil sampling and analyses	134
Statistical analyses	135
Results.....	136
Discussion.....	146
On the far “conservative” end of the leaf economics spectrum.....	147
Interconnection of N and P efficiency	148
Implications of biochemical investment of P on PPUE.....	149
Concluding remarks	151
References.....	152
Supporting Information.....	159
Chapter Five — General Discussion	174
Introduction.....	175
Physiology of carboxylate exudation.....	176
Microbe-mediated plant interactions	181
Phosphorus allocation and photosynthetic phosphorus-use efficiency.....	183
Concluding remarks	185
References.....	186
Appendix.....	196
Additional publications	197
Résumé.....	201

ACKNOWLEDGEMENTS

I am immensely grateful for the opportunity to carry on this PhD under the guidance of my supervisors, Hans Lambers, Patrick Finnegan, Kosala Ranathunge, and Patrick Hayes. Thank you for your support and patience that allowed me to acquire such invaluable skills and knowledge from each and every one of you. It all started in Alison Baird Reserve during one of our many enjoyable walks, where Hans and Pat invited me to continue doing research at the University of Western Australia. I eagerly accepted this offer, recognising it was the perfect opportunity to delve deeper into the secrets of the wonderful native plants I just became passionate about during my Masters.

Since then, I am lucky to consider Hans my mentor and friend. You have proven me wrong many times and I sure have learnt from it. Our insightful discussions, best accompanied by an excellent drop of Shiraz and a smelly cheese, have taught me a great deal, and I hope I have been able to share my passion in return. Thank you and Marion Cambridge, for your support during this journey.

Collaborations during my PhD extended beyond the confines of our stunning UWA campus, and a special thank you goes to Treena Burgess for introducing me to the enchanting realm of soil pathogens at Murdoch University. Your guidance and expertise were instrumental in the success of one of my experiments, paving the way for many more. I am also grateful to my supervisor from the shadow, Félix de Tombeur, visiting from our home country, for sharing his passion for research and writing. Meeting you led to successful collaborations and a great friendship.

I would like to extend my gratitude to the technical staff at UWA for generously sharing their expertise and resources. Special thanks to Greg Cawthray and Mike Smirk for the always longer than expected discussions on analytical techniques. I am also thankful to Erik Veneklaas for sharing his knowledge on photosynthesis but not only, Gareth Nealon for his expertise in NMR, and Rob Creasy and Bill Piasini for their assistance in the glasshouse facilities. I appreciate the support provided by Hai Ngo, Joanna Kotula, Kirsty Brooks, Chris Brouwer, and many others. I want to acknowledge Pauline Yeung, our dedicated administrative guru, whose assistance has been saving grace.

I would like to thank all my colleagues, past and present students, visitors, and staff for the diverse and memorable interactions. While it's impossible to thank each of you individually, I appreciate the role you played in this journey. Special thanks are due to Lalith Suriyagoda, Zhi Hui Wen, Patrick Hayes, Jiayin Pang, Toby Bird, Ben Nestor, Shu Tong Liu, Fiamma Riviera, Roberta Dayrell, Li Yan, Dan Tang, Hirotsuna Yamada, Manu Magar, Duccio Migliorini, Ryan Craig, Félix de Tombeur, Maëva Tremblay, Paul Dallongeville, Quentin Grébert, Etienne Regard, Haibin Kang, Michael Renton and the Eco Ag Mod group. Your contributions have been invaluable, and I am deeply grateful for your support.

I express my heartfelt gratitude to my friends back home, especially Gabriel de Gans, Natacha Kozak, Noémie Dallest-Jeanmougin, and Kenza Boubekour, for their support from afar. Thank you to Lucie Robuchon for editing my French abstract, even after all those years. Thank you to all my friends made in Perth, Monica Rothwell, Wei San Wong, Kenneth Sim, Simon Boutier, Solène Laos, and many others for all the fun times we had together. A special thank you goes to my former housemate Robert Seres. Last but not least, my deepest appreciation to Angeli Plaza for being who you are and standing by my side, for your constant motivation, support, and yummy adobo.

Finally, I wish to thank my family. Benoît et Ghislaine, Catherine, et Matilde, merci pour votre amour et votre soutien inconditionnel. Sans vous, je ne serai pas là où j'en suis aujourd'hui. Je vous aime, sans t'oublier, mon petit frère Baptiste.

This research was supported by a Scholarship for International Research Fees from the University of Western Australia and a University Postgraduate Award co-funded by the University of Western Australia and Australian Research Council grant DP200101013 to Hans Lambers and Patrick M. Finnegan. I am grateful to Craig Atkins for providing the Craig Atkins travel award and the Graduate Research School for providing a local travel award.

AUTHORSHIP DECLARATION

Chapter 2 – Details of the work:

This research manuscript is being prepared for publication in a peer-reviewed journal.

Gille CE, Grébert Q, Regard E, Yamada H, Yan L, Ranathunge K, Hayes PE, Finnegan PM, Lambers H. **2024**. Cluster-root physiology of carboxylate-releasing *Hakea* (Proteaceae) species determines manganese accumulation in leaves. *In preparation*.

Location in thesis: Chapter 2

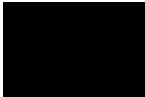
Student contribution to work:

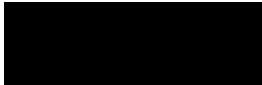
I designed this project in consultation with E/Prof. Hans Lambers, Prof. Patrick M. Finnegan and Quentin Grébert. I conducted the fieldwork and glasshouse experiment with contributions from Quentin Grébert, Etienne Regard, Hirotuna Yamada and Li Yan. I analysed the data and wrote the manuscript. All co-authors provided feedback and edits on the manuscript.

-
Quentin Grébert, 14 May 2024

-
Etienne Regard, 14 May 2024


Hirotuna Yamada, 14 May 2024


Li Yan, 14 May 2024


Kosala Ranathunge, 14 May 2024


Patrick E. Hayes, 14 May 2024


Patrick M. Finnegan, 14 May 2024


Hans Lambers, 14 May 2024

Chapter 3 – Details of the work:

This research manuscript has been published in the peer-reviewed journal *New Phytologist*, in the special issue “*Mycorrhizal research now: from the micro- to the macro-scale*” (Vol. 242, pp. 1630–1644).

Gille CE, Finnegan PM, Hayes PE, Ranathunge K, Burgess TI, de Tombeur F, Migliorini D, Dallongeville P, Glauser G, Lambers H. **2024**. Facilitative and competitive interactions between mycorrhizal and nonmycorrhizal plants in an extremely phosphorus-impooverished environment: role of ectomycorrhizal fungi and native oomycete pathogens in shaping species coexistence. *New Phytologist* **242**: 1630–1644.

Location in thesis: Chapter 3

Student contribution to work:

I designed this project in consultation with E/Prof. Hans Lambers, Prof. Patrick M. Finnegan, Prof. Treena I. Burgess and Dr. Kosala Ranathunge. I conducted the glasshouse experiment and collected growth and physiological measurements. I analysed the data and wrote the manuscript. All co-authors provided feedback and edits on the manuscript.

 Patrick M. Finnegan, 3 March 2024	 Patrick E. Hayes, 5 March 2024
 Kosala Ranathunge, 4 March 2024	 Treena I. Burgess, 1 March 2024
 Félix de Tombeur, 29 February 2024	 Duccio Migliorini, 4 March 2024
 Paul Dallongeville, 5 March 2024	 Gaétan Glauser, 29 February 2024
 Hans Lambers, 4 March 2024	

Chapter 4 – Details of the work:

This research manuscript has been submitted to the peer-reviewed journal *New Phytologist* on 29 February 2024 and is currently under review.

Gille CE, Hayes PE, Ranathunge K, Liu ST, de Tombeur F, Lambers H, Finnegan PM. **2024**. Proteaceae with high photosynthetic phosphorus-use efficiency on the conservative end of the leaf economics spectrum allocate phosphorus to biochemical fractions differently. *New Phytologist*, under review.

Location in thesis: Chapter 4

Student contribution to work:

I designed this project in consultation with Prof. Patrick M. Finnegan. I organised and conducted fieldwork in Badgingarra National Park to collect samples and field measurements with contributions from Prof. Patrick M. Finnegan, E/Prof. Hans Lambers and Dr. Shu Tong Liu. I performed all laboratory work to measure phosphorus fractions, analysed the data and wrote the manuscript. All co-authors provided feedback and edits on the manuscript.



Patrick E. Hayes, 5 March 2024



Kosala Ranathunge, 4 March 2024



Shu Tong Liu, 5 March 2024



Félix de Tombeur, 29 February 2024



Hans Lambers, 4 March 2024



Patrick M. Finnegan, 3 March 2024

Student signature:



Clément E. Gille

14 May 2024

Coordinating supervisor signature:

I, Patrick M. Finnegan certify that the student's statements regarding their contribution to each of the works listed above are correct.

As all co-authors' signatures could not be obtained for Chapter 2 (Quentin Grébert and Etienne Regard), I hereby authorise inclusion of the co-authored work in the thesis.



Patrick M. Finnegan

14 May 2024

CHAPTER ONE

General Introduction



Jacksonia floribunda (Fabaceae)

Southwest Australia, a global biodiversity hotspot

Southwest Australia stands out as one of 36 global biodiversity hotspots, boasting approximately 7,000 plant species, with around 3,000 endemics (Myers *et al.*, 2000; Hopper & Gioia, 2004; Habel *et al.*, 2019). However, southwest Australia is under increasing pressure due to climate change, land-use change, and other anthropogenic factors, with over half of its pristine habitats and up to 1,300 endemic plant species under threat (Miller *et al.*, 2007; Habel *et al.*, 2019). Similar to other biodiversity hotspots like the Cape Floristic Province in South Africa (Cowling *et al.*, 1996; Allsopp *et al.*, 2014) and the Cerrado in Brazil (Oliveira *et al.*, 2015; Silveira *et al.*, 2016), soils in south-western Australia are severely nutrient impoverished, particularly depleted in phosphorus (P) which limits plant growth (Lambers, 2014; Kooyman *et al.*, 2017). The theory of old climatically-buffered infertile landscapes (OCBIL) encompasses all these global biodiversity hotspots (Hopper, 2009, 2021). These landscapes, characterised by ancient soils that encountered little disturbance, like rejuvenation through (de)glaciation, have been subjected to prolonged weathering, leading to P depletion (Lambers *et al.*, 2010; Hopper, 2021).

Prominent plant families in the Southwest Australian biodiversity hotspot include Proteaceae, Fabaceae, Myrtaceae, Orchidaceae and Ericaceae (Lambers, 2014). Some of these families, such as Proteaceae (*e.g.*, genera *Banksia* and *Hakea*) and Myrtaceae (*e.g.*, genus *Eucalyptus*), have persisted through the breakup of the supercontinent Gondwana and are very well represented in the biodiversity hotspot (Crisp & Cook, 2013). Notably, species within these families exhibit traits that enable them to thrive in the challenging conditions in southwest Australia.

Phosphorus-acquisition strategies

Phosphorus, an essential nutrient for all life forms, is pivotal in various physiological and biochemical processes. Plants growing in P-limiting environments have evolved with specialised adaptations to acquire P efficiently that is tightly sorbed to soil particles and largely unavailable to plants. A notable example is that most Proteaceae develop cluster roots, a distinctive non-mycorrhizal root structure composed of hundreds to thousands of densely packed hairy rootlets (Shane & Lambers, 2005). In *Hakea prostrata* (Proteaceae), these ephemeral structures persist for about 21 days from formation to senescence and release exudates into the soil in an ‘exudative burst’ during maturity, which allows them to acquire P

sorbed onto soil particles (Watt & Evans, 1999; Shane *et al.*, 2004). There are different cluster-root structures. While *Hakea* species form ‘simple’ cluster roots, *Banksia* species (Proteaceae) form ‘compound’ cluster roots resembling ‘Christmas-tree’ like structures (Shane & Lambers, 2005). Additionally, some species from other families, *e.g.*, *Viminaria juncea* (Fabaceae) and *Allocasuarina humilis* (Casuarinaceae), also possess the ability to produce cluster roots (Lambers *et al.*, 2019). Similar specialised root structures are observed in various other plant families (Zemunik, 2016). Dauciform roots are produced by some Cyperaceae and while structurally distinct from cluster roots, they function similarly (Lamont, 1974; Shane *et al.*, 2005, 2006; Lambers *et al.*, 2006; Fan *et al.*, 2023). Some species from the families Haemodoraceae and Anarthriaceae produce sand-binding roots, and some Restionaceae form capillaroid roots (Lambers *et al.*, 2006, 2022; Shane *et al.*, 2011; Oliveira *et al.*, 2015). In P-impoverished environments in Brazil, Velloziaceae produce vellozioid roots (Teodoro *et al.*, 2019; Abrahão *et al.*, 2020). However, the production of cluster roots or similar specialised roots is a carbon-costly investment, explaining why it mostly occurs under severely nutrient-impoverished conditions (Lambers *et al.*, 2008; Raven *et al.*, 2018). Although all these specialised roots are structurally distinct, they are functionally analogous and release exudates that mobilise P.

Carboxylates are low-molecular-weight organic anions exuded from roots through anion channels (Zhang *et al.*, 2004). They mobilise P and a range of other elements like Mn, Fe, Zn, Si, as well as rare-earth elements (REE) (Shane *et al.*, 2004; Lambers *et al.*, 2015b; de Tombeur *et al.*, 2021; Wiche & Pourret, 2023). The physiology of carboxylate release from cluster and non-cluster roots has been extensively studied (Lambers *et al.*, 2015c). Citrate is one of the main carboxylates exuded by roots that mobilises P and other elements. Two anion channels permeable to citrate that were responsive to P availability were identified in cluster roots of white lupin (*Lupinus albus* L.) (Kihara *et al.*, 2003; Zhang *et al.*, 2004; Tomasi *et al.*, 2009; Lambers *et al.*, 2013). Other major carboxylates released by cluster roots are malate and oxalate, followed by *trans*-aconitate, *iso*-citrate, *cis*-aconitate and minor amounts of other organic acids (Roelofs *et al.*, 2001; Cawthray, 2003; Hayes *et al.*, 2024). The release of large amounts of these organic anions must be accompanied by the release of cations to balance the loss of negative charges. Citrate exudation in white lupin is dependent on an H⁺-ATPase (Tomasi *et al.*, 2009), which generates an electrochemical potential gradient that is necessary to drive anion release (Nussaume *et al.*, 2011; Poirier *et al.*, 2022). The identification of this plasma-membrane-bound proton pump associated with carboxylate release follows previous

work highlighting acidification of the rhizosphere of cluster roots in white lupin (Gardner *et al.*, 1982a,b; Dinkelaker *et al.*, 1989). While protons play a major role in acidifying the rhizosphere and further enhancing P availability in alkaline and slightly acidic soils, other cations are also mobilised by carboxylate release. In cluster roots of white lupin, the stoichiometric relationships between citrate release and the release of H⁺, K⁺, Na⁺ and Mg²⁺ are 1 : 1.3, 1 : 2.1, 1 : 1.5 and 1 : 0.47, respectively (Zhu *et al.*, 2005). By contrast, the release of malate is more strongly dependent on proton release than on other cations (Zhu *et al.*, 2005; Tomasi *et al.*, 2009). Carboxylates have different extraction potentials for inorganic elements, *e.g.*, at low pH, oxalate effectively mobilises P, while malate and citrate primarily mobilise Fe (Ström *et al.*, 1994). However, the effect of exuded counterions, other than protons, has received little attention.

In addition to carboxylates, roots also exude acid phosphatases (Ozawa *et al.*, 1995; Gilbert *et al.*, 1999; Miller *et al.*, 2001; Shane *et al.*, 2014; Png *et al.*, 2017), which allows them to access soil organic P (Tarafdar & Claassen, 1988; Turner *et al.*, 2002; George *et al.*, 2006). Organic P can represent a major fraction of the total P in agricultural soils (Hayes *et al.*, 2000; McLaren *et al.*, 2015) and also in natural soils, including those in southwest Australia (Doolette *et al.*, 2011; Turner *et al.*, 2018; Zhou *et al.*, 2019; Zhong *et al.*, 2021). Phosphatases can be categorised into different groups, including phosphomonoesterases, which hydrolyse monoesters (*e.g.*, nucleotides and sugar phosphates), and phosphodiesterases, which target phosphodiesteres (*e.g.*, nucleic acids and phospholipids). Phytate is a form of organic phosphomonoester that can be a significant fraction of organic P in soils, particularly *myo*-inositol-hexakisphosphate (Doolette *et al.*, 2011; Liu *et al.*, 2022a). Roots can release phytases that hydrolyse phytate phosphomonoesters and liberate inorganic P (Pi) available for plant uptake (Hayes *et al.*, 1999; Richardson *et al.*, 2000; Turner *et al.*, 2002; Liu *et al.*, 2022a). However, phytate is not a common P compound in P-impooverished soils (Adams & Byrne, 1989; Zhong *et al.*, 2021). Like Pi, organic P, including phytate, can be strongly bound to soil particles and accessing P in phytate requires both mobilisation by carboxylates and hydrolysis by enzymes (Giles *et al.*, 2017, 2018; Richardson *et al.*, 2022). Therefore, accessing phytate requires greater investments in carbon and energy than accessing Pi or other organic P compounds (Turner, 2008).

Symbiotic associations with mycorrhizal fungi is another common nutrient-acquisition strategy. It is found in *c.* 80% of terrestrial vascular plants (Smith & Read, 2008). Mycorrhizal

colonisation entails various benefits for the plant host, including but not exclusively enhanced mineral nutrition, water uptake and overall greater growth, and increased resistance to pathogens (Smith & Read, 2008; Brundrett, 2009; Brundrett & Tedersoo, 2018; Tedersoo *et al.*, 2020). During mycorrhizal symbioses, the fungal symbiont penetrates the root to form exchange structures. In the case of arbuscular mycorrhiza (AM), arbuscules inside root cortical cells are connected with the extraradical mycelium scavenging the soil. Ectomycorrhizal (ECM) fungi form a Hartig net between cortical cells and a fungal mantle around the root, extending to extraradical hyphae (Smith & Read, 2008). Therefore, mycorrhizal symbioses comprise a ‘scavenging’ strategy, increasing the volume of soil explored per unit of absorbing root structures. On the other hand, ‘mining’ non-mycorrhizal nutrient-acquisition strategies, *e.g.*, cluster roots, increase the local extraction efficiency of poorly-available nutrients (Lambers *et al.*, 2008). In extremely P-impoverished environments, ‘scavenging’ mycorrhizal strategies are less efficient at acquiring nutrients, particularly P, than ‘mining’ strategies (Bolan *et al.*, 1984; Abbott *et al.*, 1984; Treseder & Allen, 2002; Abrahão *et al.*, 2019; Albornoz *et al.*, 2021). Mycorrhizal symbioses also incur a greater carbon cost as soil P availability declines (Ryan *et al.*, 2012; Raven *et al.*, 2018). This higher cost explains why Southwest Australia possesses a larger proportion of non-mycorrhizal plants than nutrient-richer biomes (Brundrett & Tedersoo, 2018). However, mycorrhizal strategies are still found in extremely P-impoverished environments (Zemunik *et al.*, 2015) and might provide non-nutritional benefits to the plant host (Laliberté *et al.*, 2015; Albornoz *et al.*, 2017; Lambers *et al.*, 2018; Gille *et al.*, 2024).

Plant interactions: facilitation rather than competition

The effect of plant species diversity on productivity has been extensively studied (Cardinale *et al.*, 2009; Hendriks *et al.*, 2013; Craven *et al.*, 2016; Thakur *et al.*, 2021). However, mechanisms underlying species diversity, particularly facilitative processes in nutrient-impoverished environments, have been largely overlooked (Wright *et al.*, 2017). Facilitation plays a major role in species coexistence through fitness stabilising and equalising mechanisms (Chesson, 2000, 2018). Facilitation is characterised by a facilitator plant favouring the presence, nutrient uptake, or growth of a facilitated plant (Callaway, 2007). Along a 2-Myr dune chronosequence in south-western Australia that offers a natural gradient of soil nutrient availability, the diversity of plant nutrient-acquisition strategies increases with decreasing soil P availability (Zemunik *et al.*, 2015). The complementarity of the various nutrient-acquisition

strategies present in the system contributes to the higher species richness on older and extremely P-depleted soils through the facilitation of P acquisition (Zemunik *et al.*, 2015, 2016; Lambers *et al.*, 2018; Gille *et al.*, 2024). The exudation of carboxylates by cluster roots (or similar structures, *e.g.*, dauciform roots) of Proteaceae (or Cyperaceae) also benefits the mineral nutrition and growth of their mycorrhizal and/or non-cluster-root-forming neighbours (Lambers & Teste, 2013; Muler *et al.*, 2014; Staudinger *et al.*, 2024; Yu *et al.*, 2023; Shen *et al.*, 2024; Gille *et al.*, 2024). Facilitated species can alter biomass partitioning and root system architecture in the presence of a facilitator. Facilitation has also been reported among crop species. For example, both P uptake and biomass accumulation of wheat (*Triticum aestivum* L.) increase when intercropped with white lupin (*Lupinus albus* L.) that produces cluster roots (Cu *et al.*, 2005) or with chickpea (*Cicer arietinum* L.) that releases acid phosphatases that mobilise organic P (Li *et al.*, 2004). It is well established that low nutrient availability drives facilitative processes between species with contrasting nutrient-acquisition strategies (Callaway & Walker, 1997; Brooker *et al.*, 2008; Al-Namazi *et al.*, 2017; Lekberg *et al.*, 2018; Zhu *et al.*, 2023).

There is difficulty in assessing the expression of facilitation of P uptake in plant communities in their natural habitats. In addition to P, carboxylates also mobilise a wide range of micronutrients and beneficial elements, including Mn, Fe, Zn, Si, and REE (Lambers *et al.*, 2015b; Pang *et al.*, 2018; de Tombeur *et al.*, 2021; van der Ent *et al.*, 2023; Wiche & Pourret, 2023). At very low P supply, P uptake leads to more plant growth with little increase in leaf P concentration rather than increased leaf P storage (De Groot *et al.*, 2003; Shane *et al.*, 2003; Muler *et al.*, 2014; Gille *et al.*, 2024). Therefore, leaf P concentration is not a good indicator of the involvement of carboxylates in the facilitation of P acquisition; instead, the mobilisation of Mn by carboxylates has received increasing attention in this regard in recent years (Lambers *et al.*, 2015b, 2021; Staudinger *et al.*, 2024; Yu *et al.*, 2023). The poor control of Mn uptake by roots offers the opportunity to compare leaf Mn concentration ([Mn]) as a reflection of soil Mn availability (Baxter *et al.*, 2008). Since carboxylate exudation increases Mn availability, Lambers *et al.* (2015b, 2021) proposed that leaf [Mn] can be used as a proxy for carboxylate concentrations in the rhizosphere. This conceptual model has now been empirically validated, with strong correlations between leaf [Mn] and carboxylate concentrations in the rhizosphere among 100 chickpea genotypes with contrasting abilities to release carboxylates (Pang *et al.*, 2018). Using the same set of chickpea genotypes, Wen *et al.* (2021) proposed that leaf [Fe] and [Zn], both elements that are also mobilised by carboxylates, can also be used as a proxy for

carboxylate concentrations. However, correlations with these elements were weaker than those with leaf [Mn] due to stronger control of Fe and Zn transport and uptake (Baxter *et al.*, 2008). In a naturally-occurring P-impooverished *Banksia* woodland, leaf [Mn] of non-cluster-root-producing *Bossiaea eriocarpa* (Fabaceae) correlated with its distance to the nearest carboxylate-releasing *Banksia* (Proteaceae) plant (Staudinger *et al.*, 2024). Furthermore, the distance of a *Banksia* plant had an additional positive effect on the biomass accumulation of the facilitated *Bossiaea eriocarpa* (Staudinger *et al.*, 2024). Given that measuring carboxylate exudation in roots is a labour-intensive process and impractical for field measurement, often requiring the cultivation of plants in controlled environments, such a proxy emerges as an invaluable tool for estimating the belowground functioning of plant species. However, Mn as a proxy for a dependence of P uptake on carboxylate release requires comparing the leaf [Mn] of the target species with that of a co-occurring negative reference species, *i.e.* a species that is known not to depend on carboxylates, and with that of a positive reference species, *i.e.* a species that releases carboxylates and accumulates Mn in leaves (Lambers *et al.*, 2021). While *Banksia* species (Proteaceae) consistently accumulate relatively high concentrations of Mn in leaves, there is still a wide variation in leaf [Mn] of Proteaceae (Foulds, 1993; Roelofs *et al.*, 2001; Hayes *et al.*, 2021, 2024). The variation in leaf [Mn] is particularly strong in *Hakea* species (Proteaceae) that produce cluster roots and release carboxylates, with species that accumulate Mn but others that do not (Gille *et al.*, unpublished data; see Chapter 2). This challenges the validity of the conceptual model of leaf [Mn] as a proxy for carboxylate concentrations in the rhizosphere and the cluster-root physiology of *Hakea* species, therefore, warrants further attention.

Mycorrhizal strategies are less efficient at acquiring P than carboxylate-releasing strategies in extremely P-impooverished environments (Bolan *et al.*, 1984; Abbott *et al.*, 1984; Treseder & Allen, 2002; Albornoz *et al.*, 2021; Standish *et al.*, 2021). This is illustrated by the increase in abundance of cluster-rooted species and decrease in mycorrhizal species as soil age increases and soil P concentration decreases along a 2-Myr chronosequence in south-western Australia (Zemunik *et al.*, 2015). However, the mycorrhizal species richness and relative cover remain relatively high even on the oldest, most P-impooverished stages of the chronosequence (Zemunik *et al.*, 2015). While cluster-rooted species facilitate P uptake of mycorrhizal species, this raises the question: why do we not observe competitive exclusion of mycorrhizal species on these most P-impooverished soils and what makes them remain successful in extremely P-impooverished environments? To answer this question, we need to explore plant-plant

interactions more deeply, focusing on microbes and other biotic factors influencing these interactions.

Mycorrhizal symbiosis confers benefits besides mineral nutrition to the plant host, including enhanced protection against soil-borne pathogens through various mechanisms (Pozo & Azcón-Aguilar, 2007). Conversely, cluster-rooted species are more susceptible to soil-borne pathogens, and, therefore, a trade-off exists between efficient P acquisition and defence against pathogens (Laliberté *et al.*, 2015; Albornoz *et al.*, 2017; Lambers *et al.*, 2018). *Banksia* species lack a suberised exodermis, presumably allowing the release of large amounts of carboxylates into the rhizosphere (Lambers *et al.*, 2018). In *Hakea laurina* (Proteaceae), the release of malate originates from the cortex rather than the epidermis, supporting this hypothesis (Yamada, Wasaki *et al.*, unpublished). Conversely, most species from other families than Proteaceae do possess a suberised exodermis (Ashford *et al.*, 1989; Vesk *et al.*, 2000; Ma & Peterson, 2003; Enstone *et al.*, 2003; Brundrett & Tedersoo, 2020) that acts as a physical barrier to soilborne pathogens (Ranathunge *et al.*, 2008; Brundrett & Tedersoo, 2020). In south-western Australia, plants have co-evolved with soilborne pathogens, including native oomycete *Phytophthora* species (Ricklefs, 2010; Rea *et al.*, 2011; Albornoz *et al.*, 2017; Sarker *et al.*, 2023). Both arbuscular and ectomycorrhizal colonisation enhance the resistance of their hosts to *Phytophthora* species (Guillemin *et al.*, 1994; Branzanti *et al.*, 1999; Pozo *et al.*, 1999; Ozgonen & Erkilic, 2007; Pozo & Azcón-Aguilar, 2007). In addition to the physical protection provided by the Hartig net and fungal mantel, ectomycorrhizal fungi also release antimicrobial compounds that inhibit the growth of soilborne pathogens (Marx, 1972). Mycorrhizal colonisation also indirectly enhances the resistance of host plants to pathogens by modulating phytohormone (*e.g.*, salicylic and jasmonic acids) levels, which in turn leads to defence responses such as the induction of pathogenesis-related proteins and the production of defence-related compounds (*e.g.*, phenolics and flavonoids) involved in pathogen defence (Anfoka & Buchenauer, 1997; Durner *et al.*, 1997; Pozo *et al.*, 1999; Pozo & Azcón-Aguilar, 2007; Prithiviraj *et al.*, 2007; Ozgonen *et al.*, 2009; Avanci *et al.*, 2010; War *et al.*, 2011; Lv *et al.*, 2020; Vlot *et al.*, 2021). This trade-off between efficient P-acquisition and defence against soil-borne pathogens confers a direct advantage to mycorrhizal species that benefit from the facilitation by their non-mycorrhizal neighbours, and therefore equalises the competitive abilities of both nutrient-acquisition strategies (Laliberté *et al.*, 2015; Albornoz *et al.*, 2017; Lambers *et al.*, 2018).

A significant knowledge gap exists about the interaction between mycorrhizal fungi or mycorrhizal plant species and non-mycorrhizal cluster-rooted species. Upon establishment of the mycorrhizal symbiosis, ectomycorrhizal fungi alter the hormonal balance of the host, which inhibits defence responses (Zhang *et al.*, 2018; Basso *et al.*, 2020; Enebe & Erasmus, 2023). It has been proposed that non-host plants also contribute to the mycorrhizal network (Wang *et al.*, 2022). For example, two ectomycorrhizal fungi, *Tuber melanosporum* and *T. aestivum*, colonise the roots of non-mycorrhizal neighbouring plants but act as endophytes (Schneider-Maunoury *et al.*, 2018; Schneider-Maunoury *et al.*, 2020). In a non-host interaction with *Arabidopsis thaliana*, an arbuscular mycorrhizal fungus initiates signalling without subsequent colonisation (Fernández *et al.*, 2019). The modulation of the plant defence responses by mycorrhizal fungi, whether during host or non-host compatible interaction, occurs locally but can extend systemically (Jung *et al.*, 2012; Vlot *et al.*, 2021). It is possible that non-mycorrhizal cluster-rooted species are subjected to these types of interactions and the priming of the defences of non-mycorrhizal species in response to mycorrhizal fungi and oomycete pathogens requires further investigation. Consequently, the indirect facilitative interaction between mycorrhizal fungi and non-mycorrhizal plant species, in the context of soilborne pathogens, might contribute to the coexistence of mycorrhizal and non-mycorrhizal species in extremely P-impooverished environments.

Phosphorus-utilisation efficiency

In addition to acquiring P efficiently, numerous adaptations in Proteaceae allow them also to use it very efficiently. During leaf development, some Proteaceae exhibit a phenomenon known as ‘delayed greening’ to spread P investment over time (Sulpice *et al.*, 2014; Kuppusamy *et al.*, 2021). In delayed greening, the P-demanding growth of the leaf structure is dissociated from the development of the photosynthetic machinery, including chloroplasts (Kuppusamy *et al.*, 2014, 2021). This results in yellow-reddish young expanding leaves. The molecular basis of delayed greening has recently been unravelled, highlighting a major shift in the expression of cytosolic and mitochondrial to plastid ribosomes (Bird *et al.*, 2024). During leaf development, phospholipids are extensively replaced by other lipids that do not contain P, such as sulfolipids and galactolipids (Lambers *et al.*, 2012). Replacement of phospholipids has been described as a strategy for plants to cope with P deficiency in other species, such as *Arabidopsis thaliana* (Morcuende *et al.*, 2007), *Oryza sativa* (Hayes *et al.*, 2022), and *Eucalyptus acmenoides* (Silva *et al.*, 2022). Proteaceae function at very low abundance of rRNA and low

concentrations of protein in mature leaves (Matzek & Vitousek, 2009; Sulpice *et al.*, 2014; Liu, 2024). Some Proteaceae (*e.g.*, *Hakea prostrata*, *Banksia attenuata* and *B. thelemanniana*) restrain nitrate uptake when provided with excess nitrate (Prodhan *et al.*, 2016; Liu *et al.*, 2022b). This nitrate-uptake restraint trait is also observed in two co-occurring Myrtaceae species in a severely P-impooverished environment (Liu *et al.*, 2022b). Associated with low abundance of rRNA and low concentrations of proteins, it appears to be a convergent trait enhancing P-use efficiency in P-impooverished environments (Matzek & Vitousek, 2009; Prodhan *et al.*, 2019). Proteaceae also preferentially allocate P to photosynthetically-active mesophyll cells rather than to epidermal cells (Hayes *et al.*, 2018). Several species from other families, *e.g.*, Myrtaceae and Fabaceae, also allocate P preferentially to mesophyll cells as an adaptive response to P-impooverished environments (Guilherme Pereira *et al.*, 2018). In addition, species growing under extremely low P availability remobilise P from senescing tissues, *i.e.* senescing leaves, non-cluster and cluster roots, with high efficiency and proficiency (Shane *et al.*, 2004; Denton *et al.*, 2007; Hidaka & Kitayama, 2011; Hayes *et al.*, 2014). Taken together, all these adaptations allow Proteaceae to function at extremely low foliar P and N concentrations while maintaining relatively fast rates of CO₂ assimilation (Veneklaas *et al.*, 2012; Lambers *et al.*, 2015a) and have high photosynthetic P-use and N-use efficiency (Denton *et al.*, 2007; Lambers *et al.*, 2012; Sulpice *et al.*, 2014; Guilherme Pereira *et al.*, 2019; Shen *et al.*, 2024).

One way for plants to function at high P-use efficiency is by reducing P concentrations in leaves and partition it efficiently into different biochemical pools. Phosphorus in leaves has been conveniently categorised into five operational biochemical pools through a sequential fractionation method: nucleic acids, phospholipids, metabolic P (comprising Pi and small P-containing metabolites) and a residual fraction that likely contains phosphoproteins among other P-containing material not captured in the other fractions (Chapin & Kedrowski, 1983; Kedrowski, 1983; Hidaka & Kitayama, 2011, 2013; Yan *et al.*, 2019; Hayes *et al.*, 2022; Suriyagoda *et al.*, 2023; Tsujii *et al.*, 2023, 2024; Liu *et al.*, 2023). The lipid P fraction contains hydrophobic P-containing molecules, presumably mainly membrane lipids, including phospholipids. The replacement of phospholipids contributes to the high photosynthetic P-use efficiency (PPUE) of Proteaceae species (Lambers *et al.*, 2012). The replacement of phospholipid is a common response to P starvation in many species, including *Arabidopsis* and crops (Morcuende *et al.*, 2007; Gaude *et al.*, 2008; Nakamura *et al.*, 2009; Poitout *et al.*, 2017; Li & Yu, 2018; Wang *et al.*, 2020). However, it is usually associated with decreased

photosynthetic rates, while those sharply increase from young to mature leaves in Proteaceae species, partly contributing to their high PPUE (Lambers *et al.*, 2012). The nucleic acid P fraction is the largest organic P pool in leaves, composed mainly of RNA and some DNA, and of which up to 85% of P in this pool is in rRNA (Veneklaas *et al.*, 2012). Therefore, it is a major pool to save P for P-efficient plants. Functioning at low rRNA levels also contributes to the high PPUE of Proteaceae (Sulpice *et al.*, 2014). The metabolite P pool comprises small water-soluble phosphorylated compounds such as sugar phosphates, nucleotides, and other esterified compounds. Most metabolites in this pool (*e.g.*, glucose 6-phosphate, triose-phosphate and ATP) play a central role in photosynthesis and respiratory metabolism (Sharkey *et al.*, 1986). Therefore, metabolite P concentration and their proportion of total P are strongly correlated with photosynthetic rates (Hidaka & Kitayama, 2013; Hayes *et al.*, 2022). The fraction of cellular P in Pi is variable and spatially distinct. The cytosolic Pi is actively used for metabolism. When the cell has excess P compared with its need, the extra P is stored as Pi in the vacuole. Vacuolar Pi can be remobilised into the cytosol to meet P requirements (Poirier & Bucher, 2002; Smith *et al.*, 2003). Due to its multiple roles, especially as a storage form of P, Pi concentration increases much more than the organic P pool as the leaf total P concentration increases (Veneklaas *et al.*, 2012; Suriyagoda *et al.*, 2023). There is a tight balance between P in nucleic acids and small metabolites. Several studies have reported strong positive correlations between metabolic P (including Pi and metabolite P) or metabolite P and nucleic acid P (Hidaka & Kitayama, 2013; Yan *et al.*, 2021; Suriyagoda *et al.*, 2023). Proteaceae maintain relatively high concentrations of glucose 6-phosphate yet function at low rRNA (Sulpice *et al.*, 2014). Indeed, decreasing levels of phosphorylated intermediates would require these species to function at higher rRNA to produce enzymes, which is a far more costly P pool in leaves. In turn, Proteaceae might increase protein turnover to maintain protein to rRNA ratios (Matzek & Vitousek, 2009; Lambers, 2022). Species modulate their P-allocation patterns to these biochemical pools, particularly in low soil P availability conditions where specific adaptations have evolved (Hidaka & Kitayama, 2011, 2013; Yan *et al.*, 2019; Liu *et al.*, 2023).

Thesis outline

The primary objective of this thesis was to investigate factors underpinning plant megadiversity in an extremely P-impooverished environment. It focused on P-acquisition strategies, P-use

efficiency, and plant interactions mediated by microbes. This thesis contains four additional chapters.

Chapter 2 explores the P-acquisition strategies of *Hakea* species (Proteaceae) with contrasting leaf [Mn] that challenge the conceptual model of leaf [Mn] as a proxy for carboxylate concentrations in the rhizosphere (Lambers *et al.*, 2015b, 2021). Across a soil [P] gradient over a 2-Myr chronosequence and adjacent areas, along with a glasshouse experiment, this study explored edaphic (*e.g.*, soil pH, [Mn], and P speciation) and physiological (*e.g.*, exudation of carboxylates and cations, and acid phosphatases as alternative P-acquisition strategies) variables. I hypothesised that *Hakea* species with low leaf [Mn] rely more on additional strategies such as phosphatases than species with high leaf [Mn] and that, while all species exude carboxylates, the release of counterions associated with carboxylates determines the accumulation of Mn in leaves.

I analysed the interaction between non-mycorrhizal cluster-rooted *Banksia menziesii* (Proteaceae) and mycorrhizal *Eucalyptus todtiana* (Myrtaceae) in Chapter 3. A glasshouse experiment compared growth-related and defence-related parameters in these naturally co-occurring species, both in monoculture and in mixture, with and without ectomycorrhizal fungi and oomycete *Phytophthora* spp. pathogens. My hypotheses were based on previous studies and proposed theories (Laliberté *et al.*, 2015; Albornoz *et al.*, 2017; Lambers *et al.*, 2018), suggesting that both ectomycorrhizal fungi and oomycete pathogens would equalise competitive abilities among species with contrasting nutrient-acquisition strategies. Furthermore, I hypothesised that the ectomycorrhizal colonisation of roots of *E. todtiana* would enhance the defences of non-mycorrhizal *B. menziesii*.

Chapter 4 characterised the P-allocation patterns in major biochemical pools in leaves of 10 species of *Banksia* and *Hakea* (Proteaceae) growing in some of the most P-impoverished soils in the world in Badgingarra National Park (Western Australia). I discuss these patterns in light of the high photosynthetic P-use efficiency of both genera but with variability within each. I hypothesised that a preferential allocation of P to specific P fractions would allow species to achieve higher PPUE, with discussion on associated physiological processes.

The final chapter, the General Discussion, synthesises the findings from the previous chapters, highlighting study limitations and contextualising the results in understanding species coexistence in extremely P-impoverished and megadiverse environments.

References

- Abbott LK, Robson AD, Boer G. 1984.** The effect of phosphorus on the formation of hyphae in soil by the vesicular-arbuscular mycorrhizal fungus *Glomus fasciculatum*. *New Phytologist* **97**: 437–446.
- Abrahão A, de Britto Costa P, Lambers H, Andrade SAL, Sawaya ACHF, Ryan MH, Oliveira RS. 2019.** Soil types select for plants with matching nutrient-acquisition and -use traits in hyperdiverse and severely nutrient-impooverished *campos rupestres* and *cerrado* in Central Brazil. *Journal of Ecology* **107**: 1302–1316.
- Abrahão A, de Britto Costa P, Teodoro GS, Lambers H, Nascimento DL, Adrián López de Andrade S, Ryan MH, Silva Oliveira R. 2020.** Vellozioid roots allow for habitat specialization among rock- and soil-dwelling Velloziaceae in campos rupestres. *Functional Ecology* **34**: 442–457.
- Adams MA, Byrne LT. 1989.** ³¹P-NMR analysis of phosphorus compounds in extracts of surface soils from selected karri (*Eucalyptus diversicolor* F. Muell.) forests. *Soil Biology and Biochemistry* **21**: 523–528.
- Albornoz FE, Burgess TI, Lambers H, Etehells H, Laliberté E. 2017.** Native soilborne pathogens equalize differences in competitive ability between plants of contrasting nutrient-acquisition strategies. *Journal of Ecology* **105**: 549–557.
- Albornoz FE, Dixon KW, Lambers H. 2021.** Revisiting mycorrhizal dogmas: are mycorrhizas really functioning as they are widely believed to do? *Soil Ecology Letters* **3**: 73–82.
- Allsopp N, Colville JF, Verboom GA. 2014.** *Fynbos: ecology, evolution, and conservation of a megadiverse region*. Oxford University Press, Oxford, UK.
- Al-Namazi AA, El-Bana MI, Bonser SP. 2017.** Competition and facilitation structure plant communities under nurse tree canopies in extremely stressful environments. *Ecology and Evolution* **7**: 2747–2755.
- Anfoka G, Buchenauer H. 1997.** Systemic acquired resistance in tomato against *Phytophthora infestans* by pre-inoculation with tobacco necrosis virus. *Physiological and Molecular Plant Pathology* **50**: 85–101.
- Ashford AE, Allaway WG, Peterson CA, Cairney JWG. 1989.** Nutrient transfer and the fungus-root interface. *Australian Journal of Plant Physiology* **16**: 85–97.

- Avanci NC, Luche DD, Goldman GH, Goldman MHS. 2010.** Jasmonates are phytohormones with multiple functions, including plant defense and reproduction. *Genetics and Molecular Research* **9**: 484–505.
- Basso V, Kohler A, Miyauchi S, Singan V, Guinet F, Šimura J, Novák O, Barry KW, Amirebrahimi M, Block J, et al. 2020.** An ectomycorrhizal fungus alters sensitivity to jasmonate, salicylate, gibberellin, and ethylene in host roots. *Plant, Cell & Environment* **43**: 1047–1068.
- Baxter IR, Vitek O, Lahner B, Muthukumar B, Borghi M, Morrissey J, Guerinot M Lou, Salt DE. 2008.** The leaf ionome as a multivariable system to detect a plant's physiological status. *Proceedings of the National Academy of Sciences of the United States of America* **105**: 12081–12086.
- Bird T, Nestor BJ, Bayer PE, Wang G, Ilyasova A, Gille CE, Soraru BEH, Ranathunge K, Severn-Ellis AA, Jost R, et al. 2024.** Delayed leaf greening involves a major shift in the expression of cytosolic and mitochondrial ribosomes to plastid ribosomes in the highly phosphorus-use-efficient *Hakea prostrata* (Proteaceae). *Plant and Soil* **496**: 7–30.
- Bolan NS, Robson AD, Barrow NJ. 1984.** Increasing phosphorus supply can increase the infection of plant roots by vesicular-arbuscular mycorrhizal fungi. *Soil Biology and Biochemistry* **16**: 419–420.
- Branzanti MB, Rocca E, Pisi A. 1999.** Effect of ectomycorrhizal fungi on chestnut ink disease. *Mycorrhiza* **9**: 103–109.
- Brooker RW, Maestre FT, Callaway RM, Lortie CL, Cavieres LA, Kunstler G, Liancourt P, Tielbörger K, Travis JM, Anthelme F, et al. 2008.** Facilitation in plant communities: the past, the present, and the future. *Journal of Ecology* **96**: 18–34.
- Brundrett MC. 2009.** Mycorrhizal associations and other means of nutrition of vascular plants: understanding the global diversity of host plants by resolving conflicting information and developing reliable means of diagnosis. *Plant and Soil* **320**: 37–77.
- Brundrett MC, Tedersoo L. 2018.** Evolutionary history of mycorrhizal symbioses and global host plant diversity. *New Phytologist* **220**: 1108–1115.
- Brundrett MC, Tedersoo L. 2020.** Resolving the mycorrhizal status of important northern hemisphere trees. *Plant and Soil* **454**: 3–34.
- Callaway RM, Walker LR. 1997.** Competition and facilitation: a synthetic approach to interactions in plant communities. *Ecology* **78**: 1958–1965.
- Callaway RM. 2007.** *Positive interactions and interdependence in plant communities*. Dordrecht, the Netherlands: Springer.

- Cardinale BJ, Srivastava DS, Duffy JE, Wright JP, Downing AL, Sankaran M, Jouseau C, Cadotte MW, Carroll IT, Weis JJ, et al. 2009.** Effects of biodiversity on the functioning of ecosystems: a summary of 164 experimental manipulations of species richness. *Ecology* **90**: 854–854.
- Cawthray GR. 2003.** An improved reversed-phase liquid chromatographic method for the analysis of low-molecular mass organic acids in plant root exudates. *Journal of Chromatography A* **1011**: 233–240.
- Chapin FS, Kedrowski RA. 1983.** Seasonal changes in nitrogen and phosphorus fractions and autumn retranslocation in evergreen and deciduous Taiga trees. *Ecology* **64**: 376–391.
- Chesson P. 2000.** Mechanisms of maintenance of species diversity. *Annual Review of Ecology and Systematics* **31**: 343–366.
- Chesson P. 2018.** Updates on mechanisms of maintenance of species diversity. *Journal of Ecology* **106**: 1773–1794.
- Cowling RM, MacDonald IAW, Simmons MT. 1996.** The Cape Peninsula, South Africa: physiographical, biological and historical background to an extraordinary hot-spot of biodiversity. *Biodiversity & Conservation* **5**: 527–550.
- Craven D, Isbell F, Manning P, Connolly J, Bruelheide H, Ebeling A, Roscher C, van Ruijven J, Weigelt A, Wilsey B, et al. 2016.** Plant diversity effects on grassland productivity are robust to both nutrient enrichment and drought. *Philosophical Transactions of the Royal Society B: Biological Sciences* **371**: 20150277.
- Crisp MD, Cook LG. 2013.** How was the Australian flora assembled over the last 65 million years? A molecular phylogenetic perspective. *Annual Review of Ecology, Evolution, and Systematics* **44**: 303–324.
- Cu STT, Hutson J, Schuller KA. 2005.** Mixed culture of wheat (*Triticum aestivum* L.) with white lupin (*Lupinus albus* L.) improves the growth and phosphorus nutrition of the wheat. *Plant and Soil* **272**: 143–151.
- Denton MD, Veneklaas EJ, Freimoser FM, Lambers H. 2007.** *Banksia* species (Proteaceae) from severely phosphorus-impooverished soils exhibit extreme efficiency in the use and remobilization of phosphorus. *Plant, Cell & Environment* **30**: 1557–1565.
- Dinkelaker B, Römheld V, Marschner H. 1989.** Citric acid excretion and precipitation of calcium citrate in the rhizosphere of white lupin (*Lupinus albus* L.). *Plant, Cell & Environment* **12**: 285–292.
- Doolette AL, Smernik RJ, Dougherty WJ. 2011.** A quantitative assessment of phosphorus forms in some Australian soils. *Soil Research* **49**: 152–165.

- Durner J, Shah J, Klessig DF. 1997.** Salicylic acid and disease resistance in plants. *Trends in Plant Science* **2**: 266–274.
- Enebe MC, Erasmus M. 2023.** Susceptibility and plant immune control—a case of mycorrhizal strategy for plant colonization, symbiosis, and plant immune suppression. *Frontiers in Microbiology* **14**.
- Enstone DE, Peterson CA, Ma F. 2003.** Root endodermis and exodermis: structure, function, and responses to the environment. *Journal of Plant Growth Regulation* **21**: 335–351.
- van der Ent A, Nkrumah PN, Purwadi I, Erskine PD. 2023.** Rare earth element (hyper)accumulation in some Proteaceae from Queensland, Australia. *Plant and Soil* **485**: 247–257.
- Fan R, Hua J, Huang Y, Lin J, Ji W. 2023.** What role do dauciform roots play? Responses of *Carex filispica* to trampling in alpine meadows based on functional traits. *Ecology and Evolution* **13**: 1–11.
- Fernández I, Cosme M, Stringlis IA, Yu K, de Jonge R, van Wees SCM, Pozo MJ, Pieterse CMJ, van der Heijden MGA. 2019.** Molecular dialogue between arbuscular mycorrhizal fungi and the nonhost plant *Arabidopsis thaliana* switches from initial detection to antagonism. *New Phytologist* **223**: 867–881.
- Foulds W. 1993.** Nutrient concentrations of foliage and soil in South-western Australia. *New Phytologist* **125**: 529–546.
- Gardner WK, Parbery DG, Barber DA. 1982a.** The acquisition of phosphorus by *Lupinus albus* L. II. The effect of varying phosphorus supply and soil type on some characteristics of the soil/root interface. *Plant and Soil* **68**: 33–41.
- Gardner WK, Parbery DG, Barber DA. 1982b.** The acquisition of phosphorus by *Lupinus albus* L. I. Some characteristics of the soil/root interface. *Plant and Soil* **68**: 19–32.
- Gaude N, Nakamura Y, Scheible WR, Ohta H, Dörmann P. 2008.** Phospholipase C5 (NPC5) is involved in galactolipid accumulation during phosphate limitation in leaves of *Arabidopsis*. *Plant Journal* **56**: 28–39.
- George TS, Turner BL, Gregory PJ, Cade-Menun BJ, Richardson AE. 2006.** Depletion of organic phosphorus from Oxisols in relation to phosphatase activities in the rhizosphere. *European Journal of Soil Science* **57**: 47–57.
- Gilbert GA, Knight JD, Vance CP, Allan DL. 1999.** Acid phosphatase activity in phosphorus-deficient white lupin roots. *Plant, Cell & Environment* **22**: 801–810.
- Giles CD, Dupuy L, Boitt G, Brown LK, Condrón LM, Darch T, Blackwell MSA, Menezes-Blackburn D, Shand CA, Stutter MI, et al. 2018.** Root development impacts

on the distribution of phosphatase activity: improvements in quantification using soil zymography. *Soil Biology and Biochemistry* **116**: 158–166.

Giles CD, George TS, Brown LK, Mezeli MM, Richardson AE, Shand CA, Wendler R, Darch T, Menezes-Blackburn D, Cooper P, et al. 2017. Does the combination of citrate and phytase exudation in *Nicotiana tabacum* promote the acquisition of endogenous soil organic phosphorus? *Plant and Soil* **412**: 43–59.

Gille CE, Finnegan PM, Hayes PE, Ranathunge K, Burgess TI, de Tombeur F, Migliorini D, Dallongeville P, Glauser G, Lambers H. 2024. Facilitative and competitive interactions between mycorrhizal and nonmycorrhizal plants in an extremely phosphorus-impooverished environment: role of ectomycorrhizal fungi and native oomycete pathogens in shaping species coexistence. *New Phytologist* **242**: 1630–1644.

De Groot CC, Marcelis LFM, Van Den Boogaard R, Kaiser WM, Lambers H. 2003. Interaction of nitrogen and phosphorus nutrition in determining growth. *Plant and Soil* **248**: 257–268.

Guilherme Pereira C, Clode PL, Oliveira RS, Lambers H. 2018. Eudicots from severely phosphorus-impooverished environments preferentially allocate phosphorus to their mesophyll. *New Phytologist* **218**: 959–973.

Guilherme Pereira C, Hayes PE, O’Sullivan OS, Weerasinghe LK, Clode PL, Atkin OK, Lambers H. 2019. Trait convergence in photosynthetic nutrient-use efficiency along a 2-million year dune chronosequence in a global biodiversity hotspot. *Journal of Ecology* **107**: 2006–2023.

Guillemin J-P, Gianinazzi S, Gianinazzi-Pearson V, Marchal J. 1994. Contribution of arbuscular mycorrhizas to biological protection of micropropagated pineapple (*Ananas comosus* (L.) Merr) against *Phytophthora cinnamomi* Rands. *Agricultural and Food Science* **3**: 241–251.

Habel JC, Rasche L, Schneider UA, Engler JO, Schmid E, Rödder D, Meyer ST, Trapp N, Sos del Diego R, Eggermont H, et al. 2019. Final countdown for biodiversity hotspots. *Conservation Letters* **12**: 1–9.

Hayes PE, Adem GD, Pariasca-Tanaka J, Wissuwa M. 2022. Leaf phosphorus fractionation in rice to understand internal phosphorus-use efficiency. *Annals of Botany* **129**: 287–302.

Hayes PE, Clode PL, Lambers H. 2024. Calcifuge and soil-indifferent Proteaceae from south-western Australia: novel strategies in a calcareous habitat. *Plant and Soil* **496**: 95–122.

- Hayes PE, Clode PL, Oliveira RS, Lambers H. 2018.** Proteaceae from phosphorus-impooverished habitats preferentially allocate phosphorus to photosynthetic cells: An adaptation improving phosphorus-use efficiency. *Plant, Cell & Environment* **41**: 605–619.
- Hayes PE, Nge FJ, Cramer MD, Finnegan PM, Fu P, Hopper SD, Oliveira RS, Turner BL, Zemunik G, Zhong H, et al. 2021.** Traits related to efficient acquisition and use of phosphorus promote diversification in Proteaceae in phosphorus-impooverished landscapes. *Plant and Soil* **462**: 67–88.
- Hayes JE, Richardson AE, Simpson RJ. 1999.** Phytase and acid phosphatase activities in extracts from roots of temperate pasture grass and legume seedlings. *Australian Journal of Plant Physiology* **26**: 801–809.
- Hayes JE, Richardson AE, Simpson RJ. 2000.** Components of organic phosphorus in soil extracts that are hydrolysed by phytase and acid phosphatase. *Biology and Fertility of Soils* **32**: 279–286.
- Hayes P, Turner BL, Lambers H, Laliberté E. 2014.** Foliar nutrient concentrations and resorption efficiency in plants of contrasting nutrient-acquisition strategies along a 2-million-year dune chronosequence. *Journal of Ecology* **102**: 396–410.
- Hendriks M, Mommer L, de Caluwe H, Smit-Tiekstra AE, van der Putten WH, de Kroon H. 2013.** Independent variations of plant and soil mixtures reveal soil feedback effects on plant community overyielding. *Journal of Ecology* **101**: 287–297.
- Hidaka A, Kitayama K. 2011.** Allocation of foliar phosphorus fractions and leaf traits of tropical tree species in response to decreased soil phosphorus availability on Mount Kinabalu, Borneo. *Journal of Ecology* **99**: 849–857.
- Hidaka A, Kitayama K. 2013.** Relationship between photosynthetic phosphorus-use efficiency and foliar phosphorus fractions in tropical tree species. *Ecology and Evolution* **3**: 4872–4880.
- Hopper SD. 2009.** OCBIL theory: towards an integrated understanding of the evolution, ecology and conservation of biodiversity on old, climatically buffered, infertile landscapes. *Plant and Soil* **322**: 49–86.
- Hopper SD. 2021.** Out of the OCBILs: new hypotheses for the evolution, ecology and conservation of the eucalypts. *Biological Journal of the Linnean Society* **133**: 342–372.
- Hopper SD, Gioia P. 2004.** The Southwest Australian Floristic Region: evolution and conservation of a global hotspot of biodiversity. *Annual Review of Ecology, Evolution, and Systematics* **35**: 623–650.

- Jung SC, Martinez-Medina A, Lopez-Raez JA, Pozo MJ. 2012.** Mycorrhiza-induced resistance and priming of plant defenses. *Journal of Chemical Ecology* **38**: 651–664.
- Kedrowski RA. 1983.** Extraction and analysis of nitrogen, phosphorus and carbon fractions in plant material. *Journal of Plant Nutrition* **6**: 989–1011.
- Kihara T, Wada T, Suzuki Y, Hara T, Koyama H. 2003.** Alteration of citrate metabolism in cluster roots of white lupin. *Plant and Cell Physiology* **44**: 901–908.
- Kooyman RM, Laffan SW, Westoby M. 2017.** The incidence of low phosphorus soils in Australia. *Plant and Soil* **412**: 143–150.
- Kuppusamy T, Giavalisco P, Arvidsson S, Sulpice R, Stitt M, Finnegan PM, Scheible WR, Lambers H, Jost R. 2014.** Lipid biosynthesis and protein concentration respond uniquely to phosphate supply during leaf development in highly phosphorus-efficient *Hakea prostrata*. *Plant Physiology* **166**: 1891–1911.
- Kuppusamy T, Hahne D, Ranathunge K, Lambers H, Finnegan PM. 2021.** Delayed greening in phosphorus-efficient *Hakea prostrata* (Proteaceae) is a photoprotective and nutrient-saving strategy. *Functional Plant Biology* **48**: 218–230.
- Laliberté E, Lambers H, Burgess TI, Wright SJ. 2015.** Phosphorus limitation, soil-borne pathogens and the coexistence of plant species in hyperdiverse forests and shrublands. *New Phytologist* **206**: 507–521.
- Lambers H. 2014.** *Plant life on the sandplains in southwest Australia: a global biodiversity hotspot*. Crawley, Australia: The University of Western Australia Publishing.
- Lambers H. 2022.** Phosphorus acquisition and utilization in plants. *Annual Review of Plant Biology* **73**: 17–42.
- Lambers H, Albornoz FE, Arruda AJ, Barker T, Finnegan PM, Gille C, Gooding H, Png GK, Ranathunge K, Zhong H. 2019.** Nutrient-acquisition strategies. In: Lambers H, ed. *A Jewel in the Crown of a Global Biodiversity Hotspot*. Perth: Kwongan Foundation and the Western Australian Naturalists' Club Inc., 227–248.
- Lambers H, Albornoz FE, Kotula L, Laliberté E, Ranathunge K, Teste FP, Zemunik G. 2018.** How belowground interactions contribute to the coexistence of mycorrhizal and non-mycorrhizal species in severely phosphorus-impooverished hyperdiverse ecosystems. *Plant and Soil* **424**: 11–33.
- Lambers H, de Britto Costa P, Cawthray GR, Denton MD, Finnegan PM, Hayes PE, Oliveira RS, Power SC, Ranathunge K, Shen Q, et al. 2022.** Strategies to acquire and use phosphorus in phosphorus-impooverished and fire-prone environments. *Plant and Soil* **476**: 133–160.

- Lambers H, Brundrett MC, Raven JA, Hopper SD. 2010.** Plant mineral nutrition in ancient landscapes: high plant species diversity on infertile soils is linked to functional diversity for nutritional strategies. *Plant and Soil* **334**: 11–31.
- Lambers H, Cawthray GR, Giavalisco P, Kuo J, Laliberté E, Pearse SJ, Scheible W-R, Stitt M, Teste F, Turner BL. 2012.** Proteaceae from severely phosphorus-impooverished soils extensively replace phospholipids with galactolipids and sulfolipids during leaf development to achieve a high photosynthetic phosphorus-use-efficiency. *New Phytologist* **196**: 1098–1108.
- Lambers H, Clements JC, Nelson MN. 2013.** How a phosphorus-acquisition strategy based on carboxylate exudation powers the success and agronomic potential of lupines (*Lupinus*, Fabaceae). *American Journal of Botany* **100**: 263–288.
- Lambers H, Finnegan PM, Jost R, Plaxton WC, Shane MW, Stitt M. 2015a.** Phosphorus nutrition in Proteaceae and beyond. *Nature Plants* **1**: 15109.
- Lambers H, Hayes PE, Laliberté E, Oliveira RS, Turner BL. 2015b.** Leaf manganese accumulation and phosphorus-acquisition efficiency. *Trends in Plant Science* **20**: 83–90.
- Lambers H, Martinoia E, Renton M. 2015c.** Plant adaptations to severely phosphorus-impooverished soils. *Current Opinion in Plant Biology* **25**: 23–31.
- Lambers H, Raven JA, Shaver GR, Smith SE. 2008.** Plant nutrient-acquisition strategies change with soil age. *Trends in Ecology and Evolution* **23**: 95–103.
- Lambers H, Shane MW, Cramer MD, Pearse SJ, Veneklaas EJ. 2006.** Root structure and functioning for efficient acquisition of phosphorus: matching morphological and physiological traits. *Annals of Botany* **98**: 693–713.
- Lambers H, Teste FP. 2013.** Interactions between arbuscular mycorrhizal and non-mycorrhizal plants: do non-mycorrhizal species at both extremes of nutrient availability play the same game? *Plant, Cell & Environment* **36**.
- Lambers H, Wright IJ, Guilherme Pereira C, Bellingham PJ, Bentley LP, Boonman A, Cernusak LA, Foulds W, Gleason SM, Gray EF, et al. 2021.** Leaf manganese concentrations as a tool to assess belowground plant functioning in phosphorus-impooverished environments. *Plant and Soil* **461**: 43–61.
- Lamont B. 1974.** The biology of dauciform roots in the sedge *Cyathochaete avenacea*. *New Phytologist* **73**: 985–996.
- Lekberg Y, Bever JD, Bunn RA, Callaway RM, Hart MM, Kivlin SN, Klironomos J, Larkin BG, Maron JL, Reinhart KO, et al. 2018.** Relative importance of competition

and plant-soil feedback, their synergy, context dependency and implications for coexistence. *Ecology Letters* **21**: 1268–1281.

Li SM, Li L, Zhang FS, Tang C. 2004. Acid phosphatase role in chickpea/maize intercropping. *Annals of Botany* **94**: 297–303.

Li HM, Yu CW. 2018. Chloroplast galactolipids: the link between photosynthesis, chloroplast shape, jasmonates, phosphate starvation and freezing tolerance. *Plant and Cell Physiology* **59**: 1128–1134.

Liu ST. 2024. *Phosphorus-use and nitrogen-use strategies of native plants in south-western Australia*. University of Western Australia, Perth.

Liu ST, Gille CE, Bird T, Ranathunge K, Finnegan PM, Lambers H. 2023. Leaf phosphorus allocation to chemical fractions and its seasonal variation in south-western Australia is a species-dependent trait. *Science of the Total Environment* **901**: 166395.

Liu X, Han R, Cao Y, Turner BL, Ma LQ. 2022a. Enhancing phytate availability in soils and phytate-P acquisition by plants: a review. *Environmental Science & Technology* **56**: 9196–9219.

Liu ST, Ranathunge K, Lambers H, Finnegan PM. 2022b. Nitrate-uptake restraint in *Banksia* spp. (Proteaceae) and *Melaleuca* spp. (Myrtaceae) from a severely phosphorus-impooverished environment. *Plant and Soil* **476**: 63–77.

Lv J, Dong Y, Dong K, Zhao Q, Yang Z, Chen L. 2020. Intercropping with wheat suppressed Fusarium wilt in faba bean and modulated the composition of root exudates. *Plant and Soil* **448**: 153–164.

Ma F, Peterson CA. 2003. Current insights into the development, structure, and chemistry of the endodermis and exodermis of roots. *Canadian Journal of Botany* **81**: 405–421.

Marx DH. 1972. Ectomycorrhizae as biological deterrents to pathogenic root infections. *Annual Review of Phytopathology* **10**: 429–454.

Matzek V, Vitousek PM. 2009. N:P stoichiometry and protein:RNA ratios in vascular plants: an evaluation of the growth-rate hypothesis. *Ecology Letters* **12**: 765–771.

McLaren TI, Smernik RJ, McLaughlin MJ, McBeath TM, Kirby JK, Simpson RJ, Guppy CN, Doolette AL, Richardson AE. 2015. Complex forms of soil organic phosphorus - a major component of soil phosphorus. *Environmental Science and Technology* **49**: 13238–13245.

Miller BP, Enright NJ, Lamont BB. 2007. Record error and range contraction, real and imagined, in the restricted shrub *Banksia hookeriana* in south-western Australia. *Diversity and Distributions* **13**: 406–417.

- Miller SS, Liu J, Allan DL, Menzhuber CJ, Fedorova M, Vance CP. 2001.** Molecular control of acid phosphatase secretion into the rhizosphere of proteoid roots from phosphorus-stressed white lupin. *Plant Physiology* **127**: 594–606.
- Morcuende R, Bari R, Gibon Y, Zheng W, Pant BD, Bläsing O, Usadel B, Czechowski T, Udvardi MK, Stitt M, et al. 2007.** Genome-wide reprogramming of metabolism and regulatory networks of *Arabidopsis* in response to phosphorus. *Plant, Cell & Environment* **30**: 85–112.
- Muler AL, Oliveira RS, Lambers H, Veneklaas EJ. 2014.** Does cluster-root activity benefit nutrient uptake and growth of co-existing species? *Oecologia* **174**: 23–31.
- Myers N, Mittermeier RA, Mittermeier CG, da Fonseca GAB, Kent J. 2000.** Biodiversity hotspots for conservation priorities. *Nature* **403**: 853–858.
- Nakamura Y, Koizumi R, Shui G, Shimojima M, Wenk MR, Ito T, Ohtad H. 2009.** *Arabidopsis* lipins mediate eukaryotic pathway of lipid metabolism and cope critically with phosphate starvation. *Proceedings of the National Academy of Sciences of the United States of America* **106**: 20978–20983.
- Nussaume L, Kanno S, Javot H, Marin E, Pochon N, Ayadi A, Nakanishi TM, Thibaud MC. 2011.** Phosphate import in plants: focus on the PHT1 transporters. *Frontiers in Plant Science* **2**: 1–12.
- Oliveira RS, Galvão HC, de Campos MCR, Eller CB, Pearse SJ, Lambers H. 2015.** Mineral nutrition of campos rupestres plant species on contrasting nutrient-impooverished soil types. *New Phytologist* **205**: 1183–1194.
- Ozawa K, Osaki M, Matsui H, Honma M, Tadano T. 1995.** Purification and properties of acid phosphatase secreted from lupin roots under phosphorus-deficiency conditions. *Soil Science and Plant Nutrition* **41**: 461–469.
- Ozgonen H, Erkilic A. 2007.** Growth enhancement and *Phytophthora* blight (*Phytophthora capsici* Leonian) control by arbuscular mycorrhizal fungal inoculation in pepper. *Crop Protection* **26**: 1682–1688.
- Ozgonen H, Yardimci N, Cular Kilic H. 2009.** Induction of phenolic compounds and pathogenesis-related proteins by mycorrhizal fungal inoculations against *Phytophthora capsici* Leonian in pepper. *Pakistan Journal of Biological Sciences* **12**: 1181–1187.
- Pang J, Bansal R, Zhao H, Bohuon E, Lambers H, Ryan MH, Ranathunge K, Siddique KHM. 2018.** The carboxylate-releasing phosphorus-mobilizing strategy can be proxied by foliar manganese concentration in a large set of chickpea germplasm under low phosphorus supply. *New Phytologist* **219**: 518–529.

- Png GK, Turner BL, Albornoz FE, Hayes PE, Lambers H, Laliberté E. 2017.** Greater root phosphatase activity in nitrogen-fixing rhizobial but not actinorhizal plants with declining phosphorus availability. *Journal of Ecology* **105**: 1246–1255.
- Poirier Y, Bucher M. 2002.** Phosphate transport and homeostasis in *Arabidopsis*. *The Arabidopsis Book* **1**: e0024.
- Poirier Y, Jaskolowski A, Clúa J. 2022.** Phosphate acquisition and metabolism in plants. *Current Biology* **32**: R623–R629.
- Poitout A, Martinière A, Kucharczyk B, Queruel N, Silva-Andia J, Mashkoor S, Gamet L, Varoquaux F, Paris N, Sentenac H, et al. 2017.** Local signalling pathways regulate the *Arabidopsis* root developmental response to *Mesorhizobium loti* inoculation. *Journal of Experimental Botany* **68**: 1199–1211.
- Pozo MJ, Azcón-Aguilar C. 2007.** Unraveling mycorrhiza-induced resistance. *Current Opinion in Plant Biology* **10**: 393–398.
- Pozo MJ, Azcón-Aguilar C, Dumas-Gaudot E, Barea JM. 1999.** β -1,3-glucanase activities in tomato roots inoculated with arbuscular mycorrhizal fungi and/or *Phytophthora parasitica* and their possible involvement in bioprotection. *Plant Science* **141**: 149–157.
- Prithiviraj B, Perry LG, Badri D V., Vivanco JM. 2007.** Chemical facilitation and induced pathogen resistance mediated by a root-secreted phytotoxin. *New Phytologist* **173**: 852–860.
- Proadhan MA, Finnegan PM, Lambers H. 2019.** How does evolution in phosphorus-impooverished landscapes impact plant nitrogen and sulfur assimilation? *Trends in Plant Science* **24**: 69–82.
- Proadhan MA, Jost R, Watanabe M, Hoefgen R, Lambers H, Finnegan PM. 2016.** Tight control of nitrate acquisition in a plant species that evolved in an extremely phosphorus-impooverished environment. *Plant, Cell & Environment* **39**: 2754–2761.
- Ranathunge K, Thomas RH, Fang X, Peterson CA, Gijzen M, Bernards MA. 2008.** Soybean root suberin and partial resistance to root rot caused by *Phytophthora sojae*. *Phytopathology* **98**: 1179–1189.
- Raven JA, Lambers H, Smith SE, Westoby M. 2018.** Costs of acquiring phosphorus by vascular land plants: patterns and implications for plant coexistence. *New Phytologist* **217**: 1420–1427.
- Rea AJ, Burgess TI, Hardy GESJ, Stukely MJC, Jung T. 2011.** Two novel and potentially endemic species of *Phytophthora* associated with episodic dieback of Kwongan vegetation in the south-west of Western Australia. *Plant Pathology* **60**: 1055–1068.

- Richardson AE, George TS, Hens M, Delhaize E, Ryan PR, Simpson RJ, Hocking PJ. 2022.** Organic anions facilitate the mobilization of soil organic phosphorus and its subsequent lability to phosphatases. *Plant and Soil* **476**: 161–180.
- Richardson AE, Hadobas PA, Hayes JE. 2000.** Acid phosphomonoesterase and phytase activities of wheat (*Triticum aestivum* L.) roots and utilization of organic phosphorus substrates by seedlings grown in sterile culture. *Plant, Cell & Environment* **23**: 397–405.
- Ricklefs RE. 2010.** Evolutionary diversification, coevolution between populations and their antagonists, and the filling of niche space. *Proceedings of the National Academy of Sciences of the United States of America* **107**: 1265–1272.
- Roelofs RFR, Rengel Z, Cawthray GR, Dixon KW, Lambers H. 2001.** Exudation of carboxylates in Australian Proteaceae: chemical composition. *Plant, Cell & Environment* **24**: 891–904.
- Ryan MH, Tibbett M, Edmonds-Tibbett T, Suriyagoda LDB, Lambers H, Cawthray GR, Pang J. 2012.** Carbon trading for phosphorus gain: the balance between rhizosphere carboxylates and arbuscular mycorrhizal symbiosis in plant phosphorus acquisition. *Plant, Cell & Environment* **35**: 2170–2180.
- Sarker SR, Burgess TI, Hardy GESJ, McComb J. 2023.** Closing the gap between the number of *Phytophthora* species isolated through baiting a soil sample and the number revealed through metabarcoding. *Mycological Progress* **22**: 1–9.
- Schneider-Maunoury L, Deveau A, Moreno M, Todesco F, Belmondo S, Murat C, Courty P, Jąkalski M, Selosse M. 2020.** Two ectomycorrhizal truffles, *Tuber melanosporum* and *T. aestivum*, endophytically colonise roots of non-ectomycorrhizal plants in natural environments. *New Phytologist* **225**: 2542–2556.
- Schneider-Maunoury L, Leclercq S, Clément C, Covès H, Lambourdière J, Sauve M, Richard F, Selosse MA, Taschen E. 2018.** Is *Tuber melanosporum* colonizing the roots of herbaceous, non-ectomycorrhizal plants? *Fungal Ecology* **31**: 59–68.
- Shane MW, Cawthray GR, Cramer MD, Kuo J, Lambers H. 2006.** Specialized ‘dauciform’ roots of Cyperaceae are structurally distinct, but functionally analogous with ‘cluster’ roots. *Plant, Cell & Environment* **29**: 1989–1999.
- Shane MW, Cramer MD, Funayama-Noguchi S, Cawthray GR, Millar AH, Day DA, Lambers H. 2004.** Developmental physiology of cluster-root carboxylate synthesis and exudation in harsh hakea. Expression of phosphoenolpyruvate carboxylase and the alternative oxidase. *Plant Physiology* **135**: 549–560.

- Shane MW, Dixon KW, Lambers H. 2005.** The occurrence of dauciform roots amongst Western Australian reeds, rushes and sedges, and the impact of phosphorus supply on dauciform-root development in *Schoenus unispiculatus* (Cyperaceae). *New Phytologist* **165**: 887–898.
- Shane MW, Lambers H. 2005.** Cluster roots: a curiosity in context. *Plant and Soil* **274**: 101–125.
- Shane MW, McCully ME, Canny MJ, Pate JS, Lambers H. 2011.** Development and persistence of sandsheaths of *Lyginia barbata* (Restionaceae): relation to root structural development and longevity. *Annals of Botany* **108**: 1307–1322.
- Shane MW, Stigter K, Fedosejevs ET, Plaxton WC. 2014.** Senescence-inducible cell wall and intracellular purple acid phosphatases: implications for phosphorus remobilization in *Hakea prostrata* (Proteaceae) and *Arabidopsis thaliana* (Brassicaceae). *Journal of Experimental Botany* **65**: 6097–6106.
- Shane MW, De Vos M, De Roock S, Cawthray GR, Lambers H. 2003.** Effects of external phosphorus supply on internal phosphorus concentration and the initiation, growth and exudation of cluster roots in *Hakea prostrata* R.Br. *Plant and Soil* **248**: 209–219.
- Sharkey TD, Stitt M, Heineke D, Gerhardt R, Raschke K, Heldt HW. 1986.** Limitation of photosynthesis by carbon metabolism. II. O₂-intensive CO₂ uptake results from limitation of triose phosphate utilization. *Plant Physiology* **81**: 1123–1129.
- Shen Q, Ranathunge K, Lambers H, Finnegan PM. 2024.** *Adenanthos* species (Proteaceae) in phosphorus-impoverished environments use a variety of phosphorus-acquisition strategies and achieve high-phosphorus-use efficiency. *Annals of Botany* **133**: 483–494.
- Silva FM de O, Bulgarelli RG, Mubeen U, Caldana C, Andrade SAL, Mazzafera P. 2022.** Low phosphorus induces differential metabolic responses in eucalyptus species improving nutrient use efficiency. *Frontiers in Plant Science* **13**: 1–15.
- Silveira FAO, Negreiros D, Barbosa NPU, Buisson E, Carmo FF, Carstensen DW, Conceição AA, Cornelissen TG, Echternacht L, Fernandes GW, et al. 2016.** Ecology and evolution of plant diversity in the endangered campo rupestre: a neglected conservation priority. *Plant and Soil* **403**: 129–152.
- Smith FW, Mudge SR, Rae AL, Glassop D. 2003.** Phosphate transport in plants. *Plant and Soil* **248**: 71–83.
- Smith SE, Read DJ. 2008.** *Mycorrhizal symbiosis*. London, UK: Academic Press and Elsevier.

- Standish RJ, Albornoz FE, Morald TK, Hobbs RJ, Tibbett M. 2021.** Mycorrhizal symbiosis and phosphorus supply determine interactions among plants with contrasting nutrient-acquisition strategies. *Journal of Ecology* **109**: 3892–3902.
- Staudinger C, Renton M, Leopold M, Wasaki J, Veneklaas EJ, de Britto Costa P, Boitt G, Lambers H. 2024.** Interspecific facilitation of micronutrient uptake between cluster-root-bearing trees and non-cluster rooted-shrubs in a *Banksia* woodland. *Plant and Soil* **496**: 71–82.
- Ström L, Olsson T, Tyler G. 1994.** Differences between calcifuge and acidifuge plants in root exudation of low-molecular organic acids. *Plant and Soil* **167**: 239–245.
- Sulpice R, Ishihara H, Schlereth A, Cawthray GR, Encke B, Giavalisco P, Ivakov A, Arrivault S, Jost R, Krohn N, et al. 2014.** Low levels of ribosomal RNA partly account for the very high photosynthetic phosphorus-use efficiency of Proteaceae species. *Plant, Cell & Environment* **37**: 1276–1298.
- Suriyagoda LDB, Ryan MH, Gille CE, Dayrell RLC, Finnegan PM, Ranathunge K, Nicol D, Lambers H. 2023.** Phosphorus fractions in leaves. *New Phytologist* **237**: 1122–1135.
- Tarafdar JC, Claassen N. 1988.** Organic phosphorus compounds as a phosphorus source for higher plants through the activity of phosphatases produced by plant roots and microorganisms. *Biology and Fertility of Soils* **5**: 308–312.
- Tedersoo L, Bahram M, Zobel M. 2020.** How mycorrhizal associations drive plant population and community biology. *Science* **367**.
- Teodoro GS, Lambers H, Nascimento DL, de Britto Costa P, Flores-Borges DNA, Abrahão A, Mayer JLS, Sawaya ACHF, Ladeira FSB, Abdala DB, et al. 2019.** Specialized roots of Velloziaceae weather quartzite rock while mobilizing phosphorus using carboxylates. *Functional Ecology* **33**: 762–773.
- Thakur MP, van der Putten WH, Wilschut RA, Veen GF (Ciska), Kardol P, van Ruijven J, Allan E, Roscher C, van Kleunen M, Bezemer TM. 2021.** Plant–soil feedbacks and temporal dynamics of plant diversity–productivity relationships. *Trends in Ecology and Evolution* **36**: 651–661.
- Tomasi N, Kretschmar T, Espen L, Weisskopf L, Fuglsang AT, Palmgren MG, Neumann G, Varanini Z, Pinton R, Martinoia E, et al. 2009.** Plasma membrane H⁺-ATPase-dependent citrate exudation from cluster roots of phosphate-deficient white lupin. *Plant, Cell & Environment* **32**: 465–475.
- de Tombeur F, Cornelis JT, Lambers H. 2021.** Silicon mobilisation by root-released carboxylates. *Trends in Plant Science* **26**: 1116–1125.

- Treseder KK, Allen MF. 2002.** Direct nitrogen and phosphorus limitation of arbuscular mycorrhizal fungi: a model and field test. *New Phytologist* **155**: 507–515.
- Tsujii Y, Atwell BJ, Lambers H, Wright IJ. 2024.** Leaf phosphorus fractions vary with leaf economic traits among 35 Australian woody species. *New Phytologist* **241**: 1985–1997.
- Tsujii Y, Fan B, Atwell BJ, Lambers H, Lei Z, Wright IJ. 2023.** A survey of leaf phosphorus fractions and leaf economic traits among 12 co-occurring woody species on phosphorus-impooverished soils. *Plant and Soil* **489**: 107–124.
- Turner BL. 2008.** Resource partitioning for soil phosphorus: a hypothesis. *Journal of Ecology* **96**: 698–702.
- Turner BL, McKelvie ID, Haygarth PM. 2002.** Characterisation of water-extractable soil organic phosphorus by phosphatase hydrolysis. *Soil Biology and Biochemistry* **34**: 27–35.
- Turner BL, Hayes PE, Laliberté E. 2018.** A climosequence of chronosequences in southwestern Australia. *European Journal of Soil Science* **69**: 69–85.
- Veneklaas EJ, Lambers H, Bragg J, Finnegan PM, Lovelock CE, Plaxton WC, Price CA, Scheible W-R, Shane MW, White PJ, et al. 2012.** Opportunities for improving phosphorus-use efficiency in crop plants. *New Phytologist* **195**: 306–320.
- Vesk PA, Ashford AE, Markovina AL, Allaway WG. 2000.** Apoplasmic barriers and their significance in the exodermis and sheath of *Eucalyptus pilularis*-*Pisolithus tinctorius* ectomycorrhizas. *New Phytologist* **145**: 333–346.
- Vlot AC, Sales JH, Lenk M, Bauer K, Brambilla A, Sommer A, Chen Y, Wenig M, Nayem S. 2021.** Systemic propagation of immunity in plants. *New Phytologist* **229**: 1234–1250.
- Wang F, Ding D, Li J, He L, Xu X, Zhao Y, Yan B, Li Z, Xu J. 2020.** Characterisation of genes involved in galactolipids and sulfolipids metabolism in maize and *Arabidopsis* and their differential responses to phosphate deficiency. *Functional Plant Biology* **47**: 279–292.
- Wang Y, He X, Yu F. 2022.** Non-host plants: are they mycorrhizal networks players? *Plant Diversity* **44**: 127–134.
- War AR, Paulraj MG, War MY, Ignacimuthu S. 2011.** Role of salicylic acid in induction of plant defense system in chickpea (*Cicer arietinum* L.). *Plant Signaling & Behavior* **6**: 1787–1792.
- Watt M, Evans JR. 1999.** Proteoid roots. Physiology and development. *Plant Physiology* **121**: 317–323.

- Wen Z, Pang J, Ryan MH, Shen J, Siddique KHM, Lambers H. 2021.** In addition to foliar manganese concentration, both iron and zinc provide proxies for rhizosheath carboxylates in chickpea under low phosphorus supply. *Plant and Soil* **465**: 31–46.
- Wiche O, Pourret O. 2023.** The role of root carboxylate release on rare earth element (hyper)accumulation in plants – a biogeochemical perspective on rhizosphere chemistry. *Plant and Soil* **492**: 79–90.
- Wright AJ, Wardle DA, Callaway R, Gaxiola A. 2017.** The overlooked role of facilitation in biodiversity experiments. *Trends in Ecology & Evolution* **32**: 383–390.
- Yan L, Sunoj VSJ, Short AW, Lambers H, Elsheery NI, Kajita T, Wee AKS, Cao KF. 2021.** Correlations between allocation to foliar phosphorus fractions and maintenance of photosynthetic integrity in six mangrove populations as affected by chilling. *New Phytologist* **232**: 2267–2282.
- Yan L, Zhang X, Han Z, Pang J, Lambers H, Finnegan PM. 2019.** Responses of foliar phosphorus fractions to soil age are diverse along a 2 Myr dune chronosequence. *New Phytologist* **223**: 1621–1633.
- Yu R, Su Y, Lambers H, van Ruijven J, An R, Yang H, Yin X, Xing Y, Zhang W, Li L. 2023.** A novel proxy to examine interspecific phosphorus facilitation between plant species. *New Phytologist* **239**: 1637–1650.
- Zemunik GA. 2016.** *The response of plant community diversity and nutrient-acquisition strategies to long-term ecosystem development in nutrient-impooverished landscapes.* The University of Western Australia, Perth and the State University of Campinas, Campinas.
- Zemunik G, Turner BL, Lambers H, Laliberté E. 2015.** Diversity of plant nutrient-acquisition strategies increases during long-term ecosystem development. *Nature Plants* **1**: 1–4.
- Zemunik G, Turner BL, Lambers H, Laliberté E. 2016.** Increasing plant species diversity and extreme species turnover accompany declining soil fertility along a long-term chronosequence in a biodiversity hotspot. *Journal of Ecology* **104**: 792–805.
- Zhang F, Anasontzis GE, Labourel A, Champion C, Haon M, Kemppainen M, Commun C, Deveau A, Pardo A, Veneault-Fourrey C, et al. 2018.** The ectomycorrhizal basidiomycete *Laccaria bicolor* releases a secreted β -1,4 endoglucanase that plays a key role in symbiosis development. *New Phytologist* **220**: 1309–1321.
- Zhang WH, Ryan PR, Tyerman SD. 2004.** Citrate-permeable channels in the plasma membrane of cluster roots from white lupin. *Plant Physiology* **136**: 3771–3783.

- Zhong H, Zhou J, Azmi A, Arruda AJ, Doolette AL, Smernik RJ, Lambers H. 2021.** *Xylomelum occidentale* (Proteaceae) accesses relatively mobile soil organic phosphorus without releasing carboxylates. *Journal of Ecology* **109**: 246–259.
- Zhou J, Wu Y, Turner BL, Sun H, Wang J, Bing H, Luo J, He X, Zhu H, He Q. 2019.** Transformation of soil organic phosphorus along the Hailuoguo post-glacial chronosequence, southeastern edge of the Tibetan Plateau. *Geoderma* **352**: 414–421.
- Zhu S-G, Kiprotich W, Cheng Z, Zhou R, Fan J, Zhu H, Wang W-Y, Wang W, Wang R, Tao H, et al. 2023.** Soil phosphorus availability mediates facilitation dynamic in maize-grass pea intercropping system. *Soil and Tillage Research* **234**: 105867.
- Zhu Y, Yan F, Zörb C, Schubert S. 2005.** A link between citrate and proton release by proteoid roots of white lupin (*Lupinus albus* L.) grown under phosphorus-deficient conditions? *Plant and Cell Physiology* **46**: 892–901.

CHAPTER TWO

Cluster-root physiology of carboxylate-releasing *Hakea* (Proteaceae) species determines manganese accumulation in leaves



Hakea myrtooides × *laurina* (Proteaceae)

This chapter is being prepared for publication.

The main text is presented, followed by the Supporting Information.

Cluster-root physiology of carboxylate-releasing *Hakea* (Proteaceae) species determines manganese accumulation in leaves

Clément E. Gille, Quentin Grébert, Etienne Regard, Hirotsuna Yamada, Li Yan, Kosala Ranathunge, Patrick E. Hayes, Patrick M. Finnegan and Hans Lambers

School of Biological Sciences, The University of Western Australia, 35 Stirling Highway, Perth, WA, 6009, Australia

Author for correspondence: *Clément E. Gille*

Email: clement.gille@uwa.edu.au

Summary

- In extremely phosphorus (P)-impoverished environments, adaptations have evolved in plants that allow them to acquire P efficiently. Most Proteaceae produce cluster roots, specialised structures composed of hundreds of hairy rootlets that release carboxylates that mobilise poorly-available P sorbed onto soil particles. In addition to P, carboxylates mobilise a range of micronutrients. These include manganese (Mn), which is readily taken up by roots and translocated to leaves. As a result, leaf Mn concentration can be used as a proxy for rhizosphere carboxylate concentrations. However, some *Hakea* (Proteaceae) species that do produce cluster roots and release carboxylates do not accumulate Mn in their leaves, challenging this conceptual model.

- Using species of *Hakea* with contrasting leaf Mn concentrations, we explored the determinants of Mn accumulation in leaves. We investigated the physiology of the release of carboxylates and concomitant cations, rhizosphere phosphatase activity, and soil properties such as specific P compounds using ^{31}P -nuclear magnetic resonance (^{31}P -NMR) spectroscopy.

- Manganese accumulation in leaves did not depend on the rate of carboxylate release, but on concomitant release of cations to balance the negative charge of carboxylates. Species releasing K^+ or Mg^{2+} did not acidify the rhizosphere compared with species releasing H^+ , and therefore increased, rather than decreased the rhizosphere pH and decreased the rhizosphere Mn availability. There was a link between the ability of species to release phosphatases and access specific organic P compounds detected by ^{31}P -NMR spectroscopy.

- We highlight the limitations of using leaf Mn concentration as a proxy for rhizosphere carboxylate concentration and propose a revised model. We further discuss how the discovered alternative physiology of carboxylate exudation may contribute to the success of some species in alleviating metal-ion toxicity.

Key words: carboxylate release, cations, ion flux, ^{31}P -NMR spectroscopy, phosphatase, protons, rhizosphere acidification, root exudates.

Introduction

In severely nutrient-impoverished environments, plant adaptations have evolved to allow them to acquire scarce nutrients, particularly phosphorus (P), that pertain to the ‘do-it-yourself’ end of the root economic space (Bergmann *et al.*, 2020; Carmona *et al.*, 2021; Hayes *et al.*, 2021; Lambers *et al.*, 2022). A typical adaptation to low soil P availability is the production of cluster roots (CR) by most Proteaceae. These short-lived non-mycorrhizal roots comprise high numbers of densely packed hairy rootlets that ‘mine’ P sorbed onto soil particles by releasing large amounts of carboxylates and protons (Shane *et al.*, 2004). Species from P-impoverished environments also rely on phosphatases exuded by roots to hydrolyse P esters in organic molecules like RNA and phospholipids that are weakly bound to soil particles (Zhong *et al.*, 2021; Shen *et al.*, 2024). Root phosphatase activity also aligns with the ‘do-it-yourself’ end of the root economic space, with negative correlations between phosphatase activity and root diameter and mycorrhizal colonisation, and positive correlations with specific root length (Han *et al.*, 2022).

Carboxylates, including malate and citrate, are low-molecular-weight organic anions. Their exudation by non-cluster and cluster roots mobilises sparingly-available inorganic nutrients sorbed onto soil particles and not readily available for plant uptake. In addition to P, carboxylates also mobilise a range of micronutrients, including manganese (Mn), iron (Fe) and zinc (Zn), as well as silicon (Si), and rare earth elements (REE). The link between carboxylates in the rhizosphere and accumulation of these co-mobilised elements in leaves has recently gained substantial interest (Lambers *et al.*, 2015, 2021; de Tombour *et al.*, 2021a; Wen *et al.*, 2021; Wiche & Pourret, 2023). Assessing carboxylate exudation in roots is laborious and often requires growing plants in controlled environments with easy access to the root system. Since Mn uptake is poorly controlled (Baxter *et al.*, 2008) and likely reflects its availability in the rhizosphere, Lambers *et al.* (2015, 2021) conceptualised leaf Mn concentration ([Mn]) as a proxy for rhizosphere carboxylate concentrations. This model was supported by Pang *et al.* (2018), who found significant correlations between rhizosphere carboxylate concentration and leaf [Mn] among 100 genotypes of chickpea (*Cicer arietinum* L.) with contrasting abilities to exude carboxylates. They also found similar trends for Fe and Zn.

Carboxylate exudation by roots requires the release of cations to balance the negative charge of the organic anions released. The release of protons (H⁺) as a counter ion to carboxylate exudation has been extensively studied in various species with or without the

ability to form cluster roots (Neumann & Römheld, 1999; Roelofs *et al.*, 2001; Zhu *et al.*, 2005; Wang *et al.*, 2008). Proton release acidifies the rhizosphere and influences nutrient availability in the proximity of the roots. For example, the availability of Mn, Fe, Zn, and Cu is enhanced at lower pH (Lambers & Oliveira, 2019). This is in accordance with the concept of concomitant release of carboxylates and H⁺ leading to the accumulation of those elements in leaves (Lambers *et al.*, 2015, 2021; Pang *et al.*, 2018). However, there is a large variation in leaf [Mn] among cluster-root producing Proteaceae that presumably all release carboxylates to acquire P in P-impooverished environments (Foulds, 1993; de Tombeur *et al.*, 2021a; Hayes *et al.*, 2024). This variation in leaf [Mn] is particularly striking among species of *Hakea* (Proteaceae), which all form cluster roots and release carboxylates (Roelofs *et al.*, 2001). While *H. prostrata* accumulates Mn (Shane & Lambers, 2005; Guilherme Pereira *et al.*, 2021; Hayes *et al.*, 2024), Mn levels in leaves of *H. incrassata* and *H. flabellifolia* are more variable (de Tombeur *et al.*, 2021a; Guilherme Pereira *et al.*, 2021; Hayes *et al.*, 2024). These results challenge the proposed model and suggest that some aspects of mechanisms involved in nutrient mobilisation by carboxylates are currently overlooked.

Aluminium (Al) is a toxic element that is chelated by carboxylates (Pearse *et al.*, 2006, 2007). Like the availability of Mn, which can also be toxic for plants, Al availability increases with decreasing pH (Dong *et al.*, 1999). Species that concomitantly release H⁺ and carboxylates are expected to be more susceptible to metal ion toxicity due to rhizosphere acidification. However, carboxylates have the capacity to chelate these metal ions, rendering them non-toxic (Ryan *et al.*, 2001). Ryan *et al.* (1995) found that potassium ions (K⁺) were associated with Al-induced efflux of malate in wheat (*Triticum aestivum* L.). It is likely that the concomitant release of carboxylates with cations other than H⁺, such as K⁺, play a role in alleviating metal ion toxicity. Moreover, carboxylates have different extraction potentials for inorganic elements, *e.g.*, at low pH, oxalate effectively extracts P, while malate and citrate primarily extract Fe (Ström *et al.*, 1994). It is unclear how species in P-impooverished environments express these mechanisms to balance the release of carboxylates to satisfy P requirements with Al and Fe toxicity.

In this study, we aimed to identify determinants for accumulation of Mn and other elements in leaves of carboxylate-releasing species with contrasting leaf [Mn] in severely P-impooverished habitats. *Hakea prostrata* accumulates more Mn in mature leaves than *H. flabellifolia*, while *H. incrassata* has intermediate leaf [Mn] (Shane & Lambers, 2005;

de Tombeur *et al.*, 2021a; Guilherme Pereira *et al.*, 2021; Hayes *et al.*, 2024). Therefore, combining data from the field and a glasshouse experiment, we investigated leaf Mn accumulation in *H. prostrata*, *H. incrassata* and *H. flabellifolia* with respect to edaphic and physiological variables. We hypothesised that (1) leaf [Mn] is positively correlated with soil [Mn] and negatively correlated with soil pH for all studied species, as soil Mn availability is pH dependent (Lambers & Oliveira, 2019); (2) all species release carboxylates, but the release is accompanied by the release of species-dependent cations, *i.e.* Mn-accumulating *H. prostrata* relies mainly on H⁺ release while *H. incrassata* and *H. flabellifolia*, which accumulate less Mn, predominantly release other cations, *e.g.*, K⁺ and Mg²⁺. We also hypothesised that (3) these exudation patterns influence the accumulation of other elements for which availability varies depending on carboxylate release and soil pH, *i.e.* Ca, K, Mg, Fe, P and Zn (Lambers & Oliveira, 2019); and, finally, (4) species with low leaf [Mn] also access different forms of soil P, *e.g.*, P esters using exuded phosphatases which does not contribute to leaf Mn accumulation.

Materials and Methods

Species and site selection

At least one of the three target species in this study, *Hakea prostrata* R.Br., *H. incrassata* R.Br., and *H. flabellifolia* Meisn. were sampled at 10 locations near Jurien Bay (Western Australia), *c.* 200 km north of Perth in southwest Australia (Fig. 1). The region has a Mediterranean climate with hot dry summers and cool wet winters (Bureau of Meteorology, Australian Government; <http://www.bom.gov.au/climate/data>). The mean annual rainfall (1968–2017) is 553 mm, of which *c.* 80% falls between May and September, and the mean annual maximum temperature is 25°C (Bureau of Meteorology, Australian Government; <http://www.bom.gov.au/climate/data>).

Five sites are located along the Jurien Bay chronosequence. A detailed description of this *c.* 2-Myr-old sand dune chronosequence is presented in previous studies (Laliberté *et al.*, 2012; Turner & Laliberté, 2015; Turner *et al.*, 2018). Sites Spearwood 14 (SW14), Spearwood 34 (SW34) and Morgan's Track (MT) are located on Spearwood dunes characterised by yellow/brown shallow sand overlying pale deep sand. Sites Bassendean North Lesueur 1 (BNL1) and Powerline Track (PT) are located on Bassendean dunes characterised by pale deep sand. Five sites are located on older (> 2-Myr-old) Peron slopes and dissected lateritic plateaus

inland of the sand-dune chronosequence. Badgingarra National Park (BNP) is characterised by lateritic gravels over pale and yellow deep sand. Sites Lesueur National Park (LNP-Up, up a slope; LNP-Down, down a slope) are characterised by sedimentary (sandstone, siltstone, shale) hills. Site Cockleshell Gully (CG) is located downhill from LNP-Up and LNP-Down sites, at the boundary between Mount Lesueur and Nylagarda systems, and is characterised by brown and minor pale deep sand on the edge of an alluvial plain. Site Alexander Morrison National Park (AMNP) is characterised by sandy and lateritic gravels over pale and yellow deep sand (Fig. 1; Western Australian Department of Primary Industries and Regional Development, 2024). This series of sites offers a strong natural range of soil P concentrations (Laliberté *et al.*, 2012; Hayes *et al.*, 2014; Turner & Laliberté, 2015; Turner *et al.*, 2018). This allowed us to explore P-acquisition strategies of the three target *Hakea* species and investigate the link between their leaf [Mn] and edaphic conditions.

Leaf sampling and analyses of field plants

Mature, fully-expanded, undamaged leaves of five individuals of each target species found at each site were collected between June and August 2023. Leaves were dried at 60°C for seven days to constant weight and finely ground using a zirconium bead mill (GenoGrinder, Spex SamplePrep, Metuchen, NJ, USA). Leaf elemental concentrations were determined in *c.* 200 mg ground leaf material using inductively-coupled plasma optical emission spectroscopy (ICP-OES; Avio 560 Max, PerkinElmer, Waltham, MA, USA) after digestion with HNO₃ : HClO₄ (6 : 1 v/v) at 130°C (Zarcinas *et al.*, 1987). The use of leaf [Mn] as a proxy for carboxylate concentration in the rhizosphere requires comparing leaf [Mn] of the target species with that of a ‘positive reference’ species (Lambers *et al.*, 2021). Species of *Banksia* (Proteaceae) consistently release carboxylates and accumulate Mn in mature leaves (Lambers *et al.*, 2021; Staudinger *et al.*, 2024). Therefore, at sites where *H. prostrata*, which releases carboxylates and accumulates Mn in its leaves (Shane *et al.*, 2004; Shane & Lambers, 2005) was not found, mature leaves of a co-occurring species of *Banksia* were sampled.

Ground leaf samples (*c.* 1 mg) were analysed by combustion to measure stable carbon isotope composition ($\delta^{13}\text{C}$) using a continuous flow system (Delta V Plus mass spectrometer connected to an elemental analyser Thermo Flush 1112 via Conflo IV, Thermo-Finnigan, Bremen, Germany) at the West Australian Biogeochemistry Centre (The University of Western Australia). Stable isotope compositions were determined using international (International Atomic Energy Agency, Table S1) and laboratory standards (Skrzypek, 2013).

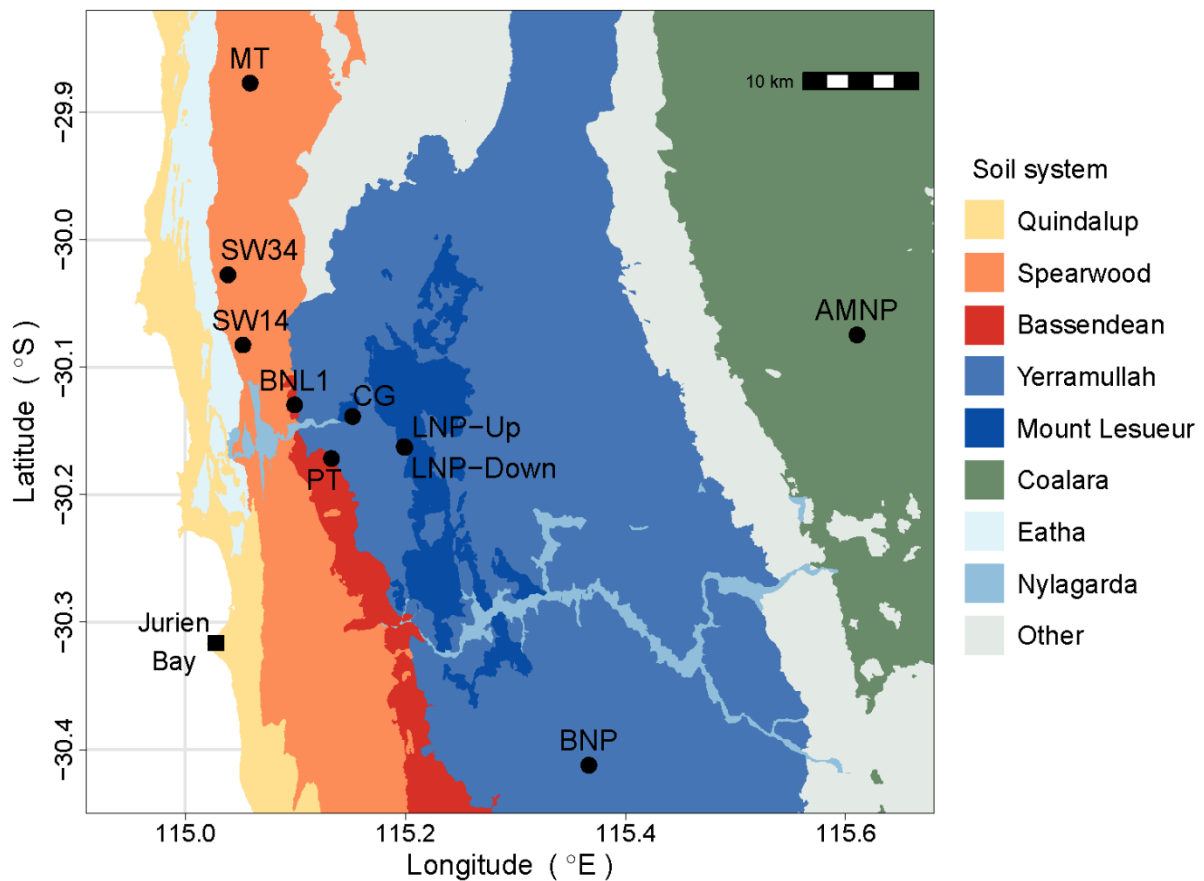


Fig. 1 Location of the 10 sites along the Jurien Bay chronosequence (Quindalup, Spearwood, and Bassendean) and surrounding area (Yerramullah, Mount Lesueur and Coalara) in south-western Australia where *Hakea prostrata*, *H. incrassata* and *H. flabellifolia* were sampled. SW14, Spearwood West 14; SW34, Spearwood West 34; MT, Morgan's track; BNL1, Bassendean North Lesueur 1; PT, Powerline track; CG, Cockleshell gully; LNP-Down, Lesueur National Park down a slope; LNP-Up, Lesueur National Park up a slope; BNP, Badgingarra National Park; AMNP, Alexander Morrison National Park. Mapping of soil systems was based on the classification of the Western Australian Department of Primary Industries and Regional Development (2024).

Soil sampling and analyses

Topsoil cores (50 mm diameter, 150 mm depth) were collected after the soil surface was cleared of litter and organic debris in open areas in the proximity of the target *Hakea* species. Samples were visually inspected to ensure they did not contain any roots to represent the 'bulk soil', *i.e.* soil available for plants to explore. Three topsoil cores were collected near one another and pooled into one soil sample, repeated five times to obtain five well-separated soil samples at

each site. Soil samples were air-dried at ambient temperature (*c.* 22°C) for two weeks and then sieved (< 2 mm stainless steel) to remove large organic debris and gravel.

Soil pH was determined in a 1:5 soil : 0.01 M CaCl₂ solution with a glass electrode (Orion Versa Star Pro, Thermo Fisher Scientific, Waltham, MA, USA). Soil total P concentration ([P]) was determined by an ignition method (Turner & Romero, 2009). In brief, air-dried soil was heated at 550°C for 1 h and allowed to cool before extraction by shaking with 1 M HCl for 16 h to determine total [P]. A second soil subsample was extracted with 1 M HCl for 16 h without prior ignition to determine inorganic [P]. Both subsamples were filtered through Whatman no. 42 paper, and soil [P] was determined colorimetrically (Motomizu *et al.*, 1983). Organic [P] was calculated by subtracting inorganic [P] from total [P]. Resin [P], a measure of ‘plant-available soil P’, was extracted using anion exchange membranes (AEM; Turner & Romero, 2009). Air-dried soil was shaken in deionised H₂O with four anionic-form AEM strips (10 × 40 mm; manufactured by BDH, Poole, UK, and distributed by VWR International) for 16 h. After shaking, the AEM strips were rinsed free of soil particles with deionised H₂O, and the Pi was recovered by shaking the strips in 0.5 M HCl for 1 h. Resin [P] in the extract was determined colorimetrically (Motomizu *et al.*, 1983). Soil P concentrations are expressed on a dry-weight (DW) basis (mg P kg⁻¹ soil DW).

Soil Mn was extracted using the aqua-regia method in a fine ground subsample of air-dried soil. In brief, *c.* 200 mg soil was digested in a mixture of concentrated 1 : 3 (v/v) HNO₃ : HCl at 130°C for 1 h and Mn concentration in the extract was determined by ICP-OES (Avio 560 Max, PerkinElmer, Waltham, MA, USA).

Solution ³¹P-NMR spectroscopy

Phosphorus speciation in soil was determined using ³¹P-nuclear magnetic resonance (³¹P-NMR) spectroscopy. Seven sites were selected as representative of the soil [P] range among the 10 sites presented in other analyses. For the seven sites selected, three soil samples were randomly selected. In brief, *c.* 10 g of air-dried soil was extracted in a 1 : 2 (w/v) soil : extraction buffer (0.25 M NaOH, 0.05 M Na₂EDTA) by shaking at *c.* 22°C for 4 h before centrifugation at 8000 g at 4°C for 30 min. The supernatant was transferred to a clean vial and freeze-dried for five days to complete dryness (VirTis BenchTop Pro ‘K’ Freeze Dryer, SP Scientific, Warminster, PA, USA). The freeze-dried material was resuspended in 5 ml of Milli-Q H₂O, and centrifuged at 8000 g at 20°C for 15 min. A 3.5 ml aliquot was transferred

into a 10-mm diameter NMR tube with 0.3 ml of deuterium oxide and 0.1 ml of 6.0 g l⁻¹ (w/v) methylenediphosphonic acid (MDP) as internal standard and samples were stored at 4°C until analysis.

Solution ³¹P-NMR spectra at 202 MHz were obtained on a Bruker AVIIIHD 500 MHz NMR spectrometer (Billerica, MA, USA) using a 10 mm broad band fluorine observe probe. Experiments were conducted using inverse gated decoupling, with a 90° pulse of 30 μs duration, a repetition time of 4 s, including an acquisition time of 0.2 s. A total of 21,500 scans were acquired, leading to an approximately 24 h total experiment time per sample. Measurement of T1 values using inversion-recovery experiments for the species present was prohibitively time consuming; therefore, the relaxation delay of 3.8 s was selected based on a preliminary experiment involving a series of measurements with relaxation delay durations from 1 s to 30 s. The relative integral against the signal of the MDP internal standard increased from a delay of 1 s to 3 s but stabilised from 3 s (Table S2). Furthermore, the integral ratio of significant peaks (*i.e.* pyrophosphate : orthophosphate, pyrophosphate : β-glycerophosphate and β-glycerophosphate : orthophosphate) was constant across relaxation delays from 3 s to 30 s (Table S2). Therefore, a relaxation delay of 3.8 s and a 0.2 s acquisition time were selected to allow quantitative analysis of the samples, whilst maintaining a minimum repetition time to improve the signal to noise ratio of the signals of interest. The chemical shift of signal peaks is reported in parts per million (ppm). Quantification of P compounds in the extracts involved deconvolution and spectral integration against the signal of the known addition of the MDP internal standard, calibrated with a chemical shift of 17 ppm. Data were analysed using MestReNova software v15.0.0. The following classes of P compounds were identified and quantified based on a series of spiking experiments with known compounds: MDP (17 ppm), orthophosphate (5.71–5.75 ppm), α-glycerophosphate (4.99–5.00 ppm), β-glycerophosphate (4.60–4.65 ppm), adenosine 5'-monophosphate (4.49–4.52 ppm), phytate (3.97, 4.11, 4.31, 4.46 and 4.81 ppm), pyrophosphate (-5.03 to -5.04 ppm). The following compounds were also spiked but not identified in the NaOH-EDTA soil extracts: phosphoenolpyruvate (0.07 ppm), ATP (-4.62 and -4.71 ppm), D-glucose 6-phosphate (5.27–5.29 ppm), and phosphonate (20.27–20.28 ppm). The identification of those peaks is consistent with previous studies (Doolette *et al.*, 2011; Doolette & Smernik, 2016; Zhong *et al.*, 2021). Significant peaks in the 3.5–5.5 ppm region without a putative identification were considered unknown phosphate monoesters (Doolette *et al.*, 2011; Doolette & Smernik, 2016; Zhong *et al.*, 2021).

Rhizobox-growth of plants and analyses

Seeds of *H. prostrata* and *H. flabellifolia* were collected at site BNP in Badgingarra National Park and at site PT along the Jurien Bay chronosequence in April 2022. Seeds were surface sterilised by submerging in 1% (w/v) NaClO for 20 s and then in 70% (v/v) ethanol for 20 s before thoroughly rinsing in deionised H₂O. Surface-sterilised seeds were sown and germinated in 1 l pots filled with Bassendean sand. Seedlings with three to four leaves were transferred from 1 l pots to rhizoboxes (35 cm length, 3 cm width, 56 cm depth) filled with triple-steam-pasteurised Bassendean sand collected at the BNL1 site. The rhizoboxes were placed at a 30°C angle to force roots to grow along the acrylic faces of the rhizoboxes, which were covered with removable black PVC sheets to avoid light exposure of the roots. The rhizoboxes were randomly moved weekly and watered two or three times per week to maintain a soil water content of *c.* 75%. Plants were grown in a glasshouse at the University of Western Australia (31.57°S, 115.47°E) from July 15th to October 8th, 2022, with minimum and maximum temperatures of 13 and 23°C, respectively. Relative humidity was maintained at approximately 60% and a shade screen was deployed if photosynthetically-active radiation exceeded 1650 $\mu\text{mol m}^{-2} \text{s}^{-1}$.

The acrylic side of the rhizobox was removed, and cluster and non-cluster roots were carefully lifted out of the sand. Roots were gently shaken to remove loosely adhering sand around the roots. The tightly adhering sand around the root was defined as rhizosheath soil (Pang *et al.*, 2017). Rhizosheath soil associated with cluster and non-cluster roots was collected using a paint brush and weighed to determine the fresh weight (FW), then transferred into a known volume of 0.02 M CaCl₂ and gently shaken by hand for 2 min. The solution was filtered through a sterile 0.22 μm syringe filter and 1 ml of the filtrate was transferred into a high-performance liquid chromatography (HPLC) vial with 20 μl of concentrated orthophosphoric acid and stored at -20°C until analysis. Carboxylates were determined by HPLC as described in Cawthray (2003) using a Prevail 250*4.6 mm column with 5 μm particle and mobile phase of 25 mM KH₂PO₄ adjusted to pH 2.5. Oxalic acid was determined using a Hypercarb 4.6*100 mm column with 5 μm particle and mobile phase of 0.1% (v/v) trifluoroacetic acid (Uloth *et al.*, 2015). Results are expressed in nmoles carboxylates g⁻¹ rhizosheath soil FW.

Acid phosphomonoesterase activity was determined in the rhizosheath soil of cluster and non-cluster roots and in the ‘bulk’ soil of each rhizobox, *i.e.* soil that was not in contact

with any root, to determine the basal microbial activity (Tabatabai & Bremner, 1969; Eivazi & Tabatabai, 1977). In brief, *c.* 1 g soil was incubated at 37°C for 1 h with 0.2 ml toluene, 4 ml tris(hydroxymethyl)aminomethane-HCl, pH 6.5, 0.1 M maleic acid, 70 mM citric acid and 0.1 M boric acid, and 1 ml 0.05 M *p*-nitrophenyl phosphate (*p*NPP). The reaction was terminated with 1 ml 0.5 M CaCl₂ and 4 ml of 0.5 M NaOH. For each sample, a blank was used, for which the *p*NPP substrate was added after the addition of CaCl₂ and NaOH. The concentration of *p*-nitrophenol (*p*NP) was determined colorimetrically at 405 nm against *p*NP working standards and the acid phosphomonoesterase activity was expressed as $\mu\text{g } p\text{NP g}^{-1}$ rhizosheath soil FW h⁻¹ after subtracting the reading of the ‘bulk’ soil sample.

Hydroponically-grown plants and analyses

One-year-old seedlings of *H. prostrata*, *H. incrassata* and *H. flabellifolia* were purchased (Natural Area Nursery, Whiteman, WA, Australia). Roots were thoroughly washed of soil particles and seedlings were transferred into a hydroponic system in a glasshouse at the University of Western Australia (31.57°S, 115.47°E) under the same environmental conditions as plants grown in rhizoboxes. Seedlings were grown in 4.5 l pots with one seedling per pot containing 4 l continuously-aerated nutrient solution (pH 5.8) with the following composition (in μM): 66.67 KNO₃, 12 MgSO₄, 0.08 MnSO₄, 0.03 ZnSO₄, 0.8 H₃BO₃, 0.01 Na₂MoO₄, 3.33 Fe-NaEDTA, 10 CaCl₂, 0.02 CuSO₄. Phosphorus was supplied separately as KH₂PO₄ at the following concentrations: 4 μM for *H. prostrata*, 2 μM for *H. flabellifolia* and *H. incrassata*. Pots were placed in cooling tanks, maintaining the nutrient solution temperature at 18–20°C and the nutrient solution was replaced every three days.

Once plants were established and root systems developed, acid phosphomonoesterase and phosphodiesterase activities were measured following Dodd *et al.* (1987) and Turner *et al.* (2001). In brief, cluster and non-cluster roots were immersed in 50 mM Na-acetate solution at 26°C for 5 min to equilibrate, then either 5 mM *p*NPP (phosphomonoesterase) or 5 mM bis-*p*NPP (phosphodiesterase) was added and the samples were incubated for another 30 min under the same conditions. The reactions were terminated by adding 0.11 M NaOH to an aliquot of the extraction solution. Samples were oven-dried to constant weight and weighed to determine DW. The concentration of *p*NP was determined colorimetrically by measuring the absorbance at 405 nm against working standards in the range 0–1000 $\mu\text{M } p\text{NP}$ and the acid phosphatase activities were expressed in $\mu\text{mol } p\text{NP g}^{-1}$ root DW h⁻¹.

Cluster and non-cluster root exudates were collected separately for the analysis of cation concentrations. Roots were excised and immersed in 20 ml 0.01 mM CaCl₂ in the dark at room temperature (*c.* 22°C) for 30 min to minimise leakage from the excision. Root samples were transferred to 20 ml fresh aerated 0.01 mM CaCl₂ and incubated in the dark at room temperature (*c.* 22°C) for 60 min. The exudate solution was then filtered through a sterile 0.22 µm syringe filter and the concentrations of cations (Ca²⁺, K⁺, Mg²⁺, Mn²⁺) were measured in the solution using ICP-OES (Ca and K; Avio 560 Max, PerkinElmer, Waltham, MA, USA) or ICP-mass spectrometry (Mg and Mn; NexION 1000, PerkinElmer, Waltham, MA, USA). The cation-exudation rates were expressed in µmol (Ca²⁺, K⁺ and Mg²⁺) or nmol (Mn²⁺) g⁻¹ root DW h⁻¹.

Statistical analyses

One-way ANOVAs were performed to test the significance of differences for all measured variables among all species at each site for leaf [Mn], among sites for soil variables (pH, soil [P] and [Mn]), or among species for both root types (*i.e.* cluster and non-cluster roots) for root physiological variables (carboxylates, phosphatase activity and cation-exudation rates), with the ‘*emmeans*’ package (Lenth, 2023). Tukey’s HSD post-hoc tests were run to determine significant pairwise differences. The homogeneity of variances was inspected using the Levene test and the normality of the residuals was inspected using the Shapiro test ($P > 0.05$). Data were log₁₀-transformed when either condition was not met. The linear regressions between leaf [Mn] and soil pH, soil [Mn] and cation-exudation rates were performed on averaged data per site, and linear regressions between leaf [Mn] and δ¹³C were performed on all individuals, but average data per site were presented for consistency. We characterised the leaf element-accumulation patterns in *Hakea* species and element concentrations in soils using principal component analyses (PCA). The PCA was performed with the ‘*FactoMineR*’ package on log₁₀-transformed data (Lê *et al.*, 2008). Ellipses were added to the output to represent the 95% confidence interval around the mean. Data were analysed using R software (R Core Team, 2023).

Results

Soil and leaf chemical properties

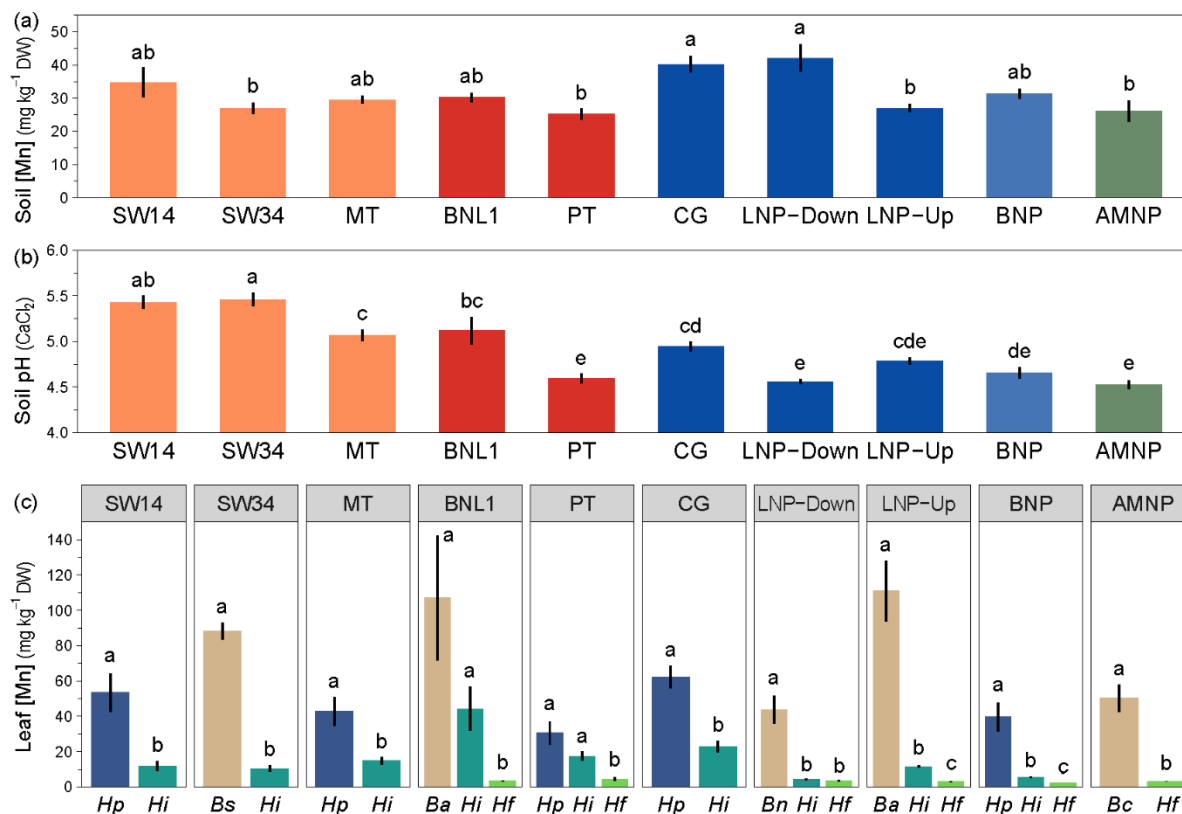


Fig. 2 (a) Soil manganese concentrations ([Mn]), (b) soil pH (CaCl₂), and (c) foliar [Mn] in leaves of *Hakea prostrata* (*Hp*), *H. incrassata* (*Hi*) and *H. flabellifolia* (*Hf*) in their natural habitats at 10 sites along the Jurien Bay chronosequence and surrounding area in south-western Australia. (a) and (b) Bar colours correspond to soil systems shown in Fig. 1; (c) Brown bars represent positive reference plants, known to release large amounts of carboxylates and accumulate leaf Mn (*Bs*, *Banksia sessilis*; *Ba*, *B. armata*; *Bn*, *B. nivea*; *Bc*, *B. candolleana*). Values are means \pm SE ($n = 5$). Different letters indicate significant differences among sites according to Tukey's HSD post-hoc test ($P < 0.05$). The site names and descriptions are given in Material and Methods.

Soil [Mn] varied across sites from 26 to 42 mg Mn kg⁻¹ soil DW for AMNP and LNP-Down, respectively (Fig. 2a). However, there were few significant ($P < 0.05$) differences among sites, with only LNP-Down and CG having higher soil [Mn] than some other sites. We observed a range of soil pH among sites along the Jurien Bay chronosequence and surrounding area, ranging from 5.5 (SW14 and SW34) to 4.5 (AMNP, BNP, and PT) (Fig. 2b).

We observed a wide range of foliar [Mn] among species and sites (Fig. 2c). *Hakea prostrata* had significantly higher [Mn] than *H. flabellifolia* at sites where both occurred (i.e. PT and BNP). *Hakea incrassata* had significantly higher foliar [Mn] than *H. flabellifolia* at all sites where they both occurred except for LNP-Down, and lower foliar [Mn] than *H. prostrata* at all sites where they both occurred except for PT. Importantly, where *H. incrassata* occurred with another of the target species, its foliar [Mn] was never higher than that of *H. prostrata* and never lower than that of *H. flabellifolia*. Foliar [Mn] of *H. prostrata* averaged at 45.8 mg Mn kg⁻¹ DW across all sites. *Hakea incrassata* had the most variable leaf [Mn] across sites, averaging 16.0 mg Mn kg⁻¹ DW, while that of *H. flabellifolia* was always relatively low, with an average of 3.3 mg Mn kg⁻¹ DW. Therefore, we refer hereafter to *H. prostrata* as ‘high Mn’, *H. incrassata* as ‘intermediate-Mn’ and *H. flabellifolia* as ‘low-Mn’, based on their leaf [Mn] values in their natural habitats.

Table 1 Soil phosphorus concentrations ([P]) at the 10 sites along the Jurien Bay chronosequence and surrounding area in south-western Australia where high-Mn *Hakea prostrata*, intermediate-Mn *H. incrassata* and low-Mn *H. flabellifolia* were sampled. Values are means \pm SE ($n = 4$ or 5). Phosphorus concentrations (total P, organic P, inorganic P and resin P) are expressed in mg P kg⁻¹ soil dry weight. Different letters indicate significant differences among sites following Tukey’s HSD post-hoc test ($P < 0.05$). Colours correspond to soil systems shown in Fig. 1 and the site names and descriptions are given in Material and Methods.

Site	Total P	Organic P	Inorganic P	Resin P
SW14	11.3 \pm 0.8 a	10.5 \pm 0.7 a	0.7 \pm 0.1 ab	0.4 \pm 0.0 bc
SW34	13.0 \pm 1.3 a	12.5 \pm 1.2 a	0.6 \pm 0.1 ab	0.4 \pm 0.1 bc
MT	6.5 \pm 0.7 b	6.1 \pm 0.6 bc	0.5 \pm 0.1 bc	0.5 \pm 0.1 ab
BNL1	7.0 \pm 0.6 b	6.7 \pm 0.5 b	0.3 \pm 0.0 cd	0.2 \pm 0.0 cde
PT	5.3 \pm 0.5 bc	5.1 \pm 0.5 bc	0.2 \pm 0.0 de	0.4 \pm 0.1 bcd
CG	12.3 \pm 1.0 a	11.4 \pm 1.0 a	0.9 \pm 0.0 a	0.7 \pm 0.1 a
LNP-Down	5.2 \pm 0.7 bc	5.0 \pm 0.7 bc	0.2 \pm 0.0 de	0.2 \pm 0.0 de
LNP-Up	7.0 \pm 0.3 b	6.7 \pm 0.3 b	0.3 \pm 0.0 cd	0.4 \pm 0.0 bcd
BNP	3.2 \pm 0.3 cd	3.1 \pm 0.3 cd	0.1 \pm 0.0 e	0.4 \pm 0.0 bcd
AMNP	1.8 \pm 0.2 d	1.7 \pm 0.2 d	0.1 \pm 0.0 f	0.1 \pm 0.0 e

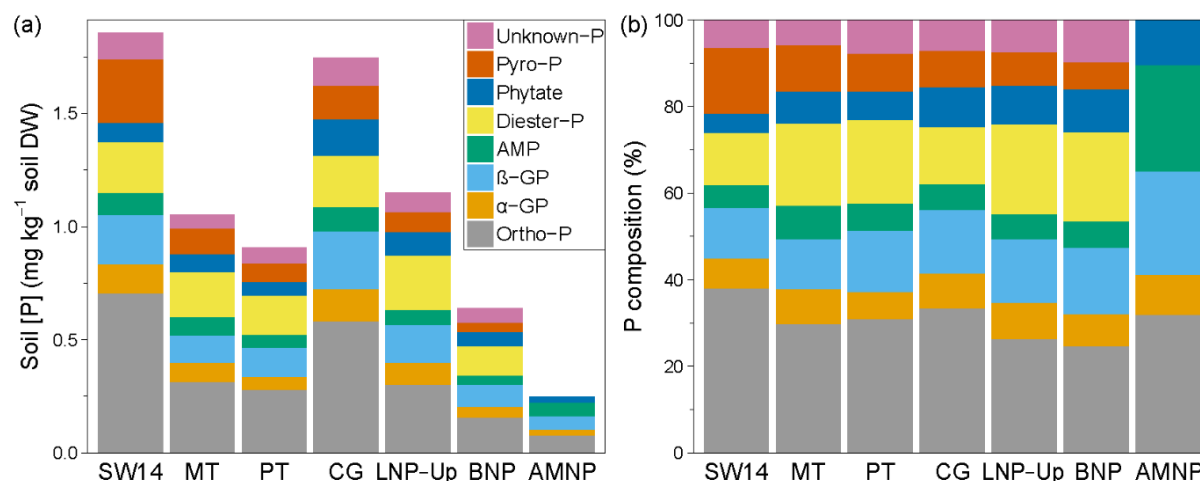


Fig. 3 Soil phosphorus concentrations ([P]) (a) and composition (b) in NaOH-EDTA extracts as detected by ^{31}P -NMR spectroscopy in bulk soil at seven sites along the Jurien Bay chronosequence and surrounding area in south-western Australia where high-manganese (Mn) *Hakea prostrata*, intermediate-Mn *H. incrassata* and low-Mn *H. flabellifolia* were sampled. Values are means ($n = 3$). Ortho-P, orthophosphate; α -GP, α -glycerophosphate; β -GP, β -glycerophosphate; AMP, adenosine 5'-monophosphate; pyro-P, pyrophosphate; unknown-P, unidentified significant peaks, likely phosphate monoesters. The site names and descriptions are given in Material and Methods.

Soil P concentrations (*i.e.* total, organic and inorganic [P]) decreased from the youngest to the oldest soils (generally moving west to east in Fig. 1), with the exception of CG (Table 1, Fig. 3a). This site, located in a gully formed by a stream flowing only in winter (Fig. 1), had a soil [P] similar to that of the youngest soils (Table 1, Fig. 3a). Interestingly, there was little variation in soil resin [P] (a measure of 'plant-available' P) compared with other forms of P (Table 1). Site CG had the highest resin [P], while AMNP had the lowest resin [P]. Although the recovery rate was lower using NaOH-EDTA extraction and ^{31}P -NMR spectroscopy quantification compared with that of HCl extraction and colorimetric quantification, both methods showed consistent results when comparing soils (Fig. S1). According to NaOH-EDTA extracts, orthophosphate was the main P compound in all soils, making up about 30% of total P in the NaOH-EDTA extracts (Table 1, Fig. 3). The differences in total [P] between soils were attributed to differences in all P compounds detected using ^{31}P -NMR spectroscopy (Fig. S2, S3). All sites had a similar P compounds composition, *i.e.* the proportion of each P compound relative to total P, except for soil at AMNP, where diesters, pyrophosphate and unidentified P compounds, likely phosphate monoesters, were not detected (Figs 3, S2, S3). This site also had a significantly higher proportion of AMP than the other sites (Fig. 3b).

Non-cluster and cluster roots physiology

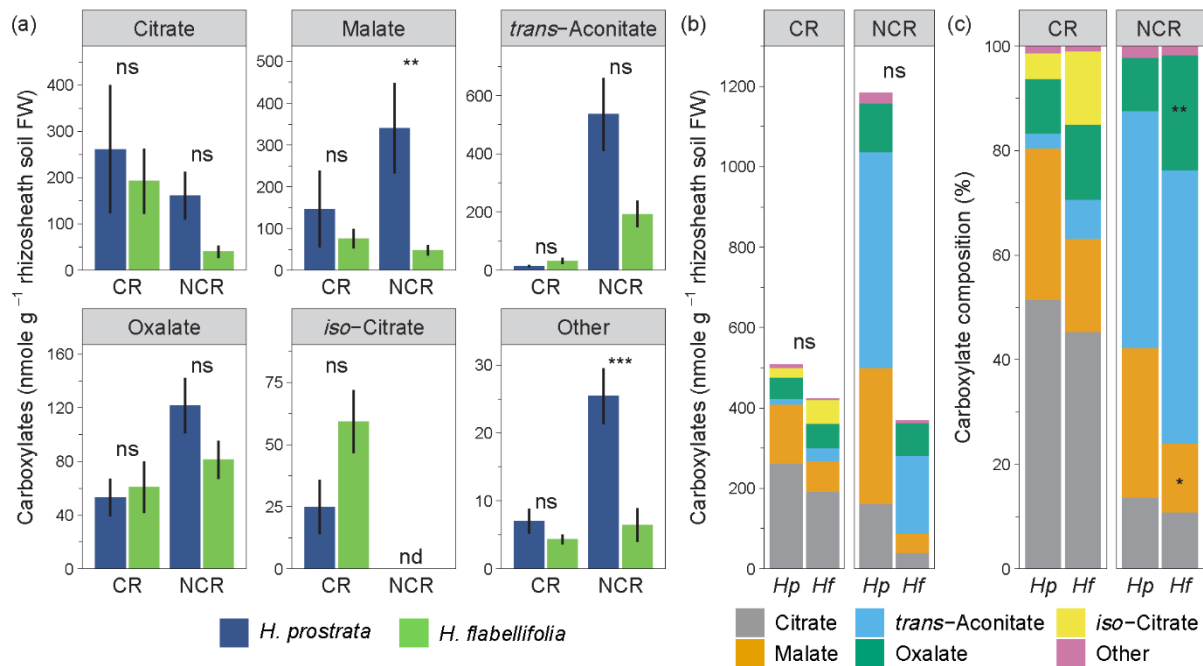


Fig. 4 Concentration (a and b) and composition profile (c) of carboxylates present in the rhizosphere soil of cluster roots (CR) and non-cluster roots (NCR) of high-manganese (Mn) *Hakea prostrata* (Hp) and low-Mn *H. flabellifolia* (Hf) grown in rhizoboxes. Significant differences between the two species were tested for each root type and carboxylate compounds using Tukey's HSD post-hoc test (*, $P < 0.05$; **, $P < 0.01$; ***, $P < 0.001$; ns, not significant, *i.e.* $P > 0.05$). 'Other' comprises fumarate, shikimate and *cis*-aconitate. nd, not detected.

There were three times more carboxylates in the rhizosphere soil of non-cluster roots of *H. prostrata* than in that of *H. flabellifolia* (Fig. 4a,b). However, this difference between the two species was not significant when considering the sum of carboxylates exuded (Fig. 4b) but reflected significant differences in the presence of individual carboxylates, *i.e.* malate and 'other' carboxylates including fumarate, shikimate and *cis*-aconitate (Fig. 4a). These other carboxylates were at concentrations that were only one-tenth of those of malate, so made up a minor component of the total carboxylates in the rhizosphere. There was no difference in the amounts of carboxylates exuded from cluster roots of the two species ($P > 0.05$; Fig. 4b). The profiles of carboxylates were also similar for both species, and for both cluster and non-cluster roots, with the most abundant carboxylates in the rhizosphere being citrate for cluster roots and *trans*-aconitate for non-cluster roots (Fig. 4c). Only the proportions of malate and oxalate were

significantly different in the rhizosphere soil of non-cluster roots of *H. prostrata* from those of *H. flabellifolia*. Malate was more abundant, and oxalate was less abundant for *H. prostrata* than for *H. flabellifolia* (Fig. 4c).

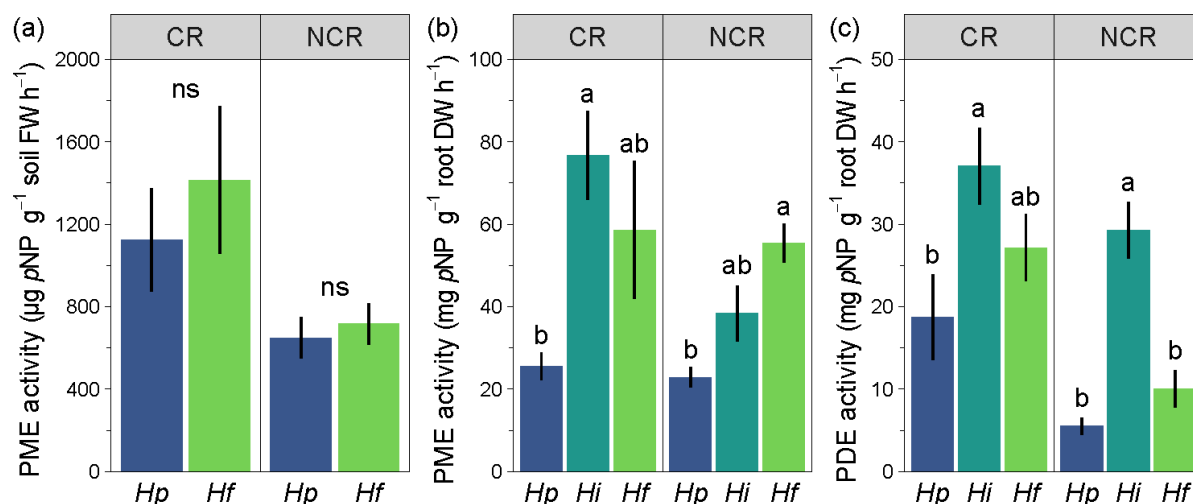


Fig. 5 Acid phosphomonoesterase (PME; a–b) and phosphodiesterase (PDE; c) activity in rhizosphere soil or in exudate-collecting solution of cluster roots (CR) and non-cluster roots (NCR) of high-manganese (Mn) *Hakea prostrata* (*Hp*), intermediate-Mn *H. incrassata* (*Hi*) and low-Mn *H. flabellifolia* (*Hf*) grown in rhizoboxes (a) and in hydroponics (b–c). Values are means \pm SE ($n = 4–11$). Different letters indicate significant differences among species for each root type according to Tukey's HSD post-hoc test ($P < 0.05$).

The acid phosphomonoesterase activity in the rhizosphere soil of both *H. prostrata* and *H. flabellifolia* grown in rhizoboxes was similar, both for cluster and non-cluster roots (Fig. 5a). However, there were significant differences in the external phosphomonoesterase and phosphodiesterase activities measured from cluster and non-cluster roots of the three *Hakea* species grown in hydroponics (Fig. 5b,c). Cluster and non-cluster roots of *H. prostrata* had a lower acid phosphomonoesterase activity in the exudate-collecting solution than the other two species. Phosphodiesterase activity was lower than that of phosphomonoesterase ($P < 0.05$), and roots of only *H. incrassata* had a higher activity than that of *H. prostrata* in both root types, and higher than that of *H. flabellifolia* in non-cluster roots (Fig. 5c).

Correlation between leaf [Mn], edaphic conditions and root physiology

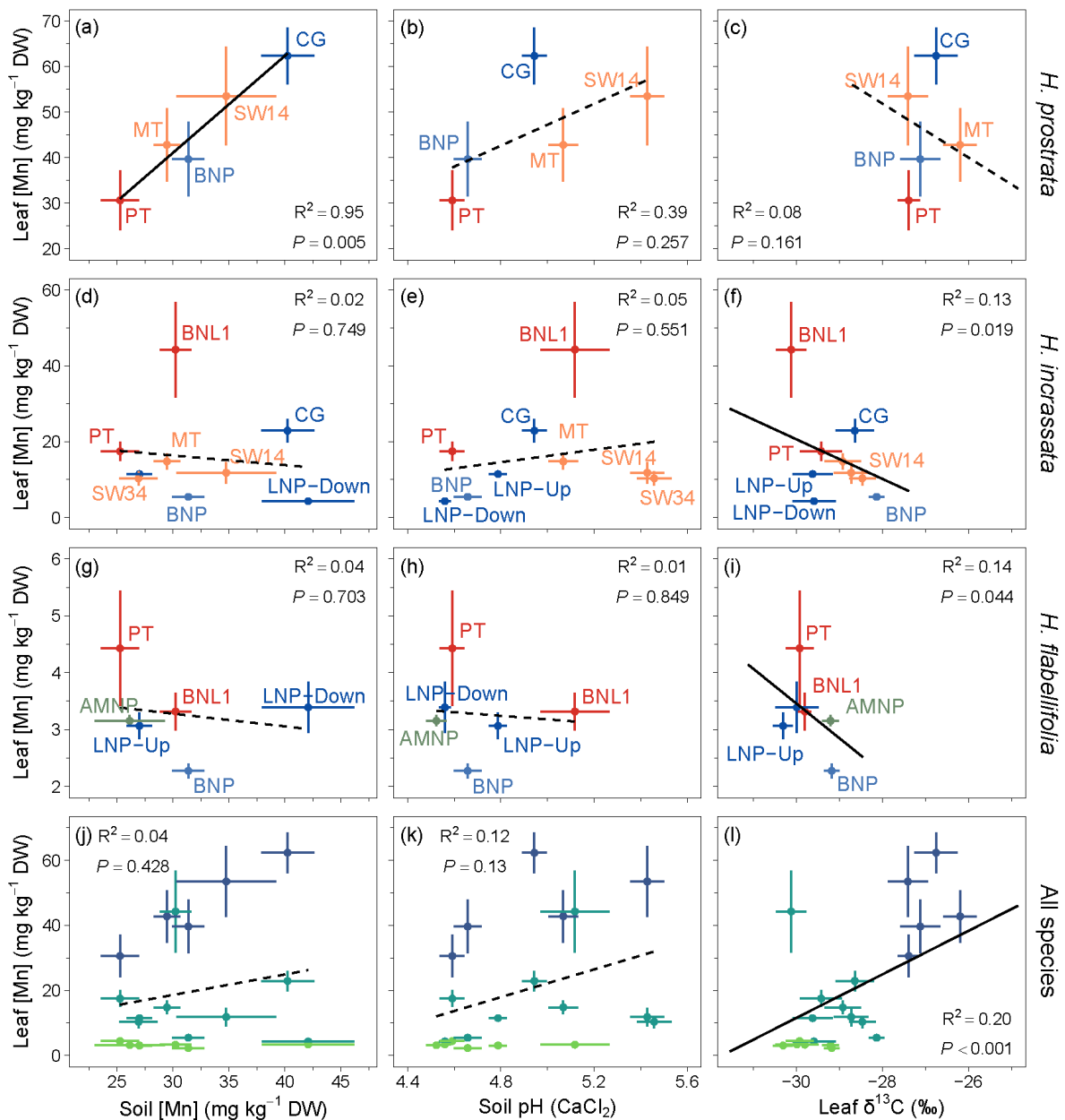


Fig. 6 Correlations between leaf manganese concentrations ([Mn]) and soil [Mn], soil pH and leaf stable carbon isotope composition ($\delta^{13}\text{C}$) for high-Mn *Hakea prostrata* (a–c), intermediate-Mn *H. incrassata* (d–f), low-Mn *H. flabellifolia* (g–i) and all species (j–l) in natural habitats at 10 sites along the Jurien Bay chronosequence and surrounding area in south-western Australia. Values are means \pm SE ($n = 5$). For pH and soil [Mn], linear regressions were analysed using averaged data per site, because the data for leaves were not paired with those for roots. For leaf $\delta^{13}\text{C}$, linear regressions were analysed using all individuals and averaged data are presented. Solid lines indicate significant correlations ($P < 0.05$), while broken lines indicate non-significant ($P > 0.05$) correlations. (a–i) Text colours correspond to soil systems shown in Fig. 1. The site names and descriptions are given in Material and Methods. (j–l) Blue, *H. prostrata*; dark green, *H. incrassata*; light green, *H. flabellifolia*.

Leaf [Mn] was significantly correlated with soil [Mn] only for *H. prostrata* (Fig. 6), despite *H. incrassata* and *H. flabellifolia* growing on sites with a similar range of soil [Mn] (Fig. 2a). Leaf [Mn] was not correlated with soil pH for any of the *Hakea* species, individually or when combined. *Hakea prostrata* had a significantly less negative $\delta^{13}\text{C}$ (-27‰) than *H. incrassata* and *H. flabellifolia* (-29.1 and -29.7‰, respectively; $P < 0.05$). Interestingly, correlations between leaf [Mn] and $\delta^{13}\text{C}$ were significant for *H. incrassata* and *H. flabellifolia*, but they only accounted for some of the variation, resulting in weak coefficients of determination ($R^2 = 0.13$ and 0.14 , respectively). The correlation between leaf [Mn] and $\delta^{13}\text{C}$ for all species was significant, but the coefficient of determination was weak ($R^2 = 0.20$), reflecting higher $\delta^{13}\text{C}$ for *H. prostrata* than for *H. incrassata* and *H. flabellifolia*.

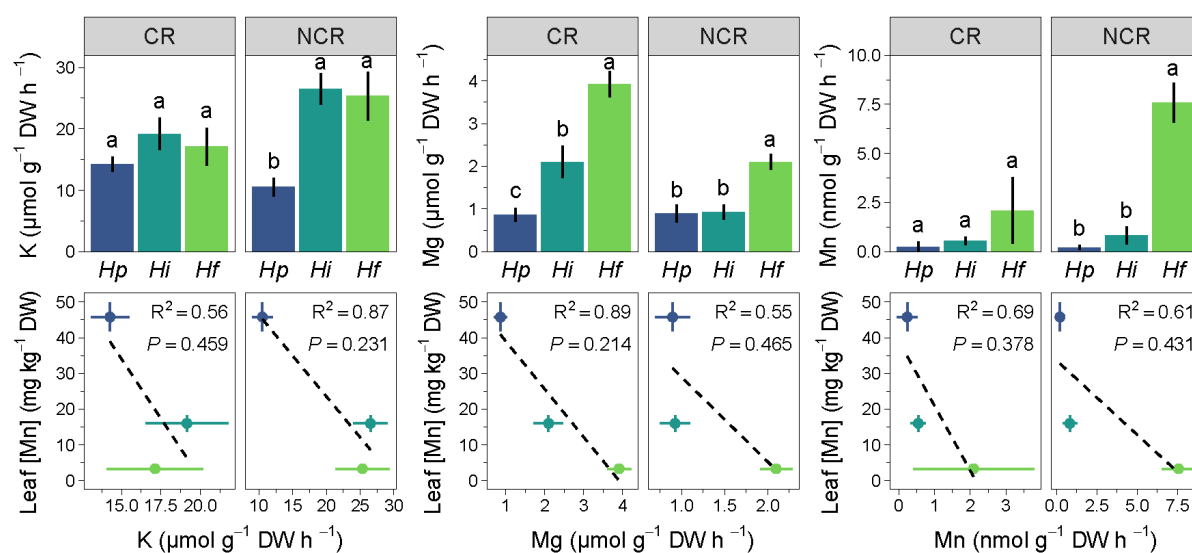


Fig. 7 Exudation rate of potassium (K), magnesium (Mg) and manganese (Mn) from cluster roots (CR) and non-cluster roots (NCR) of high-Mn *Hakea prostrata* (*Hp*), intermediate-Mn *H. incrassata* (*Hi*) and low-Mn *H. flabellifolia* (*Hf*) grown in hydroponics, and correlations between leaf Mn concentrations ([Mn]) in field-collected leaves and cation-exudation rates of hydroponically-grown plants. Values are means \pm SE ($n = 3-5$ for exudation rates; $n = 25-42$ for leaf [Mn]). Different letters indicate significant differences among species for each root type according to Tukey's HSD post-hoc test ($P < 0.05$). Correlations were calculated using averaged data because they were not paired.

All species released K, Mg, and Mn from cluster and non-cluster roots into the exudate-collection solution (Fig. 7). *Hakea incrassata* and *H. flabellifolia* released K at faster rates than *H. prostrata* did, but mainly from their non-cluster roots. Non-cluster roots of *H. flabellifolia* released Mg significantly faster than those of the other two *Hakea* species. Non-cluster roots of *H. flabellifolia* also released Mn significantly faster than those of the other two species.

The exudation rate of Mg was significantly faster from cluster roots of *H. incrassata* than from those of *H. prostrata*, but significantly slower than from those of *H. flabellifolia*. Similarly to non-cluster roots, there was a trend that cluster roots of *H. flabellifolia* released Mn faster than the cluster roots of the other two species; however, they were not statistically significant or different from each other. On average, the Mn-exudation rates were orders of magnitude slower than those of the other cations measured, *i.e.* nmol Mn vs. μmol K and Mg g^{-1} DW h^{-1} . All species took up Ca from the exudate-collecting solution, which only contained Ca^{2+} and Cl^{-} , with faster uptake rates for cluster roots than for non-cluster roots (data not shown).

The correlation between leaf [Mn] and exuded cations (K, Mg, and Mn) was not statistically significant ($P > 0.05$); it was performed on averaged data with a low sample size ($n = 3$) due to the independence of measurements. However, there were strong correlations between the three *Hakea* species for both cluster and non-cluster roots with coefficients of determination between 0.55 and 0.89, explaining a large part of the variance in leaf [Mn] among species (Fig. 7).

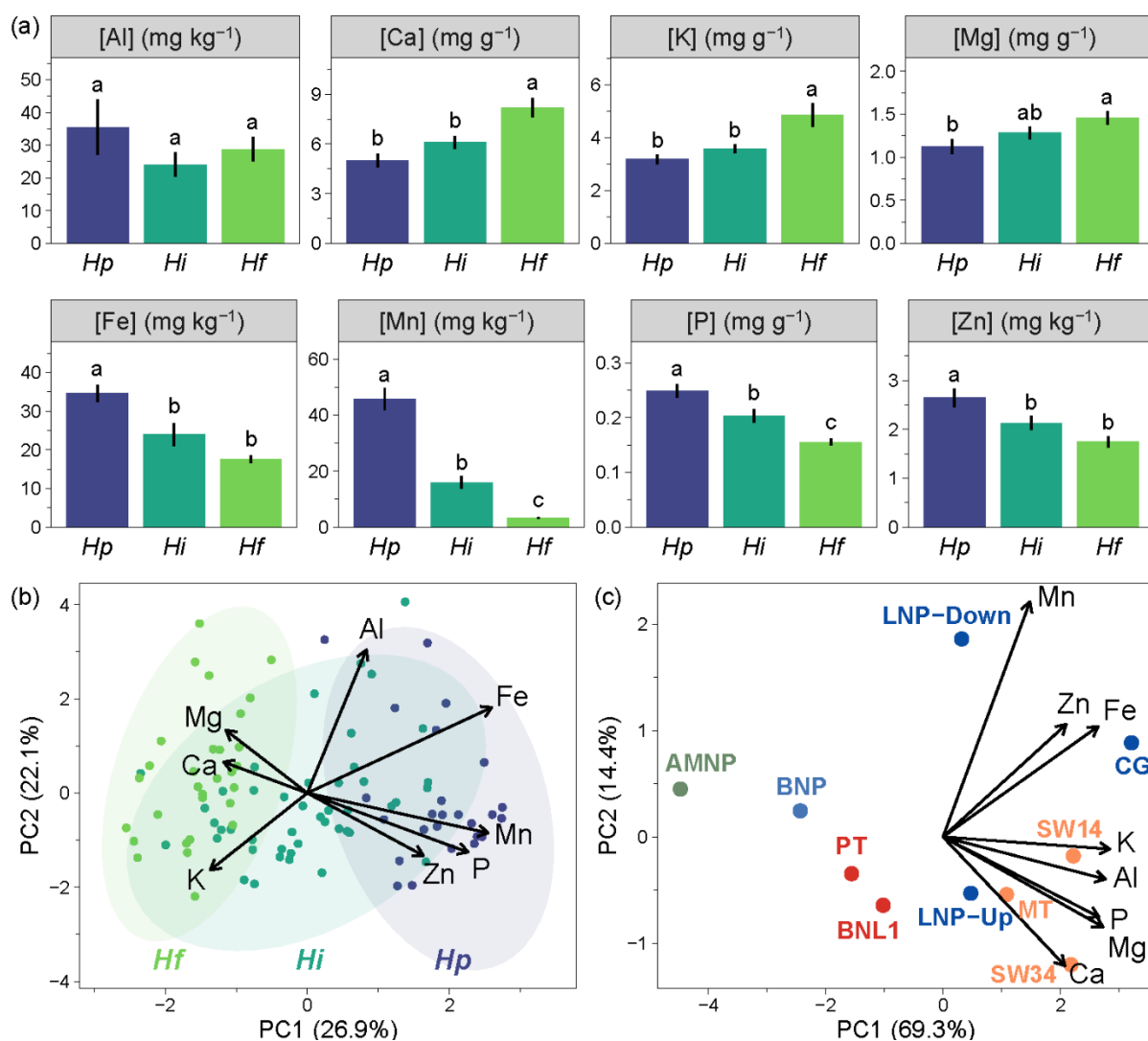


Fig. 8 Elemental concentrations (a), and principal component analysis (PCA) of elemental concentrations in leaves of high-manganese (Mn) *Hakea prostrata* (*Hp*), intermediate-Mn *H. incrassata* (*Hi*) and low-Mn *H. flabellifolia* (*Hf*) in natural habitats (b), and PCA of elemental concentrations in soil at 10 sites along the Jurien Bay chronosequence and surrounding area in south-western Australia where *Hakea* species were sampled (c). Values are means \pm SE (*Hp*, $n = 25$; *Hi*, $n = 45$; *Hf*, $n = 30$). (a) Different letters indicate significant differences among species according to Tukey's HSD post-hoc test ($P < 0.05$). (c) Text colours correspond to soil systems shown in Fig. 1. Outputs of the PCAs are given in Supporting Information Table S3. Al, aluminium; Ca, calcium; Fe, iron; K, potassium; Mg, magnesium; P, phosphorus; Zn, zinc. The site names and descriptions are given in Material and Methods.

There were significant differences in elemental concentrations in leaves of the three *Hakea* species (Fig. 8a). *Hakea prostrata* had lower leaf [Ca], [K], and [Mg] and higher leaf [Fe], [Mn], [P], and [Zn] than *H. flabellifolia*. *Hakea incrassata* generally had intermediate

concentrations of leaf elements. This trend was strongly reflected in the principal component analysis, where *H. prostrata* and *H. flabellifolia* were opposed, with *H. incrassata* spanning the entire range of distribution along PC1 (Fig. 8b). We also observed grouping among sites for elemental concentrations in soils (Fig. 8c). Soil [Al], [Fe], [K], [Mg] and [P] strongly contributed to the range observed among sites along PC1 explaining 69.3% of the variance (Fig. 8c, Table S3). Soil [Mn] contributed less to PC1 and more to PC2 than the other elements, highlighting its low level of variation among sites (Table S3).

Discussion

We explored edaphic (*i.e.* soil [P], [Mn], and pH) and physiological (*i.e.* release of carboxylates and cations from cluster and non-cluster roots and phosphatase activity) variables with respect to contrasting Mn concentrations in leaves of three *Hakea* species (Proteaceae). Our results did not fully support our first hypothesis that leaf [Mn] would be positively correlated with soil [Mn] and negatively correlated with soil pH. Instead, leaf [Mn] was neither correlated with soil [Mn] nor with soil pH. Only leaf [Mn] of *H. prostrata* was significantly correlated with soil [Mn]. However, a tight link between cations that were released with carboxylates from cluster and non-cluster roots of *Hakea* species and [Mn] in their leaves supports our second hypothesis, *i.e.* high-Mn *H. prostrata* exuded K^+ and Mg^{2+} at slower rates than the other *Hakea* species. Exudation of carboxylates is also involved in alleviating metal ion toxicity. Leaf elemental composition followed a clear pattern among species, with species exuding K^+ and Mg^{2+} at faster rates, *e.g.*, *H. flabellifolia*, having higher leaf concentrations of Ca, K and Mg, elements more available at higher soil pH, and conversely lower concentrations of Fe, Mn and Zn, which are more available at lower soil pH (Lambers & Oliveira, 2019). Plant species with lower leaf [Mn], *i.e.* *H. incrassata* and *H. flabellifolia*, also exhibited a higher rhizosphere phosphatase activity that would allow them to access more organic P than *H. prostrata* did. This more highly expressed P-acquisition strategy does not contribute to mobilising soil-bound Mn and helps to comprehend the reason for low leaf [Mn] in *H. incrassata* and *H. flabellifolia*. These results significantly advance our understanding of P-acquisition strategies within this genus.

Cations co-exuded with carboxylates explain leaf Mn accumulation

Our results confirmed the wide variation in mature leaf [Mn] among species of *Hakea*, with *H. prostrata* having consistently high leaf [Mn], compared with the relatively low leaf [Mn] of

H. flabellifolia (de Tombeur *et al.*, 2021a; Guilherme Pereira *et al.*, 2021; Hayes *et al.*, 2024). The more variable leaf [Mn] of *H. incrassata* positioned it intermediately. However, we show that high-Mn *H. prostrata* and low-Mn *H. flabellifolia* both released similar amounts of carboxylates from both their non-cluster and cluster roots. A recent study showed that carboxylate exudation rates from roots of intermediate-Mn *H. incrassata* were similar to that of high-Mn *H. prostrata* (Hayes *et al.*, 2024). This is in contradiction with the model that established leaf [Mn] as a proxy to assess belowground plant functioning, particularly the presence of carboxylates in the rhizosphere of the target species (Lambers *et al.*, 2015, 2021; Pang *et al.*, 2018; Yu *et al.*, 2023; Staudinger *et al.*, 2024). Carboxylate release is commonly associated with an acidification of the rhizosphere by the concomitant release of protons to provide the driving force for carboxylate release and balance the negative charges of the carboxylates exuded (Dinkelaker *et al.*, 1989; Neumann *et al.*, 2000; Roelofs *et al.*, 2001; George *et al.*, 2002; Zhu *et al.*, 2005). Manganese in the soil is available at pH below 7.5 with an optimum range from pH 5.0 to 6.5 (Lambers & Oliveira, 2019). The acidification of the rhizosphere towards a pH range that favours Mn bioavailability, combined with poorly-controlled Mn uptake (Baxter *et al.*, 2008), support the model of the link between leaf [Mn] and carboxylates in the rhizosphere (Lambers *et al.*, 2015, 2021). However, *H. incrassata* and *H. flabellifolia* deviated from this model and had relatively low leaf [Mn], especially *H. flabellifolia*, averaging at 3.3 mg Mn kg⁻¹ DW, while definitely releasing carboxylates into the rhizosphere. These results suggest that the accumulation of Mn in mature leaves depends not only on the exudation of carboxylates but also on concomitant proton release from the roots to the rhizosphere. Roots of both species with low leaf [Mn], *H. incrassata* and *H. flabellifolia*, released more K⁺ and Mg²⁺ in the exudate-collecting solution than *H. prostrata*, supporting this hypothesis. The release of alternative cations to H⁺, such as K⁺ or Mg²⁺, would not lead to a substantial acidification of the rhizosphere (Hinsinger *et al.*, 2003). Instead, roots are expected to take up H⁺ to drive the release of the cations via a proton cation antiport system (Hinsinger *et al.*, 2003; Hinsinger *et al.*, 2006). Therefore, this would not enhance soil Mn availability in soil and [Mn] in the leaves.

We are currently investigating cation fluxes from non-cluster roots and cluster roots of the present three *Hakea* species using a microelectrode ion flux estimation (MIFE©) system (Shabala *et al.*, 2013). This non-invasive technique allows for simultaneous measurement of several ions carrying charge from plant cells or tissues using ion-selective electrodes (see Supporting Information Method S1). Preliminary measurements show that cluster roots of

H. prostrata exhibited a greater efflux of K^+ than non-cluster roots, while both root types exhibited a similar influx of Ca^{2+} (Fig. S4). These preliminary results are in line with our measurements of K and Ca in the exudate-collecting solution using ICP-OES. We are currently developing a method to simultaneously measure H^+ , K^+ , and Na^+ fluxes as the three main cations transported across root cell membranes, according to elemental analysis from root exudates. This method will allow the measurement of ‘steady-state’ fluxes of these cations in cluster and non-cluster roots of the three *Hakea* species, *i.e.* the fluxes occurring in the absence of treatment. Further analysis involving a spike in P (as KH_2PO_4) in the solution is expected to reveal the physiological response of the roots to carboxylate exudation.

Hakea prostrata exuded K^+ and Mg^{2+} at a slower rate than *H. flabellifolia* did which must be balanced by releasing other cations to balance the release of negatively-charged carboxylates (Hinsinger, 2001; Hinsinger *et al.*, 2003). Protons are likely the other cation that high-Mn *H. prostrata* releases to drive and accompany carboxylate release (Roelofs *et al.*, 2001; Lambers *et al.*, 2006). Determining the ratio of H^+ to K^+ or other cations that are exuded will be crucial to understand the physiology of roots in relation to carboxylate exudation given the current model, which accounts for leaf Mn accumulation and carboxylate concentration in the rhizosphere. We hypothesise that low Mn-accumulating carboxylate-releasing species will have faster K^+ efflux than high Mn-accumulating species, while their H^+ efflux will be slower. The $H^+ : K^+$ ratio will reflect those differences. Faster rates of K^+ efflux compared with H^+ would not lead to a significant decrease of pH in the rhizosphere, but actually increase the pH (Hinsinger *et al.*, 2003; Hinsinger *et al.*, 2006), and hence not enhance but decrease rhizosphere Mn availability. We also hypothesise that the addition of P to the rhizosphere solution would significantly reduce the fluxes of both cations, inhibiting carboxylate exudation and confirming the coupling of the release of carboxylates and cations. However, the temporal dynamics of the response of exudation of carboxylates and cations to phosphate remains unknown.

A more highly-expressed phosphorus-acquisition strategy in *Hakea* species with low leaf Mn

Cluster and non-cluster roots of *H. incrassata* and *H. flabellifolia* had higher external phosphatase activity than those of *H. prostrata*. In addition to releasing K^+ and Mg^{2+} that contributed to less Mn accumulation in leaves, species with low leaf [Mn] exuded more phosphatases, giving them access to a pool of organic P compounds that other species such as *H. prostrata* only seem to access sparingly while relying more heavily on carboxylate release and rhizosphere acidification in P-limiting environment. The analysis of P compounds in soil

using ^{31}P -NMR spectroscopy revealed that soils at site LNP-Up, where *H. prostrata* does not occur, did not contain significantly different proportions of the various P compounds from those at the other sites. However, we did not detect phosphate diesters, pyrophosphate or unidentified phosphate monoesters in soils at site AMNP, where *H. flabellifolia* was found but not *H. prostrata*. The proportion of phosphate monoesters, *i.e.* AMP, was also higher at this site than at any other site and might be derived from the hydrolysis of P diesters (*e.g.*, RNA and DNA) that were not detected at site AMNP. *Hakea incrassata* and *H. flabellifolia* likely have greater access to these P forms through the release of greater levels of external phosphatases than *H. prostrata* did (Turner, 2008; Reitzel & Turner, 2014; Müller *et al.*, 2024). Pyrophosphate only occurs inside microorganisms and is not a P compound expected in large proportions in the soil solution (Bünemann *et al.*, 2008; Zhou *et al.*, 2019; Wimmer *et al.*, 2021). Phytate is also not a common compound in ancient and severely P-impooverished soils (Adams & Byrne, 1989; Zhong *et al.*, 2021). Accordingly, phytate concentrations were low compared with those of other P compounds, and only represented 5–10% of the soil total P. Moreover, we did not find detectable activity of external phytase exuded by either non-cluster or cluster roots of the three *Hakea* species (Supporting Information Method S2; Fig. S5). These results suggest a link between the ability of *Hakea* species to access organic P compounds via pyrophosphatase and acid phosphatase activity and their occurrence at sites where those P compounds are present in larger proportions.

Carboxylate-exudation physiology: a strategy beyond P acquisition

Soils in BNP and AMNP had a lower soil pH than those at other sites, increasing the availability of potentially toxic elements like Al and Mn at these sites (Dong *et al.*, 1999; Kochian *et al.*, 2015). Accordingly, the three *Hakea* species had higher leaf [Al] at these two sites. Interestingly, however, *H. flabellifolia* accumulated less Al than the other species. The release of H^+ , associated with acidification of the rhizosphere of *H. prostrata* and to a lesser extent *H. incrassata*, likely contributed to their greater accumulation of Al than that in *H. flabellifolia*. The importance of carboxylates in alleviating metal ion toxicity by chelation has been extensively studied (Ryan *et al.*, 1995, 2001; Kochian *et al.*, 2015). Aluminium stimulates the efflux of malate from apical cells of roots in Al-resistant wheat (*Triticum aestivum* L.), balanced by an equivalent efflux of K^+ (Ryan *et al.*, 1995). Aluminium is excluded from root tissues by the chelation of Al^{3+} by exuded carboxylates. In lead-tolerant varieties of rice (*Oryza sativa*), Yang *et al.* (2000) reported an increased exudation of oxalate that reduces Pb bioavailability. Copper induces a release of citrate associated with the efflux of K^+ from roots

of *Arabidopsis thaliana* seedlings (Murphy *et al.*, 1999). We surmise that the release of carboxylates by *Hakea* species not only contributes to the acquisition of P in extremely P-impooverished soils, but also provides benefits in avoiding toxicity by metal ions.

There were clear contrasting patterns in the foliar accumulation of elements between *H. prostrata* and *H. flabellifolia*. *Hakea prostrata* had higher leaf concentrations of the elements available at low pH (*i.e.* Zn, P, Mn and Fe) than *H. flabellifolia*. Conversely, *H. flabellifolia* accumulated higher concentrations of those more available at high pH (*i.e.* Ca, K and Mg). The release of carboxylates with specific cations, *i.e.* K⁺ rather than H⁺, might act as a dual-edge process to alleviate metal toxicity, first by reducing toxicity and uptake by chelation with carboxylates, and second by preventing the acidification of the rhizosphere, therefore limiting the availability of those metals (Hinsinger *et al.*, 2006). In line with leaf [Mn] and cation-exudation rates, *H. incrassata* was also intermediate in its element accumulation compared with the other two species. Collectively, these results suggest that specific carboxylate-exudation physiologies have evolved in *Hakea* species that allow them to acquire adequate nutrients. The variation in the strategies exhibited among species likely allows species to exist in overlapping niches.

Concluding remarks

Leaf Mn accumulation depends on various environmental and physiological factors. First, soil pH affects soil Mn availability and species can adjust their rhizosphere pH by releasing different cations, *i.e.* promote acidification by releasing H⁺ or increase the rhizosphere pH by releasing other cations, *e.g.*, K⁺ that would involve H⁺ uptake via an antiport mechanism. This ultimately influences the uptake of Mn, a process that is poorly regulated in plants which consequently leads to accumulation in mature leaves. Plants exhibit a variety of non-symbiotic P-acquisition strategies (*i.e.* carboxylate exudation and phosphatase release). A greater emphasis on an alternative strategy to carboxylate exudation can provide part of the P that is needed to meet the P requirement, reducing the importance of carboxylate exudation and, therefore, indirectly attenuate accumulation of leaf Mn. The adaptive response of roots for carboxylate exudation (*i.e.* release of cations other than protons) also provides benefits, such as avoiding the toxicity of elements like Al or Zn that are less available at higher soil pH by preventing rhizosphere acidification and are chelated by carboxylates, which renders them non-toxic.

Wen *et al.* (2021) proposed that in addition to Mn, Fe and Zn are also suitable to assess the concentration of carboxylates in the rhizosphere of chickpea (*Cicer arietinum* L.) accessions. However, neither Fe nor Zn accumulated in the leaves of *H. incrassata* or *H. flabellifolia* to the same levels as those in the leaves of *H. prostrata*. Silicon is also mobilised by carboxylate-exuding strategies (de Tombeur *et al.*, 2021a). Silicon uptake requires specific transporters and can only offer a proxy in species that possess those transporters. However, *H. incrassata* likely lacks those transporters or they are poorly expressed as it does not accumulate Si (de Tombeur *et al.*, 2021b), suggesting Si is also not a good proxy for carboxylate concentration in the rhizosphere. Rare earth elements are also mobilised in a pH-dependent manner, similar to Mn and (hyper)accumulation occurs when rhizosphere pH is below a critical value (van der Ent *et al.*, 2023; Wiche *et al.*, 2023; Wiche & Pourret, 2023). In accordance with the previous conceptual model, the accumulation of Mn as well as REE in mature leaves, in comparison with negative references, does point to species that rely on P-mining strategies (Lambers *et al.*, 2015, 2021). However, the reverse is not invariably true; that is, a low leaf [Mn] does not invariably mean that the targeted plants do not release carboxylates. We highlight the limitations of this conceptual model using carboxylate-releasing *Hakea* species and propose that leaf [Mn] is only tightly linked to the release of carboxylates when protons are the dominant counterions that balance the charge of the carboxylates.

Acknowledgements

CEG was supported by a University Postgraduate Award and Scholarship for International Research Fees from The University of Western Australia. Funding was provided by the Australian Research Council grants DP200101013 to HL and PMF and FT170100195 to KR. We are grateful to Rob Creasy and Bill Piasini for their help in the glasshouse. We thank Michael Smirk for assistance with elemental analyses and development of the ICP-MS method and Greg Cawthray for assistance with carboxylate analyses. We also thank Gareth Nealon for his help in developing the method for ³¹P-NMR spectroscopy and with analyses. Base layers in Fig. 1 were provided by the Western Australian Department of Primary Industries and Regional Development.

Author contributions

CEG, QG, PEH, KR, PMF and HL designed the study; CEG performed the experiment with various contributions from QG, ER, HY and LY; CEG analysed the data and wrote the manuscript, with feedback from PEH, KR, PMF and HL.

References

- Adams MA, Byrne LT. 1989.** ^{31}P -NMR analysis of phosphorus compounds in extracts of surface soils from selected karri (*Eucalyptus diversicolor* F. Muell.) forests. *Soil Biology and Biochemistry* **21**: 523-528.
- Baxter IR, Vitek O, Lahner B, Muthukumar B, Borghi M, Morrissey J, Guerinot ML, Salt DE. 2008.** The leaf ionome as a multivariable system to detect a plant's physiological status. *Proceedings of the National Academy of Sciences of the United States of America* **105**: 12081-12086.
- Bergmann J, Weigelt A, Van Der Plas F, Laughlin DC, Kuyper TW, Guerrero-Ramirez N, Valverde-Barrantes OJ, Bruelheide H, Fresche GT, Iversen CM, et al. 2020.** The fungal collaboration gradient dominates the root economics space in plants. *Science Advances* **6**: 1-9.
- Bünemann EK, Smernik RJ, Marschner P, McNeil AM. 2008.** Microbial synthesis of organic and condensed forms of phosphorus in acid and calcareous soils. *Soil Biology and Biochemistry* **40**: 932-946.
- Carmona CP, Bueno CG, Toussaint A, Träger S, Díaz S, Moora M, Munson AD, Pärtel M, Zobel M, Tamme R. 2021.** Fine-root traits in the global spectrum of plant form and function. *Nature* **597**: 683-687.
- Cawthray GR. 2003.** An improved reversed-phase liquid chromatographic method for the analysis of low-molecular mass organic acids in plant root exudates. *Journal of Chromatography A* **1011**: 233-240.
- de Tombeur F, Cornelis JT, Lambers H. 2021a.** Silicon mobilisation by root-released carboxylates. *Trends in Plant Science* **26**: 1116-1125.

- de Tombeur F, Laliberté E, Lambers H, Faucon MP, Zemunik G, Turner BL, Cornelis JT, Mahy G. 2021b.** A shift from phenol to silica-based leaf defences during long-term soil and ecosystem development. *Ecology Letters* **24**: 984-995.
- Dinkelaker B, Römheld V, Marschner H. 1989.** Citric acid excretion and precipitation of calcium citrate in the rhizosphere of white lupin (*Lupinus albus* L.). *Plant, Cell & Environment* **12**: 285-292.
- Dodd JC, Burton CC, Burns RG, Jeffries P. 1987.** Phosphatase activity associated with the roots and the rhizosphere of plants infected with vesicular-arbuscular mycorrhizal fungi. *New Phytologist* **107**: 163-172.
- Dong D, Xie Z, Du Y, Liu C, Wang S. 1999.** Influence of soil pH on aluminum availability in the soil and aluminum in tea leaves. *Communications in Soil Science and Plant Analysis* **30**: 873-883.
- Doolette AL, Smernik RJ. 2016.** Phosphorus speciation of dormant grapevine (*Vitis vinifera* L.) canes in the Barossa Valley, South Australia. *Australian Journal of Grape and Wine Research* **22**: 462-468.
- Doolette AL, Smernik RJ, Dougherty WJ. 2011.** A quantitative assessment of phosphorus forms in some Australian soils. *Soil Research* **49**: 152-165.
- Eivazi F, Tabatabai MA. 1977.** Phosphates in soils. *Soil Biology & Biochemistry* **9**: 167-172.
- Foulds W. 1993.** Nutrient concentrations of foliage and soil in south-western Australia. *New Phytologist* **125**: 529-546.
- George TS, Gregory PJ, Robinson JS, Buresh RJ. 2002.** Changes in phosphorus concentrations and pH in the rhizosphere of some agroforestry and crop species. *Plant and Soil* **246**: 65-73.
- Guilherme Pereira C, Hayes PE, Clode PL, Lambers H. 2021.** Phosphorus toxicity, not deficiency, explains the calcifuge habit of phosphorus-efficient Proteaceae. *Physiologia Plantarum* **172**: 1724-1739.
- Han M, Chen Y, Li R, Yu M, Fu L, Li S, Su J, Zhu B. 2022.** Root phosphatase activity aligns with the collaboration gradient of the root economics space. *New Phytologist* **234**: 837-849.
- Hayes P, Turner BL, Lambers H, Laliberté E. 2014.** Foliar nutrient concentrations and resorption efficiency in plants of contrasting nutrient-acquisition strategies along a 2-million-year dune chronosequence. *Journal of Ecology* **102**: 396-410.

- Hayes PE, Clode PL, Lambers H. 2024.** Calcifuge and soil-indifferent Proteaceae from south-western Australia: novel strategies in a calcareous habitat. *Plant and Soil* **496**: 95-122.
- Hayes PE, Nge FJ, Cramer MD, Finnegan PM, Fu P, Hopper SD, Oliveira RS, Turner BL, Zemunik G, Zhong H, et al. 2021.** Traits related to efficient acquisition and use of phosphorus promote diversification in Proteaceae in phosphorus-impooverished landscapes. *Plant and Soil* **462**: 67-88.
- Hinsinger P. 2001.** Bioavailability of soil inorganic P in the rhizosphere as affected by root-induced chemical changes: a review. *Plant and Soil* **237**: 173-195.
- Hinsinger P, Plassard C, Jaillard B. 2006.** Rhizosphere: a new frontier for soil biogeochemistry. *Journal of Geochemical Exploration* **88**: 210-213.
- Hinsinger P, Plassard C, Tang C, Jaillard B. 2003.** Origins of root-mediated pH changes in the rhizosphere and their responses to environmental constraints: a review. *Plant and Soil* **248**: 43-59.
- Kochian LV, Piñeros MA, Liu J, Magalhaes JV. 2015.** Plant adaptation to acid soils: the molecular basis for crop aluminum resistance. *Annual Review of Plant Biology* **66**: 571-598.
- Laliberté E, Turner BL, Costes T, Pearse SJ, Wyrwoll KH, Zemunik G, Lambers H. 2012.** Experimental assessment of nutrient limitation along a 2-million-year dune chronosequence in the south-western Australia biodiversity hotspot. *Journal of Ecology* **100**: 631-642.
- Lambers H, de Britto Costa P, Cawthray GR, Denton MD, Finnegan PM, Hayes PE, Oliveira RS, Power SC, Ranathunge K, Shen Q, et al. 2022.** Strategies to acquire and use phosphorus in phosphorus-impooverished and fire-prone environments. *Plant and Soil* **476**: 133-160.
- Lambers H, Hayes PE, Laliberté E, Oliveira RS, Turner BL. 2015.** Leaf manganese accumulation and phosphorus-acquisition efficiency. *Trends in Plant Science* **20**: 83-90.
- Lambers H, Oliveira RS. 2019.** *Plant Physiological Ecology*. Cham, Switzerland: Springer.
- Lambers H, Shane MW, Cramer MD, Pearse SJ, Veneklaas EJ. 2006.** Root structure and functioning for efficient acquisition of phosphorus: matching morphological and physiological traits. *Annals of Botany* **98**: 693-713.
- Lambers H, Wright IJ, Guilherme Pereira C, Bellingham PJ, Bentley LP, Boonman A, Cernusak LA, Foulds W, Gleason SM, Gray EF, et al. 2021.** Leaf manganese

- concentrations as a tool to assess belowground plant functioning in phosphorus-impooverished environments. *Plant and Soil* **461**: 43-61.
- Lê S, Josse J, Husson F. 2008.** FactoMineR: an R package for multivariate analysis. *Journal of Statistical Software* **25**: 1-18.
- Lenth R. 2023.** *emmeans: estimated marginal means, aka least-squares means*. R package v.1.8.6 [WWW document] URL <https://CRAN.R-Project.org/package=emmeans> [accessed 12 January 2024].
- Motomizu S, Wakimoto T, Tôei K. 1983.** Spectrophotometric determination of phosphate in river waters with molybdate and malachite green. *The Analyst* **108**: 361-367.
- Müller R, Elsenbeer H, Turner BL. 2024.** Evidence for soil phosphorus resource partitioning in a diverse tropical tree community. *Forests* **15**: 361-361.
- Murphy AS, Eisinger WR, Shaff JE, Kochian LV, Taiz L. 1999.** Early copper-induced leakage of K⁺ from *Arabidopsis* seedlings is mediated by ion channels and coupled to citrate efflux. *Plant Physiology* **121**: 1375-1382.
- Neumann G, Massonneau A, Langlade N, Dinkelaker B, Hengeler C, Römheld V, Martinoia E. 2000.** Physiological aspects of cluster root function and development in phosphorus-deficient white lupin (*Lupinus albus* L.). *Annals of Botany* **85**: 909-919.
- Neumann G, Römheld V. 1999.** Root excretion of carboxylic acids and protons in phosphorus-deficient plants. *Plant and Soil* **211**: 121-130.
- Pang J, Bansal R, Zhao H, Bohuon E, Lambers H, Ryan MH, Ranathunge K, Siddique KHM. 2018.** The carboxylate-releasing phosphorus-mobilizing strategy can be proxied by foliar manganese concentration in a large set of chickpea germplasm under low phosphorus supply. *New Phytologist* **219**: 518-529.
- Pang J, Ryan MH, Siddique KHM, Simpson RJ. 2017.** Unwrapping the rhizosheath. *Plant and Soil* **418**: 129-139.
- Pearse SJ, Veneklaas EJ, Cawthray G, Bolland MDA, Lambers H. 2006.** *Triticum aestivum* shows a greater biomass response to a supply of aluminium phosphate than *Lupinus albus*, despite releasing fewer carboxylates into the rhizosphere. *New Phytologist* **169**: 515-524.
- Pearse SJ, Veneklaas EJ, Cawthray G, Bolland MDA, Lambers H. 2007.** Carboxylate composition of root exudates does not relate consistently to a crop species' ability to use phosphorus from aluminium, iron or calcium phosphate sources. *New Phytologist* **173**: 181-190.
- R Core Team. 2023.** *R: a language and environment for statistical computing*. Vienna, Austria: R Foundation for Statistical Computing.

- Reitzel K, Turner BL. 2014.** Quantification of pyrophosphate in soil solution by pyrophosphatase hydrolysis. *Soil Biology and Biochemistry* **74**: 95-97.
- Roelofs RFR, Rengel Z, Cawthray GR, Dixon KW, Lambers H. 2001.** Exudation of carboxylates in Australian Proteaceae: chemical composition. *Plant, Cell & Environment* **24**: 891-904.
- Ryan PR, Delhaize E, Randall P. 1995.** Characterisation of Al-stimulated efflux of malate from the apices of Al-tolerant wheat roots. *Planta* **196**: 103-110.
- Ryan PR, Delhaize E, Jones DL. 2001.** Function and mechanism of organic anion exudation from plant roots. *Annual Review of Plant Physiology and Plant Molecular Biology* **52**: 527-560.
- Shabala S, Shabala L, Bose J, Cuin T, Newman I. 2013.** Ion flux measurements using the MIFE technique. *Methods in Molecular Biology* **953**: 171-183.
- Shane MW, Cramer MD, Funayama-Noguchi S, Cawthray GR, Millar AH, Day DA, Lambers H. 2004.** Developmental physiology of cluster-root carboxylate synthesis and exudation in harsh hakea. Expression of phosphoenolpyruvate carboxylase and the alternative oxidase. *Plant Physiology* **135**: 549-560.
- Shane MW, Lambers H. 2005.** Manganese accumulation in leaves of *Hakea prostrata* (Proteaceae) and the significance of cluster roots for micronutrient uptake as dependent on phosphorus supply. *Physiologia Plantarum* **124**: 441-450.
- Shen Q, Ranathunge K, Lambers H, Finnegan PM. 2024.** *Adenanthos* species (Proteaceae) in phosphorus-impooverished environments use a variety of phosphorus-acquisition strategies and achieve high-phosphorus-use efficiency. *Annals of Botany* **133**: 483-494.
- Skrzypek G. 2013.** Normalization procedures and reference material selection in stable HCNOS isotope analyses: an overview. *Analytical and Bioanalytical Chemistry* **405**: 2815-2823.
- Staudinger C, Renton M, Leopold M, Wasaki J, Veneklaas EJ, de Britto Costa P, Boitt G, Lambers H. 2024.** Interspecific facilitation of micronutrient uptake between cluster-root-bearing trees and non-cluster rooted-shrubs in a *Banksia* woodland. *Plant and Soil* **496**: 71-82.
- Ström L, Olsson T, Tyler G. 1994.** Differences between calcifuge and acidifuge plants in root exudation of low-molecular organic acids. *Plant and Soil* **167**: 239-245.
- Tabatabai MA, Bremner JM. 1969.** Use of *p*-nitrophenyl phosphate for assay of soil phosphatase activity. *Soil Biology and Biochemistry* **1**: 301-307.

- Turner BL. 2008.** Resource partitioning for soil phosphorus: a hypothesis. *Journal of Ecology* **96**: 698-702.
- Turner BL, Baxter R, Ellwood NTW, Whitton BA. 2001.** Characterization of the phosphatase activities of mosses in relation to their environment. *Plant, Cell & Environment* **24**: 1165-1176.
- Turner BL, Hayes PE, Laliberté E. 2018.** A climosequence of chronosequences in southwestern Australia. *European Journal of Soil Science* **69**: 69-85.
- Turner BL, Laliberté E. 2015.** Soil development and nutrient availability along a 2 million-year coastal dune chronosequence under species-rich Mediterranean shrubland in southwestern Australia. *Ecosystems* **18**: 287-309.
- Turner BL, Romero TE. 2009.** Short-term changes in extractable inorganic nutrients during storage of tropical rain forest soils. *Soil Science Society of America Journal* **73**: 1972-1979.
- Uloth MB, You MP, Cawthray G, Barbetti MJ. 2015.** Temperature adaptation in isolates of *Sclerotinia sclerotiorum* affects their ability to infect *Brassica carinata*. *Plant Pathology* **64**: 1140-1148.
- van der Ent A, Nkrumah PN, Purwadi I, Erskine PD. 2023.** Rare earth element (hyper)accumulation in some Proteaceae from Queensland, Australia. *Plant and Soil* **485**: 247-257.
- Wang B, Shen J, Tang C, Rengel Z. 2008.** Root morphology, proton release, and carboxylate exudation in lupin in response to phosphorus deficiency. *Journal of Plant Nutrition* **31**: 557-570.
- Wen Z, Pang J, Ryan MH, Shen J, Siddique KHM, Lambers H. 2021.** In addition to foliar manganese concentration, both iron and zinc provide proxies for rhizosheath carboxylates in chickpea under low phosphorus supply. *Plant and Soil* **465**: 31-46.
- Western Australian Department of Primary Industries and Regional Development. 2024.** NRInfo, [WWW document] URL <https://www.agric.wa.gov.au/resource-assessment/nrinfo-natural-resource-information-western-australia> [accessed 12 January 2024].
- Wiche O, Dittrich C, Pourret O, Monei N, Heim J, Lambers H. 2023.** Relationships between carboxylate-based nutrient-acquisition strategies, phosphorus-nutritional status and rare earth element accumulation in plants. *Plant and Soil* **489**: 645-666.
- Wiche O, Pourret O. 2023.** The role of root carboxylate release on rare earth element (hyper)accumulation in plants – a biogeochemical perspective on rhizosphere chemistry. *Plant and Soil* **492**: 79-90.

- Wimmer JLE, Kleinermanns K, Martin WF. 2021.** Pyrophosphate and irreversibility in evolution, or why PP_i is not an energy currency and why nature chose triphosphates. *Frontiers in Microbiology* **12**: 759359.
- Yang Y-Y, Jung J-Y, Song W-Y, Suh H-S, Lee Y. 2000.** Identification of rice varieties with high tolerance or sensitivity to lead and characterization of the mechanism of tolerance. *Plant Physiology* **124**: 1019-1026.
- Yu R-P, Su Y, Lambers H, van Ruijven J, An R, Yang H, Yin X-T, Xing Y, Zhang W-P, Li L. 2023.** A novel proxy to examine interspecific phosphorus facilitation between plant species. *New Phytologist* **239**: 1637-1650.
- Zarcinas BA, Cartwright B, Spouncer LR. 1987.** Nitric acid digestion and multi-element analysis of plant material by inductively coupled plasma spectrometry. *Communications in Soil Science and Plant Analysis* **18**: 131-146.
- Zhong H, Zhou J, Azmi A, Arruda AJ, Doolette AL, Smernik RJ, Lambers H. 2021.** *Xylomelum occidentale* (Proteaceae) accesses relatively mobile soil organic phosphorus without releasing carboxylates. *Journal of Ecology* **109**: 246-259.
- Zhou J, Wu Y, Turner BL, Sun H, Wang J, Bing H, Luo J, He X, Zhu H, He Q. 2019.** Transformation of soil organic phosphorus along the Hailuogou post-glacial chronosequence, southeastern edge of the Tibetan Plateau. *Geoderma* **352**: 414-421.
- Zhu Y, Yan F, Zörb C, Schubert S. 2005.** A link between citrate and proton release by proteoid roots of white lupin (*Lupinus albus* L.) grown under phosphorus-deficient conditions? *Plant and Cell Physiology* **46**: 892-901.

Supporting Information

Method S1 Potassium and calcium ion flux measurements using the non-invasive microelectrode MIFE technique.

Method S2 Phytase activity measurements in exudates of cluster and non-cluster roots of *Hakea* species.

Fig. S1 Comparison of phosphorus quantification by HCl extraction–colorimetry and NaOH extraction– ^{31}P -NMR in bulk soil at seven sites along the Jurien Bay chronosequence and surrounding area in south-western Australia.

Fig. S2 Soil phosphorus concentrations in NaOH-EDTA extracts as detected by ^{31}P -NMR spectroscopy in bulk soil at seven sites along the Jurien Bay chronosequence and surrounding area in south-western Australia.

Fig. S3 ^{31}P -NMR spectroscopy spectra of NaOH-EDTA extracts of bulk soils at three sites along the Jurien Bay chronosequence and surrounding area in south-western Australia.

Fig. S4 Microelectrode ion flux estimation of potassium and calcium in cluster and non-cluster roots of high-manganese *Hakea prostrata*.

Fig. S5 Phytase activity in exudates of cluster and non-cluster roots of high-manganese (Mn) *Hakea prostrata*, intermediate-Mn *H. incrassata* and low-Mn *H. flabellifolia*.

Table S1 Standards provided by the International Atomic Energy Agency used for normalisation of stable carbon isotope compositions.

Table S2 Comparison of the relative ^{31}P -NMR spectroscopic peak intensities as a function of the duration of the relaxation delay.

Table S3 Output of the PCA of element concentrations in leaves of high-manganese (Mn) *Hakea prostrata*, intermediate-Mn *H. incrassata* and low-Mn *H. flabellifolia* and in soil at 10 sites along the Jurien Bay chronosequence and surrounding area in south-western Australia.

Method S1 Potassium and calcium ion flux measurements using the non-invasive microelectrode MIFE technique.

Potassium (K^+) and calcium (Ca^{2+}) fluxes were measured from cluster and non-cluster roots of *Hakea prostrata* grown in hydroponics using the non-invasive Microelectrode Ion Flux Estimate (MIFE) technique (Shabala *et al.*, 2013). In brief, borosilicate glass microelectrodes were pulled using a PP-830 puller (Narishige, Tokyo, Japan), dried in an oven at 225°C overnight, and silanised with tributylchlorosilane. The electrodes were back-filled with backfilling solutions (200 mM KCl for K^+ , 500 mM $CaCl_2$ for Ca^{2+}) and front-filled with ionophore cocktails (99311 for K^+ , 99310 for Ca^{2+} , Sigma-Aldrich, St. Louis, USA). Electrodes were then calibrated in a set of standard solutions for each ion. Only electrodes with correlation coefficients > 0.999 were used. For measurements, the electrodes were mounted on a micromanipulator and positioned *c.* 50 μm away from the surface of a rootlet of cluster roots or non-cluster roots. A computer-controlled stepper motor was used to move the electrodes in a 12-s square-wave cycle between two positions (50 μm and 175 μm) away from the root surface. The potential difference between the two positions was recorded using the CHART software and net ion fluxes were calculated using the MIFEFLUX software (Newman, 2001). Ion flux measurements were performed in 10 μM $CaCl_2$ and 70 μM KCl solution, the same as the Ca and K concentrations in the hydroponic solution used to grow the plants.

Method S2 Phytase activity measurements in exudates of cluster and non-cluster roots of *Hakea* species.

Cluster and non-cluster root exudates were collected for the analysis of phytase activity, according to Hayes *et al.* (1999) and Richardson *et al.* (2000) with minor modifications. In brief, roots from the same plants used for cation-exudation rates were excised and immersed in a buffer solution (15 mM MES, 1 mM EDTA, 0.5 mM CaCl₂, pH 5.5) with 2 mM inositolhexakisphosphate (IHP) as substrate and incubated in the dark at 37°C for 1 h. The reaction was terminated by the addition of 10% (w/v) trichloroacetic acid. A set of control assays were used to determine the basal phytase activity, in which 10% (w/v) trichloroacetic acid was added before incubation and the IHP substrate after incubation. The amount of inorganic phosphate (Pi) released from the IHP substrate was determined colorimetrically (Motomizu *et al.*, 1983). The phytase activity in the exudate was expressed as $\mu\text{g Pi liberated g}^{-1} \text{ root DW h}^{-1}$ after subtracting the reading of the 'control'.

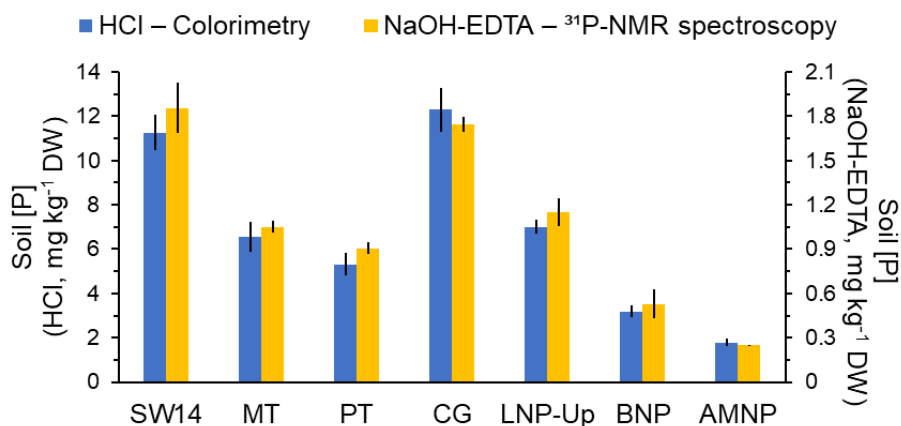


Fig. S1 Phosphorus (P) concentration in HCl (blue) and NaOH-EDTA (yellow) extracts as detected by colorimetry and ³¹P-NMR spectroscopy, respectively, of bulk soil at seven sites along the Jurien Bay chronosequence and surrounding area in south-western Australia where high-manganese (Mn) *Hakea prostrata*, intermediate-Mn *H. incrassata* and low-Mn *H. flabellifolia* were sampled. Values are means \pm SE ($n = 5$ for HCl extracts, $n = 3$ for NaOH-EDTA extracts).

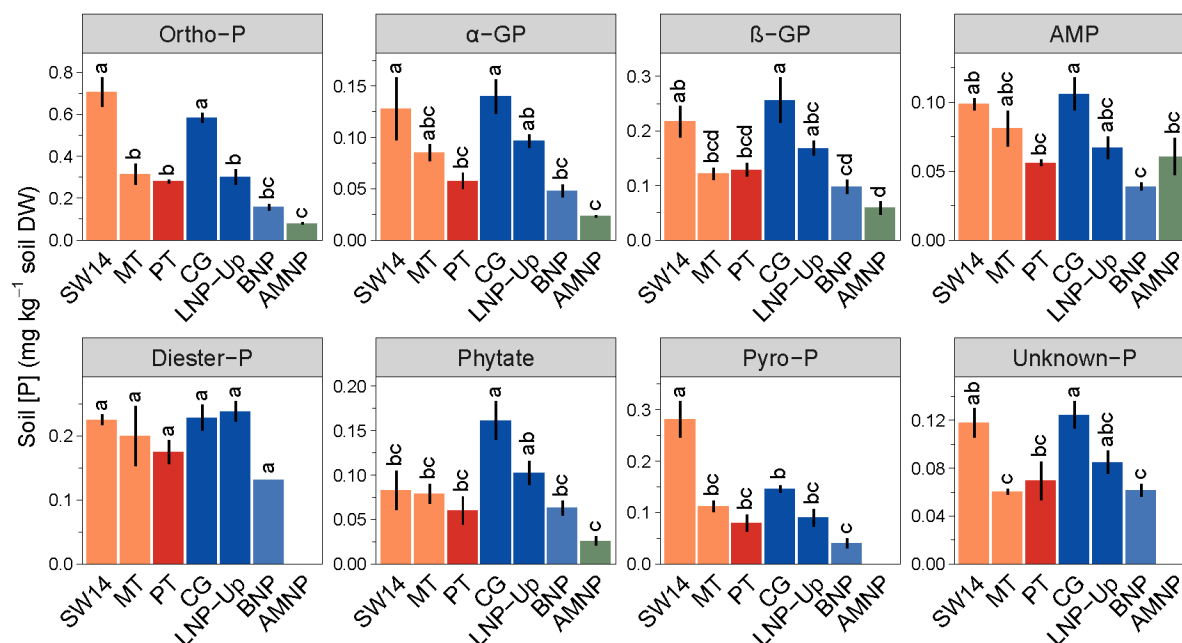
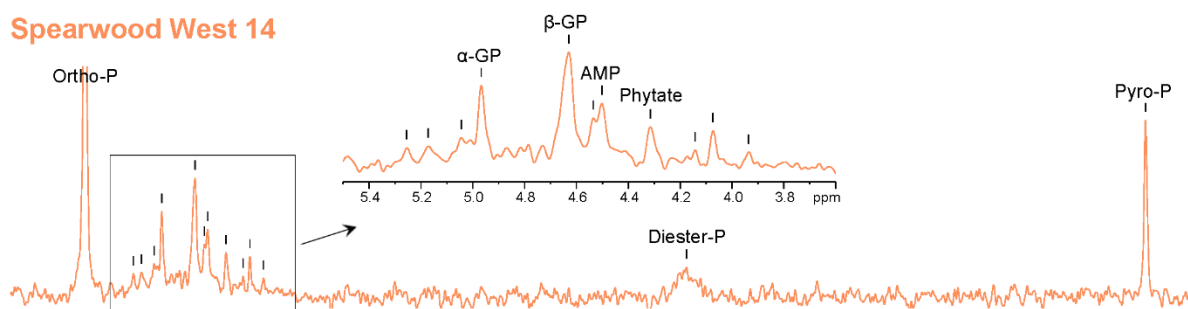
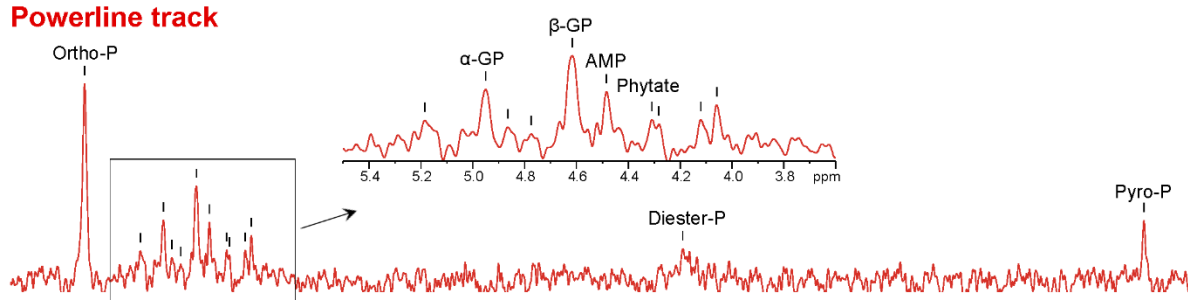


Fig. S2 Soil phosphorus concentrations ([P]) in NaOH-EDTA extracts as detected by ³¹P-NMR spectroscopy in bulk soil at seven sites along the Jurien Bay chronosequence and surrounding area in south-western Australia where high-manganese (Mn) *Hakea prostrata*, intermediate-Mn *H. incrassata* and low-Mn *H. flabellifolia* were sampled. Values are means \pm SE ($n = 3$) expressed on a soil dry weight (DW) basis. Different letters indicate significant differences among sites following Tukey's HSD post-hoc test ($P < 0.05$). Ortho-P, orthophosphate; α -GP, α -glycerophosphate; β -GP, β -glycerophosphate; AMP, adenosine 5'-monophosphate; pyro-P, pyrophosphate; unknown-P, unidentified significant peaks, likely phosphate monoesters. Bar colours correspond to soil systems shown in Fig. 1 and the site names and descriptions are given in Material and Methods.

Spearwood West 14



Powerline track



Alexander Morrison NP

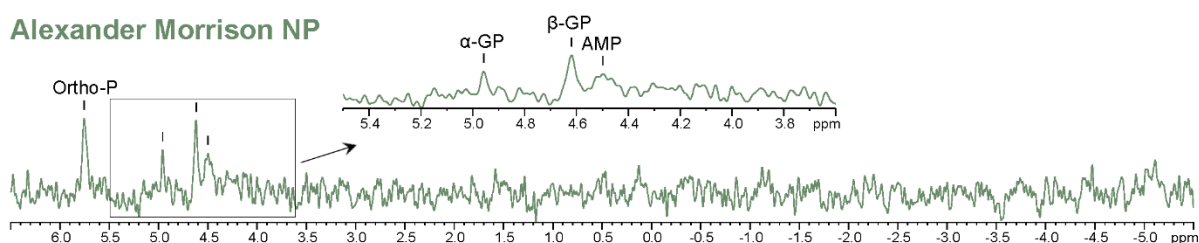


Fig. S3 ^{31}P -NMR spectroscopy spectra of NaOH-EDTA extracts of bulk soils at three sites along the Jurien Bay chronosequence and surrounding area in south-western Australia where high-manganese (Mn) *Hakea prostrata*, intermediate-Mn *H. incrassata* and low-Mn *H. flabellifolia* were sampled. Ortho-P, orthophosphate; α -GP, α -glycerophosphate; β -GP, β -glycerophosphate; AMP, adenosine 5'-monophosphate; pyro-P, pyrophosphate. Unidentified peaks in the 3.5–5.5 ppm chemical shift region likely represent phosphate monoesters.

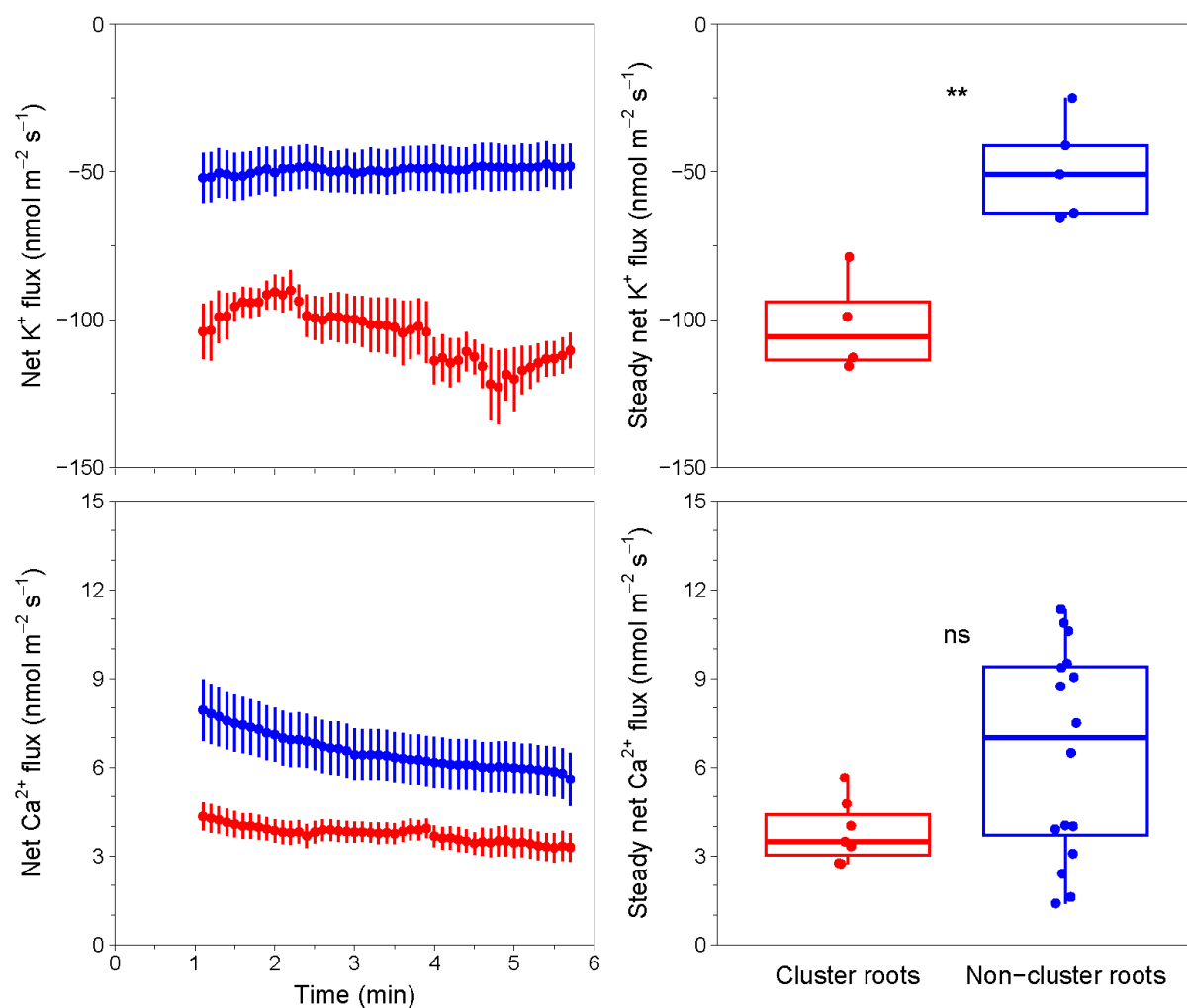


Fig. S4 Microelectrode ion flux estimation of potassium (K⁺) and calcium (Ca²⁺) in cluster roots and non-cluster roots of high-manganese *Hakea prostrata* grown in hydroponics. Values are means \pm SE (for K⁺, $n = 4$ for cluster roots and $n = 6$ for non-cluster roots, and for Ca²⁺, $n = 7$ for cluster roots and $n = 16$ for non-cluster roots). Significant differences between cluster and non-cluster roots were tested using Tukey's HSD post-hoc test (**, $P < 0.01$; ns, not significant, *i.e.* $P > 0.05$). Negative fluxes mean efflux from roots. Preliminary results courtesy of Dr. Ping Yun (UWA).

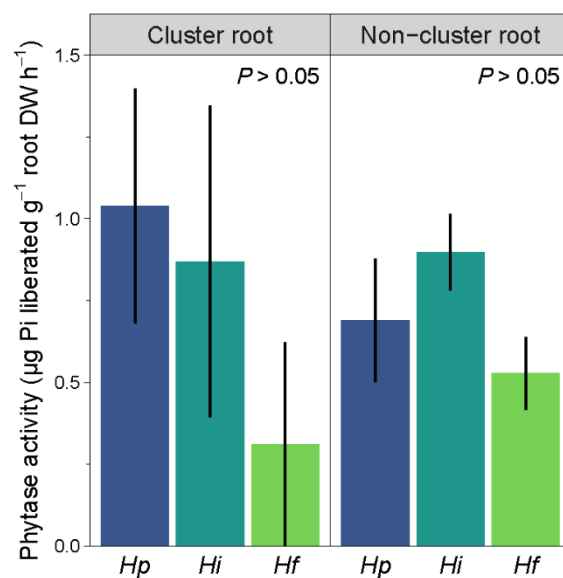


Fig. S5 Phytase activity in the exudate-collecting solution of cluster roots and non-cluster roots of high-manganese (Mn) *Hakea prostrata* (Hp), intermediate-Mn *H. incrassata* (Hi) and low-Mn *H. flabellifolia* (Hf) grown in hydroponics. Values are means \pm SE ($n = 3-8$). Differences among species for each root type were tested with Tukey's HSD post-hoc test (not significant, $P > 0.05$). Pi, inorganic phosphate.

Table S1 Standards provided by the International Atomic Energy Agency used for normalisation of stable carbon isotope compositions ($\delta^{13}\text{C}$). VPDB, Vienna PeeDee Belemnite.

Standard	$\delta^{13}\text{C}$ (‰, VPDB)
NBS22	-30.03
IAEA603	2.46
USGS24	-16.05
USGS40	-26.39

Table S2 Comparison of the relative ^{31}P -NMR spectroscopic peak intensities of a selection of phosphorus (P) compounds in NaOH-EDTA soil extracts as a function of the duration of the relaxation delay. Data shown are the relative spectral integration against the MDP standard, and the ratios of significant signal peaks. β -GP, β -glycerophosphate; ortho-P, orthophosphate; pyro-P, pyrophosphate.

	1 s	2 s	3 s	3.8 s	5 s	10 s	20 s	30 s
MDP	100	100	100	100	100	100	100	100
Ortho-P	5.5	8.5	8.1	10.3	9.8	10.1	10.1	10.8
β -GP	1.8	3.0	2.8	2.9	3.3	4.0	3.3	3.1
Pyro-P	1.5	1.8	2.4	2.8	2.7	2.9	3.1	2.9
Pyro-P : Ortho-P	0.27	0.21	0.30	0.28	0.28	0.29	0.31	0.26
Pyro-P : β -GP	0.83	0.60	0.86	0.98	0.82	0.72	0.94	0.91
β -GP : Ortho-P	0.33	0.35	0.35	0.28	0.34	0.40	0.33	0.29

Table S3 Output of the principal component analysis (PCA) of element concentrations in leaves of high-manganese (Mn) *Hakea prostrata*, intermediate-Mn *H. incrassata* and low-Mn *H. flabellifolia* (Fig. 8b) and in soil (Fig. 8c) at 10 sites along the Jurien Bay chronosequence and surrounding area in south-western Australia. Data shown are the eigenvalue, the percentage and cumulative percentage of variance explained by each subsequent principal component (PC), and the loading of each trait to each PC. The PCs explaining $\geq 10\%$ of the variance are shown. Al, aluminium; Ca, calcium; Fe, iron; K, potassium; Mg, magnesium; P, phosphorus; Zn, zinc.

	PCA leaf (Fig. 8b)				PCA soil (Fig. 8c)			
	PC1	PC2	PC3	PC4	PC1	PC2	PC3	PC4
Eigenvalue	2.2	1.8	1.3	1.0	5.5	1.2	0.7	0.4
Variance (%)	26.9	22.1	16.2	12.2	69.3	14.4	8.2	4.6
Cum. var. (%)	26.9	48.9	65.1	77.3	69.3	83.6	91.8	96.4
Al	0.24	0.87	0.07	0.30	0.94	-0.13	-0.22	-0.10
Ca	-0.34	0.19	0.79	0.17	0.70	-0.41	0.46	0.32
Fe	0.74	0.52	0.00	0.31	0.90	0.35	0.05	-0.19
K	-0.39	-0.47	0.21	0.63	0.96	-0.04	-0.11	-0.18
Mg	-0.33	0.38	0.55	-0.49	0.93	-0.29	0.05	-0.15
Mn	0.73	-0.24	0.15	-0.33	0.50	0.75	0.42	0.01
P	0.65	-0.36	0.29	0.14	0.90	-0.26	0.00	0.07
Zn	0.47	-0.38	0.46	-0.01	0.71	0.36	-0.45	0.40

Supporting Information References

- Hayes JE, Richardson AE, Simpson RJ. 1999.** Phytase and acid phosphatase activities in extracts from roots of temperate pasture grass and legume seedlings. *Australian Journal of Plant Physiology* **26**: 801-809.
- Motomizu S, Wakimoto T, Tōei K. 1983.** Spectrophotometric determination of phosphate in river waters with molybdate and malachite green. *The Analyst* **108**: 361-367.
- Newman IA. 2001.** Ion transport in roots: measurement of fluxes using ion-selective microelectrodes to characterize transporter function. *Plant, Cell & Environment* **24**: 1–14.
- Richardson AE, Hadobas PA, Hayes JE. 2000.** Acid phosphomonoesterase and phytase activities of wheat (*Triticum aestivum* L.) roots and utilization of organic phosphorus substrates by seedlings grown in sterile culture. *Plant, Cell & Environment* **23**: 397-405.
- Shabala S, Shabala L, Bose J, Cuin T, Newman I. 2013.** Ion flux measurements using the MIFE technique. *Methods in Molecular Biology* **953**: 171–183.

CHAPTER THREE

Facilitative and competitive interactions between mycorrhizal and non-mycorrhizal plants in an extremely phosphorus-impooverished environment: role of ectomycorrhizal fungi and native oomycete pathogens in shaping species coexistence



Eucalyptus todtiana (Myrtaceae)

This chapter was published in *New Phytologist* (Vol. 242, issue 4, pp. 1630–1644) in the special issue “*Mycorrhizal research now: from the micro- to the macro-scale*”.

The main text is presented, followed by the Supporting Information.

Facilitative and competitive interactions between mycorrhizal and non-mycorrhizal plants in an extremely phosphorus-impooverished environment: role of ectomycorrhizal fungi and native oomycete pathogens in shaping species coexistence

Clément E. Gille¹, Patrick M. Finnegan¹, Patrick E. Hayes¹, Kosala Ranathunge¹, Treena I. Burgess², Félix de Tombeur^{1,3}, Duccio Migliorini^{1,4}, Paul Dallongeville¹, Gaétan Glauser⁵ and Hans Lambers¹

¹School of Biological Sciences, The University of Western Australia, 35 Stirling Highway, Perth, WA, 6009, Australia; ²Phytophthora Science and Management, Harry Butler Institute, Murdoch University, Murdoch, WA, 6150, Australia; ³CEFE, CNRS, EPHE, IRD, University of Montpellier, 34000, Montpellier, France; ⁴National Research Council, Institute for Sustainable Plant Protection, Sesto Fiorentino, Florence, 50019, Italy; ⁵Neuchâtel Platform of Analytical Chemistry, University of Neuchâtel, Neuchâtel, 2000, Switzerland

Author for correspondence: *Clément E. Gille*

Email: clement.gille@uwa.edu.au

Summary

- Non-mycorrhizal cluster root-forming species enhance the phosphorus (P) acquisition of mycorrhizal neighbours in P-impoverished megadiverse systems. However, whether mycorrhizal plants facilitate the defence of non-mycorrhizal plants against soil-borne pathogens, in return and via their symbiosis, remains unknown.

- We characterised growth and defence-related compounds in *Banksia menziesii* (non-mycorrhizal) and *Eucalyptus tottiana* (ectomycorrhizal, ECM) seedlings grown either in monoculture or mixture in a multifactorial glasshouse experiment involving ECM fungi and native oomycete pathogens.

- Roots of *B. menziesii* had higher levels of phytohormones (salicylic and jasmonic acids, jasmonoyl-isoleucine and 12-oxo-phytodienoic acid) than *E. tottiana* which further activated a salicylic acid-mediated defence response in roots of *B. menziesii*, but only in the presence of ECM fungi. We also found that *B. menziesii* induced a shift in the defence strategy of *E. tottiana*, from defence-related secondary metabolites (phenolic and flavonoid) towards induced phytohormone response pathways.

- We conclude that ECM fungi play a vital role in the interactions between mycorrhizal and non-mycorrhizal plants in a severely P-impoverished environment, by introducing a competitive component within the facilitation interaction between the two plant species with contrasting nutrient-acquisition strategies. This study sheds light on the interplay between beneficial and detrimental soil microbes that shape plant–plant interaction in severely nutrient-impoverished ecosystems.

Key words: competition, defence responses, ectomycorrhiza, facilitation, phytohormones, *Phytophthora*, plant interactions, soil-borne pathogens.

Introduction

Severely phosphorus (P)-impoverished environments in southwestern Australia exhibit high plant diversity. They contain many species that evolved adaptations to enhance P-acquisition efficiency. Proteaceae, one of the most abundant families in these environments, form cluster roots (CRs), a highly efficient P-acquisition strategy (Shane & Lambers, 2005). Cluster roots are short-lived non-mycorrhizal and groups of densely packed hairy rootlets effectively ‘mine’ P sorbed onto soil particles by exuding large amounts of carboxylates (Shane *et al.*, 2004). Conversely, mycorrhizas, alternative nutrient-acquisition strategies characterised by an association of fine roots with ‘scavenging’ fungal hyphae, are less efficient at acquiring nutrients in extremely P-impoverished environments (Abbott *et al.*, 1984; Bolan *et al.*, 1984; Treseder & Allen, 2002; Albornoz *et al.*, 2021). While the abundance of cluster-rooted species increases along a 2-Myr chronosequence with declining soil P availability in southwestern Australia, that of both arbuscular mycorrhizal (AM) and ectomycorrhizal (ECM) species decreases, but they do not disappear (Zemunik *et al.*, 2015). Mobilisation of P and some micronutrients by cluster-rooted species may benefit neighbouring species with contrasting nutrient-acquisition strategies (Muler *et al.*, 2014; Shen *et al.*, 2024; Staudinger *et al.*, 2024; Yu *et al.*, 2023), and nutrient-impoverished environments are characterised by a prevalence of inter-species facilitation rather than competition (Callaway & Walker, 1997; Brooker *et al.*, 2008; Al-Namazi *et al.*, 2017; Lekberg *et al.*, 2018). The diverse array of nutrient-acquisition strategies plays a crucial role in shaping community assemblies and maintaining overall plant species diversity, particularly in severely nutrient-impoverished environments (Lambers *et al.*, 2018).

Mycorrhizal fungi, which establish symbiotic associations with *c.* 80% of terrestrial vascular plants, enhance mineral nutrition, water uptake and overall growth of their host plants (Smith & Read, 2008). Ectomycorrhizal fungi also enhance the protection of the host plants against soil-borne pathogens through various mechanisms (Pozo & Azcón-Aguilar, 2007). A trade-off exists between efficient P acquisition and root defence levels, making CRs highly susceptible to pathogens (Albornoz *et al.*, 2017; Lambers *et al.*, 2018). However, whether ECM colonisation confers pathogen tolerance to neighbouring non-mycorrhizal plants is unknown. Investigating plant–plant interactions such as these in severely nutrient-impoverished environments provides valuable insights into the mechanisms that underlie species coexistence.

Introduced pathogens pose a significant threat to plant productivity and diversity – exemplified by the devastating impact of root-rot *Phytophthora cinnamomi* in highly diverse ecosystems (Lambers *et al.*, 2013; Hardham & Blackman, 2018) – but plants have also co-evolved with soil-borne pathogens, including native oomycete species of the *Phytophthora* genus (Ricklefs, 2010; Rea *et al.*, 2011; Albornoz *et al.*, 2017; Sarker *et al.*, 2023). Previous studies have demonstrated the enhanced resistance of both AM- and ECM-colonised plants to *Phytophthora* spp. (Guillemin *et al.*, 1994; Branzanti *et al.*, 1999; Ozgonen & Erkilic, 2007; Pozo & Azcón-Aguilar, 2007). In addition to providing physical protection to the root with a fungal mantle and Hartig net, ECM fungi also release antimicrobial compounds into the rhizosphere, inhibiting the growth of pathogens (Marx, 1972). Mycorrhizal colonisation triggers the induction of pathogenesis-related (PR) proteins and/or production of phenolic compounds, which are associated with pathogen defence (Pozo *et al.*, 1999; Pozo & Azcón-Aguilar, 2007; Ozgonen *et al.*, 2009). In the intricate network of plant-defence responses, some phytohormones also play a crucial role as signalling molecules that coordinate and regulate defence pathways. Small organic molecules like salicylic acid (SA) and jasmonic acid (JA) are examples of these phytohormones that activate defence mechanisms, including the synthesis of defence compounds (Durner *et al.*, 1997; Avanci *et al.*, 2010; War *et al.*, 2011). While mycorrhizal species benefit from their symbiotic association, non-mycorrhizal plants exhibit a greater susceptibility to soil-borne pathogens. The range of susceptibility between mycorrhizal and non-mycorrhizal species potentially contributes to maintaining the megadiversity in nutrient-impooverished environments through diversity-dependent resistance mechanisms (Johnson *et al.*, 2015; Thakur *et al.*, 2021).

Recent evidence suggests that nonhost plants may participate in mycorrhizal networks, expanding the scope of these symbiotic interactions (Wang *et al.*, 2022). Interestingly, two ECM fungi, *Tuber melanosporum* and *T. aestivum*, colonise the roots of non-mycorrhizal neighbouring plants, potentially acting as root endophytes (Schneider-Maunoury *et al.*, 2018, 2020). Arbuscular mycorrhizal fungi establish early signalling interactions with nonhost *Arabidopsis thaliana*, but subsequent colonisation fails to occur (Fernández *et al.*, 2019). In a compatible interaction with *Populus tremula* × *alba*, the ECM fungus *Laccaria bicolor* actively suppresses the induction of the host-defence responses and alters the sensitivity of roots to certain phytohormones, including enhanced and diminished responsiveness to SA and JA, respectively (Basso *et al.*, 2020). Ectomycorrhizal fungi also alter sensitivity of host plants to phytohormones, particularly to JA, during the establishment of the symbiosis (Enebe &

Erasmus, 2023). The modulation of plant-defence responses occurs locally in the roots and can extend systemically throughout the plant, resulting in primed defence responses that increase the resistance of mycorrhizal plants to pathogens (Jung *et al.*, 2012; Vlot *et al.*, 2021). Understanding the responses of nonhost plants to ECM fungi and investigating the potential priming effects of these noncompatible interactions on defence responses to pathogens are critical areas for further research.

In this study, we aimed to explore the role of native oomycete pathogens, *Phytophthora* spp., and ECM fungi, in shaping the interactions between two plant species with contrasting P-acquisition strategies: *Banksia menziesii* (Proteaceae), a non-mycorrhizal CR-forming species, and *Eucalyptus todtiana* (Myrtaceae), an ECM species. In a glasshouse experiment, we cultivated *B. menziesii* and *E. todtiana* separately or together, with or without inoculation with ECM fungal spores and native oomycete (*Phytophthora* spp.). We investigated the plant growth and defence responses, and the interactions between the two species. We hypothesised that (1) the presence of native *Phytophthora* spp. will negatively impact the competitive ability of *B. menziesii*, as observed previously (Albornoz *et al.*, 2017); (2) the colonisation of *E. todtiana* roots by ECM fungi will trigger defence responses to *Phytophthora* spp. through increased levels of phytohormones and/or secondary metabolites; and (3) defence mechanisms will also be induced in the roots of *B. menziesii* when roots of *E. todtiana* are colonised by ECM fungi. By examining these interactions, we aimed to enhance our understanding of the intricate dynamics between two plant species with contrasting nutrient-acquisition strategies, native pathogens and ECM fungi, shedding light on the mechanisms underlying the coexistence of key dominant taxa of Proteaceae and Myrtaceae in a severely P-impooverished megadiverse environment.

Materials and Methods

Species selection and experimental design

Banksia menziesii R.Br. (Proteaceae) and *Eucalyptus todtiana* F.Muell. (Myrtaceae) share a similar distribution in southwestern Australia and were selected as representative of their families in kwongan vegetation (Pate & Beard, 1984) with contrasting P-acquisition strategies (*i.e.* carboxylate-exuding CRs and mycorrhizal associations, respectively).

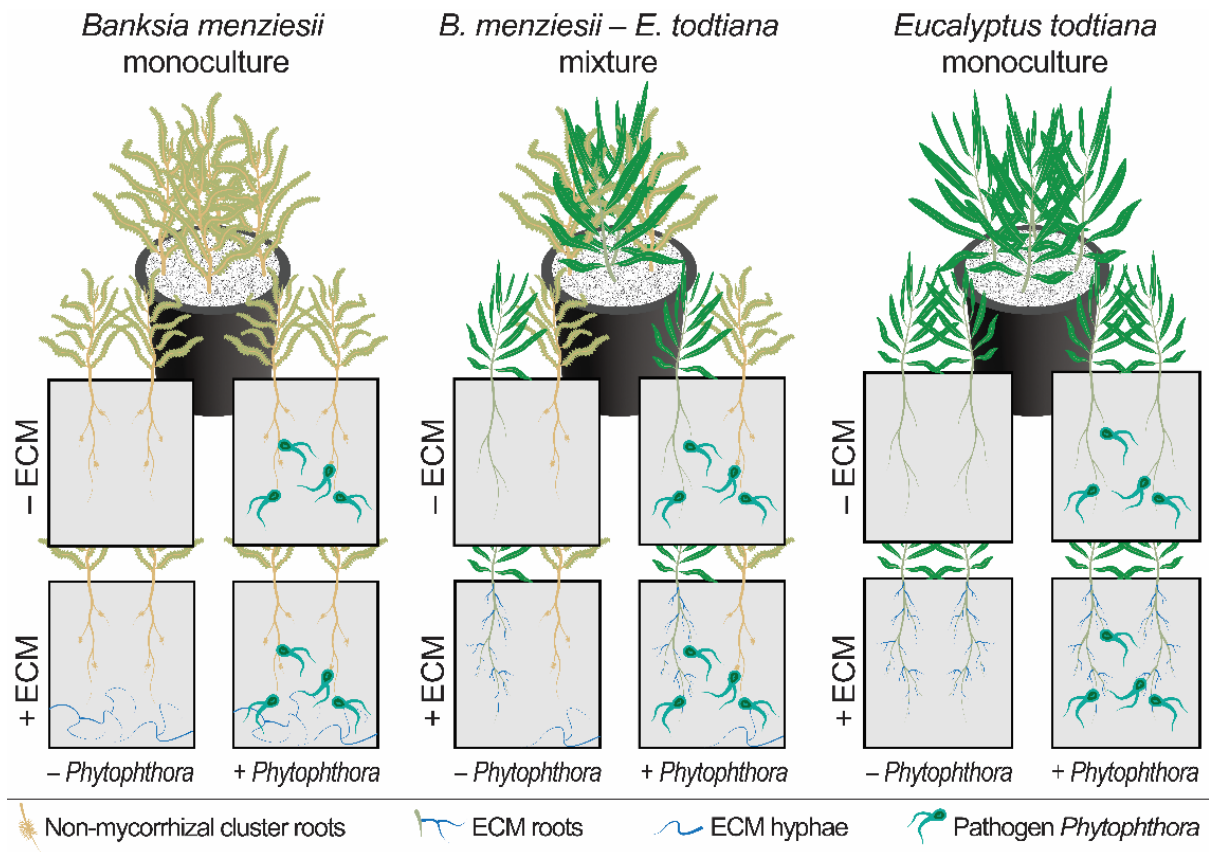


Fig. 1 Experimental design of this study conducted in a glasshouse at the University of Western Australia between August 2021 and January 2022. Seedlings of *Banksia menziesii* and *Eucalyptus tottiana* were grown in monoculture or mixture, with or without oomycete pathogens, *Phytophthora* spp., and with or without ectomycorrhizal (ECM) fungi ($n = 10$).

Seeds of *B. menziesii* and *E. tottiana* were sown and inoculated with ECM fungal spores in seedling trays on 10 August 2021, and allowed to germinate in growth chambers. Seedlings were transferred into 4.5 l pots 7 wk later, on 1 October 2021, and allowed to acclimate in controlled glasshouses, with four seedlings per pot (Fig. 1). On 31 November 2021, before inoculation with *Phytophthora* spp., six dead plants were removed from six pots. Nine weeks after transferring seedlings into final pots, on 7 December 2021, inoculum of *Phytophthora* spp. was inserted into the pots. Finally, plants were harvested 7 wk after oomycete inoculation, between 24 January and 29 January 2022. In total, there were 120 pots and 480 plants in the experiment (monocultures/mixture (three) \times ECM treatment (two) \times *Phytophthora* treatment (two) \times replication (10); Fig. 1).

Soil preparation

Bulk soil (0–200 mm) was collected from multiple spatially distributed (*c.* 10 m apart within a 100 m radius) sites within the *c.* 2-Myr-old Bassendean dune system, where both species naturally co-occur (30°10'59.4"S, 115°07'55.8"E, *c.* 230 km north of Perth, Western Australia). All sites were located within the Jurien Bay dune chronosequence. Details on the physicochemical properties of soil from Bassendean dunes and the Jurien Bay chronosequence can be found elsewhere (Laliberté *et al.*, 2012; Turner & Laliberté, 2015; Turner *et al.*, 2018). Soil was air-dried, mixed and sieved (2 mm) before being subjected to triple-steam pasteurisation at 80°C for 2 h d⁻¹ over 7 d (Albornoz *et al.*, 2017).

Inoculation of seeds with ectomycorrhizal fungi and growth conditions

Basidiocarps of the ECM fungus *Pisolithus* spp. with varied shape (round to ovoid), colour (yellow to brown) and size (30–80 mm long) were collected from different locations in Western Australia: Jurien Bay (30°11'05.8"S 115°06'39.1"E and 30°10'59.6"S 115°07'26.0"E, potential hosts *Melaleuca* sp. and *E. todtiana* trees, respectively); Lesueur National Park (30°09'41.5"S 115°11'59.1"E, potential host *E. todtiana*); Whiteman Park (31°48'59.9"S 115°55'19.2"E, potential host *E. todtiana*); and Bold Park (31°57'05.1"S 115°45'59.0"E, potential host *E. gomphocephala*). Basidiocarps were air-dried at 25°C for 48 h before the outer layer was manually broken to collect fungal spores and stored in the dark at 20°C until inoculation. Isolates of *Pisolithus* sp. 8 isolate MU98/103 (potential hosts *Eucalyptus* and *Acacia* spp.), *P. albus* isolate MH115 (potential hosts *Eucalyptus* and *Acacia* spp.) and *P. microcarpus* isolate MH97 (potential hosts *Eucalyptus* and *Melaleuca* spp.) were recovered from long-term storage from the mycology herbarium at Murdoch University and used as inoculum. GenBank accession numbers for *Pisolithus* isolates MU98/103, MH115 and MH97 are AF374663, AF374714 and AF374713, respectively (Martin *et al.*, 2002).

Seeds of *B. menziesii* and *E. todtiana* were purchased (Nindethana Seed Co. Albany, WA, Australia) after collection from natural populations in Western Australia. Seeds were surface-sterilised in 1% (w/v) NaClO for 20 s and then in 70% (v/v) ethanol for 20 s and thoroughly rinsed in deionised (DI) water. Surface-sterilised seeds were sown in seedling trays filled with soil. A subset of seeds used in the mycorrhizal treatment of both species was inoculated with *c.* 10 mg of fungal spore inoculum placed around the seeds into the soil during sowing. Seeds were germinated under artificial light (12 h : 12 h, light : dark; 300 μmol photons m⁻² s⁻¹) at 16°C until the cotyledons emerged, keeping inoculated seedling trays separate from

uninoculated ones. The temperature was then increased to 20°C : 16°C, day : night to promote the growth of the seedlings. When seedlings had their second pair of leaves, they were transferred from the seedling trays into 4.5 l pots (190 mm diameter and 180 mm deep), which were sealed with plastic bags and filled with pasteurised Bassendean soil. Four plants were transferred into each pot: four *B. menziesii* (monoculture), four *E. todtiana* (monoculture), or two *B. menziesii* and two *E. todtiana* (mixture; Fig. 1). Pots were arranged in a randomised block design with further randomisation every week, and pots were watered by weight to 75% pot capacity, twice weekly and were not fertilised. Pots were covered with a thick layer (*c.* 10 mm) of white plastic beads to avoid potential cross-contamination between ECM and pathogenic treatments and all material was disinfected between treatments during watering. Pots were placed in a controlled-environment glasshouse under natural light with temperatures of 22°C and 17°C during the day and night, respectively.

Inoculation of seedlings with *Phytophthora* spp.

Five native species of *Phytophthora* previously isolated from kwongan vegetation with reported pathogenicity on *Banksia* spp. were selected (Rea *et al.*, 2011; Simamora *et al.*, 2015; Burgess *et al.*, 2021): *P. arenaria* (CBS 125800), *P. thermophila* (PN 42.13), *P. kwonganina* (CBS 143060), *P. cooljarloo* (CBS 143062) and *P. constricta* (CPSM 21.42). GenBank accession numbers for ITS region sequences for these species are HQ013205, MF593927, JN547636, HQ012957 and OR256249, respectively. Subcultures of each species were prepared according to Belhaj *et al.* (2018), with minor modifications. In brief, subcultures were transferred onto sterile V8 agar medium at 27°C for 2 wk for growth of mycelium and then transferred into Erlenmeyer flasks with growth medium supplemented with sterilised millet seeds in the dark at 27°C for 8 wk. The flasks were sealed and shaken weekly to spread the inoculum evenly. Colonisation of the millet inoculum was confirmed and checked for contamination by plating *c.* 3 g subsamples of each species onto *Phytophthora*-selective NARPH agar medium (Hüberli *et al.*, 2000).

Nine weeks after establishment in 4.5 l pots, seedlings that were allocated to *Phytophthora* treatments were inoculated with 1 g of each millet-seed inoculum (total inoculum 5 g), according to Albornoz *et al.* (2017), with minor modifications. In brief, the inoculum was added into the void where a 15 ml Falcon tube was initially inserted into the soil in the middle of the pot. Pots without *Phytophthora* treatment were inoculated with 5 g of triple autoclaved millet-seed medium (121°C for 20 min on each of three consecutive days). Pots were watered

immediately to 100% pot capacity to facilitate colonisation of soil and roots by the pathogens. Watering was then reduced back to 75% pot capacity, twice weekly until harvest.

Harvest and growth-related measurements

Seven weeks after *Phytophthora* inoculation, plants were harvested by severing mature and other leaves (young and senescing) from the stem. All aboveground parts (stem, mature and other leaves) were oven-dried at 70°C to a constant dry weight (DW) and their combined weight was recorded as the aboveground biomass. Mature leaves were ground into a fine powder in a vertical ball-mill grinder using plastic vials and yttrium-stabilised zirconium ceramic beads (GenoGrinder, Spex SamplePrep, Metuchen, NJ, USA). Mature leaf P ([P], mg g⁻¹ DW) and Mn ([Mn], mg kg⁻¹ DW) concentrations were determined from *c.* 200 mg ground leaf material using inductively coupled plasma optical emission spectroscopy (Optima 5300DV; PerkinElmer, Waltham, MA, USA) after digestion in hot concentrated (6 : 1 v/v) HNO₃ : HClO₄ (Zarcinas *et al.*, 1987). Leaf P content (mg) was calculated as mature leaf [P] multiplied by total leaf biomass.

The root systems of each plant in the pots were gently separated by washing off adhering soil with water. Most of the roots remained attached to the primary root and stem and could easily be traced back to the plant to which they belonged. Based on the different root morphology between the two species (*i.e.* branching pattern and colour), detached roots were attributed to a species to contribute to the average biomass per species per pot (see Statistical analyses). Lateral roots were separated from the primary root and CRs were collected separately for *B. menziesii*. The primary root was oven-dried at 70°C to constant weight. Lateral roots and CR were snap-frozen in liquid nitrogen, freeze-dried for 10 d (VirTis BenchTop Pro 'K' Freeze Dryer; SP Scientific, Warminster, PA, USA), then weighed for biomass and stored at -80°C with silica desiccant, until further analyses. The weights of the primary root, lateral roots, as well as CRs for *B. menziesii*, were combined to give the belowground biomass.

Microbial colonisation

A subsample of four to five cleaned soil-free and branched lateral roots was used for microscopic observation to assess colonisation by ECM fungi and *Phytophthora* spp. in inoculated treatments or lack thereof in noninoculated controls, following Vierheilig *et al.* (1998), with minor modifications. In brief, roots were cleared in 10% (w/v) KOH for 24 h at 60°C. Clearing was continued in fresh 10% (w/v) KOH at room temperature, if required, then

the roots were rinsed in deionised water and stained with 3% (v/v) ink/vinegar for 45 min. Stained roots were rinsed with deionised water, de-stained in 1% (v/v) HCl for 35 min and stored in acidified glycerol (1% (v/v) HCl) until microscopic observation (Zeiss Axioskop fitted with Zeiss Axiocam; Zeiss).

In each treatment, three to four plants per species from each treatment were randomly selected and checked, with consistent observations as follows (Supporting Information Fig. S1). Roots of *B. menziesii* never showed any ECM fungi colonisation in either inoculated or noninoculated treatments, while those of *E. todtiana* that were inoculated were heavily colonised (> 80% of fine root tip regions observed, Fig. S1). Roots of *E. todtiana* that were not inoculated with ECM fungi did not show any colonisation. Roots of both species were abundantly colonised by *Phytophthora* oospores only in inoculated treatments.

Total root phenolics and flavonoids

Total root phenolic and flavonoid compounds were extracted from *c.* 80 mg of freeze-dried ground root material using 1.5 ml 75% (v/v) ethanol, shaken at 900 rpm at 20°C for 30 min in a thermomixer (Eppendorf, Hamburg, Germany), then incubated in an ultrasonic bath at 40 kHz for 20 min at 20°C. The extracts were cleared by centrifugation at 845 g at 20°C for 15 min. The extraction was repeated twice with 1 ml 75% (v/v) ethanol and shaking times of 45 and 90 min, respectively, followed by sonication (Romo Pérez *et al.*, 2018). The supernatants were pooled and filtered through 0.45 µm filters and kept in the dark at -20°C until quantification.

Total root phenolic compounds were quantified as in Santas *et al.* (2008), with minor modifications. In brief, 200 µl (1 : 1 v/v) ethanol root extract: 75% (v/v) ethanol was mixed with 1.5 ml (1 : 10 v/v) Folin–Ciocalteu : H₂O reagent (Sigma-Aldrich) and 1.5 ml (2% w/v) sodium carbonate and incubated in the dark at 20°C for 2 h. Absorbance was measured at 765 nm using a spectrophotometer against a blank containing 75% (v/v) ethanol. Total phenolic equivalents were determined from a calibration curve prepared from a series of gallic acid (GA; Sigma-Aldrich) standards ranging from 0 to 200 mg l⁻¹. Results were expressed as mg GA equivalents (GAE) g⁻¹ dry weight (DW).

Total root flavonoids were quantified by mixing 300 µl of root ethanol extract with 900 µl of 95% (v/v) ethanol, 60 µl of 10% (w/v) aluminium trichloride and 60 µl of 1 M potassium acetate and incubating in the dark at 20°C for 30 min. Absorbance was measured at

415 nm using a spectrophotometer against a blank containing 75% (v/v) ethanol. Total flavonoid equivalents were determined from a calibration curve prepared from a series of quercetin (Sigma-Aldrich) standards ranging from 0 to 200 mg l⁻¹. Results were expressed as mg quercetin equivalents g⁻¹ DW.

Root phytohormones

The root phytohormones SA, JA, jasmonoyl-isoleucine (JA-Ile) and 12-oxo-phytodienoic acid (OPDA) were extracted from *c.* 30 mg of freeze-dried ground root material and analysed by UHPLC–MS/MS, using an Acquity UPLC I-Class system (Waters Corp., Milford, MA, USA) connected to a QTRAP 6500+ (SCIEX, Framingham, MA, USA) as in Glauser *et al.* (2014), with minor modifications. In brief, 1 ml of ethyl acetate : formic acid (99.5 : 0.5 v/v), spiked with *d*₅-JA, ¹³C₆-JA-Ile and *d*₆-SA at 100 ng ml⁻¹, was added to ground dry root powder (25 mg) inside a 2 ml microcentrifuge tube, which also contained three or four glass beads, and was vortexed for 10 s. Hormones were further extracted in a mixer mill (Retsch MM400; Retsch GmbH, Haan, Germany) at 30 Hz for 4 min. Samples were centrifuged at 14 000 g for 4 min, and the supernatant was transferred to new tubes. The extraction step was repeated with the pellet and 0.5 ml of ethyl acetate : formic acid (99.5 : 0.5 v/v). The supernatants were combined and evaporated to dryness in a centrifugal concentrator (CentriVap Centrifugal Concentrator, Labconco, KS City, MO, USA) at 35°C. The residue was re-suspended in 200 µl 50% (v/v) methanol, and the suspension was transferred to a 0.2 ml microcentrifuge tube and centrifuged for 3 min at 14 000 g. The supernatant was transferred to HPLC glass vials for analysis. For HPLC, 2 µl of extract was injected onto an Acquity UPLC BEH C18 column (50 × 2.1 mm, 1.7 µm particle size; Waters Corp., Milford, MA, USA). Mobile phase A consisted of H₂O : formic acid (99.95 : 0.05 v/v) and mobile phase B consisted of acetonitrile : formic acid (99.95 : 0.05 v/v). A gradient of 5–65% B in 6.5 min was applied, followed by column washing with 100% B and equilibration with 5% B for 2 min. The flow rate was set to 0.4 ml min⁻¹ and the column temperature to 35°C. The mass spectrometer was operated in electrospray negative ionisation mode with multiple reaction monitoring (MRM). A six-point calibration curve (0.02, 0.1, 0.5, 5, 20 and 100 ng ml⁻¹, containing all isotopically labelled standards at 5 ng ml⁻¹) was used for quantification. Linear regressions weighted by 1/*x* were applied. ANALYST v.1.7.1 was used to control the instrument and for data processing.

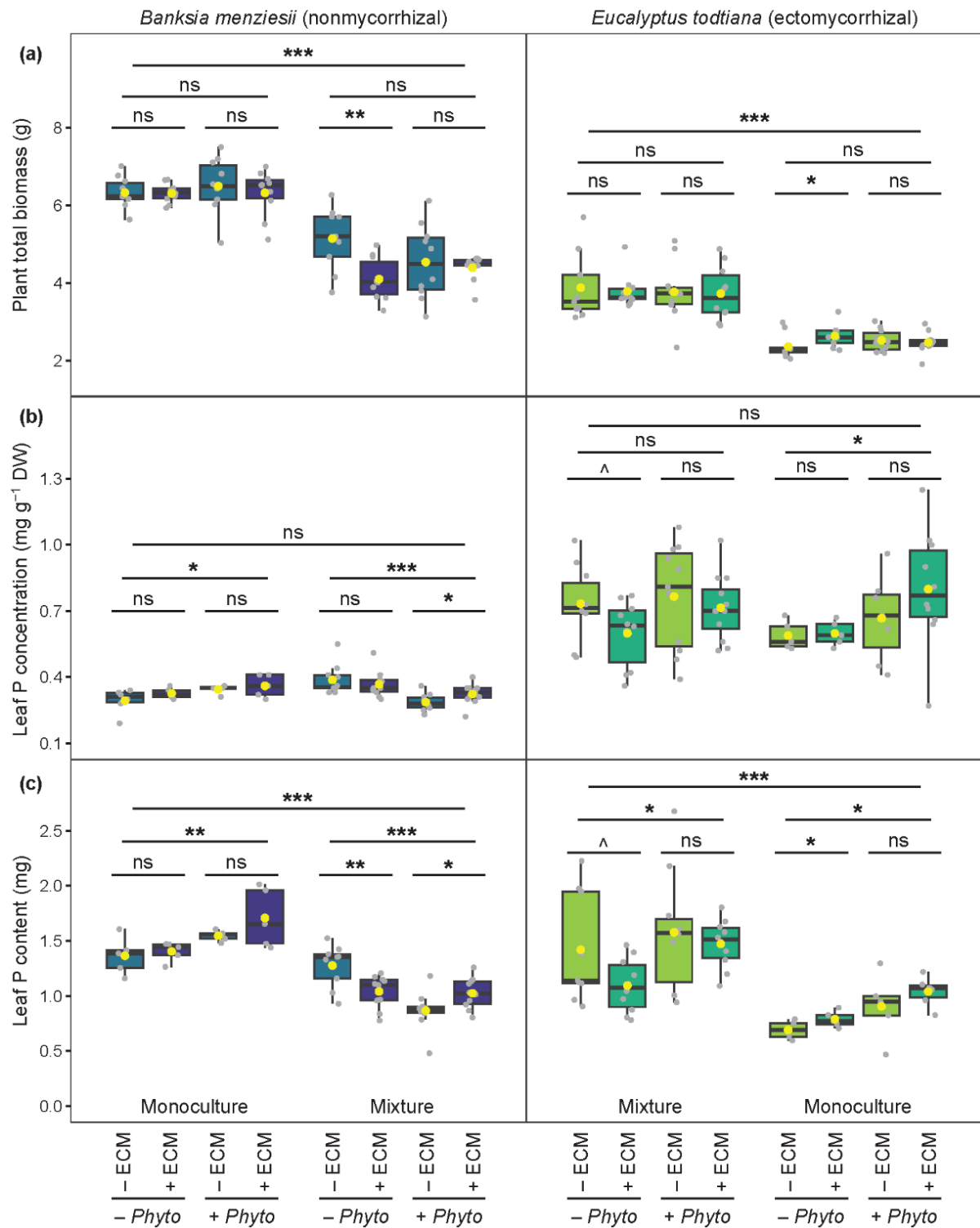
Statistical analyses

For growth-related measurements, that is aboveground, belowground, CR, non-CR and total biomass, the average of all plants from a given species within a pot constituted a data point. For example, plant total biomass was calculated as the average of the total biomass of four plants in monoculture treatments, and as the average of two plants for each species in mixture treatments. Five to twelve plants and three to five plants from each of the 12 treatments were randomly selected for leaf nutrient and defence-related measurements, respectively.

The differences among treatments were tested in all measured variables using multifactorial linear mixed-effect models, with the block as a random effect, using the NLME package (Pinheiro & Bates, 2000). Models with different variance structures were compared using the Akaike information criterion (AIC). The normality of the residuals of the best model based on the lowest AIC was checked with Shapiro–Wilks test, and \log_{10} -transformed data were used to fit models when the assumption was not respected. First, we considered the effect of the other species by comparing ‘monoculture’ vs ‘mixture’ for each species, regardless of microbial treatments. We then tested the effect of the inoculation of *Phytophthora* spp. regardless of ECM inoculation. Finally, we tested the effect of ECM inoculation. Ectomycorrhizal treatment was used as the finest level of analysis in regard to the hypotheses of the study, that is ECM colonisation contributes to defence against *Phytophthora* spp. in roots of both mycorrhizal and non-mycorrhizal plants. Pearson correlation analysis was used to analyse the correlation between defence-related compounds. We characterised the defence strategies of the two species in the treatments using a principal component analysis (PCA), considering the following traits: root concentrations of phenolics, flavonoids, SA, JA, JA-Ile and OPDA. The PCA was run with the FactoMineR package on \log_{10} -transformed data (Lê *et al.*, 2008). To test whether the defence strategies varied between the two species and in response to the treatments, the scores of each individual plant on the first two dimensions of the PCA explaining 76% and 11% of the variance, respectively, were extracted, and linear mixed-effect models were used to detect significant differences along the defence-strategy space. To compensate for interspecific variation, we characterised and analysed the distribution of each species along the defence-strategy space using species-specific PCAs and linear mixed-effect models, as described previously. Data were analysed using R software (R Core Team, 2023).

Results

Growth-related parameters of plants



Both *B. menziesii* and *E. tottiana* showed a significant effect on the growth of the other species when grown together. On average, the presence of *B. menziesii* increased the total biomass accumulation of *E. tottiana* by 52%, while its own biomass was reduced by 29% in mixture compared with monoculture (Fig. 2a; Table 1). For both species, similar patterns of biomass changes were observed for the above- and belowground biomass considered separately (Fig. S2; Table 1). Furthermore, the presence of *E. tottiana* increased the root-to-shoot ratio, CR biomass and CR-to-non-CR ratio of *B. menziesii* (Figs S2, S3; Table 1). In mixture and in the absence of pathogens, ECM fungi significantly contributed to a reduction in the growth of *B. menziesii* (Table S1). The ECM fungi had a positive effect on the growth of *E. tottiana* only in monoculture and in the absence of pathogens (Fig. 2a). Surprisingly, the presence of *Phytophthora* spp. did not affect the biomass accumulation of either species, regardless of whether they were grown in monoculture or mixture (Figs 2a, S2, S3; Table 1).

There was little variation in mature leaf [P] and [Mn] in both species grown either alone or in mixture (Figs 2b, S4; Table 1). However, inoculation with *Phytophthora* spp. significantly increased leaf [P] of *B. menziesii* in monoculture, while it was reduced in mixture (Fig. 2b; Table 1). Leaf [P] also increased in *E. tottiana* inoculated with *Phytophthora* spp. only in the monoculture (Fig. 2b; Table 1). Similar to plant biomass, leaf P content in both species was significantly impacted by the presence of the other species (Fig. 2c; Table 1). Inoculation with pathogens increased leaf P content in both species in monoculture, while it reduced that of *B. menziesii* and increased that of *E. tottiana* in mixture. Inoculation with ECM fungi reduced leaf P content in both species in mixture only in the absence of pathogens (Fig. 2c; Table 1).

◀ **Fig. 2** Total plant biomass (a), leaf phosphorus (P) concentration (b) and leaf P content (c) of *Banksia menziesii* (left panels) and *Eucalyptus tottiana* (right panels) grown in monoculture or in mixture, inoculated with *Phytophthora* pathogens (+ *Phyto*) or not (– *Phyto*) and/or with ectomycorrhizal (ECM) fungi (+ ECM, dark colour) or not (– ECM, light colour). The bottom and top of the box denote the 25th and 75th percentiles, respectively, the central line is the median, and the yellow dot represents the mean ($n = 8-10$). Whiskers extend to the most extreme data points up to a maximum of 1.5 times the lower and upper quartiles. Significant differences between treatments were tested with linear mixed-effect models (\wedge , $P < 0.1$; *, $P < 0.05$; **, $P < 0.01$; ***, $P < 0.001$; ns, not significant, *i.e.* $P > 0.1$).

Table 1 *P*-values of multifactorial linear mixed-effect models for growth-related traits of *Banksia menziesii* and *Eucalyptus todtiana* to test the significance of the effect of all treatments (*i.e.* monoculture vs mixture > – *Phyto* vs + *Phyto* > – ECM vs + ECM; ^, *P* < 0.1; *, *P* < 0.05; **, *P* < 0.01; ***, *P* < 0.001). Significant values (*P* < 0.1) are **bolded** for visualisation and the degrees of freedom (*df*) are given in brackets. ECM, ectomycorrhizal fungi; *Phyto*, *Phytophthora* spp.

	<i>B. menziesii</i> – monoculture		<i>B. menziesii</i> – mixture		<i>E. todtiana</i> – mixture		<i>E. todtiana</i> – monoculture	
	– <i>Phyto</i> +/- ECM	+ <i>Phyto</i> +/- ECM	– <i>Phyto</i> +/- ECM	+ <i>Phyto</i> +/- ECM	– <i>Phyto</i> +/- ECM	+ <i>Phyto</i> +/- ECM	– <i>Phyto</i> +/- ECM	+ <i>Phyto</i> +/- ECM
Total biomass (df = 132)	0.947 0.666 <0.001***	0.538	0.001** 0.530	0.838	0.895 0.637 <0.001***	0.936	0.027* 0.988	0.661
Aboveground biomass (df = 134)	0.422 0.265 <0.001***	0.727	0.014* 0.413	0.921	0.792 0.788 <0.001***	0.704	0.011* 0.409	0.662
Belowground biomass (df = 132)	0.395 0.508 <0.001***	0.464	<0.001*** 0.758	0.562	0.599 0.647 <0.001***	0.797	0.137 0.571	0.984
Root : Shoot ratio (df = 132)	0.270 0.371 <0.001***	0.493	0.003** 0.873	0.689	0.227 0.929 0.319	0.590	0.704 0.407	0.905
Cluster root biomass (df = 62)	0.901 0.254 0.002**	0.526	0.017* 0.888	0.281	n/a			
Cluster root : Root ratio (df = 62)	0.428 0.369 <0.001***	0.997	0.759 0.969	0.285	n/a			
Leaf [P] (df = 108)	0.211 0.049* 0.875	0.634	0.457 <0.001***	0.036*	0.074^ 0.183 0.774	0.540	0.905 0.028*	0.163
Leaf P content (df = 94)	0.599 0.001** <0.001***	0.210	0.006** <0.001***	0.035*	0.084^ 0.022* <0.001***	0.819	0.050* 0.010*	0.305
Leaf [Mn] (df = 108)	0.451 0.906 0.640	0.252	0.092^ 0.900	0.078^	0.831 0.864 0.989	0.099^	0.579 0.186	0.952

Defence-related compounds in fine roots

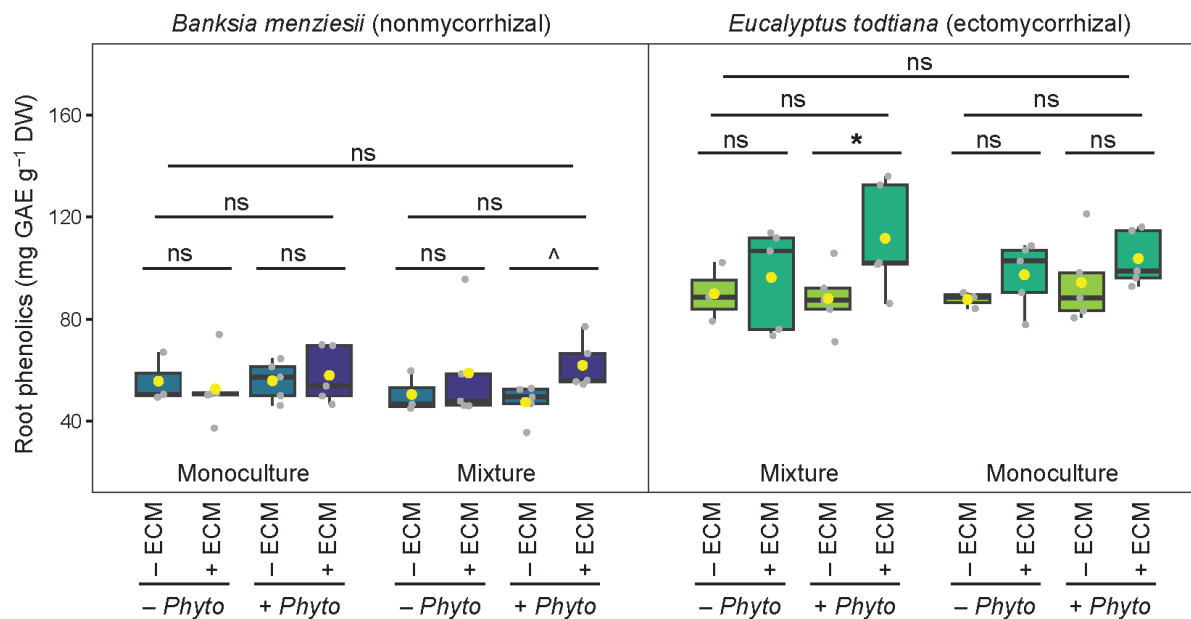


Fig. 3 Root total phenolic concentrations for *Banksia menziesii* (left panels) and *Eucalyptus tottiana* (right panels) grown in monoculture or in mixture, inoculated with *Phytophthora* pathogens (+ *Phyto*) or not (– *Phyto*) and/or with ectomycorrhizal (ECM) fungi (+ ECM, dark colour) or not (– ECM, light colour). The bottom and top of the boxes denote the 25th and 75th percentiles, respectively, and the central line is the median, and the yellow dot represents the mean ($n = 3–5$). Whiskers extend to the most extreme data points up to a maximum of 1.5 times the lower and upper quartiles. Significant differences between treatments were tested with linear mixed-effect models (^ $P < 0.1$; * $P < 0.05$; ns, not significant, *i.e.* $P > 0.1$).

Roots of *E. tottiana* had nearly twice the concentration of defence-related secondary metabolites (97 mg GAE g⁻¹ DW phenolics, 3.9 mg quercetin equivalents g⁻¹ DW flavonoids) compared with those of *B. menziesii* (55 mg GAE g⁻¹ DW phenolics, 2.4 mg quercetin equivalents g⁻¹ DW flavonoids; Figs 3, S5). The concentrations of these compounds in roots of each species were not affected by the presence of the other species. Interestingly, inoculation of *Phytophthora* pathogens also did not affect total root phenolic and flavonoid concentrations (Figs 3, S5; Table 2). By contrast, the presence of ECM fungi significantly increased the root phenolic concentrations of both species in a mixture and in the presence of pathogens (Fig. 3; Table 2).

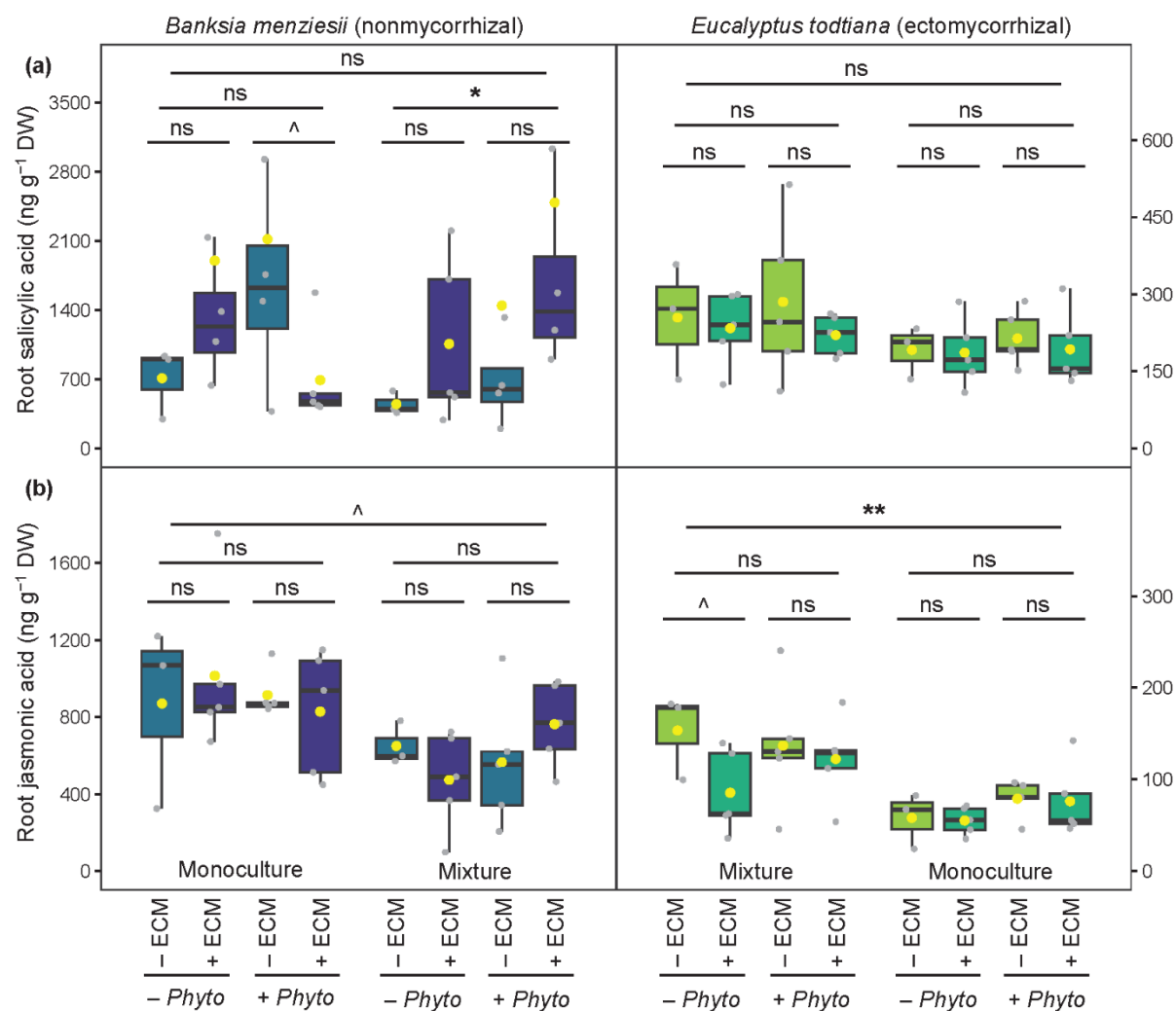


Fig. 4 Root salicylic acid (a) and jasmonic acid (b) concentrations for *Banksia menziesii* (left panels) and *Eucalyptus tottiana* (right panels) grown in monoculture or in mixture, inoculated with *Phytophthora* pathogens (+ *Phyto*) or not (- *Phyto*) and/or with ectomycorrhizal (ECM) fungi (+ ECM, dark colour) or not (- ECM, light colour). The bottom and top of the boxes denote the 25th and 75th percentiles, respectively, and the central line is the median, and the yellow dot represents the mean ($n = 3-5$). Whiskers extend to the most extreme data points up to a maximum of 1.5 times the lower and upper quartiles. Note different y-axis range for the two species. Significant differences between treatments were tested with linear mixed-effect models (^ $P < 0.1$; * $P < 0.05$; ** $P < 0.01$; ns, not significant, *i.e.* $P > 0.1$).

In contrast to those of total phenolics and flavonoids, the concentrations of all measured defence-related phytohormones (SA, JA, JA-Ile and OPDA) were higher in roots of *B. menziesii* than in those of *E. todtiana* (Figs 4, S6). The concentrations of all measured phytohormones were greater in roots of *E. todtiana* growing with *B. menziesii* than in those in the monoculture, with 1.3-, 1.8-, 3.4- and 2.3-fold greater concentrations, on average, for SA, JA, JA-Ile and OPDA, respectively (Figs 4, S6; Table 2). Conversely, the concentrations of JA and JA-Ile were lower in roots of *B. menziesii* in the mixture than in those in the monoculture (33% and 40% lower, respectively). The concentration of SA in roots of *B. menziesii* was greater when grown with *E. todtiana* in the presence of ECM fungi and significantly increased with inoculation of pathogens (Fig. 4a; Table 2). The concentration of OPDA also significantly increased in roots of *B. menziesii* in the mixture and inoculated with *Phytophthora* spp. (Fig. S6b; Table 2). The concentrations of JA were marginally lower in roots of *E. todtiana* grown in the mixture, when inoculated with ECM fungi and in the absence of *Phytophthora* spp. (Fig. 4b; Table 2).

The correlations between all defence-related compounds were significant ($P < 0.05$) with concentrations of defence-related secondary metabolites negatively correlated with phytohormone concentrations (Fig. 5a). As expected, JA-related phytohormones (JA, JA-Ile and OPDA) showed a very strong correlation among each other. The negative correlation between constitutive defence-related secondary metabolites and measured phytohormone concentrations in roots of *E. todtiana* and *B. menziesii* was reflected in a defence-strategy space along one main component in the PCA for defence-related compounds when considering individuals from both species (Fig. 5b).

The first axis of the PCA (PC1) explained 76% of the observed variance, which reflected that the presence of *B. menziesii* had a significant effect on the position of *E. todtiana* along the defence-strategy space, shifting towards higher phytohormone levels from the defence-related secondary metabolites (Figs 5b, S7). Furthermore, the presence of ECM fungi had a significant effect on the position of *E. todtiana* along PC1 in the defence-strategy space, but only in the presence of *B. menziesii*. Inoculation with *Phytophthora* spp. shifted the defence strategy of *E. todtiana* in the monoculture from defence-related secondary metabolites towards phytohormones (Fig. S7). There was very little variation among groups along PC2, with a significant shift of *B. menziesii* in the mixture and inoculated with *Phytophthora* spp., highlighting differences in concentrations of SA and flavonoids, the two variables with the largest contribution to PC2 (Figs 4a, S5, S7; Table S2).

The presence of the neighbouring species significantly shifted the distribution of both species along PC1 in individual PCAs per species (Fig. 5). In the presence of *E. tottiana*, *B. menziesii* shifted away from JA-related phytohormones (JA, JA-Ile and OPDA), strongly contributing to PC1, while we observed no differences along PC2 represented by secondary metabolites (Fig. 5c–e; Table S3). Conversely, the distribution of *E. tottiana* shifted towards JA-related phytohormones, both in the monoculture in the presence of pathogens, and in the mixture (Fig. 5f,g; Table S4). Similar to *B. menziesii*, the distribution of *E. tottiana* did not significantly change along PC2 or PC3, explained by other defence-related compounds (Fig. 5h; Table S4).

Table 2 *P*-values of multifactorial linear mixed-effect models for defence-related traits in roots of *Banksia menziesii* and *Eucalyptus tottiana* to test the statistical significance of the effect of all treatments (*i.e.* monoculture vs mixture > – *Phyto* vs + *Phyto* > – ECM vs + ECM; ^, $P < 0.1$; *, $P < 0.05$; **, $P < 0.01$; ***, $P < 0.001$; df = 47). Significant values ($P < 0.1$) are **bolded** for visualisation. ECM, ectomycorrhizal fungi; JA-Ile, jasmonoyl-isoleucine; OPDA, 12-oxo-phytodienoic acid; *Phyto*, *Phytophthora* spp.

	<i>B. menziesii</i> – monoculture		<i>B. menziesii</i> – mixture		<i>E. tottiana</i> – mixture		<i>E. tottiana</i> – monoculture	
	– <i>Phyto</i>	+ <i>Phyto</i>	– <i>Phyto</i>	+ <i>Phyto</i>	– <i>Phyto</i>	+ <i>Phyto</i>	– <i>Phyto</i>	+ <i>Phyto</i>
	+/- ECM	+/- ECM	+/- ECM	+/- ECM	+/- ECM	+/- ECM	+/- ECM	+/- ECM
Phenolics	0.720	0.779	0.319	0.053 [^]	0.572	0.025 *	0.392	0.357
	0.625		0.999		0.382		0.394	
	0.996				0.991			
Flavonoids	0.240	0.633	0.911	0.272	0.180	0.380	0.177	0.205
	0.931		0.127		0.827		0.664	
	0.958				0.526			
Salicylic acid	0.123	0.060 [^]	0.196	0.147	0.856	0.587	0.833	0.569
	0.996		0.039 *		0.930		0.672	
	0.967				0.394			
Jasmonic acid	0.499	0.596	0.163	0.185	0.065 [^]	0.847	0.911	0.755
	0.957		0.455		0.665		0.167	
	0.059 [^]				0.005 **			
JA-Ile	0.632	0.669	0.162	0.093 [^]	0.228	0.574	0.610	0.384
	0.519		0.932		0.761		0.072 [^]	
	0.034 *				<0.001 ***			
OPDA	0.859	0.696	0.403	0.105	0.188	0.379	0.292	0.135
	0.124		0.009 **		0.596		0.206	
	0.225				<0.001 ***			

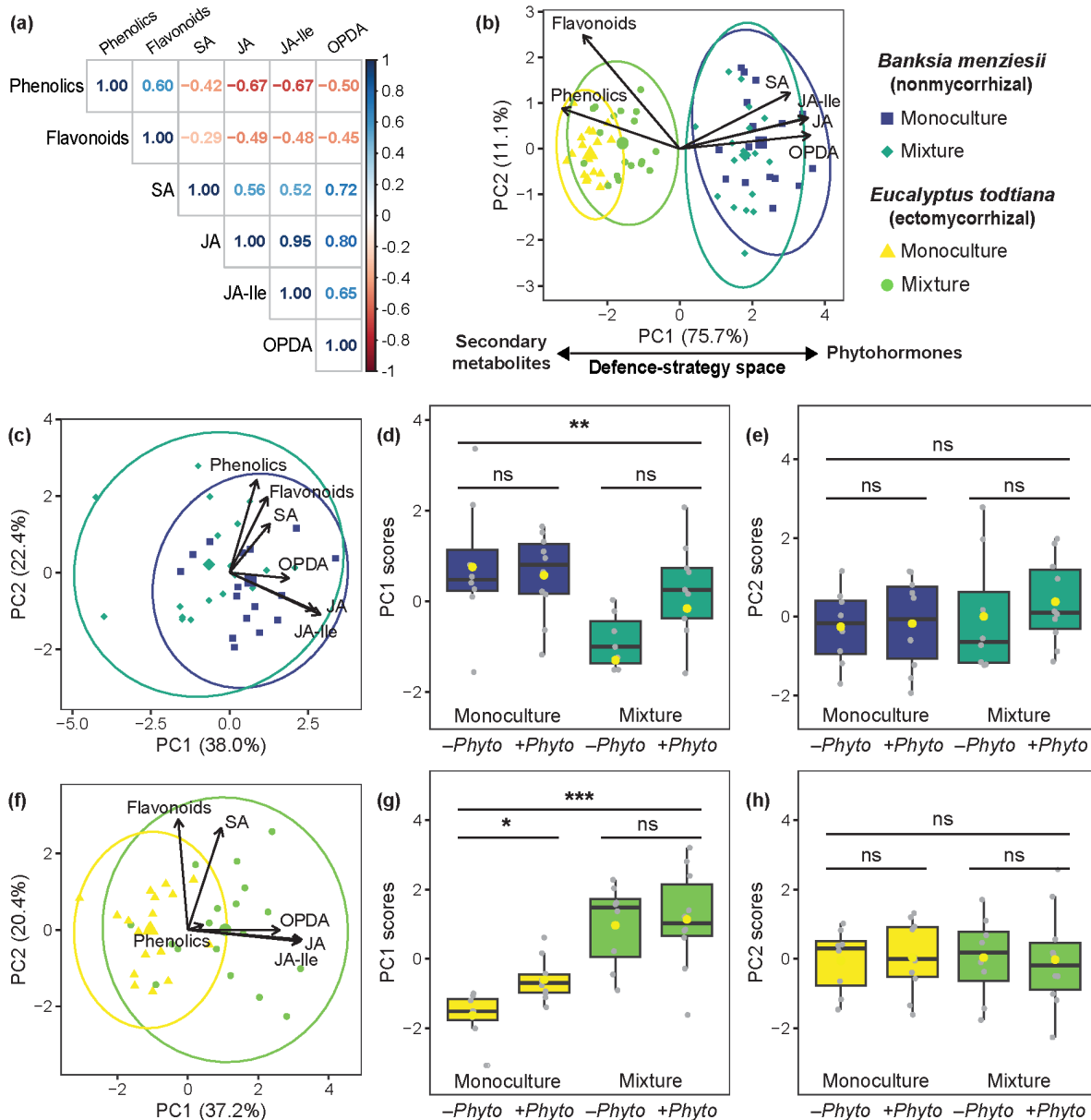


Fig. 5 Correlation matrix with Pearson's r coefficient ($P < 0.05$) (a), principal component analysis (PCA) of defence-related compounds in roots of *Banksia menziesii* and *Eucalyptus tottidiana* (b); and PCA of defence-related compounds and test of the distribution of both species and pathogen treatments along a defence-strategy space represented by the first and second dimensions of each individual PCA for *B. menziesii* (c–e) and for *E. tottidiana* (f–h). In boxplots (d, e, g and h), the bottom and top of the boxes denote the 25th and 75th percentiles, respectively, and the central line is the median, and the yellow dot represents the mean ($n = 3–5$). Whiskers extend to the most extreme data points up to a maximum of 1.5 times the lower and upper quartiles. Significant differences between treatments were tested with linear mixed-effect models (* $P < 0.05$; ** $P < 0.01$; *** $P < 0.001$; ns, not significant, *i.e.* $P > 0.05$). Outputs of the PCAs are given in Supporting Information Tables S2–S4. JA, jasmonic acid; JA-Ile, jasmonoyl-isoleucine; OPDA, 12-oxo-phytodienoic acid; *Phyto*, *Phytophthora* spp.; SA, salicylic acid.

Discussion

We explored key growth and defence-related traits in two plant species with contrasting P-acquisition strategies naturally occurring in severely P-impooverished environments and challenged by native soil-borne oomycete pathogens. Our results support the hypothesis that *B. menziesii*, a non-mycorrhizal CR-forming Proteaceae, facilitated the P acquisition and growth of *E. todtiana*, a mycorrhizal Myrtaceae that forms mycorrhizal association, but does not produce carboxylate-releasing CRs. However, the study of defence-related traits, that is constitutive defence-related secondary metabolites and signalling phytohormones, contradicted our hypotheses and the species have contrasting strategies resulted in various effects depending on the mixture of the two species, the inoculation with *Phytophthora* spp. and the presence of ECM fungi. We highlight a competitive component within the interaction between these mycorrhizal and non-mycorrhizal plants in an extremely P-impooverished environment involving a balance between the contrasting P-acquisition strategies of the plants and soil-borne microbes. This finding supports our hypothesis that native *Phytophthora* spp. impact the competitive ability of non-mycorrhizal species. This study enhances our understanding of the interactions between mycorrhizal and non-mycorrhizal plants in severely P-impooverished environments, mediated by detrimental and beneficial soil microbes, advancing on previous studies (Albornoz *et al.*, 2017; Lambers *et al.*, 2018).

Facilitative and competitive dynamics between a mycorrhizal and a non-mycorrhizal species

Surprisingly, the facilitation of the growth and P acquisition of *E. todtiana* by *B. menziesii* also involved a competitive component in the interaction. This was evident from the negative impact *E. todtiana* had on the growth and P content of *B. menziesii*. These impacts included reductions in above- and belowground bio-mass and leaf P content, as well as an increase in root-to-shoot ratio. Inclusion of *E. todtiana* also increased CR production and the CR-to-non-CR ratio in *B. menziesii*. Taken together, these results reflected the greater demand to mobilise P of *B. menziesii* in the mixture when *E. todtiana* competed for some of the mobilised P (Zhao *et al.*, 2021). Conversely, the significant increase in biomass and leaf P content without alteration of root-to-shoot ratio of *E. todtiana* indicated its P status was enhanced by facilitation by the carboxylate-releasing P-mobilising *B. menziesii*. In environments with a very low P availability, CR-forming and other carboxylate-releasing species commonly facilitate P acquisition of mycorrhizal and/or non-CR-forming neighbouring plants (Lambers & Teste, 2013; Muler *et al.*, 2014; Shen *et al.*, 2024; Staudinger *et al.*, 2024;

Yu *et al.*, 2023). For instance, in the presence of a P-mobilizing facilitator (*B. attenuata*), *Hibbertia racemosa* (a non-CR-producing mycorrhizal species) adjusts its biomass-allocation pattern and root system architecture (de Britto *et al.*, 2021). Here, we show that *E. todtiana* benefited with a net gain in above- and belowground biomass but did not exhibit a different root-to-shoot ratio when growing with *B. menziesii*. Roots of both species were highly intermingled, particularly in the close proximity of CR of *B. menziesii* where we found many roots of *E. todtiana*. Roots were not pot-bound, and we surmise that plant density likely affects the degree of facilitation and competition between the two species. We provide insights into the two-way interaction between mycorrhizal and non-mycorrhizal plants in extremely P-impooverished environments. This raises the question of the specific dynamics and mechanisms underlying the competitive effects imposed by ECM fungi that contribute to P acquisition on the present two coexisting species.

In the absence of both ECM fungi and pathogenic *Phytophthora* spp., aboveground and belowground biomass production of *B. menziesii* was reduced, whereas *B. menziesii* had a higher leaf P content in the presence of *E. todtiana*. This highlights the stronger competitive ability of non-mycorrhizal P-mining species in severely P-impooverished environments in the presence of oomycete pathogens. In the absence of these pathogens impacting their growth, however, non-mycorrhizal species strongly compete with mycorrhizal species for the acquisition of limiting P (Albornoz *et al.*, 2017; Lambers *et al.*, 2018). This further supports the view of a trade-off between nutrient-acquisition efficiency and defence against pathogens. The reduced growth of *B. menziesii* in the presence of ECM fungi, exclusively in the presence of *E. todtiana*, suggests that ECM fungi are strongly involved in nutrient acquisition by *E. todtiana*. This underscores the importance of ECM fungi in the interaction between non-mycorrhizal and mycorrhizal species, which exacerbated the competition between the two species. While facilitation of P acquisition in other species enhances their leaf [Mn] (Lambers *et al.*, 2021; Yu *et al.*, 2023), this was not the case in *E. todtiana*, indicating that mycorrhizal fungi were involved in acquiring P mobilised by *B. menziesii*.

Although there was no effect on leaf [P], despite P being the major limiting nutrient in the Bassendean soil used in this experiment (Laliberté *et al.*, 2012; Hayes *et al.*, 2014), the presence of both species significantly affected their respective growth and leaf P content. Phosphorus mobilised by CRs of *B. menziesii* and made available to roots of *E. todtiana* led to more growth in the latter. The absence of an effect on leaf [P] is because at very low P supply,

all P that is taken up leads to more growth, rather than higher leaf [P], therefore resulting in higher leaf P content (De Groot *et al.*, 2003; Shane *et al.*, 2003; Shen, 2023). In turn, both ECM fungi and pathogen inoculation affected P the nutrition and growth of both species. While facilitation of P uptake can be proxied by leaf [Mn] (Lambers *et al.*, 2021; Yu *et al.*, 2023), leaf Mn of *E. tottiana* did not vary between the monoculture and mixture. This indicates that mycorrhizas likely contributed more to the P acquisition of *E. tottiana* than its roots did, when grown alongside *B. menziesii*. Phosphorus uptake is tightly regulated in mycorrhizal roots which down-regulate their direct root Pi-uptake pathway and promote fungal hyphal uptake and translocation into the root (Smith *et al.*, 2011). Moreover, Mn did not accumulate in leaves of *E. tottiana* because mycorrhizas mainly facilitate P uptake rather than Mn (Lehmann & Rillig, 2015), and Mn is likely intercepted by the ECM network (Canton *et al.*, 2016). However, the mechanisms by which *Phytophthora* spp. altered P nutrition of both species, in balance with the ECM fungi, remain unclear.

The ECM colonisation had negligible effects on the growth of *E. tottiana*, compared with what is commonly observed in environments with moderate P limitation or when plant growth is limited by other elements (Burgess *et al.*, 1993; Montesinos-Navarro *et al.*, 2019). In severely P-impooverished environments, ECM associations likely contribute other benefits to plants that are complementary to P nutrition, such as protection against root pathogens (Marx, 1972; Standish *et al.*, 2021). Teste *et al.* (2014) showed a synergistic effect between ECM hyphal scavenging and nutrient-mobilising CRs. However, the non-nutritional roles of ectomycorrhizas on neighbouring plants deserve further attention in nutrient-poor environments.

Phytochemical responses and pathways of defence against *Phytophthora* spp.

Eucalyptus tottiana constitutively exhibited higher levels of defence-related secondary metabolites (phenolics and flavonoids) than *B. menziesii*. Furthermore, like other *Eucalyptus* species (e.g., *E. pipularis*; Ashford *et al.*, 1989; Vesik *et al.*, 2000) and most woody species (Brundrett & Tedersoo, 2020), *E. tottiana* most likely possesses a suberised exodermis that acts as a physical barrier to root pathogens (Ranathunge *et al.*, 2008). *Banksia* species lack a suberised exodermis, presumably allowing the release of large amounts of carboxylates to the rhizosphere (Lambers *et al.*, 2018). A recent study demonstrated that the release of carboxylates in *Hakea laurina* (Proteaceae) originates from the root cortex, rather than the epidermis (Hirotsuna Yamada, pers. comm.). This further supports the contention of a trade-off

between a high nutrient-acquisition efficiency in *Banksia* species and susceptibility to soil-borne pathogens, although the pathogen inoculation here did not affect biomass accumulation. While the *Phytophthora* spp. were selected to reflect the natural occurrence of native *Phytophthora* species with inoculation rates similar to previous studies (Albornoz *et al.*, 2017), we surmise that the pathogen pressure in the present study was not strong enough to suppress the growth of *B. menziesii* in monoculture, but it was strong enough to induce root phytochemical responses.

The intrinsically contrasting defence strategies observed between the present two species, that is higher levels of phytohormones in *B. menziesii* vs higher concentrations of secondary metabolites (phenolics and flavonoids) in *E. todtiana*, likely reflect divergent evolutionary adaptations of each plant to its environment. While the inoculation of *Phytophthora* spp. had little effect on the biomass of either species, we observed some relevant phytochemical responses, that is JA and JA-Ile concentrations increased in roots of *E. todtiana* inoculated with the pathogen in monoculture. This shows that *E. todtiana* perceived the inoculation of *Phytophthora* and induced a JA-related defence pathway. Interestingly, mycorrhizal associations contribute to priming the defences of their hosts by activating the JA-dependent responses (Pozo & Azcón-Aguilar, 2007). Most species of *Phytophthora* are haemibiotrophs with a variable biotrophy period before switching to necrotrophy (Sarker *et al.*, 2023). The JA pathway is commonly induced in response to necrotrophic pathogens (Glazebrook, 2005), as observed in roots of *E. todtiana* here. In roots of *B. menziesii*, the concentration of OPDA increased with pathogen inoculation. This phytohormone has previously been linked to the JA-dependent pathway and shown to be involved in defence against pathogens (Gleason *et al.*, 2016), although its role might be extended to jasmonate-independent pathways (Jimenez Aleman *et al.*, 2022). The induction of JA-related phytohormones, including OPDA, commonly leads to a vast array of defence mechanisms, for example production of defence-related secondary metabolites or the reinforcement of root physical barriers (cell-wall thickening, suberisation and lignification). However, we surmise that the basal expression of defence-related secondary metabolism in roots of *E. todtiana*, which might be genetically controlled (Kroymann, 2011), was sufficient to counteract the low pathogenicity of *Phytophthora* spp. in this trial, mimicking that in the natural environment. In the mixture of the two plant species, *Phytophthora* spp. did not trigger phytohormone responses in roots of *E. todtiana*. We surmise that the increase in belowground biomass due to the facilitation by *B. menziesii* contributed to its stronger ability to resist pathogen infection.

Interactions between ectomycorrhizal fungi and *Phytophthora* spp. alter defence responses in the non-mycorrhizal *Banksia menziesii*

The defence responses of *B. menziesii* were affected by *Phytophthora* spp. and involved ECM fungi. Inoculation of *Phytophthora* spp. increased SA and OPDA concentrations in roots of *B. menziesii* in the mixture of the two plant species. The inoculation of ECM fungi also trended towards higher concentrations of SA in roots of *B. menziesii* both with and without pathogen inoculation ($P = 0.147$ and $P = 0.196$, respectively), in marked contrast to no significant effect in the monoculture ($P = 0.996$). The activation of SA-dependent responses can be coordinated by ECM colonisation (Pozo & Azcón-Aguilar, 2007). In the presence of both ECM fungi and *Phytophthora* spp., there was even a potential association between the increase in signalling molecules (SA and JA) and a systemic response with the production of secondary metabolites (*i.e.* phenolics) for both species in the mixture. Similar results were observed in *Capsicum annuum* when simultaneously inoculated with the oomycete *Phytophthora capsici* and AM fungi (Ozgonen *et al.*, 2009). Ectomycorrhizal fungi inhibit the negative effect of two species of *Phytophthora* in *Castanea sativa* seedlings, likely by providing a physical barrier around the roots (Branzanti *et al.*, 1999). Although there is no evidence of colonisation of roots of Proteaceae like *B. menziesii* by mycorrhizal fungi, the presence of the ECM fungi induced molecular responses in roots of *B. menziesii*. We propose that the higher concentrations of SA in roots of *B. menziesii* in the presence of ECM fungi may result from (1) a negative interaction induced by incompatibility with the roots of *B. menziesii* in the presence of *E. todtiana* (Pozo *et al.*, 2015; Benjamin *et al.*, 2022) or (2) signals emitted by *E. todtiana* or mycorrhizal hyphae to the roots of *B. menziesii* (Babikova *et al.*, 2013; Gorzelak *et al.*, 2015; Johnson & Gilbert, 2015). The ECM fungi may have been perceived as potential pathogens by roots of the non-mycorrhizal *B. menziesii*, but the origin of signals in the presence of mycorrhizal *E. todtiana* remains unknown. Interactions between neighbours do not require physical contact but may involve either water-soluble or volatile signals (Birkett *et al.*, 2001; Bais *et al.*, 2006; Weston & Mathesius, 2013; Sugimoto *et al.*, 2014; Erb, 2018). Whether those putative signals contributed to priming defence responses against *Phytophthora* spp. requires further investigation.

Conclusions

This study highlights the complex and intertwined nature of facilitative and competitive interactions between a mycorrhizal and a non-mycorrhizal species and their responses to

soil-borne pathogens in extremely P-impooverished environments. Our results show that ECM fungi contributed to the competitive component of the interaction between *B. menziesii* and *E. todtiana* by inducing phytochemical responses in roots of *B. menziesii*. This highlights the importance of all four players – mycorrhizal and non-mycorrhizal plants, ECM fungi and pathogens – in shaping plant megadiversity (Laliberté *et al.*, 2015). Further investigation is warranted to explore the non-nutritional roles of ectomycorrhizas, particularly their involvement in defence against native *Phytophthora* species. Future investigations, including long-term studies, focusing on different combinations of species or considering other biotic and abiotic factors (*e.g.*, herbivory and microbiome) are needed to fully understand how interactions among plant species shape species diversity in severely nutrient-impooverished environments.

Acknowledgements

CEG is supported by a University Postgraduate Award and Scholarship for International Research Fees from The University of Western Australia. Funding was provided by the Australian Research Council grants DP200101013 to HL and PMF and FT170100195 to KR. We thank Diane White for providing the *Pisolithus* and *Phytophthora* isolates and Bill Dunstan for assistance in preparing the *Phytophthora* subcultures. We thank Megan Ryan and Felipe Albornoz for discussions on the preparation and inoculation of the ECM fungi. We thank Maëva Tremblay for assistance with secondary metabolite analyses. We thank Rob Creasy and Bill Piasini for their help in the glasshouse, and Amelia Shepherdson and Michael Ross for assistance throughout the experiment and during harvest of the plants. We thank Michael Renton and Hugo Salinas for their help with statistical analyses. Open access publishing facilitated by The University of Western Australia, as part of the Wiley - The University of Western Australia agreement via the Council of Australian University Librarians.

Author contributions

CEG, HL, PMF, KR, PEH and TIB designed the study. CEG performed the experiment and collected the data. GG performed the phytohormone analyses. CEG and DM performed microscopic observations. CEG, PMF, HL, PEH, KR and FdT analysed the data. CEG, FdT and PD developed the figures. CEG wrote the manuscript. All authors contributed critically to improve the manuscript and gave final approval for publication.

Data availability

The data that support the findings of this study are freely available at doi: [10.26182/MX6Q-GE51](https://doi.org/10.26182/MX6Q-GE51) (DATASET-Facilitative and competitive interactions between mycorrhizal and nonmycorrhizal plants in an extremely phosphorus-impooverished environment: role of ECM fungi and native oomycete pathogens in shaping species coexistence).

References

- Abbott LK, Robson AD, Boer G. 1984.** The effect of phosphorus on the formation of hyphae in soil by the vesicular-arbuscular mycorrhizal fungus *Glomus fasciculatum*. *New Phytologist* **97**: 437–446.
- Albornoz FE, Burgess TI, Lambers H, Etehellis H, Laliberté E. 2017.** Native soilborne pathogens equalize differences in competitive ability between plants of contrasting nutrient-acquisition strategies. *Journal of Ecology* **105**: 549–557.
- Albornoz FE, Dixon KW, Lambers H. 2021.** Revisiting mycorrhizal dogmas: are mycorrhizas really functioning as they are widely believed to do? *Soil Ecology Letters* **3**: 73–82.
- Al-Namazi AA, El-Bana MI, Bonser SP. 2017.** Competition and facilitation structure plant communities under nurse tree canopies in extremely stressful environments. *Ecology and Evolution* **7**: 2747–2755.
- Ashford AE, Allaway WG, Peterson CA, Cairney JWG. 1989.** Nutrient transfer and the fungus-root interface. *Australian Journal of Plant Physiology* **16**: 85–97.
- Avanci NC, Luche DD, Goldman GH, Goldman MHS. 2010.** Jasmonates are phytohormones with multiple functions, including plant defense and reproduction. *Genetics and Molecular Research* **9**: 484–505.
- Babikova Z, Gilbert L, Bruce TJA, Birkett M, Caulfield JC, Woodcock C, Pickett JA, Johnson D. 2013.** Underground signals carried through common mycelial networks warn neighbouring plants of aphid attack. *Ecology Letters* **16**: 835–843.
- Bais HP, Weir TL, Perry LG, Gilroy S, Vivanco JM. 2006.** The role of root exudates in rhizosphere interactions with plants and other organisms. *Annual Review of Plant Biology* **57**: 233–266.

- Basso V, Kohler A, Miyauchi S, Singan V, Guinet F, Šimura J, Novák O, Barry KW, Amirebrahimi M, Block J, et al. 2020.** An ectomycorrhizal fungus alters sensitivity to jasmonate, salicylate, gibberellin, and ethylene in host roots. *Plant, Cell & Environment* **43**: 1047–1068.
- Belhaj R, McComb J, Burgess TI, Hardy GESJ. 2018.** Pathogenicity of 21 newly described *Phytophthora* species against seven Western Australian native plant species. *Plant Pathology* **67**: 1140–1149.
- Benjamin G, Pandharikar G, Frendo P. 2022.** Salicylic acid in plant symbioses: beyond plant pathogen interactions. *Biology* **11**: 861.
- Birkett MA, Chamberlain K, Hooper AM, Pickett JA. 2001.** Does allelopathy offer real promise for practical weed management and for explaining rhizosphere interactions involving higher plants? *Plant and Soil* **232**: 31–39.
- Bolan NS, Robson AD, Barrow NJ. 1984.** Increasing phosphorus supply can increase the infection of plant roots by vesicular-arbuscular mycorrhizal fungi. *Soil Biology and Biochemistry* **16**: 419–420.
- Branzanti MB, Rocca E, Pisi A. 1999.** Effect of ectomycorrhizal fungi on chestnut ink disease. *Mycorrhiza* **9**: 103–109.
- de Britto Costa P, Staudinger C, Veneklaas EJ, Oliveira RS, Lambers H. 2021.** Root positioning and trait shifts in *Hibbertia racemosa* as dependent on its neighbour's nutrient-acquisition strategy. *Plant, Cell & Environment* **44**: 1257–1267.
- Brooker RW, Maestre FT, Callaway RM, Lortie CL, Cavieres LA, Kunstler G, Liancourt P, Tielbörger K, Travis JMJ, Anthelme F, et al. 2008.** Facilitation in plant communities: the past, the present, and the future. *Journal of Ecology* **96**: 18–34.
- Brundrett MC, Tedersoo L. 2020.** Resolving the mycorrhizal status of important northern hemisphere trees. *Plant and Soil* **454**: 3–34.
- Burgess TI, Edwards J, Drenth A, Massenbauer T, Cunnington J, Mostowfizadeh-Ghalamfarsa R, Dinh Q, Liew ECY, White D, Scott P, et al. 2021.** Current status of *Phytophthora* in Australia. *Persoonia - Molecular Phylogeny and Evolution of Fungi* **47**: 151–177.
- Burgess TI, Malajczuk N, Grove TS. 1993.** The ability of 16 ectomycorrhizal fungi to increase growth and phosphorus uptake of *Eucalyptus globulus* Labill. and *E. diversicolor* F. Muell. *Plant and Soil* **153**: 155–164.
- Callaway RM, Walker LR. 1997.** Competition and facilitation: a synthetic approach to interactions in plant communities. *Ecology* **78**: 1958–1965.

- Canton GC, Bertolazi AA, Cogo AJD, Eutrópio FJ, Melo J, Souza SB De, Krohling CA, Campostrini E, Gomes A, Façanha AR, et al. 2016.** Biochemical and ecophysiological responses to manganese stress by ectomycorrhizal fungus *Pisolithus tinctorius* and in association with *Eucalyptus grandis*. *Mycorrhiza* **26**: 475–487.
- De Groot CC, Marcelis LFM, Van Den Boogaard R, Kaiser WM, Lambers H. 2003.** Interaction of nitrogen and phosphorus nutrition in determining growth. *Plant and Soil* **248**: 257–268.
- Durner J, Shah J, Klessig DF. 1997.** Salicylic acid and disease resistance in plants. *Trends in Plant Science* **2**: 266–274.
- Enebe MC, Erasmus M. 2023.** Susceptibility and plant immune control—a case of mycorrhizal strategy for plant colonization, symbiosis, and plant immune suppression. *Frontiers in Microbiology* **14**: 1178258.
- Erb M. 2018.** Volatiles as inducers and suppressors of plant defense and immunity — origins, specificity, perception and signaling. *Current Opinion in Plant Biology* **44**: 117–121.
- Fernández I, Cosme M, Stringlis IA, Yu K, de Jonge R, van Wees SCM, Pozo MJ, Pieterse CMJ, van der Heijden MGA. 2019.** Molecular dialogue between arbuscular mycorrhizal fungi and the nonhost plant *Arabidopsis thaliana* switches from initial detection to antagonism. *New Phytologist* **223**: 867–881.
- Glauser G, Vallat A, Balmer D. 2014.** Hormone profiling. *Methods in Molecular Biology* **1062**: 597–608.
- Glazebrook J. 2005.** Contrasting mechanisms of defense against biotrophic and necrotrophic pathogens. *Annual Review of Phytopathology* **43**: 205–227.
- Gleason C, Leelarasamee N, Meldau D, Feussner I. 2016.** OPDA has key role in regulating plant susceptibility to the root-knot nematode *Meloidogyne hapla* in *Arabidopsis*. *Frontiers in Plant Science* **7**: 1–11.
- Gorzalak MA, Asay AK, Pickles BJ, Simard SW. 2015.** Inter-plant communication through mycorrhizal networks mediates complex adaptive behaviour in plant communities. *AoB Plants* **7**: plv050.
- Guillemin J-P, Gianinazzi S, Gianinazzi-Pearson V, Marchal J. 1994.** Contribution of arbuscular mycorrhizas to biological protection of micropropagated pineapple (*Ananas comosus* (L.) Merr) against *Phytophthora cinnamomi* Rands. *Agricultural and Food Science* **3**: 241–251.
- Hardham AR, Blackman LM. 2018.** *Phytophthora cinnamomi*. *Molecular Plant Pathology* **19**: 260–285.

- Hayes P, Turner BL, Lambers H, Laliberté E. 2014.** Foliar nutrient concentrations and resorption efficiency in plants of contrasting nutrient-acquisition strategies along a 2-million-year dune chronosequence. *Journal of Ecology* **102**: 396–410.
- Hüberli D, Tommerup IC, Hardy GESJ. 2000.** False-negative isolations or absence of lesions may cause mis-diagnosis of diseased plants infected with *Phytophthora cinnamomi*. *Australasian Plant Pathology* **29**: 164–169.
- Jimenez Aleman GH, Thirumalaikumar VP, Jander G, Fernie AR, Skirycz A. 2022.** OPDA, more than just a jasmonate precursor. *Phytochemistry* **204**: 113432.
- Johnson D, Gilbert L. 2015.** Interplant signalling through hyphal networks. *New Phytologist* **205**: 1448–1453.
- Johnson PTJ, Ostfeld RS, Keesing F. 2015.** Frontiers in research on biodiversity and disease. *Ecology Letters* **18**: 1119–1133.
- Jung SC, Martinez-Medina A, Lopez-Raez JA, Pozo MJ. 2012.** Mycorrhiza-induced resistance and priming of plant defenses. *Journal of Chemical Ecology* **38**: 651–664.
- Kroymann J. 2011.** Natural diversity and adaptation in plant secondary metabolism. *Current Opinion in Plant Biology* **14**: 246–251.
- Laliberté E, Lambers H, Burgess TI, Wright SJ. 2015.** Phosphorus limitation, soil-borne pathogens and the coexistence of plant species in hyperdiverse forests and shrublands. *New Phytologist* **206**: 507–521.
- Laliberté E, Turner BL, Costes T, Pearse SJ, Wyrwoll KH, Zemunik G, Lambers H. 2012.** Experimental assessment of nutrient limitation along a 2-million-year dune chronosequence in the south-western Australia biodiversity hotspot. *Journal of Ecology* **100**: 631–642.
- Lambers H, Ahmedi I, Berkowitz O, Dunne C, Finnegan PM, Hardy GESJ, Jost R, Laliberté E, Pearse SJ, Teste FP. 2013.** Phosphorus nutrition of phosphorus-sensitive Australian native plants: threats to plant communities in a global biodiversity hotspot. *Conservation Physiology* **1**: cot010.
- Lambers H, Albornoz FE, Kotula L, Laliberté E, Ranathunge K, Teste FP, Zemunik G. 2018.** How belowground interactions contribute to the coexistence of mycorrhizal and non-mycorrhizal species in severely phosphorus-impooverished hyperdiverse ecosystems. *Plant and Soil* **424**: 11–33.
- Lambers H, Teste FP. 2013.** Interactions between arbuscular mycorrhizal and non-mycorrhizal plants: do non-mycorrhizal species at both extremes of nutrient availability play the same game? *Plant, Cell & Environment* **36**: 1911–1915.

- Lambers H, Wright IJ, Guilherme Pereira C, Bellingham PJ, Bentley LP, Boonman A, Cernusak LA, Foulds W, Gleason SM, Gray EF, et al. 2021.** Leaf manganese concentrations as a tool to assess belowground plant functioning in phosphorus-impooverished environments. *Plant and Soil* **461**: 43–61.
- Lê S, Josse J, Husson F. 2008.** FactoMineR: an R package for multivariate analysis. *Journal of Statistical Software* **25**: 1–18.
- Lehmann A, Rillig MC. 2015.** Arbuscular mycorrhizal contribution to copper, manganese and iron nutrient concentrations in crops – a meta-analysis. *Soil Biology and Biochemistry* **81**: 147–158.
- Lekberg Y, Bever JD, Bunn RA, Callaway RM, Hart MM, Kivlin SN, Klironomos J, Larkin BG, Maron JL, Reinhart KO, et al. 2018.** Relative importance of competition and plant-soil feedback, their synergy, context dependency and implications for coexistence. *Ecology Letters* **21**: 1268–1281.
- Martin F, Diez J, Dell B, Delaruelle C. 2002.** Phylogeography of the ectomycorrhizal *Pisolithus* species as inferred from nuclear ribosomal DNA ITS sequences. *New Phytologist* **153**: 345–357.
- Marx DH. 1972.** Ectomycorrhizae as biological deterrents to pathogenic root infections. *Annual Review of Phytopathology* **10**: 429–454.
- Montesinos-Navarro A, Valiente-Banuet A, Verdú M. 2019.** Mycorrhizal symbiosis increases the benefits of plant facilitative interactions. *Ecography* **42**: 447–455.
- Muler AL, Oliveira RS, Lambers H, Veneklaas EJ. 2014.** Does cluster-root activity benefit nutrient uptake and growth of co-existing species? *Oecologia* **174**: 23–31.
- Ozgonen H, Erkilic A. 2007.** Growth enhancement and Phytophthora blight (*Phytophthora capsici* Leonian) control by arbuscular mycorrhizal fungal inoculation in pepper. *Crop Protection* **26**: 1682–1688.
- Ozgonen H, Yardimci N, Cular Kilic H. 2009.** Induction of phenolic compounds and pathogenesis-related proteins by mycorrhizal fungal inoculations against *Phytophthora capsici* Leonian in pepper. *Pakistan Journal of Biological Sciences* **12**: 1181–1187.
- Pate JS, Beard JS. 1984.** *Kwongan, plant life of the sandplain*. Nedlands, WA, Australia: University of Western Australia Press.
- Pinheiro J, Bates D. 2000.** *Mixed-effects models in S and S-PLUS*. New York, NY, USA: Springer.
- Pozo MJ, Azcón-Aguilar C. 2007.** Unraveling mycorrhiza-induced resistance. *Current Opinion in Plant Biology* **10**: 393–398.

- Pozo MJ, Azcón-Aguilar C, Dumas-Gaudot E, Barea JM. 1999.** β -1,3-glucanase activities in tomato roots inoculated with arbuscular mycorrhizal fungi and/or *Phytophthora parasitica* and their possible involvement in bioprotection. *Plant Science* **141**: 149–157.
- Pozo MJ, López-Ráez JA, Azcón-Aguilar C, García-Garrido JM. 2015.** Phytohormones as integrators of environmental signals in the regulation of mycorrhizal symbioses. *New Phytologist* **205**: 1431–1436.
- R Core Team. 2023.** *R: a language and environment for statistical computing*. Vienna, Austria: R Foundation for Statistical Computing.
- Ranathunge K, Thomas RH, Fang X, Peterson CA, Gijzen M, Bernards MA. 2008.** Soybean root suberin and partial resistance to root rot caused by *Phytophthora sojae*. *Phytopathology* **98**: 1179–1189.
- Rea AJ, Burgess TI, Hardy GESJ, Stukely MJC, Jung T. 2011.** Two novel and potentially endemic species of *Phytophthora* associated with episodic dieback of Kwongan vegetation in the south-west of Western Australia. *Plant Pathology* **60**: 1055–1068.
- Ricklefs RE. 2010.** Evolutionary diversification, coevolution between populations and their antagonists, and the filling of niche space. *Proceedings of the National Academy of Sciences of the United States of America* **107**: 1265–1272.
- Romo Pérez M, Merkt N, Zikeli S, Zörb C. 2018.** Quality aspects in open-pollinated onion varieties from Western Europe. *Journal of Applied Botany and Food Quality* **91**: 69–78.
- Santas J, Carbó R, Gordon MH, Almajano MP. 2008.** Comparison of the antioxidant activity of two Spanish onion varieties. *Food Chemistry* **107**: 1210–1216.
- Sarker SR, Burgess TI, Hardy GESJ, McComb J. 2023.** Closing the gap between the number of *Phytophthora* species isolated through baiting a soil sample and the number revealed through metabarcoding. *Mycological Progress* **22**: 39.
- Schneider-Maunoury L, Deveau A, Moreno M, Todesco F, Belmondo S, Murat C, Courty P, Jąkalski M, Selosse M. 2020.** Two ectomycorrhizal truffles, *Tuber melanosporum* and *T. aestivum*, endophytically colonise roots of non-ectomycorrhizal plants in natural environments. *New Phytologist* **225**: 2542–2556.
- Schneider-Maunoury L, Leclercq S, Clément C, Covès H, Lambourdière J, Sauve M, Richard F, Selosse MA, Taschen E. 2018.** Is *Tuber melanosporum* colonizing the roots of herbaceous, non-ectomycorrhizal plants? *Fungal Ecology* **31**: 59–68.
- Shane MW, Cramer MD, Funayama-Noguchi S, Cawthray GR, Millar AH, Day DA, Lambers H. 2004.** Developmental physiology of cluster-root carboxylate synthesis and

exudation in harsh hakea. Expression of phosphoenolpyruvate carboxylase and the alternative oxidase. *Plant Physiology* **135**: 549–560.

Shane MW, De Vos M, De Roock S, Cawthray GR, Lambers H. 2003. Effects of external phosphorus supply on internal phosphorus concentration and the initiation, growth and exudation of cluster roots in *Hakea prostrata* R.Br. *Plant and Soil* **248**: 209–219.

Shane MW, Lambers H. 2005. Cluster roots: a curiosity in context. *Plant and Soil* **274**: 101–125.

Shen Q. 2023. *Phosphorus-acquisition and phosphorus-utilisation strategies of native plants in south-western Australia*. Perth, WA, Australia: University of Western Australia.

Shen Q, Ranathunge K, Zhong H, Finnegan PM, Lambers H. 2024. Facilitation of phosphorus acquisition by *Banksia attenuata* allows *Adenanthos cygnorum* (Proteaceae) to extend its range into severely phosphorus-impooverished habitats. *Plant and Soil* **496**: 51–70.

Simamora A V., Stukely MJC, St Hardy GEJ, Burgess TI. 2015. *Phytophthora boodjera* sp. nov., a damping-off pathogen in production nurseries and from urban and natural landscapes, with an update on the status of *P. alticola*. *IMA Fungus* **6**: 319–335.

Smith SE, Jakobsen I, Grønlund M, Smith FA. 2011. Roles of arbuscular mycorrhizas in plant phosphorus nutrition: interactions between pathways of phosphorus uptake in arbuscular mycorrhizal roots have important implications for understanding and manipulating plant phosphorus acquisition. *Plant Physiology* **156**: 1050–1057.

Smith SE, Read DJ. 2008. *Mycorrhizal Symbiosis*. London: Academic Press and Elsevier.

Standish RJ, Albornoz FE, Morald TK, Hobbs RJ, Tibbett M. 2021. Mycorrhizal symbiosis and phosphorus supply determine interactions among plants with contrasting nutrient-acquisition strategies. *Journal of Ecology* **109**: 3892–3902.

Staudinger C, Renton M, Leopold M, Wasaki J, Veneklaas EJ, de Britto Costa P, Boitt G, Lambers H. 2024. Interspecific facilitation of micronutrient uptake between cluster-root-bearing trees and non-cluster rooted-shrubs in a *Banksia* woodland. *Plant and Soil* **496**: 71–82.

Sugimoto K, Matsui K, Iijima Y, Akakabe Y, Muramoto S, Ozawa R, Uefune M, Sasaki R, Alamgir KM, Akitake S, et al. 2014. Intake and transformation to a glycoside of (Z)-3-hexenol from infested neighbors reveals a mode of plant odor reception and defense. *Proceedings of the National Academy of Sciences of the United States of America* **111**: 7144–7149.

- Teste FP, Veneklaas EJ, Dixon KW, Lambers H. 2014.** Complementary plant nutrient-acquisition strategies promote growth of neighbour species. *Functional Ecology* **28**: 819–828.
- Thakur MP, van der Putten WH, Wilschut RA, Veen GF (Ciska.), Kardol P, van Ruijven J, Allan E, Roscher C, van Kleunen M, Bezemer TM. 2021.** Plant–soil feedbacks and temporal dynamics of plant diversity–productivity relationships. *Trends in Ecology and Evolution* **36**: 651–661.
- Treseder KK, Allen MF. 2002.** Direct nitrogen and phosphorus limitation of arbuscular mycorrhizal fungi: a model and field test. *New Phytologist* **155**: 507–515.
- Turner BL, Hayes PE, Laliberté E. 2018.** A climosequence of chronosequences in southwestern Australia. *European Journal of Soil Science* **69**: 69–85.
- Turner BL, Laliberté E. 2015.** Soil development and nutrient availability along a 2 million-year coastal dune chronosequence under species-rich Mediterranean shrubland in southwestern Australia. *Ecosystems* **18**: 287–309.
- Vesk PA, Ashford AE, Markovina AL, Allaway WG. 2000.** Apoplasmic barriers and their significance in the exodermis and sheath of *Eucalyptus pilularis*-*Pisolithus tinctorius* ectomycorrhizas. *New Phytologist* **145**: 333–346.
- Vierheilig H, Coughlan AP, Wyss U, Piché Y. 1998.** Ink and vinegar, a simple staining technique for arbuscular-mycorrhizal fungi. *Applied and Environmental Microbiology* **64**: 5004–5007.
- Vlot AC, Sales JH, Lenk M, Bauer K, Brambilla A, Sommer A, Chen Y, Wenig M, Nayem S. 2021.** Systemic propagation of immunity in plants. *New Phytologist* **229**: 1234–1250.
- Wang Y, He X, Yu F. 2022.** Non-host plants: are they mycorrhizal networks players? *Plant Diversity* **44**: 127–134.
- War AR, Paulraj MG, War MY, Ignacimuthu S. 2011.** Role of salicylic acid in induction of plant defense system in chickpea (*Cicer arietinum* L.). *Plant Signaling & Behavior* **6**: 1787–1792.
- Weston LA, Mathesius U. 2013.** Flavonoids: their structure, biosynthesis and role in the rhizosphere, including allelopathy. *Journal of Chemical Ecology* **39**: 283–297.
- Yu R, Su Y, Lambers H, van Ruijven J, An R, Yang H, Yin X, Xing Y, Zhang W, Li L. 2023.** A novel proxy to examine interspecific phosphorus facilitation between plant species. *New Phytologist* **239**: 1637–1650.

Zarcinas BA, Cartwright B, Spouncer LR. 1987. Nitric acid digestion and multi-element analysis of plant material by inductively coupled plasma spectrometry. *Communications in Soil Science and Plant Analysis* **18**: 131–146.

Zemunik G, Turner BL, Lambers H, Laliberté E. 2015. Diversity of plant nutrient-acquisition strategies increases during long-term ecosystem development. *Nature Plants* **1**: 15050.

Zhao X, Lyu Y, Jin K, Lambers H, Shen J. 2021. Leaf phosphorus concentration regulates the development of cluster roots and exudation of carboxylates in *Macadamia integrifolia*. *Frontiers in Plant Science* **11**: 610591.

Supporting Information

Fig. S1 Colonisation of roots of *Eucalyptus todtiana* and *Banksia menziesii* by ectomycorrhizal fungi and *Phytophthora* species.

Fig. S2 Below- and aboveground biomass and root-to-shoot ratios of *Banksia menziesii* and *Eucalyptus todtiana* in monoculture and in mixture, subjected to *Phytophthora* spp. and ectomycorrhizal treatments.

Fig. S3 Cluster-root (CR) biomass and CR-to-non-CR ratios of *Banksia menziesii* in monoculture and in mixture with *Eucalyptus todtiana*, subjected to *Phytophthora* spp. and ectomycorrhizal treatments.

Fig. S4 Manganese concentrations in leaves of *Banksia menziesii* and *Eucalyptus todtiana* in monoculture and in mixture, subjected to *Phytophthora* spp. and ectomycorrhizal treatments.

Fig. S5 Total flavonoid concentrations in roots of *Banksia menziesii* and *Eucalyptus todtiana* in monoculture and in mixture, subjected to *Phytophthora* spp. and ectomycorrhizal treatments.

Fig. S6 Jasmonoyl-isoleucine (JA-Ile) and 12-oxo-phytodienoic acid (OPDA) concentrations in roots of *Banksia menziesii* and *Eucalyptus todtiana* in monoculture and in mixture, subjected to *Phytophthora* spp. and ectomycorrhizal treatments.

Fig. S7 Distribution of *Banksia menziesii* and *Eucalyptus todtiana* in monoculture and in mixture, subjected to *Phytophthora* spp. and ectomycorrhizal treatments, along a defence-strategy space.

Table S1 Output of multifactorial linear mixed-effect models for growth-related traits of *Banksia menziesii* in the mixture.

Table S2 Output of the principal component analysis of defence-related compounds in roots of *Banksia menziesii* and *Eucalyptus todtiana*.

Table S3 Output of the principal component analysis of defence-related compounds in roots of *Banksia menziesii*.

Table S4 Output of the principal component analysis of defence-related compounds in roots of *Eucalyptus todtiana*.

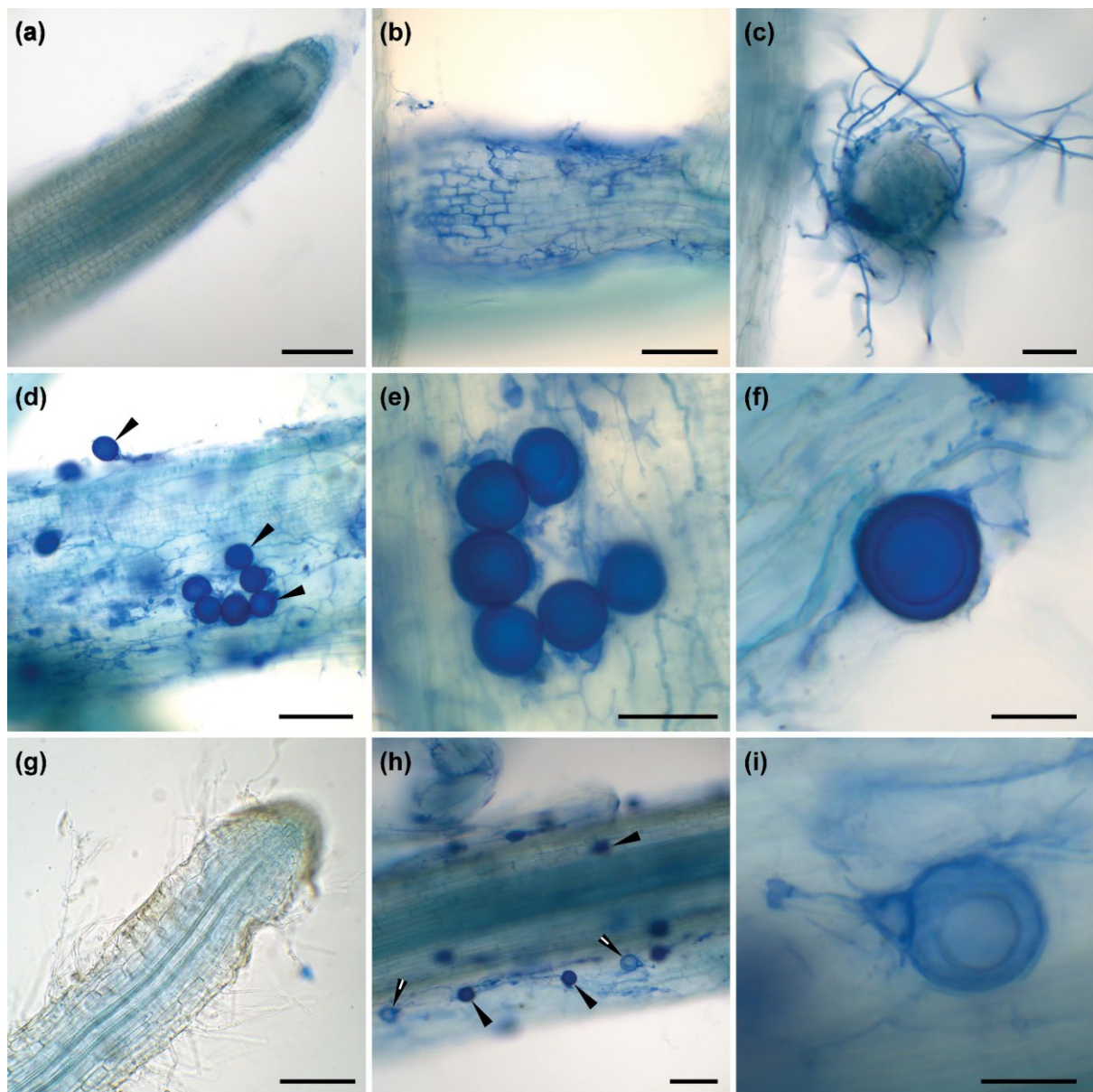


Fig. S1 Colonisation of roots of *Eucalyptus todtiana* (a–f) and *Banksia menziesii* (g–i) by ectomycorrhizal (ECM) fungi and *Phytophthora* spp. pathogens. (a) Root tip region of *E. todtiana*; (b–c) root colonisation by ECM fungi showing fungal sheath and extraradical hyphae; (d) extensive colonisation at the root surface of *E. todtiana* by *Phytophthora* spp. showing hyphae and oospores (pointing arrowheads); (e–f) oospores of *Phytophthora* spp. at the root surface of *E. todtiana*; (g) root tip region of *B. menziesii* showing extensive root hair development; (h) extensive colonisation at the root surface of *B. menziesii* by *Phytophthora* spp. showing hyphae, oospores and aborted oospores (pointing split arrowheads); (i) aborted oospore at the root surface of *B. menziesii*. Scale bars = 100 μm for (a), (b), (d), (g) and (h); 50 μm for (c) and (e); and 25 μm for (f) and (i).

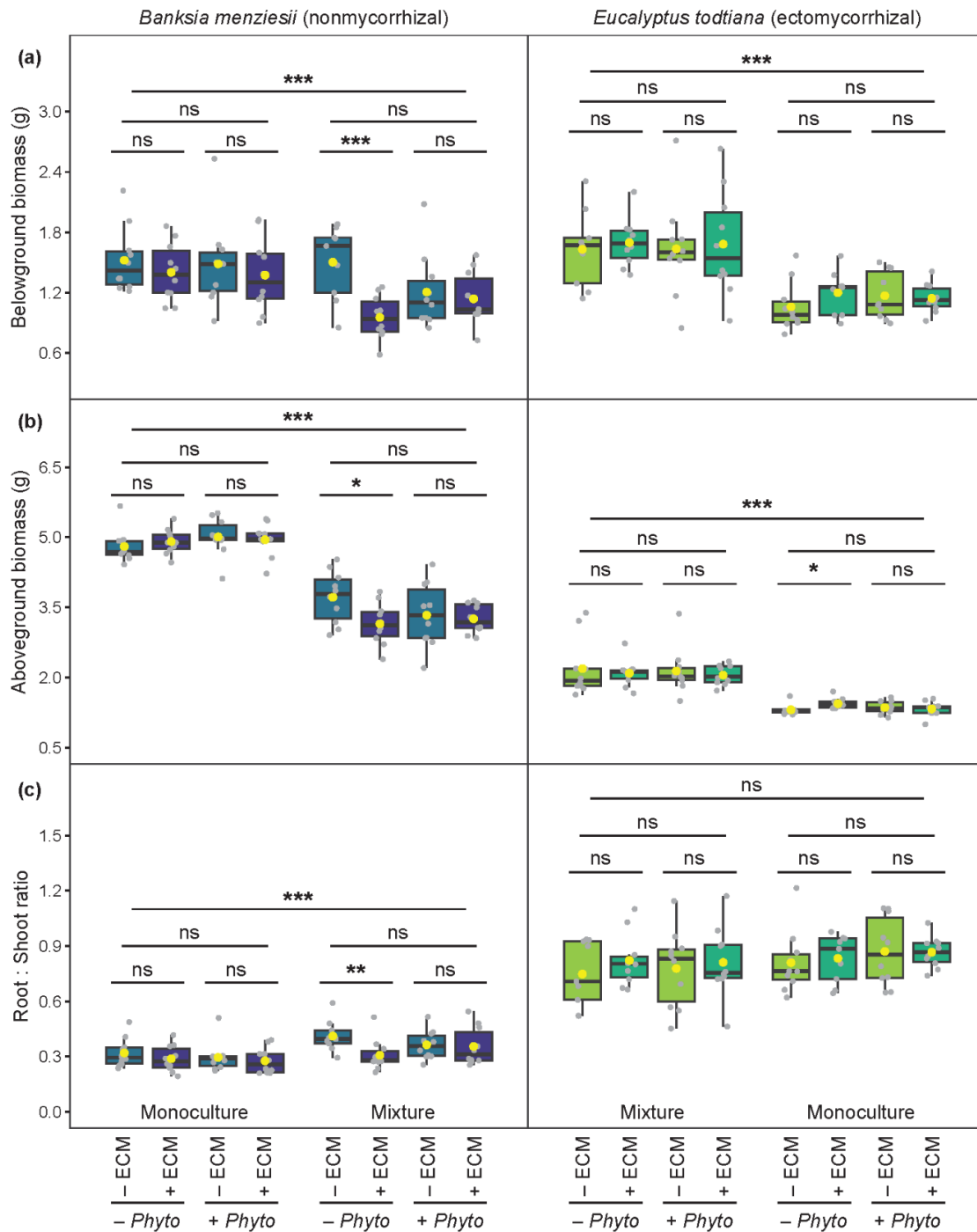


Fig. S2 Belowground (a), aboveground (b) biomass, and root to shoot ratios (c) of *Banksia menziesii* (left panels) and *Eucalyptus tottiana* (right panels) grown in monoculture or in mixture, inoculated with *Phytophthora* pathogens (+ *Phyto*) or not (- *Phyto*) and/or with ectomycorrhizal (ECM) fungi (+ ECM, dark colour) or not (- ECM, light colour). The bottom and top of the boxes denote the 25th and 75th percentiles, respectively, and the central line is the median, and the yellow dot represents the mean ($n = 8-10$). Whiskers extend to the most extreme data points up to a maximum of 1.5 times the lower and upper quartiles. Significant differences between treatments were tested with linear mixed-effect models (* $P < 0.05$; ** $P < 0.01$; *** $P < 0.001$; ns, not significant, *i.e.* $P > 0.1$).

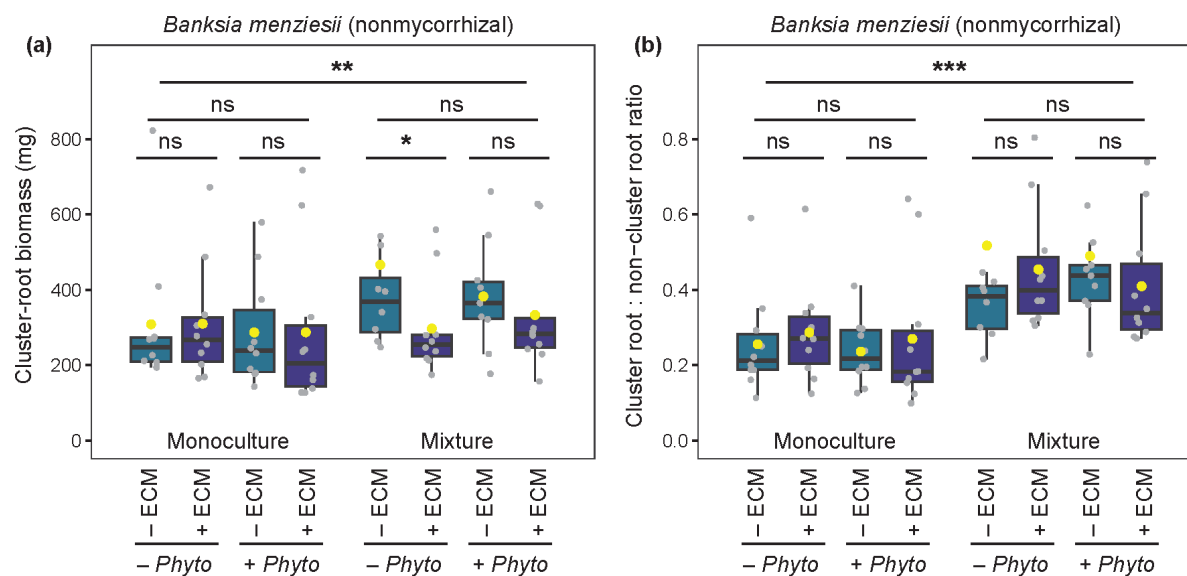


Fig. S3 Cluster-root (CR) biomass (a) and CR to non-CR ratios (b) of *Banksia menziesii* grown in monoculture or in mixture, inoculated with *Phytophthora* pathogens (+ *Phyto*) or not (– *Phyto*) and/or with ectomycorrhizal (ECM) fungi (+ ECM, dark colour) or not (– ECM, light colour). The bottom and top of the boxes denote the 25th and 75th percentiles, respectively, and the central line is the median, and the yellow dot represents the mean ($n = 8-10$). Whiskers extend to the most extreme data points up to a maximum of 1.5 times the lower and upper quartiles. Significant differences between treatments were tested with linear mixed-effect models (* $P < 0.05$; ** $P < 0.01$; *** $P < 0.001$; ns, not significant, *i.e.* $P > 0.1$).

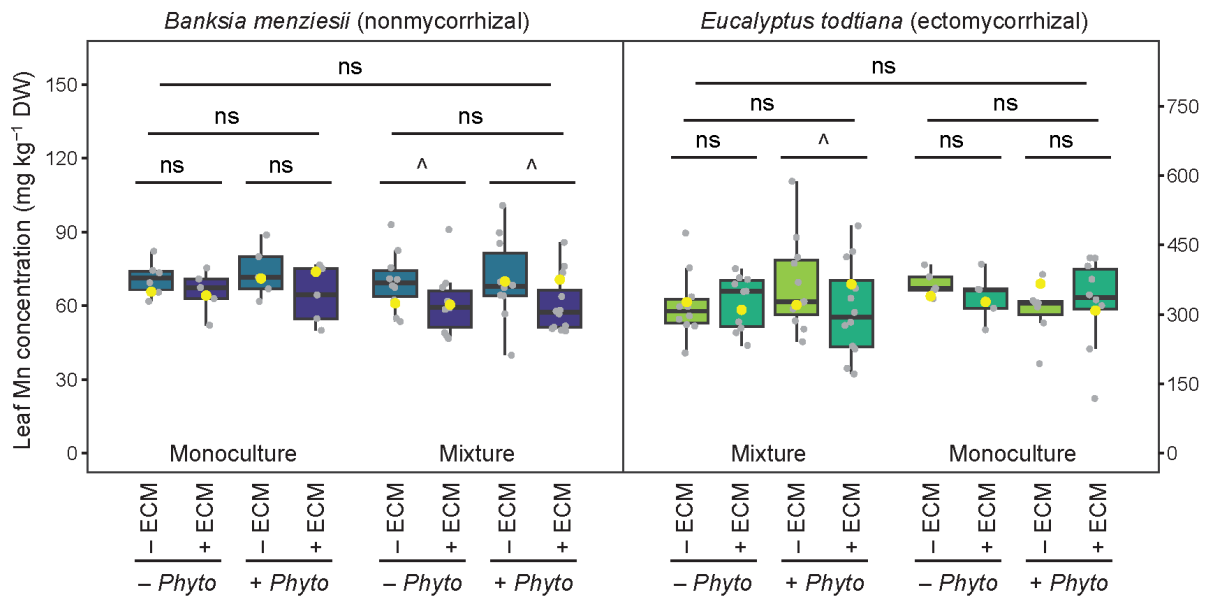


Fig. S4 Total leaf manganese (Mn) concentration of *Banksia menziesii* (left panel) and *Eucalyptus tottiana* (right panel) grown in monoculture or in mixture, inoculated with *Phytophthora* pathogens (+ *Phyto*) or not (– *Phyto*) and/or with ectomycorrhizal (ECM) fungi (+ ECM, dark colour) or not (– ECM, light colour). The bottom and top of the boxes denote the 25th and 75th percentiles, respectively, and the central line is the median, and the yellow dot represents the mean ($n = 8–10$). Whiskers extend to the most extreme data points up to a maximum of 1.5 times the lower and upper quartiles. Note different y-axis range for the two species. Significant differences between treatments were tested with linear mixed-effect models (^ $P < 0.1$; ns, not significant, *i.e.* $P > 0.1$).

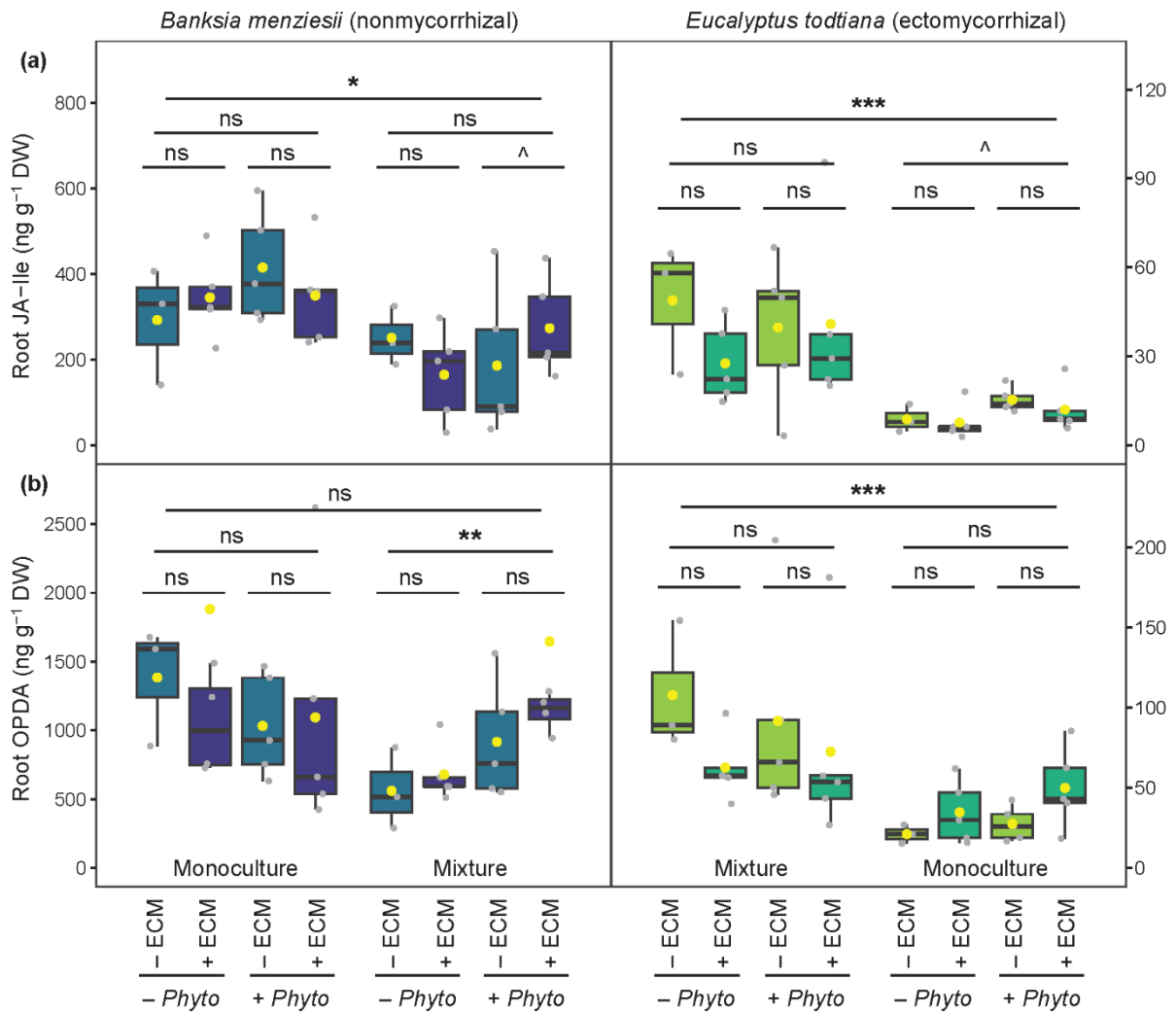


Fig. S6 Root jasmonoyl-isoleucine (JA-Ile) (a) and 12-oxo-phytodienoic acid (OPDA) (b) concentrations for *Banksia menziesii* (left panels) and *Eucalyptus tottiana* (right panels) grown in monoculture or in mixture, inoculated with *Phytophthora* pathogens (+ *Phyto*) or not (- *Phyto*) and/or with ectomycorrhizal (ECM) fungi (+ ECM, dark colour) or not (- ECM, light colour). The bottom and top of the boxes denote the 25th and 75th percentiles, respectively, and the central line is the median, and the yellow dot represents the mean ($n = 3-5$). Whiskers extend to the most extreme data points up to a maximum of 1.5 times the lower and upper quartiles. Note different y-axis range for the two species. Significant differences between treatments were tested with linear mixed-effect models (^ $P < 0.1$; * $P < 0.05$; ** $P < 0.01$; *** $P < 0.001$; ns, not significant, *i.e.* $P > 0.1$).

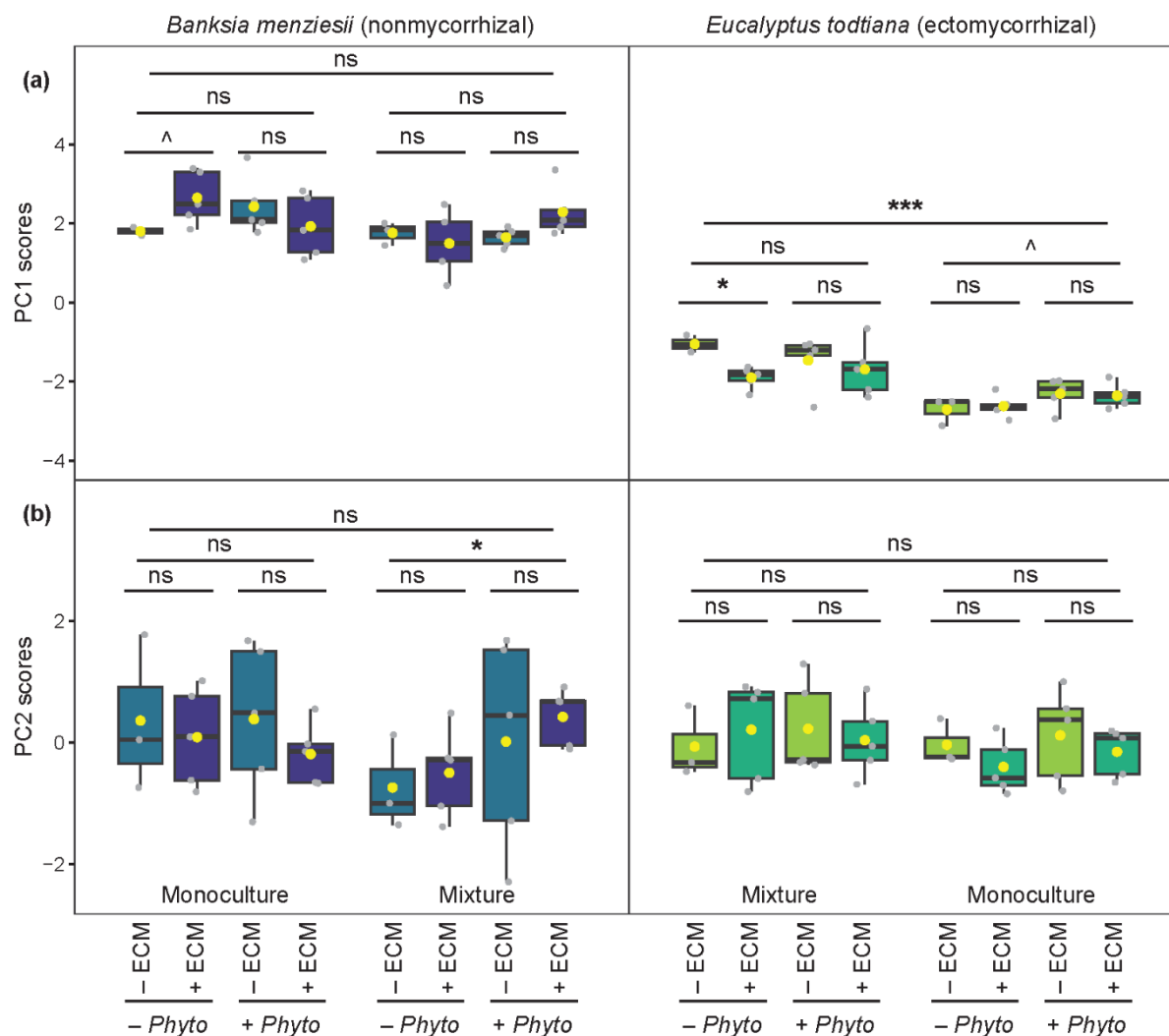


Fig. S7 Distribution of *Banksia menziesii* and *Eucalyptus tottiana* along the defence-strategy space defined in the principal component analysis (PCA) shown in Fig. 5b. Differences between *B. menziesii* (left panels) and *E. tottiana* (right panels) grown in monoculture or in mixture, inoculated with *Phytophthora* pathogens (+ *Phyto*) or not (- *Phyto*) and/or with ectomycorrhizal (ECM) fungi (+ ECM, dark colour) or not (- ECM, light colour) were tested along the first (a) and second (b) principal components of the PCA. Output of the PCA is given in Table S2. The bottom and top of the boxes denote the 25th and 75th percentiles, respectively, and the central line is the median, and the yellow dot represents the mean ($n = 3-5$). Whiskers extend to the most extreme data points up to a maximum of 1.5 times the lower and upper quartiles. Significant differences between treatments were tested with linear mixed-effect models (^ $P < 0.1$; * $P < 0.05$; ** $P < 0.01$; *** $P < 0.001$; ns, not significant, *i.e.* $P > 0.1$).

Table S1 The *P*-values of multifactorial linear mixed-effect models for growth-related traits of *Banksia menziesii* in the mixture, and the significance of differences between – *Phyto*/– ECM and other treatments; ^ $P < 0.1$; * $P < 0.05$; ** $P < 0.01$; *** $P < 0.001$. Significant values ($P < 0.1$) are **bolded** for visualisation and the degrees of freedom (*df*) are given in brackets. ECM, ectomycorrhizal fungi; *Phyto*, *Phytophthora* spp.

	– <i>Phyto</i>		+ <i>Phyto</i>	
	+ ECM	– ECM	– ECM	+ ECM
Total biomass (df = 132)	0.006**	0.389	0.389	0.055^
Aboveground biomass (df = 134)	0.064^	0.459	0.459	0.113
Belowground biomass (df = 132)	<0.001***	0.032*	0.032*	0.035*
Root : Shoot ratio (df = 132)	0.017*	0.630	0.630	0.390
Cluster-root biomass (df = 62)	0.076^	0.853	0.853	0.256
Cluster root : Root ratio (df = 62)	0.990	0.915	0.915	0.979
Leaf [P] (df = 108)	0.878	<0.001***	<0.001***	0.042*
Leaf P content (df = 94)	0.032*	<0.001***	<0.001***	0.014*

Table S2 Output of the principal component analysis (PCA) of defence-related compounds in roots of *Banksia menziesii* and *Eucalyptus tottiana*, as shown in Fig. 5b. Data shown are the eigenvalue, the percentage and cumulative percentage of variance explained by each subsequent principal component (PC), and the contribution of each trait to the PCs. The PCs explaining $\geq 95\%$ of the cumulated variance are shown. The largest contribution for each trait is **bolded** for visualisation. JA, jasmonic acid; JA-Ile, jasmonoyl-isoleucine; OPDA, 12-oxo-phytodienoic acid; SA, salicylic acid.

	PC1	PC2	PC3	PC4
Eigenvalue	4.5	0.7	0.4	0.3
Variance (%)	75.7	11.1	6.3	4.5
Cumulated variance (%)	75.7	86.8	93.1	97.6
Phenolics	-0.86	0.23	0.04	0.45
Flavonoids	-0.71	0.66	0.09	-0.23
SA	0.81	0.33	-0.48	0.06
JA	0.94	0.18	0.26	0.06
JA-Ile	0.93	0.18	0.26	0.07
OPDA	0.95	0.08	0.00	0.05

Table S3 Output of the principal component analysis (PCA) of defence-related compounds in roots of *Banksia menziesii*, as shown in Fig. 5c. Data shown are the eigenvalue, the percentage and cumulative percentage of variance explained by each subsequent principal component (PC), and the contribution of each trait to the PCs. The PCs explaining $\geq 90\%$ of the cumulated variance are shown. The largest contribution for each trait is **bolded** for visualisation. JA, jasmonic acid; JA-Ile, jasmonoyl-isoleucine; OPDA, 12-oxo-phytodienoic acid; SA, salicylic acid.

	PC1	PC2	PC3	PC4
Eigenvalue	2.3	1.3	1.2	0.7
Variance (%)	38.0	22.4	19.2	11.3
Cumulated variance (%)	38.0	60.4	79.6	90.9
Phenolics	0.27	0.76	-0.13	0.52
Flavonoids	0.38	0.62	-0.45	-0.33
SA	0.40	0.40	0.63	-0.45
JA	0.91	-0.34	-0.18	0.06
JA-Ile	0.85	-0.31	-0.31	-0.08
OPDA	0.59	-0.05	0.64	0.30

Table S4 Output of the principal component analysis (PCA) of defence-related compounds in roots of *Eucalyptus tottiana*, as shown in Fig. 5f. Data shown are the eigenvalue, the percentage and cumulative percentage of variance explained by each subsequent principal component (PC), and the contribution of each trait to the PCs. The PCs explaining $\geq 90\%$ of the cumulated variance are shown. The largest contribution for each trait is **bolded** for visualisation. JA, jasmonic acid; JA-Ile, jasmonoyl-isoleucine; OPDA, 12-oxo-phytodienoic acid; SA, salicylic acid.

	PC1	PC2	PC3	PC4	PC5
Eigenvalue	2.2	1.2	1.1	0.7	0.5
Variance (%)	37.2	20.4	18.9	12.3	9.1
Cumulated variance (%)	37.2	57.6	76.5	88.8	97.9
Phenolics	0.12	0.04	0.88	0.44	-0.11
Flavonoids	-0.08	0.81	0.33	-0.40	0.27
SA	0.27	0.75	-0.37	0.36	-0.31
JA	0.89	-0.08	0.26	-0.26	-0.06
JA-Ile	0.90	-0.07	-0.07	-0.24	-0.25
OPDA	0.73	-0.00	-0.20	0.36	0.54

CHAPTER FOUR

Proteaceae with high photosynthetic phosphorus-use efficiency on the conservative end of the leaf economics spectrum allocate phosphorus to biochemical fractions differently



Banksia ericifolia (Proteaceae)

This chapter was submitted to *New Phytologist* on 29 February 2024
and is currently under review.

The main text is presented, followed by the Supporting Information.

Proteaceae with high photosynthetic phosphorus-use efficiency on the conservative end of the leaf economics spectrum allocate phosphorus to biochemical fractions differently

Clément E. Gille¹, Patrick E. Hayes¹, Kosala Ranathunge¹, Shu Tong Liu¹, Félix de Tombeur^{1,2}, Hans Lambers¹ and Patrick M. Finnegan¹

¹School of Biological Sciences, The University of Western Australia, 35 Stirling Highway, Perth, WA, 6009, Australia; ²CEFE, CNRS, EPHE, IRD, University of Montpellier, 34000, Montpellier, France

Author for correspondence: *Clément E. Gille*

Email: clement.gille@uwa.edu.au

Summary

- In severely phosphorus (P)-impoverished environments, plants have evolved adaptations allowing them to use P very efficiently. Yet, it is unclear how P allocation in leaves contributes to their photosynthetic P-use efficiency (PPUE) and position along the leaf economics spectrum (LES). We address this question in five highly P-efficient species from each of two Proteaceae genera: *Banksia* and *Hakea*.

- We characterised traits in leaves of *Banksia* and *Hakea* associated with the LES: leaf mass per area (LMA), light-saturated photosynthetic rates, P and nitrogen concentrations, and PPUE. We also determined leaf P partitioning to five biochemical fractions (lipid P, nucleic acid P, metabolite P, inorganic P, residual P).

- For both genera, PPUE was negatively and positively correlated with fractional allocation of P to lipids and metabolites, respectively, but PPUE was negatively correlated with residual P only for *Banksia* species. Phosphorus-allocation patterns significantly explained PPUE but not to the position of *Banksia* and *Hakea* species at the conservative end of the LES (*i.e.* highly-conservative traits, high LMA, low nutrient concentrations).

- We conclude that distinct P-allocation patterns enable species from different genera to achieve high PPUE in extremely P-impoverished environments and provide insights into the interplay between the various P fractions.

Key words: leaf economics spectrum, nitrogen, nucleic acids, nutrient-use efficiency, phospholipids, phosphorus fractions, Proteaceae, stoichiometry.

Introduction

Phosphorus (P) is an essential nutrient for plant growth and is involved in many physiological processes. Thus, P fertilisation is pivotal to high productivity in agriculture. However, rock-derived P fertilisers are not renewable and global reserves continue to be consumed, mainly in the agricultural sector, due to the dependence of current agricultural systems on P fertilisers (Fixen & Johnston, 2012). Moreover, P limitation in natural terrestrial ecosystems has been widely underestimated (Hou *et al.*, 2020) and is becoming more critical under global change (Wassen *et al.*, 2005; Tian *et al.*, 2022). As such, it is essential to understand how plants use P efficiently to sustain growth under P-limiting conditions.

The leaf economics spectrum (LES) defines a global trade-off that contrasts fast-growing species characterised by acquisitive traits, such as fast nutrient acquisition and mass-based photosynthetic rates, with slow-growing species characterised by conservative traits, such as stronger investment in structure and storage, accompanied with long-lived leaves (Wright *et al.*, 2004). Plants growing on infertile soils, including P-impooverished sites, tend to exhibit more conservative growth strategies and retain scarce nutrients in the soil-plant system (Hayes *et al.*, 2014; Guilherme Pereira *et al.*, 2019). For instance, along a 2-million-year dune chronosequence in south-western Australia, plants growing on older severely P-impooverished dunes have higher leaf mass per area (LMA), leaf dry matter content (LDMC) and defence strategies based on silicon, a beneficial nutrient, but lower concentrations of essential nutrients (*i.e.* P and nitrogen (N)) than plants growing on younger P-richer dunes (Hayes *et al.*, 2014; Guilherme Pereira *et al.*, 2019; de Tombeur *et al.*, 2020, 2021). While LMA increases with declining soil P availability, photosynthetic rates do not decrease, either when expressed on an area or mass basis (Guilherme Pereira *et al.*, 2019). However, it is not clear how plants allocate nutrients within their leaves, particularly P, to achieve high photosynthetic P-use efficiency (PPUE) and how P allocation and leaf traits associated with the LES drive photosynthetic nutrient-use efficiency in severely P-impooverished environments.

One way for plants to adapt or acclimate to P limitation is by reducing the concentration of P in their leaves (Veneklaas *et al.*, 2012). Phosphorus in leaves comprises five operational biochemical pools: nucleic acids, phospholipids, metabolic P (comprising inorganic P (Pi) and small P-containing metabolites) and a residual fraction that likely contains phosphorylated proteins among other P-containing chemical compounds not captured in other fractions (Hidaka & Kitayama, 2011, 2013; Mo *et al.*, 2019; Yan *et al.*, 2019; Liu *et al.*, 2023). Along a

120-year deglaciation chronosequence on the eastern Tibetan Plateau with varying soil P speciation and availability, evergreen species maintain their PPUE by decreasing the total amount of P in their leaves and by adjusting the allocation of P among fractions, with fast and slow economic strategies driving plant succession along the chronosequence (Lei *et al.*, 2021). Similar results were reported for a fast-growing *Banksia sessilis* (Proteaceae), allocating more P to nucleic acids than the slow-growing *B. attenuata* in severely P-impooverished soil (Han *et al.*, 2021). A recent survey demonstrated a partial association between variation in P allocation along the LES in 12 evergreen species co-occurring on P-impooverished soils in south-eastern Australia (Tsuji *et al.*, 2023). However, it is not clear how the allocation of P to different P fractions by highly P-efficient plant species integrates within the LES framework under extreme P limitation.

South-western Australia is one of the most nutrient-impooverished regions in the world (Lambers *et al.*, 2010; Viscarra Rossel & Bui, 2016; Kooyman *et al.*, 2017) and is recognised as a global biodiversity hotspot (Myers *et al.*, 2000; Williams *et al.*, 2011). The Proteaceae family is prominent, with most species in the family being endemic to the region (Beard *et al.*, 2000; Hopper, 2009). Adaptations have evolved in the Proteaceae that provide them with a high P-acquisition efficiency in extremely P-impooverished soils (Hayes *et al.*, 2021; Lambers, 2022). The high P-acquisition efficiency is complemented by numerous adaptations that also give Proteaceae a high internal P-use efficiency (Hayes *et al.*, 2021). Proteaceae function at a very low abundance of ribosomal RNA (rRNA) and low concentrations of protein in mature leaves (Lambers *et al.*, 2015a; Liu *et al.*, 2022). During leaf development, Proteaceae replace phospholipids with lipids that do not contain P, such as sulfolipids and galactolipids (Lambers *et al.*, 2012). The demand for P is further spread over time with the leaf growth being dissociated from the P-demanding development of the photosynthetic apparatus, a phenomenon known as ‘delayed greening’ (Lambers *et al.*, 2011; Kuppusamy *et al.*, 2014, 2021; Bird *et al.*, 2024). These adaptations have allowed Proteaceae to function at low foliar P and N concentrations ([P] and [N], respectively) without compromising photosynthetic performance, as is usually the case under extremely low P availability (Veneklaas *et al.*, 2012; Guilherme Pereira *et al.*, 2019; Hayes *et al.*, 2021). This results in a high leaf PPUE and PNUE (Denton *et al.*, 2007; Lambers *et al.*, 2012; Sulpice *et al.*, 2014; Hayes *et al.*, 2018; Guilherme Pereira *et al.*, 2019). Liu *et al.* (2023) showed that P-allocation patterns among a wide range of species from different families in south-western Australia are species dependent. However, it

remains unknown how the P investment at the biochemical level explains the relatively high PPUE of species from different genera within the Proteaceae.

In this study, we combined major leaf traits associated with the LES framework (*i.e.* LMA, mass-based photosynthetic rates, leaf [P] and [N]) with the allocation of P to the major biochemical fractions described above in a range of species of *Banksia* and *Hakea* that occur on extremely P-impooverished soils in Badgingarra National Park, Western Australia. *Banksia* and *Hakea* are emblematic and phylogenetically well-separated genera of the Proteaceae family, with long evolutionary histories and strong diversification (Hopper, 2009; Hayes *et al.*, 2021). We aimed to determine the dependence of physiological processes such as photosynthesis and PPUE on P allocation in leaves and how P-allocation patterns integrate with traits associated with the LES. We hypothesised that (1) the allocation of P to lipids and small metabolites would be negatively and positively correlated with PPUE, respectively, as observed in other studies (Hidaka & Kitayama, 2013; Suriyagoda *et al.*, 2023); (2) in relation to their evolutionary history, *Banksia* and *Hakea* species would be positioned at the highly-conservative end of the LES and P allocation, particularly that in lipids, metabolites and nucleic acids would contribute to the position of these species along the LES.

Materials and Methods

Species selection and study area

Five *Banksia* species (Proteaceae) and five *Hakea* species (Proteaceae) were selected as the highly-abundant species in the targeted extremely P-impooverished area of Badgingarra National Park (S30.412, E115.367), *c.* 200 km north of Perth, Western Australia (Fig. 1). The vegetation is kwongan heath, dominated by sclerophyllous shrubs of the family Proteaceae, followed by Myrtaceae and Fabaceae (Pate & Beard, 1984). The climate is Mediterranean with hot dry summers and cool wet winters, with a mean annual maximum temperature of 26°C and a mean annual rainfall of 440 mm (1999-2018, Badgingarra Research Station, Australian Bureau of Meteorology, <http://www.bom.gov.au>). Five individuals of each species were sampled at four sites along a *c.* 8 m elevation gradient with contrasting soils (Fig. 1), with one species (*Hakea conchifolia*) found at two sites (Fig. 1c,e).

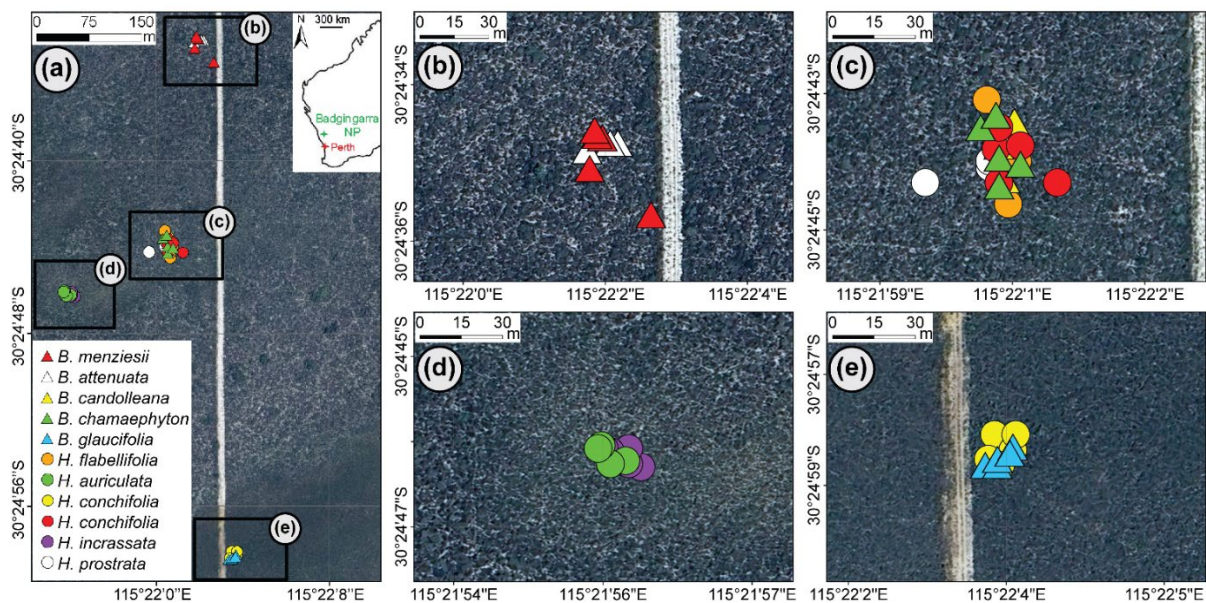


Fig. 1 Sampling location of five *Banksia* species (triangles) and five *Hakea* species (circles) naturally occurring at four extremely P-impoorished sites along a slight elevation gradient in Badgingarra National Park, Western Australia: (a) overall study area; the inset shows the location of Badgingarra National Park in south-western Australia, c. 200 km north of Perth; (b) ‘bottom’ site with silty sand; (c) ‘slope’ site with sand; (d) ‘top’ site with exposed laterite interspersed with sand; and (e) ‘laterite’ site with little sand. Elevation differs c. 8 m from (b) to (e). Elevation at (c) was similar to (d). The maps were edited using ArcMap 10.8.2 GIS software using Google Earth imagery (Google Inc.).

Leaf characteristics and nutrient analyses

Mature, fully-expanded, undamaged and sun-exposed leaves were collected, scanned with an optical scanner (Epson Perfection V800 Photo, Epson, Los Alamitos, USA) and the images analysed for projected leaf area (WinRHIZO Pro software, Regent Instruments Inc., Quebec, Canada). Leaf thickness was measured using a portable digital calliper and calculated as the average thickness of three positions on the lamina along the axis from the base to the tip of the leaf. Leaves were oven-dried for one week at 70°C to a constant weight and leaf mass per area (LMA; g m⁻²) was calculated as the total dry weight of the sample divided by its total area.

Fresh mature leaf material was snap-frozen in liquid N and stored at -80°C before being freeze-dried for seven days (VirTis BenchTop Pro ‘K’ Freeze Dryer, SP Scientific, Warminster, PA, USA). Freeze-dried material was finely ground using plastic vials and zirconium beads in a vertical ball-mill grinder (GenoGrinder, Spex SamplePrep, Metuchen,

NJ, USA). Leaf total [N] was determined by combustion with a glutamic acid standard using a CN analyser (Elementar Vario Macro CNS analyser, Langenselbold, Hesse, Germany). Leaf total [P] was determined by inductively coupled plasma optical emission spectrometry (ICP-OES, Optima 5300DV, PerkinElmer, Waltham, MA, USA) following acid digestion with a mixture of concentrated nitric and perchloric acids (Zarcinas *et al.*, 1987).

Analysis of leaf P fractions

Leaf inorganic P (Pi) concentration was determined after extraction with acetic acid (Hurley *et al.*, 2010). In brief, freeze-dried and ground leaf material was mixed with cold 1% (v/v) acetic acid, shaken with zirconium beads in bursts of 5000 rpm at 4°C for 15 s with 5 min breaks between bursts (Precellys 24 Tissue Homogenizer, Bertin Instruments, Montigny-le-Bretonneux, France). After clarification by centrifugation at 14000 g at 4°C for 15 min, the extract was purified with activated charcoal (Dayrell *et al.*, 2022) and the Pi concentration was determined colorimetrically using a malachite green-based method (Motomizu *et al.*, 1983).

Foliar P was separated into lipid P, metabolic P (comprising both metabolite P and Pi), nucleic acid P and a residual P fraction by sequential extraction based on the differential solubility of each class of P-containing compound using a modification of the method from (Kedrowski, 1983; Hidaka & Kitayama, 2013; Hayes *et al.*, 2022). In brief, ground leaf material was extracted with 12 : 6 : 1 (v/v/v) chloroform : methanol : formic acid, then with 1 : 2 : 0.8 (v/v/v) chloroform : methanol : water. The extracts were combined and extracted with chloroform-saturated water into an organic phase and an aqueous phase, which contained the lipid P and metabolic P fractions, respectively. The pellet was resuspended in 85% (v/v) methanol and extracted with 5% (w/v) trichloroacetic acid (TCA). After centrifugation of the sample at 5000 g at 4°C for 15 min, the clear supernatant was added to the metabolic P fraction. The pellet was resuspended in 2.5% (w/v) TCA at 95°C to extract the nucleic acids. The pellet was then transferred to a digestion flask by suspending in 85% (v/v) methanol three times to make the residual P fraction. All fractions were dried at *c.* 50°C and digested with a mixture of concentrated nitric and perchloric acids to hydrolyse esterified P (Zarcinas *et al.*, 1987). The Pi concentration in each fraction was determined colorimetrically as described above (Motomizu *et al.*, 1983). Metabolite P was calculated by subtracting Pi from metabolic P, where Pi was determined as described above. The recovery rate (%) was calculated as the sum of all P fractions divided by total P measured directly from the ground leaves by ICP-OES and

ranged from 86% to 94% for our P fractionation method (Table S1). Therefore, we present total P as the sum of the four P fractions (lipid P, metabolic P, nucleic acid P and residual P).

Gas exchange measurements

Leaf gas exchange was measured on clear sunny days between 8:30 am and 10:30 am on June 16th and 17th, 2020, on leaves with similar attributes to those used for leaf trait measurement. Light-saturated net photosynthetic rates of leaves were measured using a portable open-system infrared gas analyser (LI6400XT, LI-COR Biosciences, Lincoln, NE, USA) with 1500 $\mu\text{mol}^{-1} \text{s}^{-1}$ photosynthetic photon flux density, 400 $\mu\text{mol mol}^{-1} \text{CO}_2$ with a chamber temperature of $23 \pm 1^\circ\text{C}$ and relative humidity of 55 to 70%. When the chamber area (6 cm^2) was not completely filled, the leaf area inside the chamber was measured by scanning as described above. Photosynthetic rates were expressed on a leaf area basis ($A_{\text{sat,area}}$; $\mu\text{mol CO}_2 \text{m}^{-2} \text{s}^{-1}$) and on a leaf dry mass basis, using LMA for conversion ($A_{\text{sat,mass}}$; $\text{nmol CO}_2 \text{g}^{-1} \text{s}^{-1}$). Photosynthetic P-use efficiency (PPUE) and photosynthetic N-use efficiency (PNUE) were calculated as the rate of net photosynthetic CO_2 assimilation per unit P ($\mu\text{mol CO}_2 \text{g}^{-1} \text{P s}^{-1}$) and N ($\mu\text{mol CO}_2 \text{g}^{-1} \text{N s}^{-1}$), respectively.

Soil sampling and analyses

Three soil samples were collected within 300 mm around the base of three plants of each targeted species at each site on June 16th, 2023. The three subsamples of soil from each plant were collected using a hand trowel (depth = 100 mm) and mixed to form one soil sample for each plant. The soil samples were air-dried at room temperature (*c.* 20°C) for two weeks and then sieved ($< 2 \text{ mm}$) to remove gravel and large organic debris, including roots.

Soil pH and electrical conductivity (EC) were measured in deionised water (1 : 5 (w/v) soil : water) using pH and EC probes calibrated with pH 4 and 7 buffers or a $1314 \mu\text{S cm}^{-1}$ solution, respectively. Soil pH was also measured in 0.01 M CaCl_2 (1 : 5 (w/v) soil : solution; Orion Versa Star Pro, Thermo Fisher Scientific, Waltham, MA, USA).

Soil total [P] was determined by ignition (Saunders & Williams, 1955). In brief, air-dried soil was heated at 550°C for 1 h and allowed to cool before extraction by shaking with 1 M HCl (1 : 30 (w/v) soil : solution) for 16 h. A second soil subsample was extracted with 1 M HCl (1 : 10 (w/v) soil : solution) for 16 h without prior ignition for the determination of inorganic P (Saunders & Williams, 1955). Both subsamples were filtered using Whatman

No.42 filter papers, and the [P] was determined colorimetrically (Motomizu *et al.*, 1983). Organic P (Po) was calculated by subtracting the [P] in the non-ignited sample from the [P] in the ignited sample.

Resin P, a measure of ‘plant-available’ soil P, was extracted using anion exchange membranes (AEM (Turner & Romero, 2009)). Air-dried soil was shaken in deionised H₂O (1 : 6 (w/v) soil : water) with four anionic-form AEM strips (10 × 40 mm; manufactured by BDH, Poole, UK, and distributed by VWR International) for 16 h. After shaking, the AEM strips were rinsed free of soil particles with deionised H₂O and the P_i was recovered by shaking the strips in 10 ml of 0.5 M HCl for 1 h. Resin [P] in the extract was determined colorimetrically (Motomizu *et al.*, 1983). Soil [P] was expressed on a dry-weight basis (mg P kg⁻¹ soil DW).

Statistical analyses

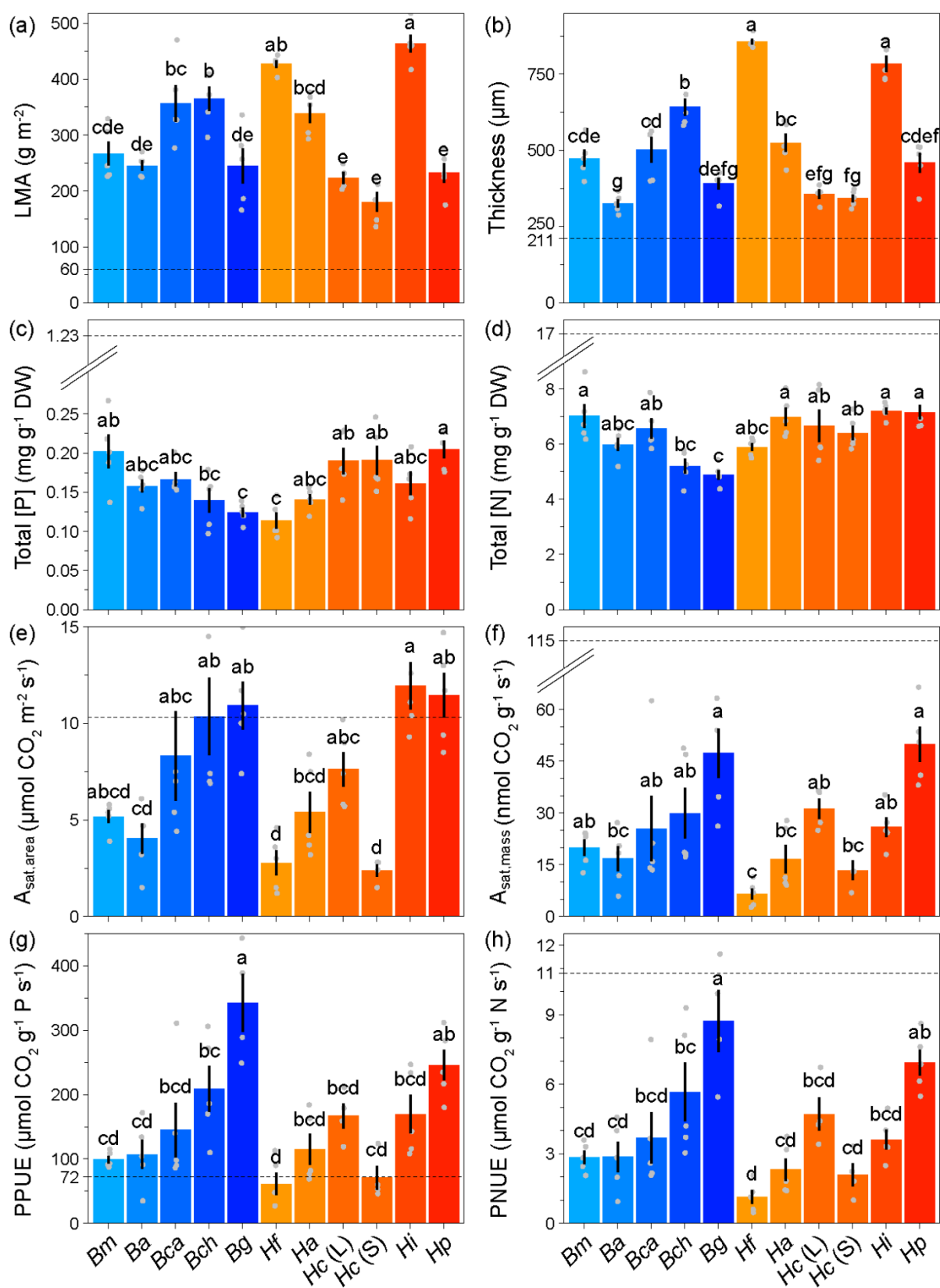
Data were analysed using the R software platform (R Core Team, 2023). One-way ANOVAs were performed to test the significance of differences in all measured variables among all species or among species within both genera, and Tukey’s HSD post-hoc tests were run to determine significant differences. The homogeneity of variances was inspected using the Levene’s test and the normality of the residuals was inspected using the Shapiro-Wilk test ($P > 0.05$). Data were log₁₀-transformed when either condition was not met. The linear regressions between leaf [P] and soil [P] were run on unmatched averaged data. The principal component analyses (PCAs) characterising functional foliar traits defining LES and P-related traits were run using the ‘*FactoMineR*’ package on log₁₀-transformed data (Lê *et al.*, 2008). Missing values were imputed and the number of principal components (PCs) retained in the PCA was decided using the ‘*missMDA*’ package (Josse & Husson, 2016). In the case of no missing data, PCs explaining $\geq 90\%$ of the variation were retained. Pearson’s correlation analysis was used to analyse the correlation between the allocation of P to the different fractions and the individual coordinates extracted from individual PCAs for each genus. Global averages for leaf traits presented in Fig. 2 were extracted with permission from the published TRY plant trait database (Kattge *et al.*, 2011) and global data presented in Fig. S1 were extracted with permission from the GLOPNET dataset from the leaf economics spectrum initiative (Wright *et al.*, 2004).

Results

Banksia and *Hakea* species had a high leaf mass per unit area (LMA), averaging 306 g m^{-2} , compared with a global average of 60 g m^{-2} (Figs 2a, S1). However, there was a wide variation, reflecting differences in leaf structure among species. The LMA closely aligned with leaf thickness (Fig. 2b). Leaf [P] were low compared with a global average with *Banksia* species ranging from 0.124 to $0.202 \text{ mg P g}^{-1} \text{ DW}$ for *B. glaucifolia* and *B. menziesii*, respectively, and *Hakea* species ranging from 0.114 to $0.205 \text{ mg P g}^{-1} \text{ DW}$ for *H. flabellifolia* and *H. prostrata*, respectively (Figs 2c, S1). Leaf [N] were also low compared with a global average, between 4.9 and $7.2 \text{ mg N g}^{-1} \text{ DW}$, with only *B. chamaephyton* and *B. glaucifolia* having significantly lower [N] than some of the other species (Figs 2d, S1). Foliar [N] was relatively more conserved among all Proteaceae tested than foliar [P] (1.5-fold and 1.8-fold variation across all species, respectively). This conservation was particularly pronounced among *Hakea* species (1.2-fold variation), which an average of $6.7 \text{ mg N g}^{-1} \text{ DW}$ with no strictly-significant differences within this genus ($P > 0.05$; Fig. 2d). The average N : P ratio for the 10 species was 41, which was notably high compared with a global average of 13 (Fig. S2).

Light-saturated photosynthetic rates were more variable than leaf [P] and [N] within each genus (Fig. 2e,f). Area-based photosynthetic rates ($A_{\text{sat,area}}$) were spanning the entire range of that measured in the LES (Fig. S1), although most species had slower rates than the global average. However, when expressed on a mass basis, photosynthetic rates ($A_{\text{sat,mass}}$) were no more than 6% (*H. flabellifolia*) to 43% (*H. prostrata*) of the global average rate, reflecting the high LMA of these species (Fig. 2a,f).

The photosynthetic P-use efficiency (PPUE) of the study group ranged from $61 \mu\text{mol CO}_2 \text{ g}^{-1} \text{ P s}^{-1}$ for *H. flabellifolia* to 375 and $246 \mu\text{mol CO}_2 \text{ g}^{-1} \text{ P s}^{-1}$ for *B. glaucifolia* and *H. prostrata*, respectively (Fig. 2g). Therefore, the values were at or above the global average value. The photosynthetic N-use efficiency (PNUE) followed the same relative pattern across species as the PPUE, but the values were all less than half of the global average, except for *B. glaucifolia*, which was near the global average (Fig. 2h). Both PPUE and PNUE were similar between *Banksia* and *Hakea* ($P > 0.05$), but varied among species within each genus (Fig. 2g,h).



There were no significant differences in pH or EC in the soil under any of the species (Table 1). Soil total [P] was significantly higher under *B. glaucifolia* and *H. conchifolia*, the two species found on the lateritic site, consistent with higher soil organic [P] under these plants (Fig. S3a; Table 1). There were no significant differences in soil resin P under any of the species (Fig. S3b; Table 1). In contrast to the species level comparison, combining the data from these same soils by site revealed differences in soil [P] (Table S2). The soil at the upper-most laterite site had the highest soil [P], while the bottom and slope sites had the lowest soil total [P], respectively. The soil at the top site was between these extremes. Soil total [P] at the site level were consistent with soil Pi and Po concentrations. Interestingly, the slope and top sites, which were intermediate in elevation, had the lowest and highest resin [P], respectively (Table S2). Despite these differences in soil total [P] and resin [P] among the four sites, there was no significant correlation between leaf [P] and either soil total [P] or resin [P] (Fig. S3).

◀ **Fig. 2** Foliar traits of five *Banksia* and five *Hakea* species naturally occurring on extremely P-impooverished soils: (a) leaf mass per unit area (LMA), (b) leaf thickness, (c) leaf phosphorus concentration ([P]), (d) leaf nitrogen concentration ([N]), (e) area-based light-saturated photosynthetic rate ($A_{\text{sat,area}}$), (f) mass-based light-saturated photosynthetic rate ($A_{\text{sat,mass}}$), (g) photosynthetic P-use efficiency (PPUE) and (h) photosynthetic N-use efficiency (PNUE). Values are means \pm SE ($n = 4$ or 5). Different letters indicate significant differences among species (post-hoc Tukey's HSD test, $P < 0.05$). The horizontal dashed lines represent mean global averages extracted from the TRY plant trait database (Kattge *et al.*, 2011). *Bm*, *Banksia menziesii*; *Ba*, *B. attenuata*; *Bca*, *B. candolleana*; *Bch*, *B. chamaephyton*; *Bg*, *B. glaucifolia*; *Hf*, *Hakea flabellifolia*; *Ha*, *H. auriculata*; *Hc*, *H. conchifolia* (Laterite and Slope); *Hi*, *H. incrassata*; *Hp*, *H. prostrata*.

Table 1 Soil chemical characteristics of the top layer (0 to 100 mm depth) under five *Banksia* and five *Hakea* species naturally occurring on extremely P-impooverished soils. Values are means \pm SE ($n = 3$). Different letters indicate significant differences among species (post-hoc Tukey's HSD test, $P < 0.05$). DW, dry weight; EC, electrical conductivity.

Species	Site	EC ($\mu\text{S cm}^{-1}$)	pH (CaCl ₂)	pH (H ₂ O)	
<i>B. menziesii</i>	Bottom	17 \pm 1 a	4.5 \pm 0 b	6.1 \pm 0 a	
<i>B. attenuata</i>	Bottom	14 \pm 1 a	4.5 \pm 0.1 b	6.1 \pm 0 a	
<i>B. candolleana</i>	Slope	17 \pm 1 a	4.6 \pm 0.1 b	6.0 \pm 0.1 a	
<i>B. chamaephyton</i>	Slope	15 \pm 5 a	4.6 \pm 0 ab	6.0 \pm 0 a	
<i>B. glaucifolia</i>	Laterite	23 \pm 4 a	4.6 \pm 0.1 b	5.9 \pm 0.1 a	
<i>H. flabellifolia</i>	Slope	27 \pm 7 a	4.7 \pm 0.1 ab	5.9 \pm 0.1 a	
<i>H. auriculata</i>	Top	21 \pm 4 a	5.0 \pm 0.1 a	6.2 \pm 0 a	
<i>H. conchifolia</i>	Laterite	27 \pm 1 a	4.5 \pm 0 b	5.9 \pm 0 a	
<i>H. conchifolia</i>	Slope	21 \pm 5 a	4.6 \pm 0 b	5.9 \pm 0.1 a	
<i>H. incrassata</i>	Top	22 \pm 2 a	4.8 \pm 0.1 ab	6.1 \pm 0 a	
<i>H. prostrata</i>	Slope	22 \pm 6 a	4.5 \pm 0.1 b	5.7 \pm 0.3 a	

Species	Site	Total P (mg kg ⁻¹ DW)	Inorganic P (mg kg ⁻¹ DW)	Organic P (mg kg ⁻¹ DW)	Resin P (mg kg ⁻¹ DW)
<i>B. menziesii</i>	Bottom	4.5 \pm 0.6 c	0.18 \pm 0.01 ab	4.3 \pm 0.5 c	0.23 \pm 0.00 a
<i>B. attenuata</i>	Bottom	3.9 \pm 0.5 c	0.19 \pm 0.03 ab	3.7 \pm 0.4 c	0.22 \pm 0.04 a
<i>B. candolleana</i>	Slope	4.2 \pm 0.8 c	0.16 \pm 0.05 abc	4.0 \pm 0.7 c	0.27 \pm 0.01 a
<i>B. chamaephyton</i>	Slope	3.4 \pm 0.6 c	0.12 \pm 0.01 abc	3.3 \pm 0.5 c	0.24 \pm 0.05 a
<i>B. glaucifolia</i>	Laterite	12.2 \pm 2.6 ab	0.48 \pm 0.12 a	11.7 \pm 2.5 ab	0.16 \pm 0.04 a
<i>H. flabellifolia</i>	Slope	5.5 \pm 1.1 c	0.07 \pm 0.03 bc	5.4 \pm 1.0 c	0.17 \pm 0.02 a
<i>H. auriculata</i>	Top	8.3 \pm 0.9 bc	0.12 \pm 0.02 abc	8.2 \pm 0.9 bc	0.10 \pm 0.02 a
<i>H. conchifolia</i>	Laterite	16.7 \pm 1.8 a	0.52 \pm 0.13 a	16.2 \pm 1.6 a	0.11 \pm 0.02 a
<i>H. conchifolia</i>	Slope	4.2 \pm 0.7 c	0.05 \pm 0.02 c	4.2 \pm 0.7 c	0.23 \pm 0.07 a
<i>H. incrassata</i>	Top	9.0 \pm 1.1 bc	0.15 \pm 0.03 abc	8.9 \pm 1.1 bc	0.14 \pm 0.03 a
<i>H. prostrata</i>	Slope	4.5 \pm 1.5 c	0.08 \pm 0.03 bc	4.4 \pm 1.5 c	0.20 \pm 0.08 a

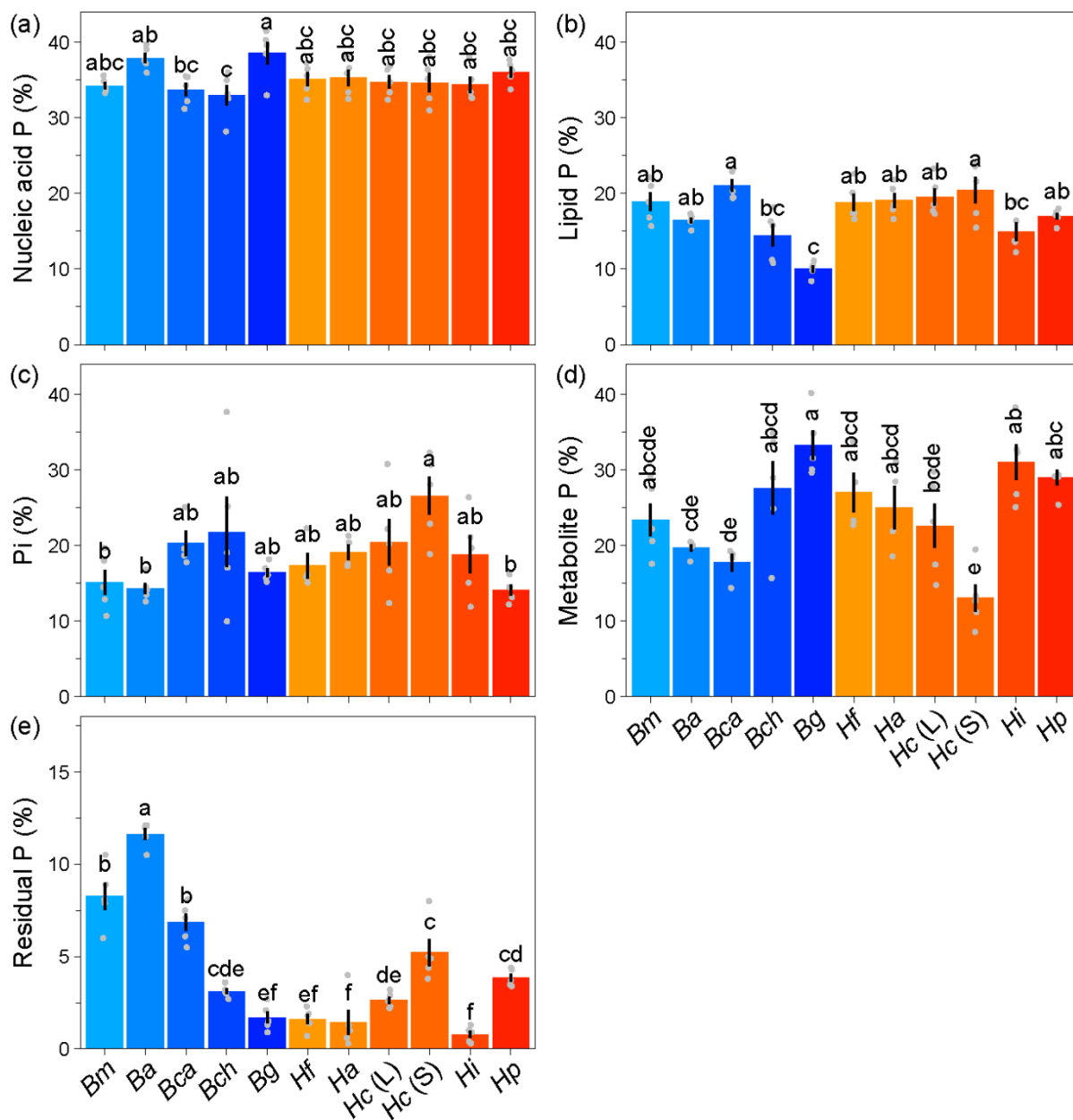


Fig. 3 Phosphorus (P) allocation to five biochemical fractions as a proportion of total foliar P for five *Banksia* and five *Hakea* species naturally occurring on extremely P-impooverished soils: (a) nucleic acid P, (b) lipid P, (c) inorganic P (Pi), (d) metabolite P (metabolic P – Pi) and (e) residual P. Values are means \pm SE ($n = 4$ or 5). Different letters indicate significant differences among species (post-hoc Tukey's HSD test, $P < 0.05$). Actual concentrations of P (mg P g^{-1} DW) in each fraction are given in Supporting Information Figure S3. Bm, *Banksia menziesii*; Ba, *B. attenuata*; Bca, *B. candolleana*; Bch, *B. chamaephyton*; Bg, *B. glaucifolia*; Hf, *Hakea flabellifolia*; Ha, *H. auriculata*; Hc, *H. conchifolia* (Laterite and Slope); Hi, *H. incrassata*; Hp, *H. prostrata*.

There was a high level of consistency in the proportion of P each species allocated to nucleic acid P, with an overall average of 36.6% of total P allocated to this fraction (Fig. 3a). The proportional allocation of P to lipids was also relatively conserved across species, particularly among *Hakea* species, with the greatest variation of 1.4-fold between *H. conchifolia* (on the slope) and *H. incrassata* (Fig. 3b). Interestingly, *Hakea* species had an overall greater allocation of P to lipids than *Banksia* species did ($P = 0.037$). The allocation of P to Pi was also conserved across all species with no differences among *Banksia* species ($P > 0.05$). The only statistically-significant differences among all species were that *H. conchifolia* (on the slope) had a greater P allocation to Pi than *H. prostrata*, *B. menziesii* and *B. attenuata* (Fig. 3c).

The allocation of P to small metabolites and the residual fraction was much more variable, with a 2.5-fold and 14.9-fold variation among all species, respectively (Fig. 3d,e). Within the respective genera, *B. glaucifolia* had a higher proportion of P allocated to small metabolites than *B. attenuata* and *B. candolleana*, while *H. conchifolia* (on the slope) had a lower proportional allocation than the other *Hakea* species ($P < 0.05$; Fig. 3d). Although residual P only represented a small proportion of foliar total P compared with the other fractions, it significantly differed ($P < 0.001$) at the genus level between *Banksia* and *Hakea* with averages of 6.5% and 2.6% of total P, respectively (Fig. 3e).

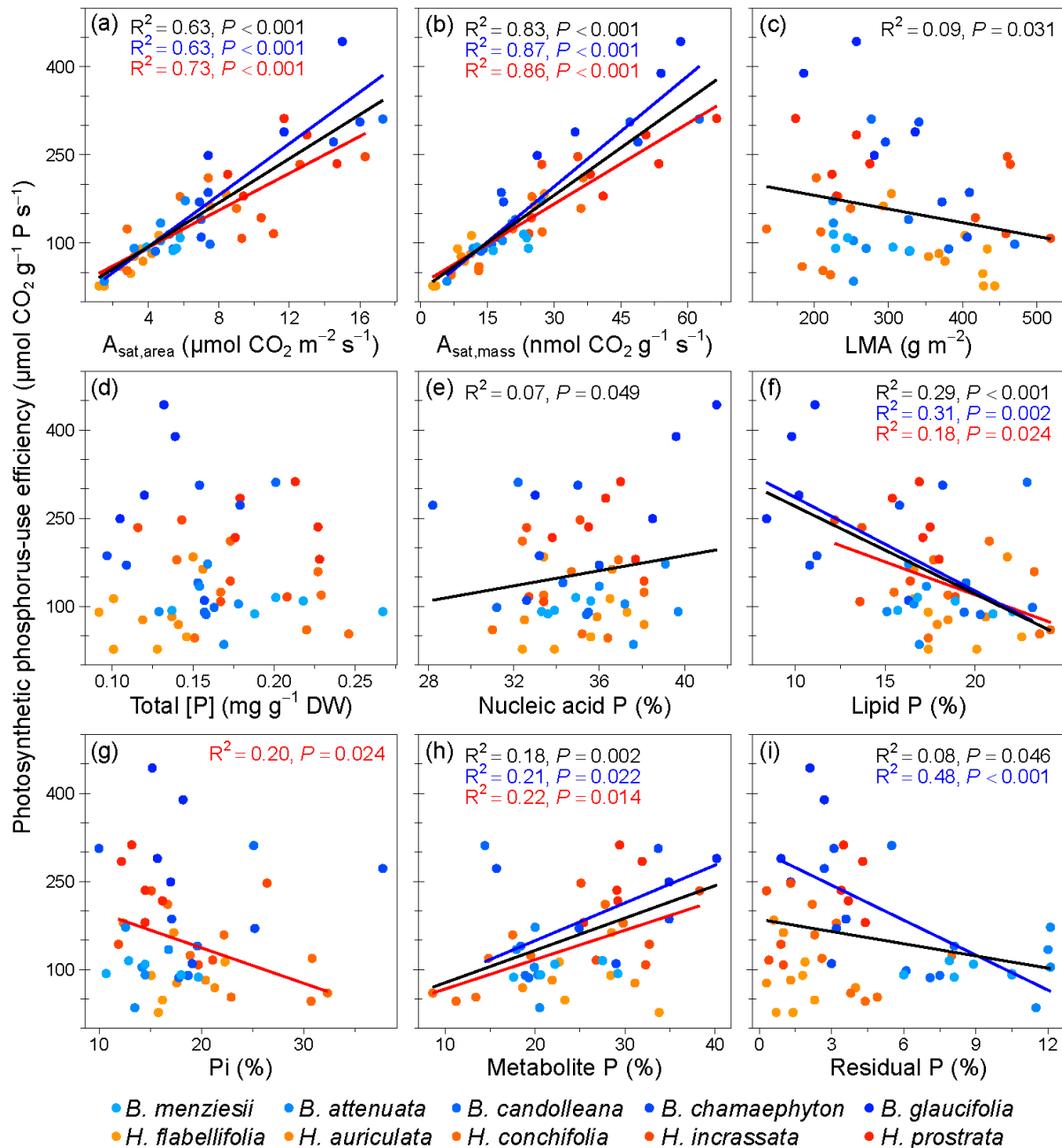


Fig. 4 Correlations between photosynthetic phosphorus (P)-use efficiency (PPUE) and leaf traits for five *Banksia* and five *Hakea* species naturally occurring on extremely P-impooverished soils. Correlations between PPUE and major leaf traits (a) area-based light-saturated photosynthetic rate ($A_{\text{sat,area}}$), (b) mass-based light-saturated photosynthetic rate ($A_{\text{sat,mass}}$), (c) leaf mass per unit area (LMA), (d) leaf P concentration, and correlations between PPUE and percentages of P allocated to (e) nucleic acid P, (f) lipid P, (g) inorganic P (Pi), (h) metabolite P (metabolic P – Pi) and (i) residual P. Solid lines indicate significant linear correlations (black: among all individuals, $N = 52$ to 55 ; blue: among *Banksia* species, $N = 24$ or 25 ; and red: among *Hakea* species, $N = 28$ to 30 ; $P < 0.05$).

A correlation analysis across the two genera showed significant correlations between PPUE and most of the leaf traits, as well as P fractions expressed on a fractional basis (Fig. 4). The strongest correlations were between PPUE and $A_{\text{sat,area}}$ and $A_{\text{sat,mass}}$ which were supported by strong correlations for each genus examined individually. In contrast, there was a weak correlation between PPUE and LMA that was not sustained by either genus individually. Interestingly, no correlation was found between PPUE and total foliar [P], despite a nearly two-fold variation in leaf [P] within each genus (Fig. 2). Thus, the differences in PPUE were associated with differences in photosynthetic rates, rather than leaf [P]. Like PPUE, PNUE was strongly correlated with photosynthetic rates, rather than foliar [N] or LMA (Fig. S5). Therefore, PPUE and PNUE were strongly correlated ($R^2 = 0.97$ and $R^2 = 0.88$ for *Banksia* and *Hakea* species, respectively; $P < 0.001$; Fig. S5).

The only correlations between PPUE and the fractional allocation of P that was supported by both genera assessed individually was a negative correlation of PPUE with lipid P (Fig. 4f) and a positive correlation of PPUE with metabolite P (Fig. 4h). There was a weak positive correlation of PPUE with nucleic acid P, but this was not supported by either genus individually. At the level of all plants examined, there was a negative correlation between PPUE and residual P. This correlation was driven by the *Banksia* species, but not by the *Hakea* species. Conversely, there was a negative correlation between PPUE and Pi only for the *Hakea* species examined.

Correlations specific to each genus were also found when fractions were expressed as an absolute concentration of P, *i.e.* PPUE correlated with P concentration in lipids for *Banksia* species and P concentration in metabolites for *Hakea* species (Fig. S6). Also, there was a strong correlation for *Banksia* species between PPUE and the absolute P concentration in the residual fraction. Interestingly, P allocated to the lipid and residual fractions (both fractional and actual concentrations) were positively correlated with leaf [N] only for the *Banksia* species. Moreover, there was a strong correlation between leaf [N] and nucleic acid P concentrations supported by both genera assessed individually (Fig. S7).

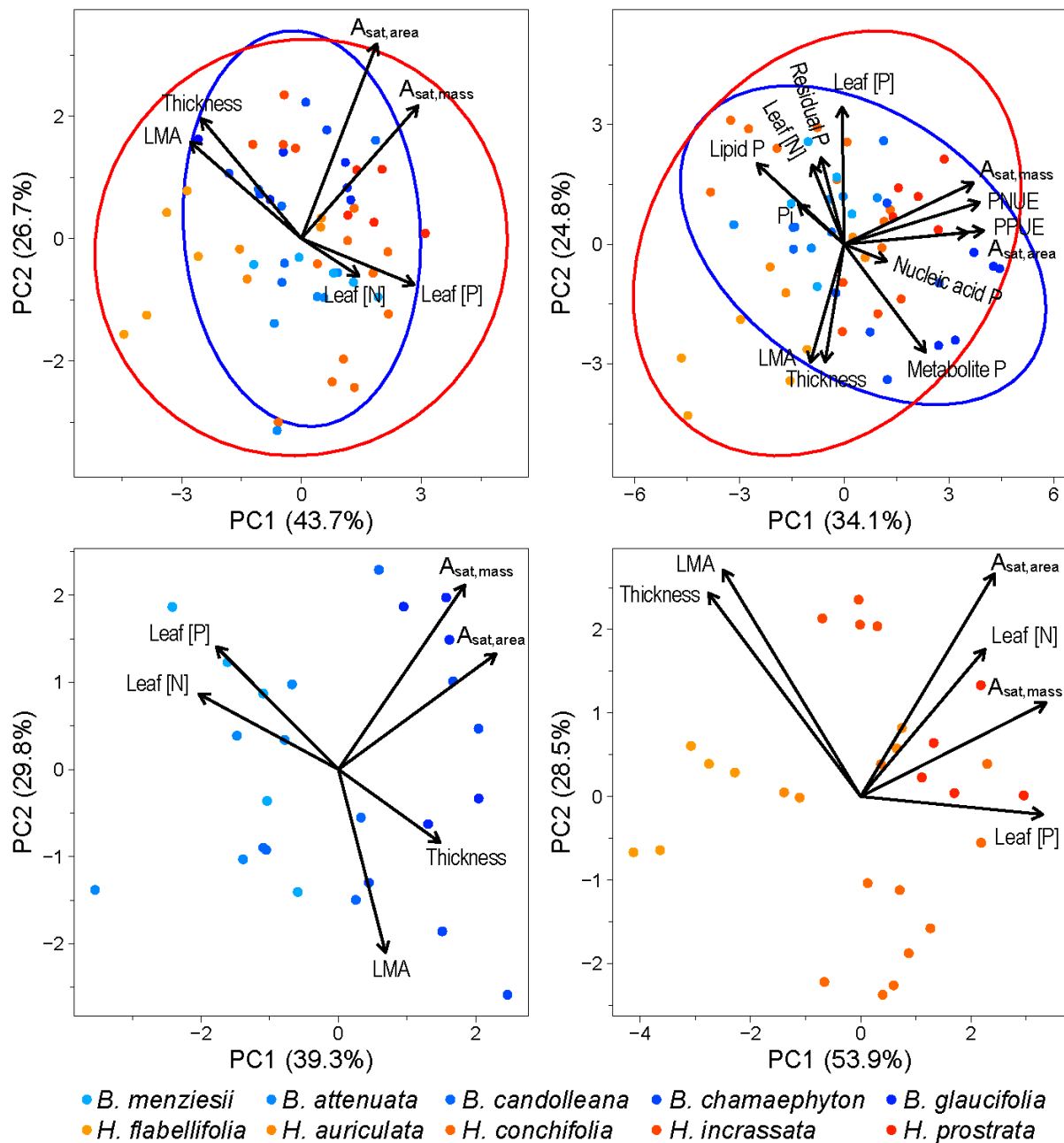


Fig. 5 Principal component analysis (PCA) of (a) functional leaf traits defining the leaf economics spectrum and (b) after adding in phosphorus (P)-related leaf traits of five *Banksia* (blue) and five *Hakea* species (red) naturally occurring on extremely P-impooverished soils; PCA of functional leaf traits of (c) *Banksia* species and (d) *Hakea* species. Detailed results are presented in Supporting Information Tables S3–S4. Nucleic acid P, lipid P, inorganic P (Pi), metabolite P and residual P are expressed as a fraction of leaf total P concentration ([P]). $A_{\text{sat,area}}$, area-based light-saturated photosynthetic rate; $A_{\text{sat,mass}}$, mass-based light-saturated photosynthetic rate; LMA, leaf mass per unit area; PNUE, photosynthetic nitrogen-use efficiency; PPUE, photosynthetic P-use efficiency.

Table 2 Correlations between the position of individuals of *Banksia* and *Hakea* along the dimensions defining the leaf economics spectrum in each individual principal component analysis (PCA) and phosphorus (P) allocated to five biochemical fractions, expressed as a percentage of total P and absolute concentration. Significant linear correlations ($P < 0.05$) are shown in **bold**. Detailed results of the PCAs are presented in Supporting Information Table S4. Correlations are shown in Supporting Information Fig. S8.

	<i>Banksia</i>				<i>Hakea</i>	
	PC1		PC2		PC1	
	<i>P</i>	R ²	<i>P</i>	R ²	<i>P</i>	R ²
Nucleic acid P	0.637	0.010	0.479	0.023	0.922	0.000
Lipid P	0.002**	0.356	0.444	0.027	0.611	0.011
Pi	% 0.165	0.086	0.660	0.009	0.864	0.001
Metabolite P	0.002**	0.353	0.424	0.029	0.434	0.026
Residual P	<0.001***	0.643	0.573	0.015	0.052	0.149
Nucleic acid P	<0.001***	0.498	0.002**	0.353	<0.001***	0.756
Lipid P	0.001**	0.376	0.063	0.149	<0.001***	0.419
Pi	mg P g ⁻¹ DW 0.660	0.009	0.068	0.144	0.014*	0.226
Metabolite P	0.943	0.000	0.140	0.096	0.009**	0.254
Residual P	<0.001***	0.772	0.755	0.005	0.003**	0.318

In a principal component analysis (PCA), the first two principal components (PCs) explained 70% of the total variance for all individuals of *Banksia* and *Hakea* when describing functional foliar traits associated with the LES (Fig. 5a; Table S3). When P-related foliar traits were combined with the foliar functional traits, PC1 and PC2 encompassed 59% of the variation in all individuals (Fig. 5b; Table S3). There was no distinction between the two genera when all traits were considered together. However, in accordance with the LES framework, structural traits (*i.e.* LMA and leaf thickness) were placed opposite to total leaf [P] and [N]. in both PCAs (Fig. 5a,b; Table S3). Surprisingly, photosynthesis-related traits (*i.e.* $A_{\text{sat,area}}$, $A_{\text{sat,mass}}$, PPUE, and PNUE) were dissociated from the contrasts between structural traits and nutrient concentrations and were placed along a different PC.

The fractional allocation of P to metabolites and lipids grouped with and opposite to photosynthesis-related traits, respectively, along PC1 in the PCA describing functional and P-related traits. The allocation to residual P was strongly associated with leaf [N] along PC2, but not with nucleic acid P that was placed on PC3 (Fig. 5b, Table S3).

The individual PCAs of functional leaf traits comprising the LES for *Banksia* (Fig. 5c) and *Hakea* species (Fig. 5d) showed similar patterns with structural traits opposed to nutrient concentrations. However, photosynthesis-related traits were disconnected from that axis for *Banksia* species, while they grouped together with nutrient concentrations for *Hakea* species (Fig. 5c,d; Table S4). For *Banksia* species, PC2 opposed structural traits to both nutrient concentrations and photosynthesis-related traits, which we define as the LES for this genus (Fig. 5c; Table S4). However, PC1 opposed nutrient concentrations to both structural and photosynthesis-related traits. Therefore, we define PC2 as the axis comprising the LES for *Banksia* species, but also present correlations between the allocation of P to the different fractions for PC1 (Fig. 5c; Tables 2, S4). For *Hakea* species, there was a clear contrast between structural and physiological traits along PC1 that we define as the LES axis for this genus (Fig. 5c; Table S4).

All five P fractions expressed as an absolute P concentration were significantly positively correlated with the distribution along PC1 for *Hakea* species, but we did not observe any significant correlations between the fractional P allocation and the distribution along PC1 (Table 2; Fig. S8). This highlights the tight link between an increase in P in those fractions and increase in total [P]. Similarly for *Banksia* species, most P fractions except Pi and metabolite P concentrations significantly correlated with PC1, driven by total [P] (Table 2, Fig. S8). Only nucleic acid P concentration significantly correlated with PC2, defined as the LES, but this was not retained for the percentage of P allocated to nucleic acids (Table 2). The percentage of P allocated to lipid P, metabolite P and residual P significantly correlated with the distribution along PC1, substantiating the correlations found between those P fractions and PPUE for *Banksia* species (Fig. 4).

Discussion

Our results support the notion that Proteaceae naturally occurring in extremely nutrient-impoverted environments modulate the allocation of P in their leaves to achieve high PPUE. Of the five P fractions measured, the allocation of P to lipids and to small metabolites were the allocations most closely associated with variation in PPUE. The allocation of P to other fractions, especially to nucleic acids and Pi, was more conserved among species of both genera. These observations support our first hypothesis that the allocation of P to lipids and

small metabolites would be negatively and positively correlated with PPUE, respectively. The variation in photosynthetic nutrient-use efficiency (PPUE and PNUE) was largely determined by the variation in photosynthetic rates ($A_{\text{sat,area}}$ and $A_{\text{sat,mass}}$), which were more variable among the species and spanned the range of global values, although they were generally below global averages (Wright *et al.*, 2004; Kattge *et al.*, 2011, 2020). All species had highly conservative leaf traits, such as extremely high LMA and low leaf nutrient concentrations, placing them on the far conservative end of the LES, supporting our second hypothesis. Our correlation analyses showed that the P-allocation patterns of *Banksia* and *Hakea* species contributed differently, at least in part, to their high PPUE, but not to their distribution along a genus-defined LES axis opposing structural and physiological traits. These findings did not align with our second hypothesis.

On the far “conservative” end of the leaf economics spectrum

Leaf [P] of *Banksia* and *Hakea* growing on extremely P-impooverished soils were extremely low with an average of 0.16 mg P g⁻¹ DW, which is even lower than in plants found in typical kwongan vegetation (c. 0.3 mg P g⁻¹ DW; Hayes *et al.*, 2018; Guilherme Pereira *et al.*, 2019). Leaf [P] in this study were among the lowest recorded worldwide (worldwide average: 1.23 mg P g⁻¹ DW (Wright *et al.*, 2004; Kattge *et al.*, 2011, 2020)). In alignment with low leaf total [P], all P fractions had significantly lower concentrations than the global averages for perennial species (Suriyagoda *et al.*, 2023). All Proteaceae in this study had similarly conservative leaf traits, *e.g.*, low $A_{\text{sat,mass}}$ and high LMA associated with scleromorphy. Slight variation in soil total [P] and resin [P] were not associated with higher leaf [P]. On the lateritic site, soil was shallower than on the sandy non-lateritic sites. Yet, cluster-rooted species like *Banksia* and *Hakea* are able to efficiently access sufficient nutrients from this lower soil volume and also directly from lateritic gravels (Han *et al.*, 2021). Moreover, at a very low P supply like that of our study site in Badgingarra National Park, which has some of the most P impooverished soils in the world (Kooyman *et al.*, 2017), P that is taken up by plants is mainly distributed to support growth, rather than accumulating in leaves to a high [P] (De Groot *et al.*, 2003; Shane *et al.*, 2003; Gille *et al.*, 2024). Accumulating more biomass rather than increasing leaf [P] further emphasises the extreme P-conserving strategy of these species.

We observed some variation in structural (*e.g.*, LMA) and physiological (*e.g.*, A_{sat} , nutrient concentrations) traits among species of both genera. These two sets of traits comprising the LES were well separated from each other in the PCA including both *Banksia* and *Hakea*

species, as well as in genus-specific PCAs. However, there was a disconnection between nutrient concentrations and photosynthesis-related traits, particularly for *Banksia* species. Moreover, we did not find significant correlations between P-allocation patterns (*i.e.* percentage of P allocated to each fraction) and the distribution of individuals along the axes defining the LES, despite species among each genus being positioned differently along those axes. However, we highlight different strategies in the two genera to achieve high PPUE and discuss below the implications of P allocation on physiological processes.

Higher LMA is usually associated with slower growth rates, long leaf lifespans and lower leaf protein concentrations (Poorter *et al.*, 2009). Our high-LMA leaves had low leaf [N] and nucleic acid [P], indicative of low protein and rRNA concentrations, respectively, suggesting a low capacity to produce and replace proteins. *Hakea prostrata* had a higher leaf nucleic acid P concentration, but similar leaf total [N], as the other *Hakea* species. This indicates that mature *H. prostrata* leaves function at a lower leaf protein : rRNA ratio, suggesting a faster protein turnover rate than that of other species of *Hakea* (Matzek & Vitousek, 2009; Lambers, 2022). In a glasshouse experiment conducted in acidic soil similar to that found at our study site in Badgingarra National Park, *H. prostrata* and *B. menziesii* had faster relative growth rates than *H. incrassata* (Hayes *et al.*, 2024). However, the potential correlation between P fractions, leaf [N] and protein turnover has yet to be explored. For this exploration, it will be crucial to consider expanding leaves of species with contrasting growth rates.

Interconnection of N and P efficiency

Leaf N and nucleic acid P proportions were remarkably conserved among all Proteaceae in our study. *Hakea prostrata*, *B. attenuata* and *B. thelemanniana* restrain their nitrate uptake even when provided with a large amount of nitrate (Prodhan *et al.*, 2016; Liu *et al.*, 2022). This nitrate-uptake restraint trait is also found in two Myrtaceae co-occurring with Proteaceae in a highly P-impoverished environment, suggesting that it is a convergent trait in species that evolved in these environments (Liu *et al.*, 2022). Limiting N uptake appears to be a strategy that allows plants to enhance P-use efficiency, and is associated with low concentrations of rRNA and, therefore, proteins (Matzek & Vitousek, 2009; Prodhan *et al.*, 2019). The low leaf [N] and extremely high N : P ratios in leaves of all species in this study, as well as the lack of variation among species, suggest nitrate-restraint in these species which would substantiate

nitrate-uptake restraint as an adaptation to low-P environments. Further studies need to be carried out to explore the prevalence of this trait among Proteaceae.

The lack of correlation between photosynthetic rates and [N] or nucleic acid P concentrations indicates that photosynthesis was limited by metabolic factors other than protein concentration (Sulpice *et al.*, 2014; Ellsworth *et al.*, 2022). Moreover, a recent study demonstrated that two Proteaceae species from south-western Australia, *Grevillea thelemanniana* and *Hakea ceratophylla*, prioritise leaf N investment to photosynthesis-related proteins while sacrificing proteins related to abiotic stress tolerance to maintain rapid photosynthetic rates at low leaf [N], compared with *Arabidopsis thaliana* (Liu, 2024). However, we suggest that *Banksia* species might also function with higher enzyme concentrations in parallel with lower substrate abundance, considering the strong correlation for this genus only found between PPUE and residual P, which likely contains phosphorylated proteins involved in photosynthetic and respiratory metabolism. The lack of correlation between PPUE and the P concentration in small metabolites in *Banksia* species supports the theory of a tight balance between substrate and enzyme abundance (Dourado *et al.*, 2021). The lack of correlation between residual P and either leaf [N] or PPUE for *Hakea* species highlights the different biochemical strategies in this genus to adapt to the extremely nutrient-impooverished environment compared with the *Banksia* species. *Hakea* species potentially function at higher substrate concentrations than *Banksia* species, which exhibited a positive correlation between PPUE and P concentration in small metabolites. Determining the content of the residual P fraction and its proportion of phosphorylated proteins is an essential challenge to the recently evolving field of P fractions in leaves (Suriyagoda *et al.*, 2023; Liu *et al.*, 2023; Tsujii *et al.*, 2024).

Implications of biochemical investment of P on PPUE

Foliar lipid P concentrations among the *Banksia* and *Hakea* species examined here were low and similar to those found in several other species growing in severely P-impooverished environments (Hidaka & Kitayama, 2011, 2013; Lambers *et al.*, 2012; Yan *et al.*, 2019). It is likely that all Proteaceae in this study replaced phospholipids by other lipids that do not contain P, such as sulfolipids and galactolipids as previously determined for five of the present species (Lambers *et al.*, 2012). The endoplasmic reticulum (ER) contains > 60% phospholipid by mass in a variety of cells (Lagace & Ridgway, 2013). Therefore, the negative correlation between lipid P and PPUE may indicate that the replacement of phospholipids involves a trade-off

between saving P and maintaining the function of cellular membranes, particularly that of the ER. The ER is involved in synthesising proteins destined for endomembranes or export (Sadowski *et al.*, 2008), so the trade-off may be associated with both low protein and rRNA concentrations. The link between phospholipids in the ER membranes and protein synthesis, as well as protein turnover, in relation to P limitation requires further attention.

Inorganic phosphate concentration is tightly linked with that of small metabolites via phosphorylation (Plaxton & Tran, 2011). The fact that PPUE was positively correlated with metabolite P but not with Pi indicates that plants growing under extremely low P availability function at the lower limit of Pi concentrations. Excess Pi is stored in the vacuole and remobilised for metabolism when needed. One of the typical P-starvation responses in a wide range of species is the reduction of the concentration of Pi (Bielecki, 1968; Veneklaas *et al.*, 2012; Yan *et al.*, 2019). Using ³¹P-nuclear magnetic resonance (³¹P-NMR), Pratt *et al.* (2009) showed that a decrease in cytosolic Pi concentration is the first response following Pi starvation but that Pi efflux from the vacuole is not sufficient to fully compensate for the lack of Pi supply in *Acer pseudoplatanus* (Sapindaceae) and *Arabidopsis thaliana* (Brassicaceae). Further investigation is required to identify the extent of the metabolic importance of both cytosolic and vacuolar Pi pools under very low P availability. These aspects can be measured using metabolomics approaches combined with ³¹P-NMR (Pratt *et al.*, 2009; Gout *et al.*, 2011).

Positive correlations between PPUE and the fractional allocation of P to small metabolites are consistent with previous studies (Wen *et al.*, 2023), although we were able to distinguish low-molecular-weight esterified metabolites (metabolite P) from Pi which are sometimes pooled as metabolic P (Hidaka & Kitayama, 2013). A decrease in the concentration of phosphorylated metabolites involved in major metabolic pathways, *e.g.*, Benson-Bassham-Calvin cycle and glycolysis, decreases their activity unless compensated by increases in enzyme quantity that use these metabolites or changes in the catalytic properties of the enzymes (Lambers *et al.*, 2015b). Producing more enzyme is unlikely to occur under low P availability as it would require a greater investment of P in rRNA to support protein synthesis (Veneklaas *et al.*, 2012; Lambers, 2022). To achieve higher PPUE, *Banksia* and *Hakea* species might increase P allocation to small metabolites to support greater enzyme activity (*i.e.* higher substrate concentration) and maintain relatively fast photosynthetic rates. However, we observed a positive correlation between nucleic acid P and metabolite P ($R^2 = 0.18$, $P = 0.002$), consistent with previous studies (Hidaka & Kitayama, 2013; Yan *et al.*, 2021; Suriyagoda *et*

al., 2023), but contradictory to the idea that lower enzyme concentration is compensated for by higher small metabolite concentration. Some metabolites are products of those enzymes (*e.g.*, glucose 1-P, fructose 6-P) and understanding how the concentrations of phosphorylated metabolites are regulated and at which scale the composition of this pool is regulated is warranted.

Concluding remarks

This study highlights critical differences in P-allocation patterns to achieve high PPUE between two genera of Proteaceae found on extremely P-impooverished soils. The 10 Proteaceae studied functioned remarkably conservatively, *i.e.* high LMA and low nutrient concentrations, positioning them at the far conservative end of the LES. However, the studied *Banksia* and *Hakea* species allocated P differently, whilst both genera achieved high PPUE. Our results show that high PPUE was achieved by a high P allocation to small metabolites and low P allocation to lipids for both *Banksia* and *Hakea* species. Interestingly, for the *Banksia* species only, the actual concentration and relative proportion of P allocated to the residual fraction, likely containing phosphorylated proteins, was negatively correlated with PPUE and positively with leaf [N]. These findings have clear implications and further our understanding of the differences and similarities of plant functional traits related to biochemical, physiological, and structural parameters, as well as trade-offs, that impact the fitness, survival, growth, and performance of Proteaceae. Further investigation is necessary to explore the nature of molecules comprising those P fractions, particularly the small P metabolites and the residual fraction.

Acknowledgements

CEG is supported by a Scholarship for International Research Fees from The University of Western Australia and a University Postgraduate Award co-funded by The University of Western Australia and Australian Research Council grant DP200101013 to HL and PMF. Project funding was provided by the Australian Research Council grants DP200101013 to HL and PMF and FT170100195 Future Fellowship to KR. FdT is supported by the EU Horizon 2020 Research and Innovation Program under Marie Skłodowska-Curie grant agreement 101021641. We are grateful to Toby Bird, Li Yan and Hirotuna Yamada for assistance with fieldwork.

Author contributions

CEG and PMF designed the study; CEG performed the experiment and collected the data with contributions from HL, STL and PMF; CEG, PEH, FdT, PMF, KR and HL analysed the data; and CEG wrote the manuscript. All authors contributed critically to improve the final version of the manuscript and gave approval for publication.

Data availability

The data that support the findings of this study will available upon acceptance at doi: [10.26182/xqvw-y130/](https://doi.org/10.26182/xqvw-y130/) (DATASET-BadgingarraNP-Pfractions-LES).

References

- Beard JS, Chapman AR, Gioia P. 2000.** Species richness and endemism in the Western Australian flora. *Journal of Biogeography* **27**: 1257–1268.
- Bieleski RL. 1968.** Effect of phosphorus deficiency on levels of phosphorus compounds in *Spirodela*. *Plant Physiology* **43**: 1309–1316.
- Bird T, Nestor BJ, Bayer PE, Wang G, Ilyasova A, Gille CE, Soraru BEH, Ranathunge K, Severn-Ellis AA, Jost R, et al. 2024.** Delayed leaf greening involves a major shift in the expression of cytosolic and mitochondrial ribosomes to plastid ribosomes in the highly phosphorus-use-efficient *Hakea prostrata* (Proteaceae). *Plant and Soil* **496**: 7–30.
- Dayrell RLC, Cawthray GR, Lambers H, Ranathunge K. 2022.** Using activated charcoal to remove substances interfering with the colorimetric assay of inorganic phosphate in plant extracts. *Plant and Soil* **476**: 755–764.
- Denton MD, Veneklaas EJ, Freimoser FM, Lambers H. 2007.** *Banksia* species (Proteaceae) from severely phosphorus-impooverished soils exhibit extreme efficiency in the use and re-mobilization of phosphorus. *Plant, Cell & Environment* **30**: 1557–1565.
- Dourado H, Mori M, Hwa T, Lercher MJ. 2021.** On the optimality of the enzyme–substrate relationship in bacteria. *PLOS Biology* **19**: e3001416.
- Ellsworth DS, Crous KY, De Kauwe MG, Verryckct LT, Goll D, Zaehle S, Bloomfield KJ, Ciais P, Cernusak LA, Domingues TF, et al. 2022.** Convergence in phosphorus

constraints to photosynthesis in forests around the world. *Nature Communications* **13**: 5005.

Fixen PE, Johnston AM. 2012. World fertilizer nutrient reserves: a view to the future. *Journal of the Science of Food and Agriculture* **92**: 1001–1005.

Gille CE, Finnegan PM, Hayes PE, Ranathunge K, Burgess TI, de Tombeur F, Migliorini D, Dallongeville P, Glauser G, Lambers H. 2024. Facilitative and competitive interactions between mycorrhizal and nonmycorrhizal plants in an extremely phosphorus-impooverished environment: role of ectomycorrhizal fungi and native oomycete pathogens in shaping species coexistence. *New Phytologist* **242**: 1630–1644.

Gout E, Bligny R, Douce R, Boisson A, Rivasseau C. 2011. Early response of plant cell to carbon deprivation: in vivo ^{31}P -NMR spectroscopy shows a quasi-instantaneous disruption on cytosolic sugars, phosphorylated intermediates of energy metabolism, phosphate partitioning, and intracellular pHs. *New Phytologist* **189**: 135–147.

De Groot CC, Marcelis LFM, Van Den Boogaard R, Kaiser WM, Lambers H. 2003. Interaction of nitrogen and phosphorus nutrition in determining growth. *Plant and Soil* **248**: 257–268.

Guilherme Pereira C, Hayes PE, O’Sullivan OS, Weerasinghe LK, Clode PL, Atkin OK, Lambers H. 2019. Trait convergence in photosynthetic nutrient-use efficiency along a 2-million year dune chronosequence in a global biodiversity hotspot. *Journal of Ecology* **107**: 2006–2023.

Han Z, Shi J, Pang J, Yan L, Finnegan PM, Lambers H. 2021. Foliar nutrient allocation patterns in *Banksia attenuata* and *Banksia sessilis* differing in growth rate and adaptation to low-phosphorus habitats. *Annals of Botany* **128**: 419–430.

Hayes PE, Adem GD, Pariasca-Tanaka J, Wissuwa M. 2022. Leaf phosphorus fractionation in rice to understand internal phosphorus-use efficiency. *Annals of Botany* **129**: 287–302.

Hayes PE, Clode PL, Lambers H. 2024. Calcifuge and soil-indifferent Proteaceae from south-western Australia: novel strategies in a calcareous habitat. *Plant and Soil* **496**: 95–122.

Hayes PE, Clode PL, Oliveira RS, Lambers H. 2018. Proteaceae from phosphorus-impooverished habitats preferentially allocate phosphorus to photosynthetic cells: an adaptation improving phosphorus-use efficiency. *Plant, Cell & Environment* **41**: 605–619.

Hayes PE, Nge FJ, Cramer MD, Finnegan PM, Fu P, Hopper SD, Oliveira RS, Turner BL, Zemunik G, Zhong H, et al. 2021. Traits related to efficient acquisition and use of

- phosphorus promote diversification in Proteaceae in phosphorus-impooverished landscapes. *Plant and Soil* **462**: 67–88.
- Hayes P, Turner BL, Lambers H, Laliberté E. 2014.** Foliar nutrient concentrations and resorption efficiency in plants of contrasting nutrient-acquisition strategies along a 2-million-year dune chronosequence. *Journal of Ecology* **102**: 396–410.
- Hidaka A, Kitayama K. 2011.** Allocation of foliar phosphorus fractions and leaf traits of tropical tree species in response to decreased soil phosphorus availability on Mount Kinabalu, Borneo. *Journal of Ecology* **99**: 849–857.
- Hidaka A, Kitayama K. 2013.** Relationship between photosynthetic phosphorus-use efficiency and foliar phosphorus fractions in tropical tree species. *Ecology and Evolution* **3**: 4872–4880.
- Hopper SD. 2009.** OCBIL theory: towards an integrated understanding of the evolution, ecology and conservation of biodiversity on old, climatically buffered, infertile landscapes. *Plant and Soil* **322**: 49–86.
- Hou E, Luo Y, Kuang Y, Chen C, Lu X, Jiang L, Luo X, Wen D. 2020.** Global meta-analysis shows pervasive phosphorus limitation of aboveground plant production in natural terrestrial ecosystems. *Nature Communications* **11**: 637.
- Hurley BA, Tran HT, Marty NJ, Park J, Snedden WA, Mullen RT, Plaxton WC. 2010.** The dual-targeted purple acid phosphatase isozyme AtPAP26 is essential for efficient acclimation of *Arabidopsis* to nutritional phosphate deprivation. *Plant Physiology* **153**: 1112–1122.
- Josse J, Husson F. 2016.** missMDA: a package for handling missing values in multivariate data analysis. *Journal of Statistical Software* **70**: 1–31.
- Kattge J, Bönisch G, Díaz S, Lavorel S, Prentice IC, Leadley P, Tautenhahn S, Werner GDA, Aakala T, Abedi M, et al. 2020.** TRY plant trait database – enhanced coverage and open access. *Global Change Biology* **26**: 119–188.
- Kattge J, Díaz S, Lavorel S, Prentice IC, Leadley P, Bönisch G, Garnier E, Westoby M, Reich PB, Wright IJ, et al. 2011.** TRY - a global database of plant traits. *Global Change Biology* **17**: 2905–2935.
- Kedrowski RA. 1983.** Extraction and analysis of nitrogen, phosphorus and carbon fractions in plant material. *Journal of Plant Nutrition* **6**: 989–1011.
- Kooyman RM, Laffan SW, Westoby M. 2017.** The incidence of low phosphorus soils in Australia. *Plant and Soil* **412**: 143–150.

- Kuppusamy T, Giavalisco P, Arvidsson S, Sulpice R, Stitt M, Finnegan PM, Scheible W-R, Lambers H, Jost R. 2014.** Lipid biosynthesis and protein concentration respond uniquely to phosphate supply during leaf development in highly phosphorus-efficient *Hakea prostrata*. *Plant Physiology* **166**: 1891–1911.
- Kuppusamy T, Hahne D, Ranathunge K, Lambers H, Finnegan PM. 2021.** Delayed greening in phosphorus-efficient *Hakea prostrata* (Proteaceae) is a photoprotective and nutrient-saving strategy. *Functional Plant Biology* **48**: 218–230.
- Lagace TA, Ridgway ND. 2013.** The role of phospholipids in the biological activity and structure of the endoplasmic reticulum. *Biochimica et Biophysica Acta - Molecular Cell Research* **1833**: 2499–2510.
- Lambers H. 2022.** Phosphorus acquisition and utilization in plants. *Annual Review of Plant Biology* **73**: 17–42.
- Lambers H, Brundrett MC, Raven JA, Hopper SD. 2010.** Plant mineral nutrition in ancient landscapes: high plant species diversity on infertile soils is linked to functional diversity for nutritional strategies. *Plant and Soil* **334**: 11–31.
- Lambers H, Cawthray GR, Giavalisco P, Kuo J, Laliberté E, Pearse SJ, Scheible W-R, Stitt M, Teste F, Turner BL. 2012.** Proteaceae from severely phosphorus-impooverished soils extensively replace phospholipids with galactolipids and sulfolipids during leaf development to achieve a high photosynthetic phosphorus-use-efficiency. *New Phytologist* **196**: 1098–1108.
- Lambers H, Clode PL, Hawkins H, Laliberté E, Oliveira RS, Reddell P, Shane MW, Stitt M, Weston P. 2015a.** Metabolic adaptations of the non-mycotrophic Proteaceae to soils with low phosphorus availability. In: Plaxton WC, Lambers H, eds. *Annual Plant Reviews, Volume 48, Phosphorus Metabolism in Plants*. Chichester: John Wiley & Sons, 289–336.
- Lambers H, Finnegan PM, Jost R, Plaxton WC, Shane MW, Stitt M. 2015b.** Phosphorus nutrition in Proteaceae and beyond. *Nature Plants* **1**: 15109.
- Lambers H, Finnegan PM, Laliberté E, Pearse SJ, Ryan MH, Shane MW, Veneklaas EJ. 2011.** Phosphorus nutrition of Proteaceae in severely phosphorus-impooverished soils: are there lessons to be learned for future crops? *Plant Physiology* **156**: 1058–1066.
- Lê S, Josse J, Husson F. 2008.** FactoMineR: an R package for multivariate analysis. *Journal of Statistical Software* **25**: 1–18.
- Lei Y, Du L, Chen K, Plenković-Moraj A, Sun G. 2021.** Optimizing foliar allocation of limiting nutrients and fast-slow economic strategies drive forest succession along a glacier retreating chronosequence in the eastern Tibetan Plateau. *Plant and Soil* **462**: 159–174.

- Liu ST. 2024.** *Phosphorus-use and nitrogen-use strategies of native plants in south-western Australia*. Perth, WA, Australia: University of Western Australia.
- Liu ST, Gille CE, Bird T, Ranathunge K, Finnegan PM, Lambers H. 2023.** Leaf phosphorus allocation to chemical fractions and its seasonal variation in south-western Australia is a species-dependent trait. *Science of the Total Environment* **901**: 166395.
- Liu ST, Ranathunge K, Lambers H, Finnegan PM. 2022.** Nitrate-uptake restraint in *Banksia* spp. (Proteaceae) and *Melaleuca* spp. (Myrtaceae) from a severely phosphorus-impooverished environment. *Plant and Soil* **476**: 63–77.
- Matzek V, Vitousek PM. 2009.** N:P stoichiometry and protein:RNA ratios in vascular plants: an evaluation of the growth-rate hypothesis. *Ecology Letters* **12**: 765–771.
- Mo Q, Li Z, Sayer EJ, Lambers H, Li Y, Zou B, Tang J, Heskell M, Ding Y, Wang F. 2019.** Foliar phosphorus fractions reveal how tropical plants maintain photosynthetic rates despite low soil phosphorus availability. *Functional Ecology* **33**: 1–11.
- Motomizu S, Wakimoto T, Tōei K. 1983.** Spectrophotometric determination of phosphate in river waters with molybdate and malachite green. *The Analyst* **108**: 361–367.
- Myers N, Mittermeier RA, Mittermeier CG, da Fonseca GAB, Kent J. 2000.** Biodiversity hotspots for conservation priorities. *Nature* **403**: 853–858.
- Pate JS, Beard JS. 1984.** *Kwongan, plant life of the sandplain*. Nedlands, WA, Australia: University of Western Australia Press.
- Plaxton WC, Tran HT. 2011.** Metabolic adaptations of phosphate-starved plants. *Plant Physiology* **156**: 1006–1015.
- Poorter H, Niinemets Ü, Poorter L, Wright IJ, Villar R. 2009.** Causes and consequences of variation in leaf mass per area (LMA): a meta-analysis. *New Phytologist* **182**: 565–588.
- Pratt J, Boisson AM, Gout E, Bligny R, Douce R, Aubert S. 2009.** Phosphate (Pi) starvation effect on the cytosolic Pi concentration and Pi exchanges across the tonoplast in plant cells: an in vivo ³¹P-nuclear magnetic resonance study using methylphosphonate as a Pi analog. *Plant Physiology* **151**: 1646–1657.
- Proadhan MA, Finnegan PM, Lambers H. 2019.** How does evolution in phosphorus-impooverished landscapes impact plant nitrogen and sulfur assimilation? *Trends in Plant Science* **24**: 69–82.
- Proadhan MA, Jost R, Watanabe M, Hoefgen R, Lambers H, Finnegan PM. 2016.** Tight control of nitrate acquisition in a plant species that evolved in an extremely phosphorus-impooverished environment. *Plant, Cell & Environment* **39**: 2754–2761.

- R Core Team. 2023.** *R: a language and environment for statistical computing*. Vienna, Austria: R Foundation for Statistical Computing.
- Sadowski PG, Groen AJ, Dupree P, Lilley KS. 2008.** Sub-cellular localization of membrane proteins. *Proteomics* **8**: 3991–4011.
- Saunders WMH, Williams EG. 1955.** Observations on the determination of total organic phosphorus in soils. *Journal of Soil Science* **6**: 254–267.
- Shane MW, De Vos M, De Roock S, Cawthray GR, Lambers H. 2003.** Effects of external phosphorus supply on internal phosphorus concentration and the initiation, growth and exudation of cluster roots in *Hakea prostrata* R.Br. *Plant and Soil* **248**: 209–219.
- Sulpice R, Ishihara H, Schlereth A, Cawthray GR, Encke B, Giavalisco P, Ivakov A, Arrivault S, Jost R, Krohn N, et al. 2014.** Low levels of ribosomal RNA partly account for the very high photosynthetic phosphorus-use efficiency of Proteaceae species. *Plant, Cell & Environment* **37**: 1276–1298.
- Suriyagoda LDB, Ryan MH, Gille CE, Dayrell RLC, Finnegan PM, Ranathunge K, Nicol D, Lambers H. 2023.** Phosphorus fractions in leaves. *New Phytologist* **237**: 1122–1135.
- Tian Q, Lu P, Zhai X, Zhang R, Zheng Y, Wang H, Nie B, Bai W, Niu S, Shi P, et al. 2022.** An integrated belowground trait-based understanding of nitrogen-driven plant diversity loss. *Global Change Biology* **28**: 3651–3664.
- de Tombeur F, Laliberté E, Lambers H, Faucon M, Zemunik G, Turner BL, Cornelis J, Mahy G. 2021.** A shift from phenol to silica-based leaf defences during long-term soil and ecosystem development. *Ecology Letters* **24**: 984–995.
- de Tombeur F, Turner BL, Laliberté E, Lambers H, Mahy G, Faucon M-P, Zemunik G, Cornelis J-T. 2020.** Plants sustain the terrestrial silicon cycle during ecosystem retrogression. *Science* **369**: 1245–1248.
- Tsujii Y, Atwell BJ, Lambers H, Wright IJ. 2024.** Leaf phosphorus fractions vary with leaf economic traits among 35 Australian woody species. *New Phytologist* **241**: 1985–1997.
- Tsujii Y, Fan B, Atwell BJ, Lambers H, Lei Z, Wright IJ. 2023.** A survey of leaf phosphorus fractions and leaf economic traits among 12 co-occurring woody species on phosphorus-impooverished soils. *Plant and Soil* **489**: 107–124.
- Turner BL, Romero TE. 2009.** Short-term changes in extractable inorganic nutrients during storage of tropical rain forest soils. *Soil Science Society of America Journal* **73**: 1972–1979.

- Veneklaas EJ, Lambers H, Bragg J, Finnegan PM, Lovelock CE, Plaxton WC, Price CA, Scheible W-R, Shane MW, White PJ, et al. 2012.** Opportunities for improving phosphorus-use efficiency in crop plants. *New Phytologist* **195**: 306–320.
- Viscarra Rossel RA, Bui EN. 2016.** A new detailed map of total phosphorus stocks in Australian soil. *Science of the Total Environment* **542**: 1040–1049.
- Wassen MJ, Venterink HO, Lapshina ED, Tanneberger F. 2005.** Endangered plants persist under phosphorus limitation. *Nature* **437**: 547–550.
- Wen Z, Pang J, Wang X, Gille CE, De Borda A, Hayes PE, Clode PL, Ryan MH, Siddique KHM, Shen J, et al. 2023.** Differences in foliar phosphorus fractions, rather than in cell-specific phosphorus allocation, underlie contrasting photosynthetic phosphorus use efficiency among chickpea genotypes. *Journal of Experimental Botany* **74**: 1974–1989.
- Williams KJ, Ford A, Rosauer DF, De Silva N, Mittermeier R, Bruce C, Larsen FW, Margules C. 2011.** Forests of east Australia: the 35th biodiversity hotspot. In: Zachos F, Habel J, eds. *Biodiversity Hotspots*. Berlin, Germany: Berlin: Springer, 295–310.
- Wright IJ, Reich PB, Westoby M, Ackerly DD, Baruch Z, Bongers F, Cavender-Bares J, Chapin T, Cornelissen JHC, Diemer M, et al. 2004.** The worldwide leaf economics spectrum. *Nature* **428**: 821–827.
- Yan L, Sunoj VSJ, Short AW, Lambers H, Elsheery NI, Kajita T, Wee AKS, Cao KF. 2021.** Correlations between allocation to foliar phosphorus fractions and maintenance of photosynthetic integrity in six mangrove populations as affected by chilling. *New Phytologist* **232**: 2267–2282.
- Yan L, Zhang X, Han Z, Pang J, Lambers H, Finnegan PM. 2019.** Responses of foliar phosphorus fractions to soil age are diverse along a 2 Myr dune chronosequence. *New Phytologist* **223**: 1621–1633.
- Zarcinas BA, Cartwright B, Spouncer LR. 1987.** Nitric acid digestion and multi-element analysis of plant material by inductively coupled plasma spectrometry. *Communications in Soil Science and Plant Analysis* **18**: 131–146.

Supporting Information

Fig. S1 Distribution of five *Banksia* and five *Hakea* species in the space defined by the leaf economics spectrum.

Fig. S2 Leaf nitrogen to phosphorus ratio.

Fig. S3 Correlations between foliar total phosphorus (P) concentrations and soil total P and soil resin P concentrations.

Fig. S4 Phosphorus allocated to five major biochemical fractions in leaves of five *Banksia* and five *Hakea* species.

Fig. S5 Correlations between photosynthetic nitrogen-use efficiency and major leaf traits.

Fig. S6 Correlations between photosynthetic phosphorus (P)-use efficiency and P allocated to five major leaf biochemical fractions.

Fig. S7 Correlations between leaf nitrogen concentrations and P allocated to five major biochemical fractions.

Fig. S8 Correlations between the position of *Banksia* and *Hakea* species along the leaf economics spectrum and phosphorus allocated to five major biochemical fractions.

Table S1 Recovery rate of the phosphorus-fractionation method.

Table S2 Soil chemical characteristics at four locations in Badgingarra National Park.

Table S3 Output of the principal component analyses of functional leaf traits defining the leaf economics spectrum and combined with phosphorus-related traits of five *Banksia* and five *Hakea* species.

Table S4 Output of the principal component analyses of functional leaf traits of five *Banksia* and five *Hakea* species.

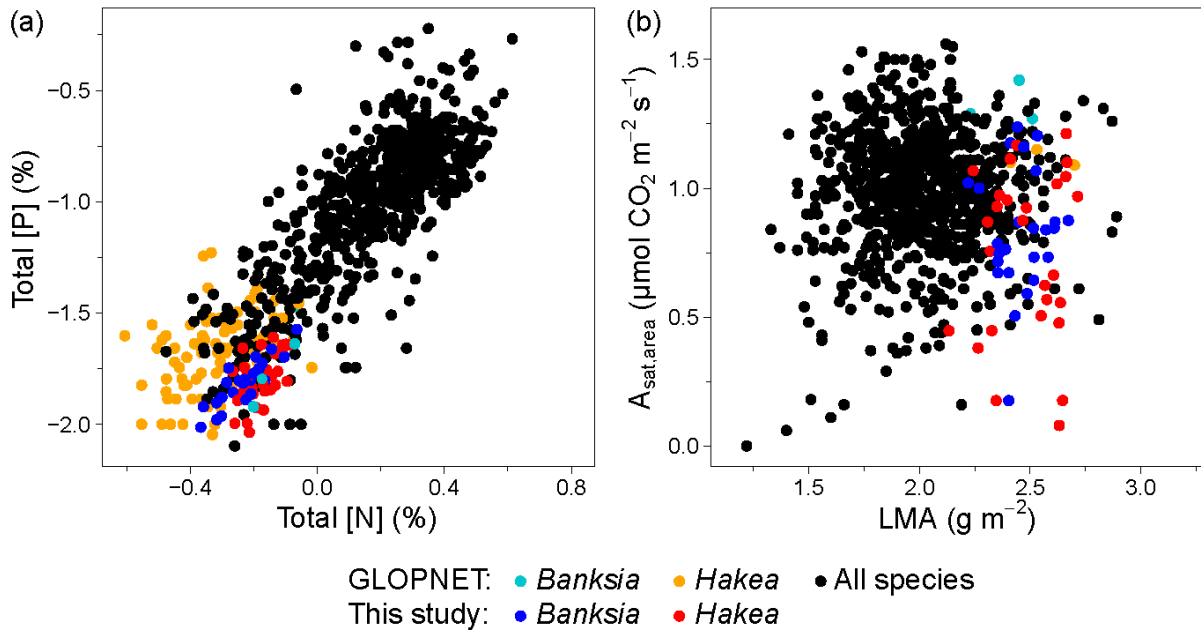


Fig. S1 Major leaf traits associated with the leaf economics spectrum (LES) for five *Banksia* (blue) and five *Hakea* (red) species naturally occurring on extremely phosphorus (P)-impoverished soils, and global data points (black) extracted from the GLOPNET dataset (Wright *et al.*, 2004). (a) Leaf total P vs. total leaf nitrogen concentrations ($n = 836$, 25 and 30 for GLOPNET, *Banksia* and *Hakea*, respectively); (b) light-saturated area-based photosynthetic rate ($A_{\text{sat,area}}$) vs. leaf mass per unit area (LMA) ($N = 764$, 25, 28 for GLOPNET, *Banksia* and *Hakea*, respectively). Data are \log_{10} -transformed to fit the regressions defined by the LES (Wright *et al.*, 2004).

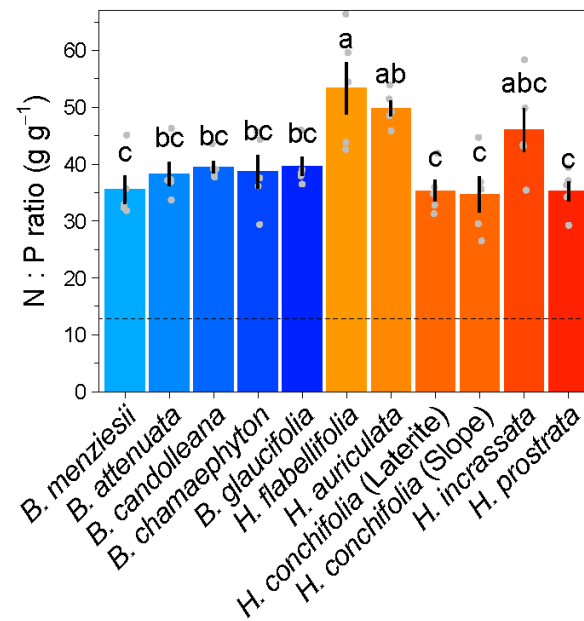


Fig. S2 Nitrogen (N) to phosphorus (P) ratio in leaves of five *Banksia* and five *Hakea* species naturally occurring on extremely P-impoverished soils. Values are means \pm SE ($n = 5$). Different letters indicate significant differences among species (post-hoc Tukey's HSD test, $P < 0.05$). The horizontal dashed lines represent mean global averages extracted from the TRY plant trait database (Kattge *et al.*, 2011).

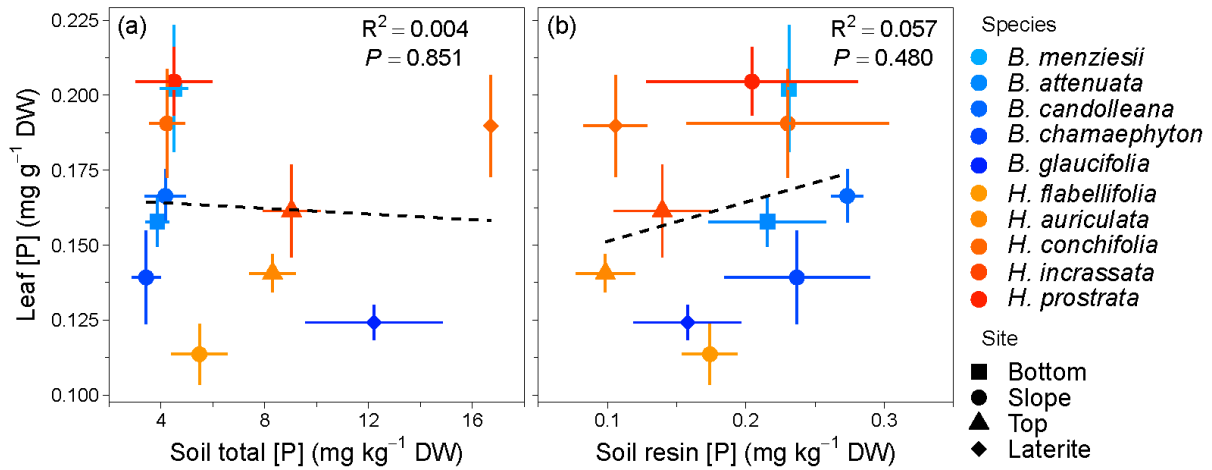


Fig. S3 Correlations between foliar total phosphorus (P) concentrations and (a) soil total P and (b) soil resin P concentrations for five *Banksia* and five *Hakea* species naturally occurring on extremely P-impoorished soils. Values are means \pm SE ($n = 5$ for leaf P, $n = 3$ for soil P). Dashed lines indicate non-significant linear regressions ($N = 11$; $P > 0.05$).

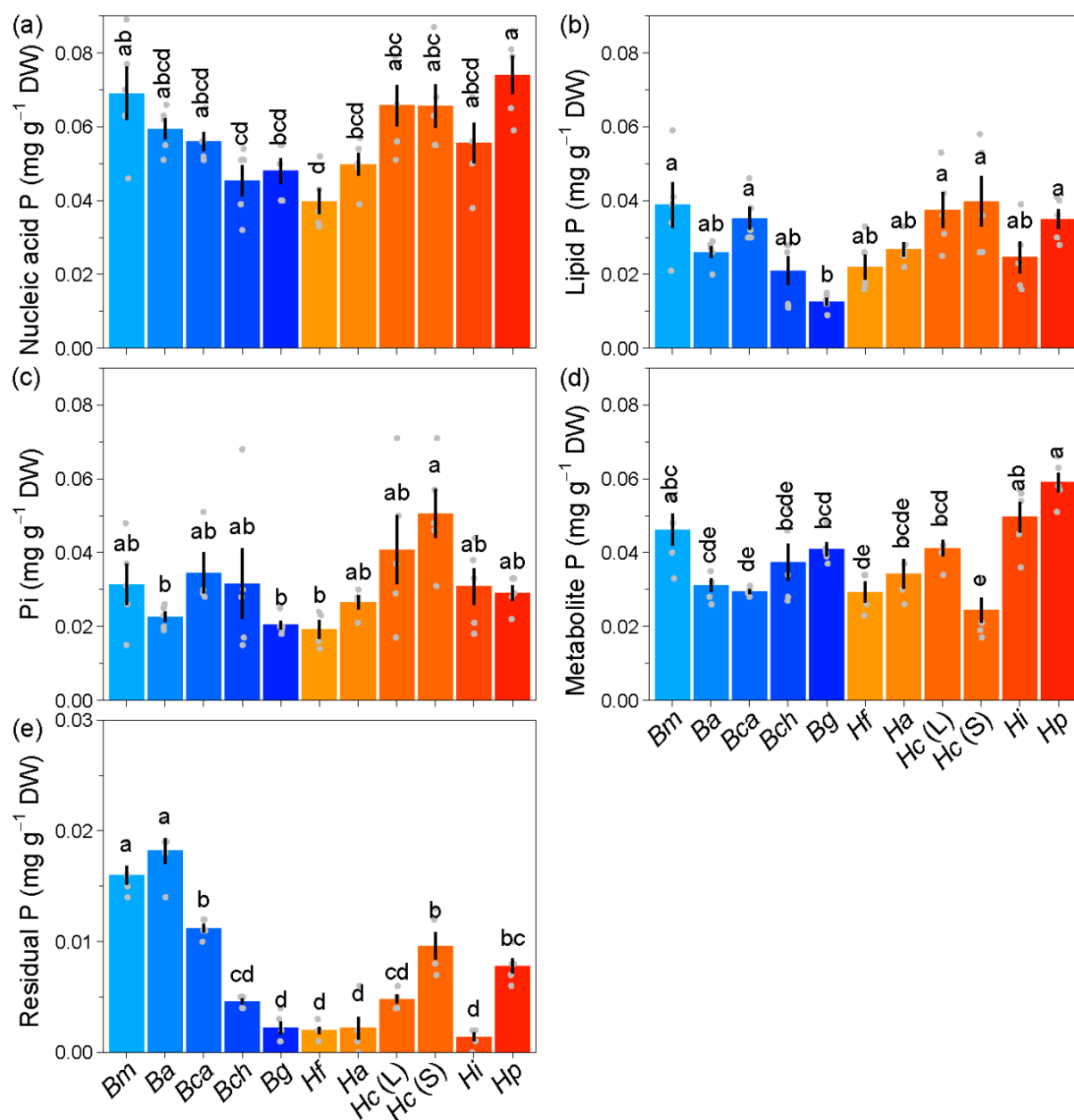


Fig. S4 Phosphorus (P) allocation to five major biochemical fractions in leaves of five *Banksia* and five *Hakea* species naturally occurring on extremely P-impoverished soils: (a) nucleic acid P, (b) lipid P, (c) inorganic P (Pi), (d) metabolite P (metabolic P – Pi) and (e) residual P. Values are means \pm SE ($n = 5$). Different lowercase letters indicate significant differences among species (post-hoc Tukey's HSD test, $P < 0.05$). *Bm*, *Banksia menziesii*; *Ba*, *B. attenuata*; *Bca*, *B. candolleana*; *Bch*, *B. chamaephyton*; *Bg*, *B. glaucifolia*; *Hf*, *Hakea flabellifolia*; *Ha*, *H. auriculata*; *Hc*, *H. conchifolia* (Laterite and Slope); *Hi*, *H. incrassata*; *Hp*, *H. prostrata*.

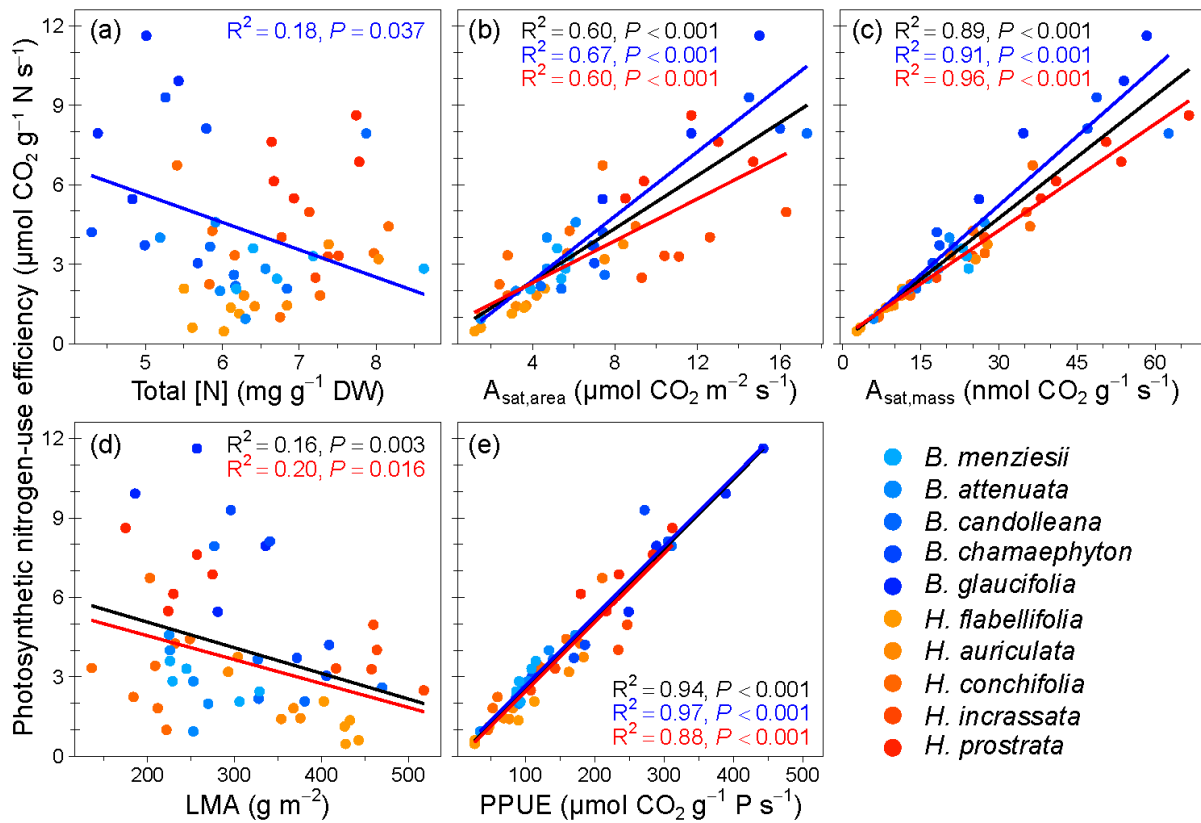


Fig. S5 Correlations between photosynthetic nitrogen (N)-use efficiency (PNUE) and major leaf traits of five *Banksia* and five *Hakea* species naturally occurring on extremely P-impooverished soils. Correlations between PNUE and (a) leaf N concentrations, (b) area-based light-saturated photosynthetic rates ($A_{\text{sat,area}}$), (c) mass-based light-saturated photosynthetic rates ($A_{\text{sat,mass}}$), (d) leaf mass per unit area (LMA) and (e) photosynthetic phosphorus-use efficiency (PPUE). Solid lines indicate significant linear correlations (black: among all individuals, blue: among *Banksia* species and red: among *Hakea* species, $P < 0.05$).

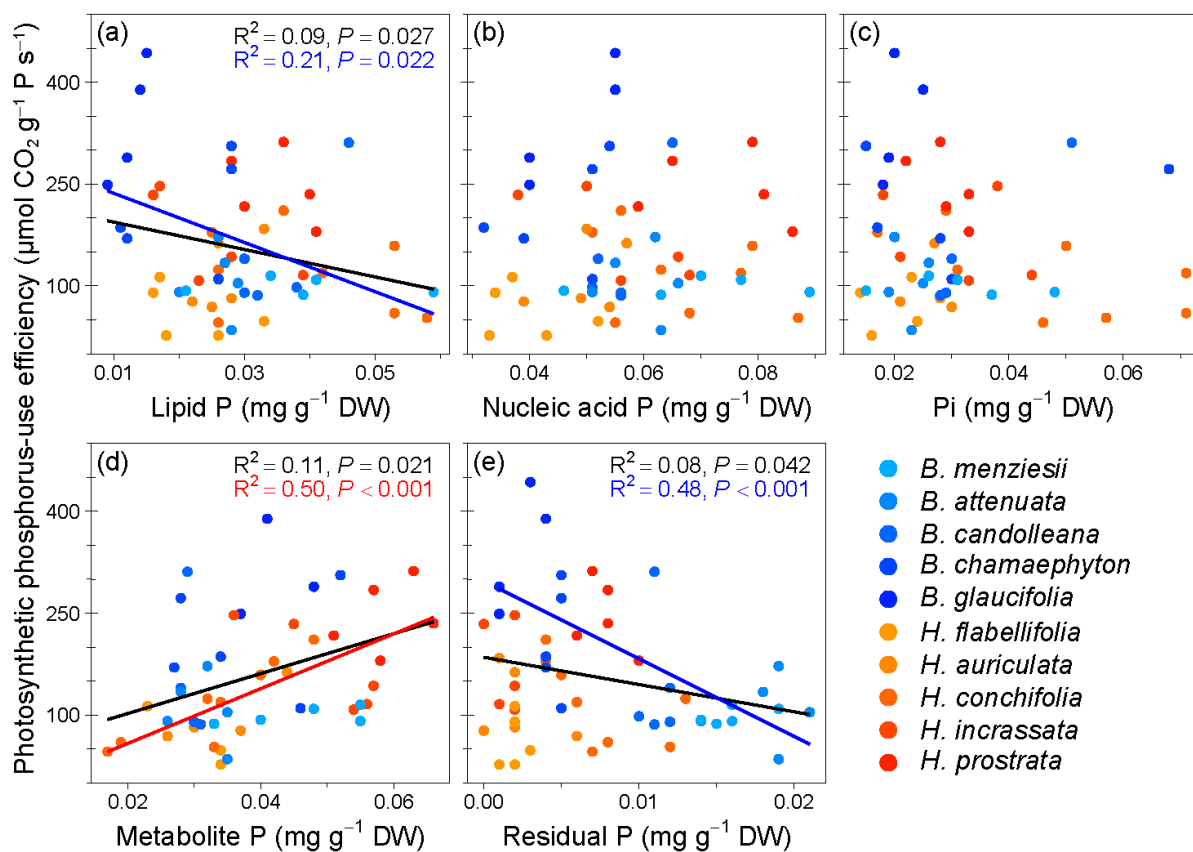


Fig. S6 Correlations between photosynthetic phosphorus (P)-use efficiency (PPUE) and P allocated to five major biochemical fractions in leaves of five *Banksia* and five *Hakea* species naturally occurring on extremely P-impooverished soils. Correlations between PPUE and (a) lipid P, (b) nucleic acid P, (c) inorganic P (Pi), (d) metabolite P (metabolic P – Pi) and (e) residual P. Solid lines indicate significant linear correlations (black: among all individuals, blue: among *Banksia* species and red: among *Hakea* species, $P < 0.05$).

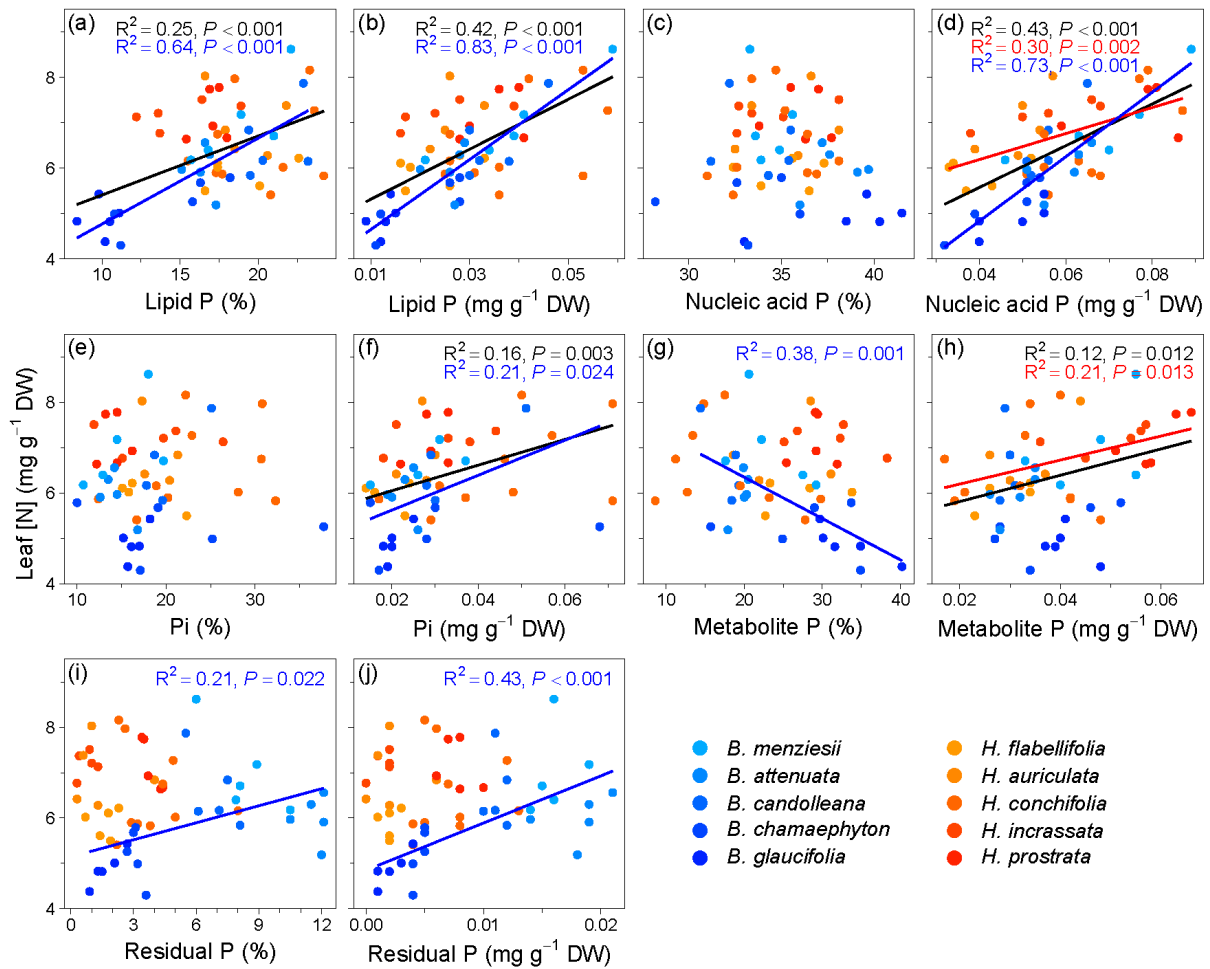


Fig. S7 Correlations between leaf nitrogen (N) concentrations ([N]) and phosphorus (P) allocated to five biochemical fractions as a proportion of leaf total P and P concentration in leaves of five *Banksia* and five *Hakea* species naturally occurring on extremely P-impooverished soils. Correlations between leaf [N] and (a–b) lipid P; (c–d) nucleic acid P; (e–f) inorganic P (Pi); (g–h) metabolite P (metabolic P – Pi); (i–j) residual P. Solid lines indicate significant linear correlations (black: among all individuals, $N = 52$ to 55 ; blue: among *Banksia* species, $N = 24$ or 25 ; and red: among *Hakea* species, $N = 28$ to 30 ; $P < 0.05$).

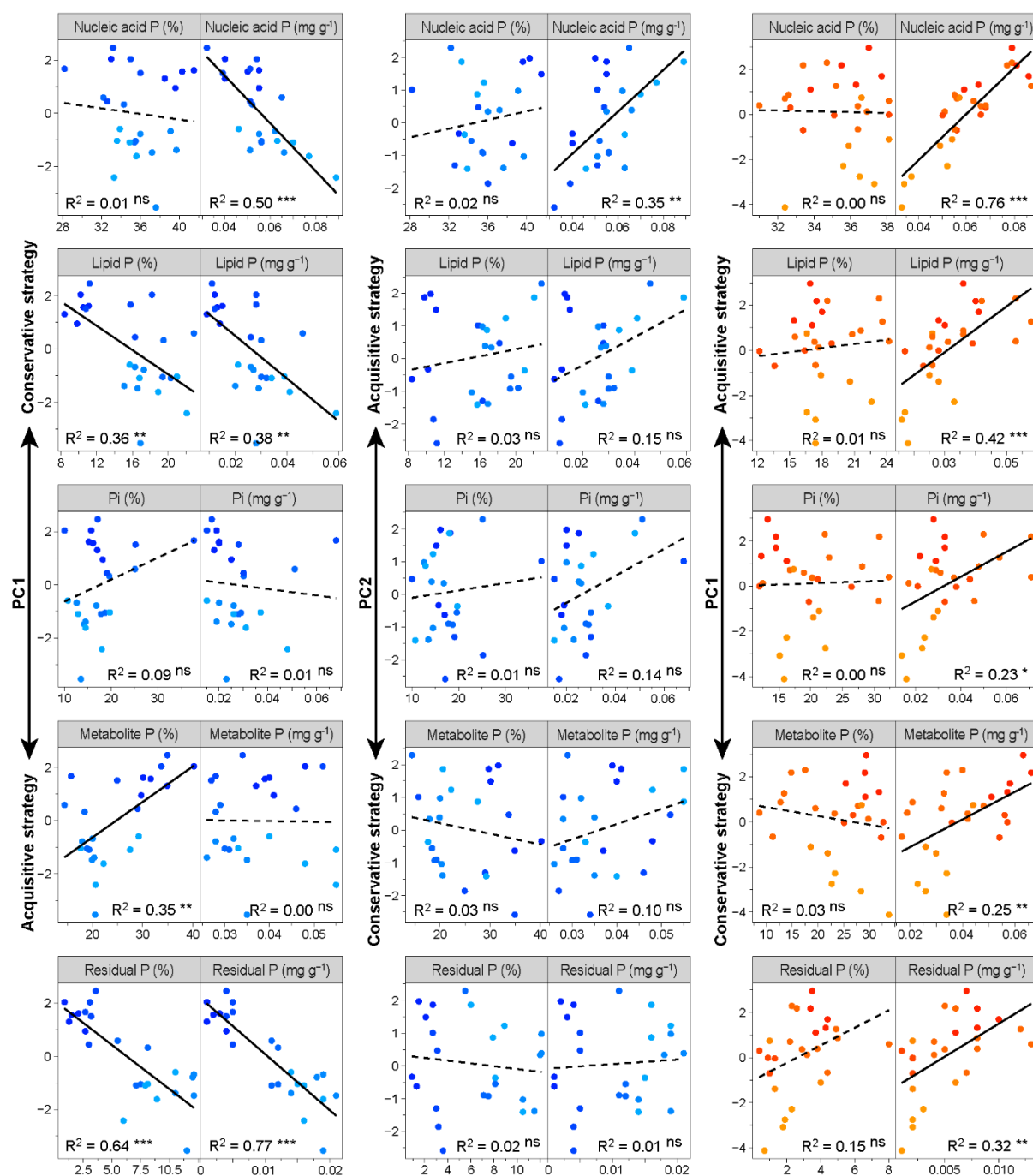


Fig. S8 Correlations between the position of individuals of *Banksia* (blue) and *Hakea* (red) along the dimensions defining the leaf economics spectrum in each individual principal component analysis (PCA) defined in Fig. 5 and P allocated to five biochemical fractions, expressed as a percentage of total P and absolute concentration. Solid and broken lines represent significant ($P < 0.05$) and non-significant ($P > 0.05$) linear correlations, respectively. Detailed results of the PCAs are presented in Supplementary Information Table S4.

Table S1 Recovery rate of phosphorus (P) in the four fractions in leaves of five *Banksia* and five *Hakea* species naturally occurring on extremely P-impooverished soils, showing high levels of recovery and consistency of the P-fractionation method. Values are means \pm SE ($n = 4-5$). DW, dry weight; ICP-OES, inductively coupled plasma optical emission spectroscopy.

	Sum P fractions (mg g ⁻¹ DW)	Leaf [P] (ICP-OES) (mg g ⁻¹ DW)	Recovery rate (%)	<i>n</i>
<i>B. menziesii</i>	0.171 \pm 0.03	0.198 \pm 0.03	86 \pm 10	4
<i>B. attenuata</i>	0.137 \pm 0.01	0.158 \pm 0.01	87 \pm 1	5
<i>B. candolleana</i>	0.145 \pm 0.01	0.166 \pm 0.01	87 \pm 3	5
<i>B. chamaephyton</i>	0.119 \pm 0.02	0.139 \pm 0.02	86 \pm 6	5
<i>B. glaucifolia</i>	0.117 \pm 0.01	0.124 \pm 0.00	94 \pm 2	5
<i>H. flabellifolia</i>	0.100 \pm 0.01	0.114 \pm 0.01	88 \pm 1	5
<i>H. auriculata</i>	0.128 \pm 0.01	0.141 \pm 0.01	91 \pm 2	5
<i>H. conchifolia</i> (Laterite)	0.163 \pm 0.02	0.190 \pm 0.02	86 \pm 3	5
<i>H. conchifolia</i> (Slope)	0.164 \pm 0.02	0.190 \pm 0.02	86 \pm 3	5
<i>H. incrassata</i>	0.144 \pm 0.02	0.162 \pm 0.02	89 \pm 3	5
<i>H. prostrata</i>	0.188 \pm 0.01	0.204 \pm 0.01	92 \pm 1	5
All	0.143 \pm 0.01	0.162 \pm 0.01	88 \pm 1	54

Table S2 Soil chemical characteristics of the top layer (0-100 mm depth) under five *Banksia* and five *Hakea* species naturally occurring on extremely phosphorus (P)-impoverished soils at four locations in Badgingarra National Park. Values are means \pm SE ($n = 6-15$). Different letters indicate significant differences among sites (post-hoc Tukey's HSD test, $P < 0.05$). DW, dry weight; EC, electrical conductivity.

Site	EC ($\mu\text{S cm}^{-1}$)	pH (CaCl₂)	pH (H₂O)	
Bottom	15 \pm 1 a	4.5 \pm 0 b	6.1 \pm 0 a	
Slope	20 \pm 2 a	4.6 \pm 0 b	5.9 \pm 0.1 a	
Top	21 \pm 2 a	4.9 \pm 0.1 a	6.1 \pm 0 a	
Laterite	24 \pm 2 a	4.5 \pm 0 b	5.9 \pm 0 a	

Site	Total P (mg kg^{-1} DW)	Inorganic P (mg kg^{-1} DW)	Organic P (mg kg^{-1} DW)	Resin P (mg kg^{-1} DW)
Bottom	4.2 \pm 0.4 c	0.18 \pm 0.01 b	4.0 \pm 0.3 b	0.22 \pm 0.02 ab
Slope	4.4 \pm 0.4 c	0.10 \pm 0.02 b	4.3 \pm 0.4 b	0.22 \pm 0.02 a
Top	8.7 \pm 0.7 b	0.14 \pm 0.02 b	8.5 \pm 0.6 a	0.12 \pm 0.02 b
Laterite	14.5 \pm 1.7 a	0.50 \pm 0.08 a	14.0 \pm 1.7 a	0.13 \pm 0.02 ab

Table S3 Results of the principal component analyses (PCAs) of functional leaf traits defining the leaf economics spectrum (Fig. 5a) and functional and phosphorus (P)-related traits (Fig. 5b) of five *Banksia* and five *Hakea* species naturally occurring on extremely P-impooverished soils. Data shown are the eigenvalue, the percentage and cumulative percentage of variance explained by each subsequent principal component (PC), and the loading of each trait to each PC. The PCs explaining $\geq 90\%$ of the cumulated variance or retained in the PCA after imputing missing values are shown. The loadings $\geq |0.50|$ for each trait are shown in bold. $A_{\text{sat,area}}$, area-based light-saturated photosynthetic rate; $A_{\text{sat,mass}}$, mass-based light-saturated photosynthetic rate; LMA, leaf mass per unit area; P_i , inorganic P; PNUE, photosynthetic nitrogen-use efficiency; PPUE, photosynthetic P-use efficiency.

	Fig. 6a Functional traits			Fig. 6b Functional + P-related traits		
	PC1	PC2	PC3	PC1	PC2	PC3
Eigenvalue	2.6	1.6	1.4	4.4	3.2	2.1
Variance (%)	43.7	26.7	22.8	34.1	24.8	16.2
Cumulated variance (%)	43.7	70.4	93.2	34.1	58.9	75.1
Thickness	-0.68	0.53	0.39	-0.13	-0.72	0.54
LMA	-0.75	0.42	0.40	-0.24	-0.72	0.46
Leaf [P]	0.76	-0.20	0.52	-0.01	0.84	0.32
Leaf [N]	0.39	-0.16	0.86	-0.22	0.48	0.43
$A_{\text{sat,mass}}$	0.79	0.58	-0.19	0.90	0.37	0.20
$A_{\text{sat,area}}$	0.51	0.86	-0.02	0.86	0.07	0.45
PPUE				0.97	0.08	0.10
PNUE				0.95	0.26	0.11
Lipid P (%)				-0.61	0.49	0.35
Nucleic acid P (%)				0.30	-0.10	-0.70
Metabolite P (%)				0.57	-0.66	-0.03
P_i (%)				-0.32	0.24	0.42
Residual P (%)				-0.16	0.53	-0.51

Table S4 Results of the principal component analysis (PCA) of functional leaf traits defining the leaf economics spectrum of five *Banksia* species (Fig. 5c) and five *Hakea* species (Fig. 5d) naturally occurring on extremely P-impooverished soils. Data shown are the eigenvalue, the percentage and cumulative percentage of variance explained by each subsequent principal component (PC), and the loading of each trait to each PC. The PCs explaining $\geq 90\%$ of the cumulated variance are shown. The loadings $\geq |0.50|$ for each trait are shown in bold. $A_{\text{sat,area}}$, area-based light-saturated photosynthetic rate; $A_{\text{sat,mass}}$, mass-based light-saturated photosynthetic rate; LMA, leaf mass per unit area.

	<i>Banksia</i>			<i>Hakea</i>		
	PC1	PC2	PC3	PC1	PC2	PC3
Eigenvalue	2.4	1.8	1.5	3.2	1.7	0.7
Variance (%)	39.3	29.8	24.7	53.9	28.5	11.6
Cumulated variance (%)	39.3	69.1	93.8	53.9	82.4	94.0
LMA	0.24	-0.75	0.53	-0.66	0.71	0.15
Thickness	0.53	-0.30	0.71	-0.72	0.64	-0.08
Leaf [N]	-0.72	0.31	0.57	0.59	0.46	0.62
Leaf [P]	-0.63	0.50	0.54	0.87	-0.06	0.23
$A_{\text{sat,mass}}$	0.65	0.75	0.04	0.88	0.29	-0.36
$A_{\text{sat,area}}$	0.82	0.47	0.28	0.64	0.70	-0.32

Supporting Information References

Kattge J, Díaz S, Lavorel S, Prentice IC, Leadley P, Bönisch G, Garnier E, Westoby M, Reich PB, Wright IJ, *et al.* 2011. TRY - a global database of plant traits. *Global Change Biology* **17**: 2905–2935.

Wright IJ, Reich PB, Westoby M, Ackerly DD, Baruch Z, Bongers F, Cavender-Bares J, Chapin T, Cornelissen JHC, Diemer M, *et al.* 2004. The worldwide leaf economics spectrum. *Nature* **428**: 821–827.

CHAPTER FIVE

General Discussion



Hakea obliqua (Proteaceae)

Introduction

The astonishing plant diversity found in the Southwest Australian biodiversity hotspot is under increasing threat (Hopper & Gioia, 2004; Miller *et al.*, 2007; Habel *et al.*, 2019). Among this diversity, Proteaceae is an emblematic family and many adaptations have evolved in this family, allowing them to acquire and use phosphorus (P) efficiently. This offers remarkable opportunities to investigate factors driving the success of this family in such an extremely P-impooverished environment (Lambers, 2014; Lambers *et al.*, 2015a; Hayes *et al.*, 2021).

A striking example allowing Proteaceae to acquire P very efficiently is the production of cluster roots – ephemeral non-mycorrhizal root structures composed of hundreds to thousands of densely-packed hairy lateral rootlets (Shane & Lambers, 2005). Functionally analogous structures that significantly increase root surface area to effectively mine poorly-available P are observed in other families co-occurring with Proteaceae in south-western Australia, *e.g.*, dauciform roots in Cyperaceae, and sand-binding roots in Haemodoraceae and Anarthriaceae (Lamont, 1974; Shane *et al.*, 2005, 2006, 2011; Lambers *et al.*, 2006). Carboxylates released in large amounts by these specialised P-acquisition structures not only mobilise P but also manganese (Mn). Because the uptake of Mn by plants is poorly regulated (Baxter *et al.*, 2008), it accumulates in mature leaves, and, thus, it has been proposed that this can be used as a proxy for the release of carboxylates (Lambers *et al.*, 2015b, 2021). However, some inconsistencies, *i.e.* low Mn levels in cluster-root-bearing *Hakea* species (Proteaceae), challenge the proposed conceptual model of leaf [Mn] as a proxy for carboxylate concentration in the rhizosphere. I explored the physiology of carboxylate exudation in *Hakea* species in Chapter 2.

In comparison with cluster-rooted species, mycorrhizal species are less efficient at acquiring P at very low P availability (Treseder & Allen, 2002; Abrahão *et al.*, 2019; Albornoz *et al.*, 2021), yet significantly contribute to the exceptional diversity in the Southwest Australian biodiversity hotspot (Zemunik *et al.*, 2015, 2016). Chapter 3 aimed to elucidate the non-nutritional role of mycorrhizal fungi and the characteristics of the interaction between mycorrhizal and non-mycorrhizal cluster-rooted species.

Proteaceae function at extremely low leaf P levels and use P very efficiently (Lambers *et al.*, 2011, 2015a; Lambers, 2022). Sequential P fractionation is an effective method to investigate P allocation in leaves (Chapin & Kedrowski, 1983; Kedrowski, 1983; Suriyagoda

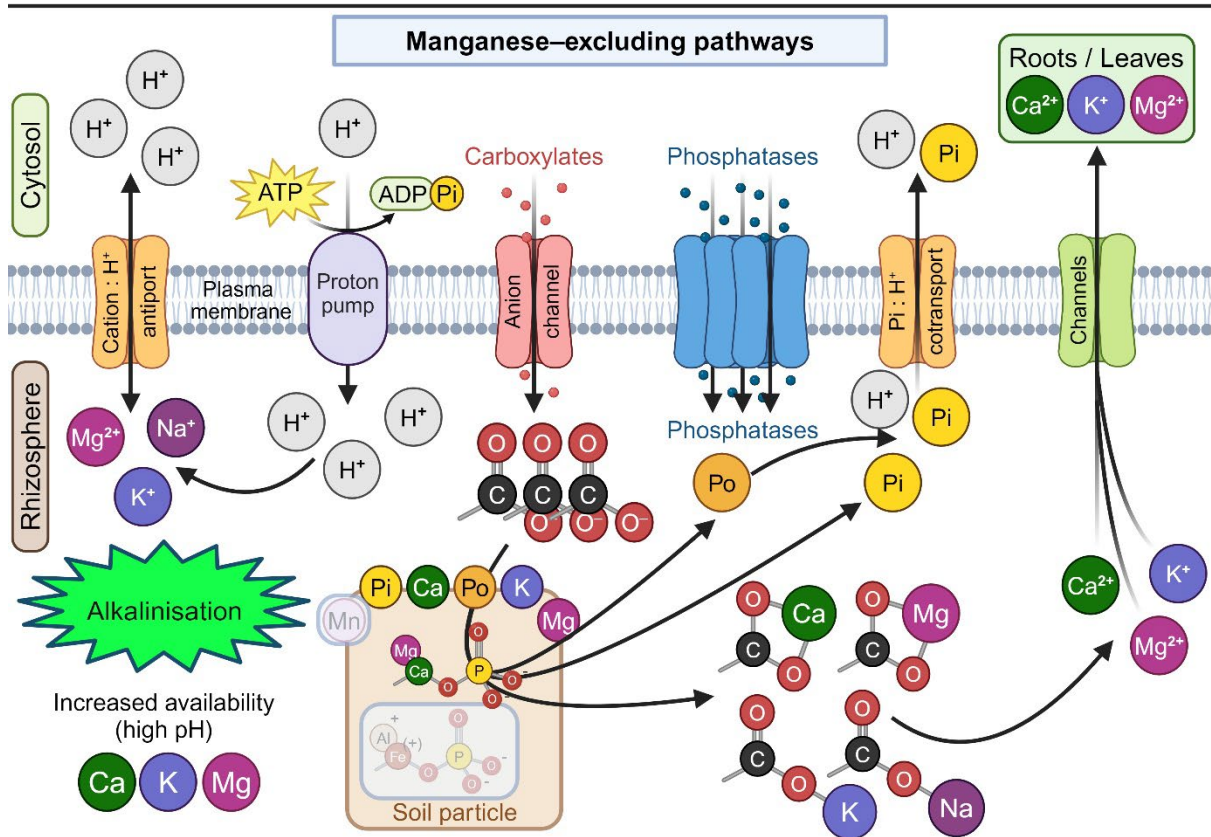
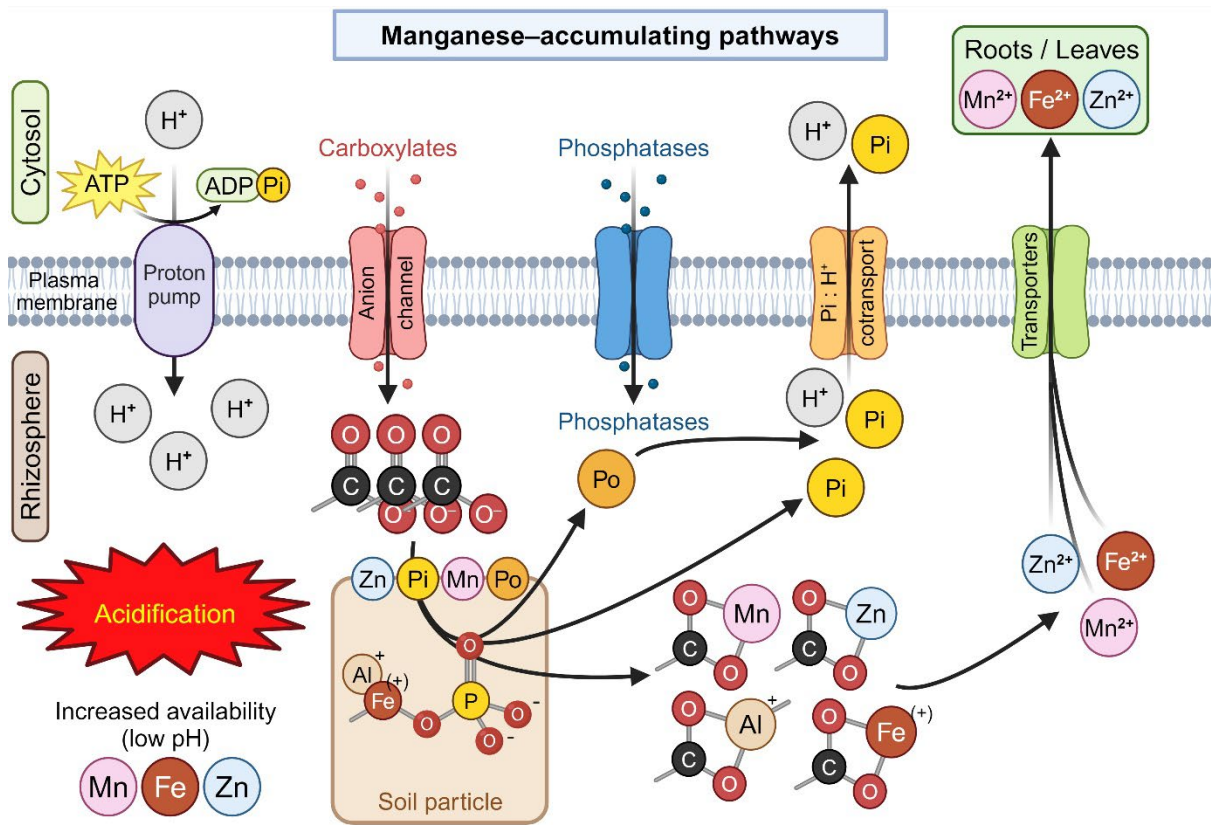
et al., 2023). Phosphorus allocation in leaves appears to be a largely species-dependent trait in south-western Australia (Liu *et al.*, 2023). In Chapter 4, I aimed to elucidate P-allocation patterns in regard to the high, yet variable photosynthetic P-use efficiency (PPUE) among *Banksia* and *Hakea* species, two iconic genera from the Proteaceae.

An understanding of the factors underpinning biodiversity in south-western Australia is crucial to ensure sustainable conservation and restoration. This thesis highlights a variety of complementary strategies, from belowground functioning and interactions to efficient P-use in leaves, that presumably all contribute to the coexistence and success of native plants in an extremely P-impooverished environment.

Physiology of carboxylate exudation

Chapter 2 explored the P-acquisition strategies of three *Hakea* species (Proteaceae) in relation to their leaf [Mn]. In support of my hypothesis, *Hakea* species with low leaf [Mn] (*H. incrassata* and *H. flabellifolia*) released similar amounts of carboxylates in rhizosphere but released cations other than protons (*e.g.*, K^+ , Mg^{2+}) at faster rates, than the high leaf-[Mn] species, *H. prostrata*. Low leaf [Mn] species also had higher rhizosphere root phosphatase (both mono- and di-esterase) activity than *H. prostrata*. These findings both contradict and support a previously established model (Lambers *et al.*, 2015b, 2021), as detailed below.

The release of ‘alternative counterions’ to H^+ with carboxylates, *e.g.*, K^+ , Mg^{2+} , Na^+ , does not promote the acidification of the rhizosphere. Some protons exported into the rhizosphere as the result of the activity of an H^+ -ATPase that provides the driving force for carboxylate release are imported back into the cytosol of the roots for the export of these cations via an antiport system (Fig. 1). Contrary to the physiology solely relying on the activity of the proton pump, this results in less H^+ accumulation in the rhizosphere. In turn, the net reduction of H^+ in the rhizosphere results in less acidification and may even lead to alkalisation. Anecdotal measurements in the nutrient solution of the three *Hakea* species grown in hydroponics revealed an increased pH of the solution in which *H. incrassata* and *H. flabellifolia* are grown, but not in that of *H. prostrata*. As a revision to the model, I propose that this alternative physiological pathway for the release of carboxylates explains, in part, why some carboxylate-releasing species do not accumulate Mn in leaves (Fig. 1). I show that low leaf [Mn] does not necessarily equate to the absence of carboxylates in the rhizosphere, but might result from an altered physiology to that initially proposed.



Considering natural reserves of non-renewable phosphate rock are being depleted (Scholz & Wellmer, 2013), carboxylate release is a desirable trait to understand and enhance P acquisition in crop species. However, measuring carboxylate concentrations in the rhizosphere or exudation rates is not feasible in the field, particularly in species-rich habitats where it would lead to species-specific estimation errors (Pérez-Harguindeguy *et al.*, 2013; Freschet *et al.*, 2021). Therefore, utilising leaf [Mn] as a proxy constitutes a valuable screening tool, although care must be taken in the interpretation of the results, as shown in this study. In P-impooverished environments, particularly for species with specialised P-mining structures like cluster roots, high leaf [Mn] is a strong indicator of the ability of a species to release carboxylates or being facilitated by carboxylate-releasing neighbours. However, species with low leaf [Mn] should receive further physiological assessment before they are defined as non-carboxylate-releasing species.

◀ **Fig. 1** Conceptual model of the effects of carboxylate-exudation physiology on the accumulation of elements in plants. Carboxylates are released via anion channels (Diatloff *et al.*, 2004). Inorganic phosphorus (Pi), desorbed from soil particles or released through hydrolysis by phosphatases from organic P (Po), which may also need to be mobilised by carboxylates, is taken up by a Pi : H⁺ cotransporter (Poirier *et al.*, 2022). The mechanism of release of phosphatases from the cytosol into the rhizosphere is not known. Carboxylates are released down an electrochemical potential gradient generated by an H⁺ gradient through the activity of a proton pump (Nussaume *et al.*, 2011). In manganese (Mn)-accumulating species (top panel), the release of carboxylates is strongly dependent on the activity of the proton pump, resulting in acidification of the rhizosphere. This increases the availability of metal cations like Fe²⁺, Zn²⁺ and Mn²⁺ that are transported into the roots by non-specific Fe²⁺ transporters (*e.g.*, IRT1 and NRAMP; Bereczky *et al.*, 2003). Moreover, Fe, Mn and Zn cations are chelated by free carboxylates. In Mn-excluding species (bottom panel), the release of carboxylates is also driven by the activity of a proton pump. However, some of the H⁺ ions exported are taken up in a cotransport mechanism leading to a release of ‘alternative cations’, *e.g.*, K⁺, Mg²⁺ and Na⁺ via a cation : H⁺ antiporter also dependent on the activity of the proton pump (Sze & Chanroj, 2018). This mechanism leads to less H⁺ accumulation in the rhizosphere, therefore contributing to less acidification and potentially alkalinisation of the rhizosphere, and increasing the availability of K, Mg and Ca that are subsequently taken up by various channels (Ashley *et al.*, 2006; Gebert *et al.*, 2010; Lambers & Oliveira, 2019). In this strategy, the availability of Mn, Fe and Zn decreases. This figure was created using BioRender, adapted from Lambers *et al.* (2015b) with permission.

On the young alkaline soils (pH 6 to 8) of the 2-Myr Jurien Bay chronosequence, the release of carboxylates is an effective strategy to mobilise P (Hayes *et al.*, 2014). On these alkaline soils, it is likely that carboxylates are accompanied by H⁺ release to enhance P availability which also enhances Mn availability. Interestingly, not many Proteaceae occur on these young soils. Along with a few species of *Banksia*, *H. prostrata* is found on alkaline soils, but not *H. incrassata* and *H. flabellifolia*. Manganese availability increases with declining soil pH, down to *c.* pH 5, below which Mn availability decreases (Lambers & Oliveira, 2019). On slightly acidic soils (pH 5 to 6), such as those on the oldest dunes of the Jurien Bay chronosequence where P-mining species are prominent (Zemunik *et al.*, 2015, 2016), carboxylate release is also the most effective strategy, as P is tightly bound to soil particles. On even more acidic soils in campos rupestres (Brazil) with soil pH < 5, non-mycorrhizal P-mining strategies are still prominent, and species accumulate Mn in leaves (Abrahão *et al.*, 2014; Oliveira *et al.*, 2015). In such acidic and P-limiting environments, it is likely that species release counterions other than H⁺ which acidifies less or potentially alkalinises the rhizosphere and increases P availability. However, the non-mycorrhizal *Discocactus placentiformis* (Cactaceae) native to campos rupestres releases carboxylates and acidifies the rhizosphere (Abrahão *et al.*, 2014). This highlights the complexity of the physiology of carboxylate release as a species-specific trait and that carboxylate release can also be involved in processes other than P mobilisation.

The release of alternative counterions may also alleviate the toxicity of certain metal ions (Ryan *et al.*, 1995, 2001; Kochian *et al.*, 2015). Previous studies have established the release of carboxylates in response to certain elements. Aluminium stimulates the efflux of malate associated with an efflux of K⁺ from roots of Al-resistant wheat (Ryan *et al.*, 1995). In addition to the carboxylates chelating toxic Al³⁺ ions, the release of K⁺ instead of H⁺ may contribute to acidifying less or even alkalinising the rhizosphere and reduce the availability of Al³⁺. Similar responses have been observed in other species with other toxic elements. For example, *Arabidopsis thaliana* releases citrate and K⁺ in response to copper exposure (Murphy *et al.*, 1999). A lead-tolerant variety of rice (*Oryza sativa*) exhibits a faster exudation of oxalate than a non-tolerant variety (Yang *et al.*, 2000). It is unclear, however, why *H. prostrata* always accumulates Mn, even in soils with low pH and, therefore, higher availability of toxic elements. *Hakea flabellifolia* was found exclusively on soils with pH < 5, and I highlighted its capacity to release alternative counterions at faster rates than *H. prostrata*. Also, *H. prostrata* occurs on soils with pH > 5. *Hakea flabellifolia* appeared less plastic than *H. prostrata* in its

carboxylate-release physiology, *i.e.* its leaf [Mn] was low and highly conserved across a large number of sites. This low plasticity likely contributes to its restricted distribution and restrains it from occurring on more alkaline and calcareous sites, unlike *H. prostrata*. Further research is warranted to elucidate the plasticity of the physiology of carboxylate release and to what extent it is involved, beyond acquiring P, in alleviating toxicity of metal ions in extremely P-impooverished soils.

The elemental analysis of the exudation assay solution of the three *Hakea* species with contrasting leaf [Mn] allowed me to measure concentrations of K and Mg, but not the concentration of H⁺. Microelectrode ion flux estimation (MIFE) provides a valuable complementary tool to measure direct ion fluxes from non-cluster-roots and cluster roots (Shabala *et al.*, 2013). It allows simultaneous measurement of ion fluxes from root tissues, including that of H⁺, K⁺, Na⁺, Mg²⁺. This tool could be considered for further studies on the physiology of carboxylate release, for example as a suitable trait for crop improvement.

Accessing organic P is also a strategy in extremely P-impooverished environments (Zhong *et al.*, 2021; Lambers *et al.*, 2022; Shen *et al.*, 2024). While I highlighted the limitation of leaf [Mn] as a proxy for carboxylate concentration in the rhizosphere, some of my results are in accordance with the original model. The higher phosphatase activity in roots of the low-leaf [Mn] *H. incrassata* and *H. flabellifolia* compared with that of *H. prostrata* indirectly contributed to their relatively low leaf Mn levels. This P-acquisition strategy does not enhance soil Mn availability, *i.e.* neither by acidifying the rhizosphere nor by mobilising soil-bound Mn, although some soil-bound organic P, *e.g.*, phytate, requires prior mobilisation by carboxylates (Giles *et al.*, 2017, 2018; Richardson *et al.*, 2022). Therefore, carboxylate-releasing species with higher exuded phosphatase activity might be able to meet their P needs by releasing less carboxylates and thus accumulate less Mn in leaves (Zhong *et al.*, 2021). However, this was not the case in the *Hakea* species studied that all released non-significantly different amounts of carboxylates. The increase in species diversity with declining soil P availability is also accompanied by an increase in nutrient-acquisition diversity (Zemunik *et al.*, 2015, 2016). By accessing different soil P species, the functional diversity of P-acquisition strategies contributes to the species coexistence in extremely P-impooverished environments (Turner, 2008; Raven *et al.*, 2018).

Microbe-mediated plant interactions

In Chapter 3, I showed that the competitive ability of non-mycorrhizal *Banksia menziesii* to acquire P was reduced in the presence of either beneficial or detrimental soil microbes and mycorrhizal *Eucalyptus tottiana*. This confirms previous models that both mycorrhizal fungi and pathogens contribute to maintaining plant diversity in extremely P-impoverished environments (Fig. 2; Laliberté *et al.*, 2015; Albornoz *et al.*, 2017; Lambers *et al.*, 2018). In the mixture only, we observed more complex defence responses in roots of *B. menziesii*, *i.e.* increased levels of phytohormones, and increased concentrations of phenolic compounds in roots of both species. *Eucalyptus tottiana* exhibited stronger defence responses in the monoculture, irrespective of its mycorrhizal status, *i.e.* colonised or not, emphasising the positive effect of the facilitation by *B. menziesii* to mediate pathogen infection.

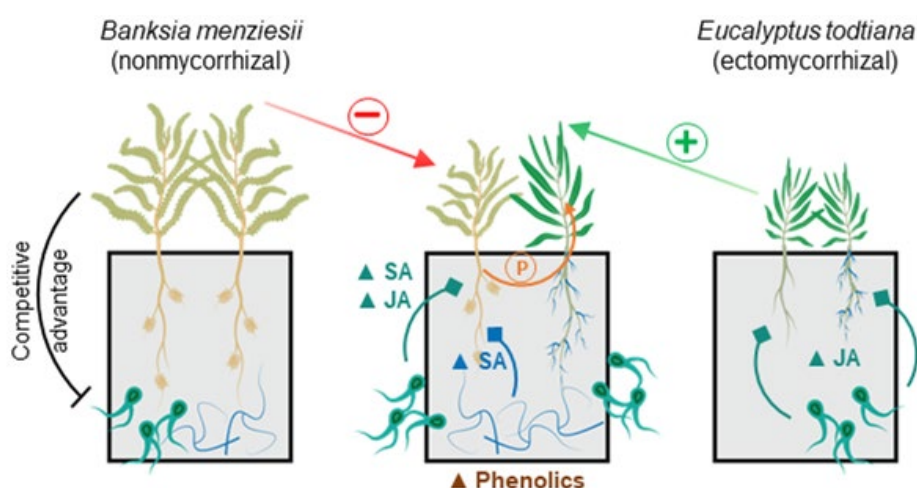


Fig. 2 Conceptual model of the interactions between non-mycorrhizal cluster-rooted *Banksia menziesii* (Proteaceae) and ectomycorrhizal *Eucalyptus tottiana* (Myrtaceae) mediated by soil microbes. Ectomycorrhizal fungi and oomycete *Phytophthora* spp. pathogens did not induce defence responses in roots of *B. menziesii* grown in a monoculture, likely as a result of the stronger growth of *B. menziesii* compared with that in mixture with *E. tottiana*. However, both salicylic (SA) and jasmonic acid (JA)-dependent responses were induced in roots of *B. menziesii* in the mixture, in association with competition with *E. tottiana* for resource acquisition (*i.e.* phosphorus (P) uptake) and growth. Conversely, the growth advantage of *E. tottiana* from the facilitation in the mixture with *B. menziesii* suppressed the JA-dependent response to oomycete pathogens observed in the monoculture. In the mixture, the presence of *E. tottiana* induced an SA-dependent effect in roots of *B. menziesii* in response to the ectomycorrhizal fungi. Both beneficial and detrimental microbes contributed to increase phenolic levels in roots of both species in the mixture. Adapted from Gille *et al.* (2024).

Facilitation, rather than competition, is prevalent in stressful environments (Callaway, 2007; Lekberg *et al.*, 2018). In extremely P-impooverished environments such as south-western Australia, many species rely on positive interactions with their P-mobilising neighbours to acquire scarce nutrients. In the presence of a P-mobilising facilitator, *Hibbertia racemosa* (Dilleniaceae), which does not produce cluster roots, adjusts its biomass-allocation pattern by decreasing its root to shoot ratio and alters its root system architecture by orienting roots toward the P-mobilising roots of the facilitator (de Britto Costa *et al.*, 2021). Intermingling between carboxylate-releasing roots of one species and non-carboxylate-releasing roots of a facilitated species is the first step of the facilitation (Teste *et al.*, 2020a). Subsequently, non-cluster-rooted and/or non-mycorrhizal plants can access P mobilised by carboxylates (Lambers & Teste, 2013; Muler *et al.*, 2014; Yu *et al.*, 2023; Staudinger *et al.*, 2024). However, I showed, for the first time, that the facilitation of the growth and P uptake of *E. todtiana* by *B. menziesii* comprised a competitive component in the interaction (Fig. 2). In the absence of soil microbes, this competitive component was weaker, further emphasising the trade-off between efficient P acquisition and defence against pathogens.

There is a wealth of evidence of the benefits of either arbuscular (AM) or ectomycorrhizal (ECM) fungal colonisation on the nutritional status of the plant host, particularly P uptake (Smith & Read, 2008; Smith *et al.*, 2011; Ferrol *et al.*, 2019). However, mycorrhizal symbiosis is not an effective strategy for nutrient acquisition under extremely P-limiting conditions (Parfit, 1979; Bolan *et al.*, 1984; Abbott *et al.*, 1984; Treseder & Allen, 2002; Albornoz *et al.*, 2021). Mycorrhizal symbiosis provides other benefits to the hosts, including water uptake, soil aggregation, or disease resistance (Delavaux *et al.*, 2017; Qin *et al.*, 2021). Facilitation of the defence against pathogens can take many forms; *e.g.*, ECM fungi provide a physical barrier to pathogens with their Hartig net and fungal mantle, direct chemical defence (antimicrobial compounds), or induction of the plant-host defence (Pozo & Azcón-Aguilar, 2007). Interestingly, ECM fungi induced a phytohormone response in roots of *B. menziesii* only in the presence of *E. todtiana*. I suggest that ectomycorrhizal fungi contribute to the priming of the defence responses of the non-mycorrhizal *B. menziesii* by initiating a non-host incompatible interaction, or that signals were emitted from the roots of *E. todtiana* or its associated microbiome via the mycorrhizal hyphae. This interaction involving putative signals between mycorrhizal fungi, and mycorrhizal and non-mycorrhizal plants warrants further investigation.

The dominance of ECM fungi decreases along ecological gradients like soil nutrient availability, in contrast with that of AM fungi (Teste *et al.*, 2020b). Conversely, AM fungal colonisation increases with plant age (Teste *et al.*, 2020b). In *Acacia rostellifera* (Fabaceae) and *Melaleuca systena* (Myrtaceae), two species endemic to south-western Australia naturally that occur along a gradient of soil age along the 2-Myr Jurien Bay chronosequence, the root colonisation by AM fungi decreases while that of ECM fungi increases with increasing soil age (Zemunik *et al.*, 2015; Albornoz *et al.*, 2016a). *Eucalyptus todtiana* and *B. menziesii* are iconic species in south-western Australia and co-occur on some of the most ancient and P-impooverished soils (Hopper, 2021; Ritchie *et al.*, 2021). The dominance of ECM fungi in extremely P-impooverished soils was the rationale behind the choice of inoculum comprising various ECM fungal species, of which *Pisolithus* spp. are the most common (Burgess *et al.*, 1993; Martin *et al.*, 2002), to study the defences of two species with contrasting nutrient-acquisition strategies. However, AM and ECM symbioses act differently on the biology of their hosts (Brundrett & Tedersoo, 2020; Tedersoo *et al.*, 2020). Moreover, there is evidence of a switch between mycorrhizal symbiosis types with plant age (Teste *et al.*, 2020b). For example, seedlings of *Eucalyptus globulus* and *E. urophylla* switch from AM to ECM fungal colonisation with seedling development between 8 and 16 weeks (Chen *et al.*, 2000). In addition to the shift in mycorrhizal type that dominates along the Jurien Bay chronosequence (Albornoz *et al.*, 2016a), the community composition of ECM fungi changes (Albornoz *et al.*, 2016b). Moreover, some plants, including native species from south-western Australia from multiple families, have the ability to form dual mycorrhizal symbioses, *i.e.* they associate with both AM and ECM fungi simultaneously on different parts of the roots (Albornoz *et al.*, 2016a; Teste & Laliberté, 2019; Teste *et al.*, 2020b; Frew & Aguilar-Trigueros, 2023). While the present study provides insights into the non-nutritional benefits of ECM fungi to their hosts, *i.e.* defence against oomycete pathogens, further comprehensive studies should investigate the role of AM fungi and their interaction with ECM fungi in an ecological perspective (Chaudhary *et al.*, 2022).

Phosphorus allocation and photosynthetic phosphorus-use efficiency

Proteaceae both acquire and use P very efficiently. All species studied in Chapter 4 had a PPUE near or higher than the global average (Kattge *et al.*, 2011). Photosynthetic rates and PPUE were very strongly correlated, while PPUE and leaf [P] were not. This indicates that Proteaceae in this study used P for photosynthesis very efficiently, but photosynthetic rates did not exceed

the global average (Kattge *et al.*, 2011). While all species had very high PPUE, we observed variation within both genera of *Banksia* and *Hakea*. There was a certain degree of convergence in P-allocation patterns between the two genera, with both allocating more P to small metabolites and less to lipids to achieve high PPUE. However, correlations between PPUE and Pi or residual P, likely containing phosphorylated proteins, were not consistent for both genera. Accordingly, we suggest a trade-off between substrate and enzyme abundance, particularly in *Banksia* species.

The analysis of P fractions in leaves has gained substantial interest in recent years, with various applications in understanding plant species' functioning (Yan *et al.*, 2021; Suriyagoda *et al.*, 2023; Tsujii *et al.*, 2023, 2024; Wen *et al.*, 2023; Liu *et al.*, 2023). However, very little is known about what comprises those P fractions, particularly metabolite P and residual P. The metabolite P pool presumably contains small water-soluble phosphorylated compounds, while the residual P fraction contains P-containing molecules that did not partition into the previous solvents used in the sequential extraction (Chapin & Kedrowski, 1983). It is crucial to elucidate the nature of those fractions to enhance our understanding of their metabolic involvement, particularly in photosynthetic performance. What are the most abundant compounds in the metabolite P fraction? How do they vary among species? It is also essential to discern the cellular distribution of those compounds. For example, Proteaceae preferentially allocate P to photosynthetically-active mesophyll cells rather than epidermal cells, contributing to their high PPUE (Guilherme Pereira *et al.*, 2018; Hayes *et al.*, 2018). Vacuolar Pi is not metabolically active (Yang *et al.*, 2017), but Pi is withdrawn from this pool into the cytoplasm in response to Pi starvation (Pratt *et al.*, 2009). To what extent do Proteaceae with low foliar total [P] allocate Pi, still representing *c.* 20% of total P, to the vacuolar compartment? To address these outstanding questions, it is fundamental to combine the P-fractionation method used here with other techniques such as microscopy (*e.g.*, cryo-SEM; Hayes *et al.*, 2018), -omics approaches, and ³¹P-NMR (Gout *et al.*, 2011).

All species examined had extremely low leaf [P], which also contributed to their high PPUE. In addition, I observed very high LMA, typical for the high levels of scleromorphy observed in leaves of Proteaceae (Jordan *et al.*, 2005). These traits place these species on the far 'conservative' end of the leaf economics spectrum (LES), as previously described (Westoby & Falster, 2021). Interestingly, P-allocation patterns did not explain the position of the species along the LES, *i.e.* there was no correlation between P fractions as a percentage of total P and

the distribution of the species along the axes opposing the acquisitive and conservative resource-utilisation strategies. There were strong correlations between the distribution of the species along these axes and P fractions in absolute concentrations, reflecting the greater investment of P in a given fraction contributed to higher leaf total [P]. However, how P-allocation patterns influence the distribution of species from other families co-occurring with Proteaceae in extremely P-impooverished environments requires further attention. In a meta-analysis, Suriyagoda *et al.* (2023) reported a larger variability of P allocation into P fractions among families than between species in a family. How do species from families, *e.g.*, *Eucalyptus* sp. (Myrtaceae) and *Acacia* sp. (Fabaceae), with less conservative leaf traits than Proteaceae, *i.e.* lower LMA, higher leaf [P], allocate P and how does this allocation contribute to their more variable position along the LES? In addition to complementarity in P-acquisition strategies, P-allocation patterns contribute to the functional diversity in extremely P-impooverished megadiverse south-western Australia.

Concluding remarks

I examined aspects of functional diversity among native species in an extremely P-impooverished environment in south-western Australia. *Hakea* species displayed contrasting physiologies of carboxylate exudation resulting in variable leaf Mn accumulation. Leaf [Mn] is a valuable practical tool to predict carboxylate concentration in the rhizosphere, considering how challenging it is to assess belowground functioning. However, I highlight the limitations of this model. In the revised model I propose, leaf [Mn] is a proxy for carboxylate exudation depending on protons as counterion. Moreover, contrasting physiology of carboxylate exudation, *i.e.* the dependence on different counterions, aids in explaining the distribution of *Hakea* species along the natural gradient of soil P and pH found along the Jurien Bay chronosequence. By accessing different forms of P and being restricted to certain soil conditions, cluster-root physiology contributes to the diversity of *Hakea* species. These findings have important implications for the distribution of species relying on carboxylate exudation for nutrient acquisition.

Cluster-rooted Proteaceae can facilitate P acquisition by their non-cluster-rooted neighbours. Although I highlight a competitive component in the facilitative interaction between a non-mycorrhizal Proteaceae and a mycorrhizal Myrtaceae, both species contributed to their relative success when experiencing pathogen infection. This is another example of the importance of functional diversity driving species diversity in stressful environments.

I also observed a diversity in P-allocation patterns among *Banksia* and *Hakea* species, two co-occurring genera. This physiological diversity does not contribute to the functional diversity as I propose for P-acquisition strategies and plant-plant interactions. However, these findings highlight the importance of the diversity among P-efficient native plant species in extremely P-impooverished environments.

Future research is required to further explore the present findings, for example assessing the physiology of carboxylate exudation in *Banksia* species that consistently accumulate Mn in leaves. It is also unclear to what extent different counterions restrain the distribution of carboxylate-releasing species in relation to toxic metal elements. There are many nutrient-acquisition strategies in addition to carboxylate release (Lambers *et al.* 2022). However, little is known about the interaction between plants with those contrasting nutrient-acquisition strategies, and how various biotic and abiotic factors influence those interactions. The P-use efficiency also deserves further attention in species with contrasting growth habits from genera co-occurring with Proteaceae in these environments. My thesis lays the groundwork in understanding how functional diversity of below- and aboveground physiological traits contributes to species diversity and their success in extremely P-impooverished megadiverse environment in south-western Australia.

References

- Abbott LK, Robson AD, Boer G. 1984.** The effect of phosphorus on the formation of hyphae in soil by the vesicular-arbuscular mycorrhizal fungus *Glomus fasciculatum*. *New Phytologist* **97**: 437–446.
- Abrahão A, de Britto Costa P, Lambers H, Andrade SAL, Sawaya ACHF, Ryan MH, Oliveira RS. 2019.** Soil types select for plants with matching nutrient-acquisition and -use traits in hyperdiverse and severely nutrient-impooverished *campos rupestres* and *cerrado* in Central Brazil. *Journal of Ecology* **107**: 1302–1316.
- Abrahão A, Lambers H, Sawaya ACHF, Mazzafera P, Oliveira RS. 2014.** Convergence of a specialized root trait in plants from nutrient-impooverished soils: phosphorus-acquisition strategy in a nonmycorrhizal cactus. *Oecologia* **176**: 345–355.

- Albornoz FE, Burgess TI, Lambers H, Etehellis H, Laliberté E. 2017.** Native soilborne pathogens equalize differences in competitive ability between plants of contrasting nutrient-acquisition strategies. *Journal of Ecology* **105**: 549–557.
- Albornoz FE, Dixon KW, Lambers H. 2021.** Revisiting mycorrhizal dogmas: are mycorrhizas really functioning as they are widely believed to do? *Soil Ecology Letters* **3**: 73–82.
- Albornoz FE, Lambers H, Turner BL, Teste FP, Laliberté E. 2016a.** Shifts in symbiotic associations in plants capable of forming multiple root symbioses across a long-term soil chronosequence. *Ecology and Evolution* **6**: 2368–2377.
- Albornoz FE, Teste FP, Lambers H, Bunce M, Murray DC, White NE, Laliberté E. 2016b.** Changes in ectomycorrhizal fungal community composition and declining diversity along a 2-million-year soil chronosequence. *Molecular ecology* **25**: 4919–4929.
- Ashley MK, Grant M, Grabov A. 2006.** Plant responses to potassium deficiencies: a role for potassium transport proteins. *Journal of Experimental Botany* **57**: 425–436.
- Baxter IR, Vitek O, Lahner B, Muthukumar B, Borghi M, Morrissey J, Guerinot M Lou, Salt DE. 2008.** The leaf ionome as a multivariable system to detect a plant's physiological status. *Proceedings of the National Academy of Sciences of the United States of America* **105**: 12081–12086.
- Berezky Z, Wang H-Y, Schubert V, Ganai M, Bauer P. 2003.** Differential regulation of *nramp* and *irt* metal transporter genes in wild type and iron uptake mutants of tomato. *Journal of Biological Chemistry* **278**: 24697–24704.
- Bolan NS, Robson AD, Barrow NJ. 1984.** Increasing phosphorus supply can increase the infection of plant roots by vesicular-arbuscular mycorrhizal fungi. *Soil Biology and Biochemistry* **16**: 419–420.
- de Britto Costa P, Staudinger C, Veneklaas EJ, Oliveira RS, Lambers H. 2021.** Root positioning and trait shifts in *Hibbertia racemosa* as dependent on its neighbour's nutrient-acquisition strategy. *Plant, Cell & Environment* **44**: 1257–1267.
- Brundrett MC, Tedersoo L. 2020.** Resolving the mycorrhizal status of important northern hemisphere trees. *Plant and Soil* **454**: 3–34.
- Burgess TI, Malajczuk N, Grove TS. 1993.** The ability of 16 ectomycorrhizal fungi to increase growth and phosphorus uptake of *Eucalyptus globulus* Labill. and *E. diversicolor* F. Muell. *Plant and Soil* **153**: 155–164.
- Callaway RM. 2007.** *Positive interactions and interdependence in plant communities*. Dordrecht, the Netherlands: Springer.

- Chapin FS, Kedrowski RA. 1983.** Seasonal changes in nitrogen and phosphorus fractions and autumn retranslocation in evergreen and deciduous Taiga trees. *Ecology* **64**: 376–391.
- Chaudhary VB, Holland EP, Charman-Anderson S, Guzman A, Bell-Dereske L, Cheeke TE, Corrales A, Duchicela J, Egan C, Gupta MM, et al. 2022.** What are mycorrhizal traits? *Trends in Ecology and Evolution* **37**: 573–581.
- Chen YL, Brundrett MC, Dell B. 2000.** Effects of ectomycorrhizas and vesicular–arbuscular mycorrhizas, alone or in competition, on root colonization and growth of *Eucalyptus globulus* and *E. urophylla*. *New Phytologist* **146**: 545–555.
- Delavaux CS, Smith-Ramesh LM, Kuebbing SE. 2017.** Beyond nutrients: a meta-analysis of the diverse effects of arbuscular mycorrhizal fungi on plants and soils. *Ecology* **98**: 2111–2119.
- Diatloff E, Roberts M, Sanders D, Roberts SK. 2004.** Characterization of anion channels in the plasma membrane of *Arabidopsis* epidermal root cells and the identification of a citrate-permeable channel induced by phosphate starvation. *Plant Physiology* **136**: 4136–4149.
- Ferrol N, Azcón-Aguilar C, Pérez-Tienda J. 2019.** Review: arbuscular mycorrhizas as key players in sustainable plant phosphorus acquisition: an overview on the mechanisms involved. *Plant Science* **280**: 441–447.
- Freschet GT, Pagès L, Iversen CM, Comas LH, Rewald B, Roumet C, Klimešová J, Zadworny M, Poorter H, Postma JA, et al. 2021.** A starting guide to root ecology: strengthening ecological concepts and standardising root classification, sampling, processing and trait measurements. *New Phytologist* **232**: 973–1122.
- Frew A, Aguilar-Trigueros CA. 2023.** Australia offers unique insight into the ecology of arbuscular mycorrhizal fungi: an opportunity not to be lost. *Austral Ecology* **48**: 1713–1720.
- Gebert M, Meschenmoser K, Svidová S, Weghuber J, Schweyen R, Eifler K, Lenz H, Weyand K, Knoop V. 2010.** A root-expressed magnesium transporter of the *MRS2/MGT* gene family in *Arabidopsis thaliana* allows for growth in low-Mg²⁺ environments. *Plant Cell* **21**: 4018–4030.
- Giles CD, Dupuy L, Boitt G, Brown LK, Condrón LM, Darch T, Blackwell MSA, Menezes-Blackburn D, Shand CA, Stutter MI, et al. 2018.** Root development impacts on the distribution of phosphatase activity: improvements in quantification using soil zymography. *Soil Biology and Biochemistry* **116**: 158–166.

- Giles CD, George TS, Brown LK, Mezeli MM, Richardson AE, Shand CA, Wendler R, Darch T, Menezes-Blackburn D, Cooper P, et al. 2017.** Does the combination of citrate and phytase exudation in *Nicotiana tabacum* promote the acquisition of endogenous soil organic phosphorus? *Plant and Soil* **412**: 43–59.
- Gille CE, Finnegan PM, Hayes PE, Ranathunge K, Burgess TI, de Tombeur F, Migliorini D, Dallongeville P, Glauser G, Lambers H. 2024.** Facilitative and competitive interactions between mycorrhizal and nonmycorrhizal plants in an extremely phosphorus-impooverished environment: role of ectomycorrhizal fungi and native oomycete pathogens in shaping species coexistence. *New Phytologist* **242**: 1630–1644.
- Gout E, Bligny R, Douce R, Boisson A, Rivasseau C. 2011.** Early response of plant cell to carbon deprivation: in vivo ^{31}P -NMR spectroscopy shows a quasi-instantaneous disruption on cytosolic sugars, phosphorylated intermediates of energy metabolism, phosphate partitioning, and intracellular pHs. *New Phytologist* **189**: 135–147.
- Guilherme Pereira C, Clode PL, Oliveira RS, Lambers H. 2018.** Eudicots from severely phosphorus-impooverished environments preferentially allocate phosphorus to their mesophyll. *New Phytologist* **218**: 959–973.
- Habel JC, Rasche L, Schneider UA, Engler JO, Schmid E, Rödder D, Meyer ST, Trapp N, Sos del Diego R, Eggermont H, et al. 2019.** Final countdown for biodiversity hotspots. *Conservation Letters* **12**: e12668.
- Hayes PE, Clode PL, Oliveira RS, Lambers H. 2018.** Proteaceae from phosphorus-impooverished habitats preferentially allocate phosphorus to photosynthetic cells: An adaptation improving phosphorus-use efficiency. *Plant, Cell & Environment* **41**: 605–619.
- Hayes PE, Nge FJ, Cramer MD, Finnegan PM, Fu P, Hopper SD, Oliveira RS, Turner BL, Zemunik G, Zhong H, et al. 2021.** Traits related to efficient acquisition and use of phosphorus promote diversification in Proteaceae in phosphorus-impooverished landscapes. *Plant and Soil* **462**: 67–88.
- Hayes P, Turner BL, Lambers H, Laliberté E. 2014.** Foliar nutrient concentrations and resorption efficiency in plants of contrasting nutrient-acquisition strategies along a 2-million-year dune chronosequence. *Journal of Ecology* **102**: 396–410.
- Hopper SD. 2021.** Out of the OCBILs: new hypotheses for the evolution, ecology and conservation of the eucalypts. *Biological Journal of the Linnean Society* **133**: 342–372.
- Hopper SD, Gioia P. 2004.** The Southwest Australian Floristic Region: evolution and conservation of a global hotspot of biodiversity. *Annual Review of Ecology, Evolution, and Systematics* **35**: 623–650.

- Jordan GJ, Dillon RA, Weston PH. 2005.** Solar radiation as a factor in the evolution of scleromorphic leaf anatomy in Proteaceae. *American Journal of Botany* **92**: 789–796.
- Kattge J, Díaz S, Lavorel S, Prentice IC, Leadley P, Bönlisch G, Garnier E, Westoby M, Reich PB, Wright IJ, et al. 2011.** TRY - a global database of plant traits. *Global Change Biology* **17**: 2905–2935.
- Kedrowski RA. 1983.** Extraction and analysis of nitrogen, phosphorus and carbon fractions in plant material. *Journal of Plant Nutrition* **6**: 989–1011.
- Kochian L V., Piñeros MA, Liu J, Magalhaes J V. 2015.** Plant adaptation to acid soils: the molecular basis for crop aluminum resistance. *Annual Review of Plant Biology* **66**: 571–598.
- Laliberté E, Lambers H, Burgess TI, Wright SJ. 2015.** Phosphorus limitation, soil-borne pathogens and the coexistence of plant species in hyperdiverse forests and shrublands. *New Phytologist* **206**: 507–521.
- Lambers H. 2014.** *Plant life on the sandplains in southwest Australia: a global biodiversity hotspot*. Crawley, Australia: The University of Western Australia Publishing.
- Lambers H. 2022.** Phosphorus acquisition and utilization in plants. *Annual Review of Plant Biology* **73**: 17–42.
- Lambers H, Albornoz FE, Kotula L, Laliberté E, Ranathunge K, Teste FP, Zemunik G. 2018.** How belowground interactions contribute to the coexistence of mycorrhizal and non-mycorrhizal species in severely phosphorus-impooverished hyperdiverse ecosystems. *Plant and Soil* **424**: 11–33.
- Lambers H, de Britto Costa P, Cawthray GR, Denton MD, Finnegan PM, Hayes PE, Oliveira RS, Power SC, Ranathunge K, Shen Q, et al. 2022.** Strategies to acquire and use phosphorus in phosphorus-impooverished and fire-prone environments. *Plant and Soil* **476**: 133–160.
- Lambers H, Finnegan PM, Jost R, Plaxton WC, Shane MW, Stitt M. 2015a.** Phosphorus nutrition in Proteaceae and beyond. *Nature Plants* **1**: 15109.
- Lambers H, Finnegan PM, Laliberté E, Pearse SJ, Ryan MH, Shane MW, Veneklaas EJ. 2011.** Phosphorus nutrition of Proteaceae in severely phosphorus-impooverished soils: are there lessons to be learned for future crops? *Plant Physiology* **156**: 1058–1066.
- Lambers H, Hayes PE, Laliberté E, Oliveira RS, Turner BL. 2015b.** Leaf manganese accumulation and phosphorus-acquisition efficiency. *Trends in Plant Science* **20**: 83–90.
- Lambers H, Oliveira RS. 2019.** *Plant Physiological Ecology*. Cham, Switzerland: Springer.

- Lambers H, Shane MW, Cramer MD, Pearse SJ, Veneklaas EJ. 2006.** Root structure and functioning for efficient acquisition of phosphorus: matching morphological and physiological traits. *Annals of Botany* **98**: 693–713.
- Lambers H, Teste FP. 2013.** Interactions between arbuscular mycorrhizal and non-mycorrhizal plants: do non-mycorrhizal species at both extremes of nutrient availability play the same game? *Plant, Cell & Environment* **36**: 1911–1915.
- Lambers H, Wright IJ, Guilherme Pereira C, Bellingham PJ, Bentley LP, Boonman A, Cernusak LA, Foulds W, Gleason SM, Gray EF, et al. 2021.** Leaf manganese concentrations as a tool to assess belowground plant functioning in phosphorus-impooverished environments. *Plant and Soil* **461**: 43–61.
- Lamont B. 1974.** The biology of dauciform roots in the sedge *Cyathochaete avenacea*. *New Phytologist* **73**: 985–996.
- Lekberg Y, Bever JD, Bunn RA, Callaway RM, Hart MM, Kivlin SN, Klironomos J, Larkin BG, Maron JL, Reinhart KO, et al. 2018.** Relative importance of competition and plant-soil feedback, their synergy, context dependency and implications for coexistence. *Ecology Letters* **21**: 1268–1281.
- Liu ST, Gille CE, Bird T, Ranathunge K, Finnegan PM, Lambers H. 2023.** Leaf phosphorus allocation to chemical fractions and its seasonal variation in south-western Australia is a species-dependent trait. *Science of the Total Environment* **901**: 166395.
- Martin F, Diez J, Dell B, Delaruelle C. 2002.** Phylogeography of the ectomycorrhizal *Pisolithus* species as inferred from nuclear ribosomal DNA ITS sequences. *New Phytologist* **153**: 345–357.
- Miller BP, Enright NJ, Lamont BB. 2007.** Record error and range contraction, real and imagined, in the restricted shrub *Banksia hookeriana* in south-western Australia. *Diversity and Distributions* **13**: 406–417.
- Muler AL, Oliveira RS, Lambers H, Veneklaas EJ. 2014.** Does cluster-root activity benefit nutrient uptake and growth of co-existing species? *Oecologia* **174**: 23–31.
- Murphy AS, Eisinger WR, Shaff JE, Kochian L V, Taiz L. 1999.** Early copper-induced leakage of K⁺ from *Arabidopsis* seedlings is mediated by ion channels and coupled to citrate efflux. *Plant Physiology* **121**: 1375–1382.
- Nussaume L, Kanno S, Javot H, Marin E, Pochon N, Ayadi A, Nakanishi TM, Thibaud MC. 2011.** Phosphate import in plants: focus on the PHT1 transporters. *Frontiers in Plant Science* **2**: 83.

- Oliveira RS, Galvão HC, de Campos MCR, Eller CB, Pearse SJ, Lambers H. 2015.** Mineral nutrition of campos rupestres plant species on contrasting nutrient-impooverished soil types. *New Phytologist* **205**: 1183–1194.
- Parfitt RL. 1979.** The availability of P from phosphate-goethite bridging complexes. Desorption and uptake by ryegrass. *Plant and Soil* **53**: 55–65.
- Pérez-Harguindeguy N, Díaz S, Garnier E, Lavorel S, Poorter H, Jaureguiberry P, Bret-Harte MS, Cornwell WK, Craine JM, Gurvich DE, et al. 2013.** New handbook for standardised measurement of plant functional traits worldwide. *Australian Journal of Botany* **61**: 167–234.
- Poirier Y, Jaskolowski A, Clúa J. 2022.** Phosphate acquisition and metabolism in plants. *Current Biology* **32**: R623–R629.
- Pozo MJ, Azcón-Aguilar C. 2007.** Unraveling mycorrhiza-induced resistance. *Current Opinion in Plant Biology* **10**: 393–398.
- Pratt J, Boisson AM, Gout E, Bligny R, Douce R, Aubert S. 2009.** Phosphate (Pi) starvation effect on the cytosolic Pi concentration and Pi exchanges across the tonoplast in plant cells: an in vivo ³¹P-nuclear magnetic resonance study using methylphosphonate as a Pi analog. *Plant Physiology* **151**: 1646–1657.
- Qin J, Geng Y, Li X, Zhang C, Zhao X, von Gadow K. 2021.** Mycorrhizal type and soil pathogenic fungi mediate tree survival and density dependence in a temperate forest. *Forest Ecology and Management* **496**: 119459.
- Raven JA, Lambers H, Smith SE, Westoby M. 2018.** Costs of acquiring phosphorus by vascular land plants: patterns and implications for plant coexistence. *New Phytologist* **217**: 1420–1427.
- Richardson AE, George TS, Hens M, Delhaize E, Ryan PR, Simpson RJ, Hocking PJ. 2022.** Organic anions facilitate the mobilization of soil organic phosphorus and its subsequent lability to phosphatases. *Plant and Soil* **476**: 161–180.
- Ritchie AL, Svejcar LN, Ayre BM, Bolleter J, Brace A, Craig MD, Davis B, Davis RA, Van Etten EJB, Fontaine JB, et al. 2021.** A threatened ecological community: research advances and priorities for *Banksia* woodlands. *Australian Journal of Botany* **69**: 53–84.
- Ryan P, Delhaize E, Jones D. 2001.** Function and mechanism of organic anion exudation from plant roots. *Annual Review of Plant Physiology and Plant Molecular Biology* **52**: 527–560.
- Ryan P, Delhaize E, Randall P. 1995.** Characterisation of Al-stimulated efflux of malate from the apices of Al-tolerant wheat roots. *Planta* **196**: 103–110.

- Scholz RW, Wellmer FW. 2013.** Approaching a dynamic view on the availability of mineral resources: what we may learn from the case of phosphorus? *Global Environmental Change* **23**: 11–27.
- Shabala S, Shabala L, Bose J, Cuin T, Newman I. 2013.** Ion flux measurements using the MIFE technique. In: *Methods in Molecular Biology*. 171–183.
- Shane MW, Cawthray GR, Cramer MD, Kuo J, Lambers H. 2006.** Specialized ‘dauciform’ roots of Cyperaceae are structurally distinct, but functionally analogous with ‘cluster’ roots. *Plant, Cell & Environment* **29**: 1989–1999.
- Shane MW, Dixon KW, Lambers H. 2005.** The occurrence of dauciform roots amongst Western Australian reeds, rushes and sedges, and the impact of phosphorus supply on dauciform-root development in *Schoenus unispiculatus* (Cyperaceae). *New Phytologist* **165**: 887–898.
- Shane MW, Lambers H. 2005.** Cluster roots: a curiosity in context. *Plant and Soil* **274**: 101–125.
- Shane MW, McCully ME, Canny MJ, Pate JS, Lambers H. 2011.** Development and persistence of sandsheaths of *Lyginia barbata* (Restionaceae): relation to root structural development and longevity. *Annals of Botany* **108**: 1307–1322.
- Shen Q, Ranathunge K, Lambers H, Finnegan PM. 2024.** *Adenanthos* species (Proteaceae) in phosphorus-impooverished environments use a variety of phosphorus-acquisition strategies and achieve high-phosphorus-use efficiency. *Annals of Botany* **133**: 483–494.
- Smith SE, Jakobsen I, Grønlund M, Smith FA. 2011.** Roles of arbuscular mycorrhizas in plant phosphorus nutrition: interactions between pathways of phosphorus uptake in arbuscular mycorrhizal roots have important implications for understanding and manipulating plant phosphorus acquisition. *Plant Physiology* **156**: 1050–1057.
- Smith SE, Read DJ. 2008.** *Mycorrhizal symbiosis*. London, UK: Academic Press and Elsevier.
- Staudinger C, Renton M, Leopold M, Wasaki J, Veneklaas EJ, de Britto Costa P, Boitt G, Lambers H. 2024.** Interspecific facilitation of micronutrient uptake between cluster-root-bearing trees and non-cluster rooted-shrubs in a *Banksia* woodland. *Plant and Soil* **496**: 71–82.
- Suriyagoda LDB, Ryan MH, Gille CE, Dayrell RLC, Finnegan PM, Ranathunge K, Nicol D, Lambers H. 2023.** Phosphorus fractions in leaves. *New Phytologist* **237**: 1122–1135.
- Sze H, Chanroj S. 2018.** Plant endomembrane dynamics: studies of K⁺/H⁺ antiporters provide insights on the effects of pH and ion homeostasis. *Plant Physiology* **177**: 875–895.

- Tedersoo L, Bahram M, Zobel M. 2020.** How mycorrhizal associations drive plant population and community biology. *Science* **367**: eaba1223.
- Teste FP, Dixon KW, Lambers H, Zhou J, Veneklaas EJ. 2020a.** The potential for phosphorus benefits through root placement in the rhizosphere of phosphorus-mobilising neighbours. *Oecologia* **193**: 843–855.
- Teste FP, Jones MD, Dickie IA. 2020b.** Dual-mycorrhizal plants: their ecology and relevance. *New Phytologist* **225**: 1835–1851.
- Teste FP, Laliberté E. 2019.** Plasticity in root symbioses following shifts in soil nutrient availability during long-term ecosystem development. *Journal of Ecology* **107**: 633–649.
- Treseder KK, Allen MF. 2002.** Direct nitrogen and phosphorus limitation of arbuscular mycorrhizal fungi: a model and field test. *New Phytologist* **155**: 507–515.
- Tsujii Y, Atwell BJ, Lambers H, Wright IJ. 2024.** Leaf phosphorus fractions vary with leaf economic traits among 35 Australian woody species. *New Phytologist* **241**: 1985–1997.
- Tsujii Y, Fan B, Atwell BJ, Lambers H, Lei Z, Wright IJ. 2023.** A survey of leaf phosphorus fractions and leaf economic traits among 12 co-occurring woody species on phosphorus-impooverished soils. *Plant and Soil* **489**: 107–124.
- Turner BL. 2008.** Resource partitioning for soil phosphorus: a hypothesis. *Journal of Ecology* **96**: 698–702.
- Wen Z, Pang J, Wang X, Gille CE, De Borda A, Hayes PE, Clode PL, Ryan MH, Siddique KHM, Shen J, et al. 2023.** Differences in foliar phosphorus fractions, rather than in cell-specific phosphorus allocation, underlie contrasting photosynthetic phosphorus use efficiency among chickpea genotypes. *Journal of Experimental Botany* **74**: 1974–1989.
- Westoby M, Falster DS. 2021.** The conservative low-phosphorus niche in Proteaceae. *Plant and Soil* **462**: 89–93.
- Yan L, Sunoj VSJ, Short AW, Lambers H, Elsheery NI, Kajita T, Wee AKS, Cao KF. 2021.** Correlations between allocation to foliar phosphorus fractions and maintenance of photosynthetic integrity in six mangrove populations as affected by chilling. *New Phytologist* **232**: 2267–2282.
- Yang SY, Huang TK, Kuo HF, Chiou TJ. 2017.** Role of vacuoles in phosphorus storage and remobilization. *Journal of Experimental Botany* **68**: 3045–3055.
- Yang Y, Jung J, Song W, Suh H, Lee Y. 2000.** Identification of rice varieties with high tolerance or sensitivity to lead and characterization of the mechanism of tolerance. *Plant Physiology* **124**: 1019–1026.

- Yu R, Su Y, Lambers H, van Ruijven J, An R, Yang H, Yin X, Xing Y, Zhang W, Li L. 2023.** A novel proxy to examine interspecific phosphorus facilitation between plant species. *New Phytologist* **239**: 1637–1650.
- Zemunik G, Turner BL, Lambers H, Laliberté E. 2015.** Diversity of plant nutrient-acquisition strategies increases during long-term ecosystem development. *Nature Plants* **1**: 15050.
- Zemunik G, Turner BL, Lambers H, Laliberté E. 2016.** Increasing plant species diversity and extreme species turnover accompany declining soil fertility along a long-term chronosequence in a biodiversity hotspot. *Journal of Ecology* **104**: 792–805.
- Zhong H, Zhou J, Azmi A, Arruda AJ, Doolette AL, Smernik RJ, Lambers H. 2021.** *Xylomelum occidentale* (Proteaceae) accesses relatively mobile soil organic phosphorus without releasing carboxylates. *Journal of Ecology* **109**: 246–259.

APPENDIX

Additional publications during PhD



Verticordia ovalifolia (Myrtaceae)

During my PhD, I co-authored the following publications in peer-reviewed journals.

The frontpages of four selected publications, highly relevant to the work presented in this thesis, are presented.

Suriyagoda LDB, Ryan MH, Gille CE, Dayrell RLC, Finnegan PM, Ranathunge K, Nicol D, Lambers H. 2023. Phosphorus fractions in leaves. *New Phytologist* 237: 1122–1135.

Review

New
Phytologist *Research review*

Phosphorus fractions in leaves

Author for correspondence:


Lalith D. B. Suriyagoda

Email: lalith.suriyagoda@agri.pdn.ac.lk;

lalith.suriyagoda@uwa.edu.au

Received: 12 July 2022

Accepted: 25 October 2022

Lalith D. B. Suriyagoda^{1,2} , Megan H. Ryan^{3,4} , Clément E. Gille² ,
Roberta L. C. Dayrell² , Patrick M. Finnegan² , Kosala Ranathunge² ,
Dion Nicol^{3,4,5} and Hans Lambers^{2,4} 

¹Department of Crop Science, Faculty of Agriculture, University of Peradeniya, Peradeniya 20400, Sri Lanka; ²School of Biological Sciences, The University of Western Australia, 35 Stirling Highway, Perth, WA 6009, Australia; ³UWA School of Agriculture and Environment, The University of Western Australia, 35 Stirling Highway, Perth, WA 6009, Australia; ⁴Institute of Agriculture, The University of Western Australia, 35 Stirling Highway, Perth, WA 6009, Australia; ⁵Department of Primary Industries and Regional Development, Western Australia, Dryland Research Institute, Merredin, WA 6415, Australia

New Phytologist (2023) 237: 1122–1135
doi: 10.1111/nph.18588

Key words: crop improvement, organic phosphorus, phospholipids, phosphorus fractions, phosphorus-use efficiency.

Summary

Leaf phosphorus (P) comprises four major fractions: inorganic phosphate (P_i), nucleic acids, phospholipids, P-containing metabolites and a residual fraction. In this review paper, we investigated whether allocation of P fractions varies among groups of terrestrial vascular plants, and is indicative of a species' strategy to use P efficiently. We found that as leaf total P concentration increases, the P_i fraction increases the most, without a plateau, while other fractions plateau. Variability of the concentrations of leaf P fractions is greatest among families > species(family) > regions > plant life forms. The percentage of total P allocated to nucleic acid-P (20–35%) and lipid-P (14–34%) varies less among families/species. High photosynthetic P-use efficiency is associated with low concentrations of all P fractions, and preferential allocation of P to metabolite-P and mesophyll cells. Sequential resorption of P from senescing leaves starts with P_i , followed by metabolite-P, and then other organic P fractions. Allocation of P to leaf P fractions varies with season. Leaf phytate concentrations vary considerably among species, associated with variation in photosynthesis and defence. Plasticity of P allocation to its fractions is important for acclimation to low soil P availability, and species-specific P allocation is needed for co-occurrence with other species.

Introduction

Phosphorus (P) frequently limits plant productivity, and its availability in soil determines species distribution in many terrestrial ecosystems (Veneklaas *et al.*, 2012; Zemunik *et al.*, 2015). Molecules that contain P are involved in many metabolic processes (Bielecki, 1973). Based on their chemical structure, leaf P compounds are broadly divided into four chemical fractions: inorganic phosphate (P_i) and three organic P (P_o) fractions (small metabolites, nucleic acids and phospholipids), as well as a residual fraction of uncharacterised composition (Bielecki, 1973; Chapin III & Bielecki, 1982; Veneklaas *et al.*, 2012; Hidaka & Kitayama, 2013). The metabolically active P_i fraction is located in the cytoplasm within a narrow range of concentrations (Bielecki, 1968; Mimura *et al.*, 1996), and excess P_i is stored in the cell

vacuole as a buffer to regulate [P_i] in the cytoplasm (Bielecki, 1968; Tachibana, 1987; Lee & Ratcliffe, 1993), or in other membrane-surrounded structures and organelles presently poorly characterised (Ryan *et al.*, 2019). Small metabolites represent low-molecular-weight P-esters, such as sugar phosphates and nucleotides (e.g. ATP and NAD(P)H). Inorganic P and small metabolites are sometimes reported together as the 'metabolic' P pool, which is inappropriate as only a fraction of the P_i is metabolically active (Bielecki, 1968; Veneklaas *et al.*, 2012). Nucleic acids are the major P_o fraction in leaves, of which up to 85% is RNA and the remainder is DNA (Bielecki, 1968; Tachibana, 1987; Matzek & Vitousek, 2009). Phospholipids are components of cellular membranes including endoplasmic reticulum, plasmalemma, Golgi apparatus and tonoplast, as well as membranes of the nucleus, mitochondria and chloroplasts (Jouhet *et al.*, 2004; Andersson

Liu ST, Gille CE, Bird T, Ranathunge K, Finnegan PM, Lambers H. 2023. Leaf phosphorus allocation to chemical fractions and its seasonal variation in south-western Australia is a species-dependent trait. *Science of the Total Environment* 901: 166395.

Science of the Total Environment 901 (2023) 166395



Contents lists available at ScienceDirect

Science of the Total Environment

journal homepage: www.elsevier.com/locate/scitotenv



Leaf phosphorus allocation to chemical fractions and its seasonal variation in south-western Australia is a species-dependent trait

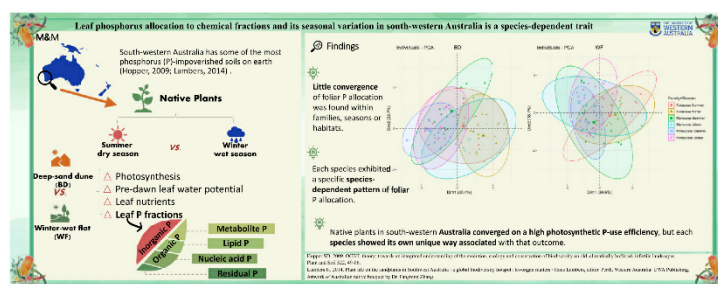
Shu Tong Liu^{*}, Clément E. Gille, Toby Bird, Kosala Ranathunge, Patrick M. Finnegan, Hans Lambers

School of Biological Sciences, The University of Western Australia, 35 Stirling Highway, Perth, WA 6009, Australia

HIGHLIGHTS

- Little convergence of foliar P allocation was found within family, season or habitat.
- Plants in south-western Australia exhibited species-dependent foliar P-allocation patterns.
- Species converged on high photosynthetic P-use efficiency, each with their specific way.

GRAPHICAL ABSTRACT



ARTICLE INFO

Editor: Charlotte Poschenrieder

Keywords:

Habitat
Leaf phosphorus fractions
Phosphorus
Photosynthesis
Seasonality
South-western Australia

ABSTRACT

South-western Australia is a global biodiversity hotspot and has some of the oldest and most phosphorus (P)-impoverished soils in the world. Proteaceae is one of the dominant P-efficient plant families there, but it is unknown how leaf P concentrations and foliar P allocation of Proteaceae and coexisting dominant plant families vary between seasons and habitats. To investigate this, we selected 18 species from Proteaceae, Myrtaceae and Fabaceae, six from each family, in two habitats from Alison Baird Reserve (32°1'19"S 15°58'52"E) in Western Australia. Total leaf P and nitrogen (N) concentrations, leaf mass per area, photosynthetic rate, pre-dawn leaf water potential and foliar P fractions were determined for each species both at the end of summer (March 2019 and early April 2020) and at the end of winter (September 2019). Soil P availability was also determined for each site. This is the very first study that focused on seasonal changes of foliar P fractions from different P-impoverished environments in three plant families. However, contrary to our expectation, we found little evidence for convergence of foliar P allocation within family, season or habitat. Each species exhibited a specific species-dependent pattern of foliar P allocation, and many species showed differences between seasons. Native plants in south-western Australia converged on a high photosynthetic P-use efficiency, but each species showed its own unique way associated with that outcome.

^{*} Corresponding author.

E-mail addresses: shutong.liu@uwa.edu.au (S.T. Liu), clement.gille@uwa.edu.au (C.E. Gille), toby.bird@research.uwa.edu.au (T. Bird), kosala.ranathunge@uwa.edu.au (K. Ranathunge), patrick.finnegan@uwa.edu.au (P.M. Finnegan), hans.lambers@uwa.edu.au (H. Lambers).

<https://doi.org/10.1016/j.scitotenv.2023.166395>

Received 23 May 2023; Received in revised form 15 August 2023; Accepted 16 August 2023

Available online 18 August 2023

0048-9697/© 2023 The Authors. Published by Elsevier B.V. This is an open access article under the CC BY-NC-ND license (<http://creativecommons.org/licenses/by-nc-nd/4.0/>).

Wen Z, Pang J, Wang X, Gille CE, De Borda A, Hayes PE, Clode PL, Ryan MH, Siddique KHM, Shen J, *et al.* 2023. Differences in foliar phosphorus fractions, rather than in cell-specific phosphorus allocation, underlie contrasting photosynthetic phosphorus use efficiency among chickpea genotypes. *Journal of Experimental Botany* 74: 1974–1989.



Journal of Experimental Botany, Vol. 74, No. 6 pp. 1974–1989, 2023
<https://doi.org/10.1093/jxb/erac519> Advance Access Publication 28 December 2022



RESEARCH PAPER

Differences in foliar phosphorus fractions, rather than in cell-specific phosphorus allocation, underlie contrasting photosynthetic phosphorus use efficiency among chickpea genotypes

Zhihui Wen^{1,2}, Jiayin Pang^{3,4,*}, Xiao Wang^{2,3}, Clément E. Gille², Axel De Borda^{2,5}, Patrick E. Hayes², Peta L. Clode^{2,6}, Megan H. Ryan^{3,4}, Kadambot H. M. Siddique^{3,4}, Jianbo Shen^{1,*} and Hans Lambers^{1,2,3}

¹ Department of Plant Nutrition, College of Resources and Environmental Sciences; National Academy of Agriculture Green Development; Key Laboratory of Plant-Soil Interactions, Ministry of Education, China Agricultural University, Beijing 100193, China

² School of Biological Sciences, The University of Western Australia, Perth, WA 6009, Australia

³ The UWA Institute of Agriculture, The University of Western Australia, Perth, WA 6009, Australia

⁴ UWA School of Agriculture and Environment, The University of Western Australia, Perth, WA 6009, Australia

⁵ Agronomy Engineering School of Purpan, 75 Voie du Toec-BP 57611, 31076 Toulouse, France

⁶ Centre for Microscopy, Characterisation and Analysis, The University of Western Australia, Perth, WA 6009, Australia

* Correspondence: jbshen@cau.edu.cn or jiayin.pang@uwa.edu.au

Received 4 August 2022; Editorial decision 22 December 2022; Accepted 26 December 2022

Editor: Guohua Xu, Nanjing Agricultural University, China

Abstract

Although significant intraspecific variation in photosynthetic phosphorus (P) use efficiency (PPUE) has been shown in numerous species, we still know little about the biochemical basis for differences in PPUE among genotypes within a species. Here, we grew two high PPUE and two low PPUE chickpea (*Cicer arietinum*) genotypes with low P supply in a glasshouse to compare their photosynthesis-related traits, total foliar P concentration ([P]) and chemical P fractions (i.e. inorganic P (Pi), metabolite P, lipid P, nucleic acid P, and residual P). Foliar cell-specific nutrient concentrations including P were characterized using elemental X-ray microanalysis. Genotypes with high PPUE showed lower total foliar [P] without slower photosynthetic rates. No consistent differences in cellular [P] between the epidermis and mesophyll cells occurred across the four genotypes. In contrast, high PPUE was associated with lower allocation to Pi and metabolite P, with PPUE being negatively correlated with the percentage of these two fractions. Furthermore, a lower allocation to Pi and metabolite P was correlated with a greater allocation to nucleic acid P, but not to lipid P. Collectively, our results suggest that a different allocation to foliar P fractions, rather than preferential P allocation to specific leaf tissues, underlies the contrasting PPUE among chickpea genotypes.















Keywords: Leaf elemental distribution, leaf phosphorus fractions, phosphorus allocation, photosynthetic phosphorus use efficiency, scanning electron microscopy, X-ray microanalysis.

Bird T, Nestor BJ, Bayer PE, Wang G, Ilyasova A, Gille CE, Soraru BEH, Ranathunge K, Severn-Ellis AA, Jost R, *et al.* 2024. Delayed leaf greening involves a major shift in the expression of cytosolic and mitochondrial ribosomes to plastid ribosomes in the highly phosphorus-use-efficient *Hakea prostrata* (Proteaceae). *Plant and Soil* 496: 7–30.

Plant Soil (2024) 496:7–30
<https://doi.org/10.1007/s11104-023-06275-1>

RESEARCH ARTICLE

Delayed leaf greening involves a major shift in the expression of cytosolic and mitochondrial ribosomes to plastid ribosomes in the highly phosphorus-use-efficient *Hakea prostrata* (Proteaceae)

Toby Bird  · Benjamin J. Nestor  · Philipp E. Bayer  · Guannan Wang  · Albina Ilyasova · Clément E. Gille  · Bryce E. H. Soraru · Kosala Ranathunge  · Anita A. Severn-Ellis  · Ricarda Jost  · Wolf-Rüdiger Scheible  · Maheshi Dassanayake  · Jacqueline Batley  · David Edwards  · Hans Lambers  · Patrick M. Finnegan 

Received: 21 April 2023 / Accepted: 31 August 2023 / Published online: 27 September 2023
 © The Author(s) 2023

Abstract

Background and aims *Hakea prostrata* (Proteaceae) is a highly phosphorus-use-efficient plant native to southwest Australia. It maintains a high photosynthetic rate at low leaf phosphorus (P) and exhibits delayed leaf greening, a convergent adaptation that increases nutrient-use efficiency. This study aimed to

provide broad physiological and gene expression profiles across leaf development, uncovering pathways leading from young leaves as nutrient sinks to mature leaves as low-nutrient, energy-transducing sources.

Methods To explore gene expression underlying delayed greening, we analysed a de novo transcriptome for *H. prostrata* across five stages of leaf development. Photosynthesis and respiration rates, and foliar pigment, P and nitrogen (N) concentrations were determined, including the division of P into five biochemical fractions.

Key results Transcripts encoding functions associated with leaf structure generally decreased in abundance across leaf development, concomitant with decreases in foliar concentrations of 85% for

Responsible Editor: Mian Gu.

Toby Bird and Benjamin J. Nestor are co-first authors of this article.

Supplementary Information The online version contains supplementary material available at <https://doi.org/10.1007/s11104-023-06275-1>.

T. Bird (✉) · B. J. Nestor (✉) · P. E. Bayer · A. Ilyasova · C. E. Gille · B. E. H. Soraru · K. Ranathunge · A. A. Severn-Ellis · R. Jost · J. Batley · D. Edwards · H. Lambers · P. M. Finnegan
 School of Biological Sciences, University of Western Australia, Perth, WA 6009, Australia
 e-mail: toby.bird@research.uwa.edu.au

B. J. Nestor
 e-mail: benjamin.nestor@research.uwa.edu.au

P. E. Bayer
 e-mail: philipp.bayer@uwa.edu.au

A. Ilyasova
 e-mail: albina.ilyasova6012@gmail.com

C. E. Gille
 e-mail: clement.gille@research.uwa.edu.au

B. E. H. Soraru
 e-mail: bsoraru@gmail.com

K. Ranathunge
 e-mail: kosala.ranathunge@uwa.edu.au

A. A. Severn-Ellis
 e-mail: anita.severn-ellis@dpird.wa.gov.au

R. Jost
 e-mail: R.Jost@latrobe.edu.au

J. Batley
 e-mail: jacqueline.batley@uwa.edu.au

D. Edwards
 e-mail: dave.edwards@uwa.edu.au

H. Lambers
 e-mail: hans.lambers@uwa.edu.au

RÉSUMÉ

(French Abstract)

Facteurs influençant la mégadiversité végétale dans le Sud-Ouest australien, point chaud de biodiversité extrêmement appauvri en phosphore

Le point chaud de biodiversité du Sud-Ouest australien abrite une diversité d'espèces végétales exceptionnelle. Les sols sont extrêmement appauvris en nutriments, particulièrement en phosphore (P). Des adaptations ont évolué chez ces espèces, leur permettant d'acquérir et d'utiliser efficacement les nutriments peu abondants. La plupart des Protéacées, une famille de plantes emblématique et écologiquement importante de la région, forment des « racines *cluster* ». Ces structures racinaires fascinantes sont non-mycorhiziennes et éphémères, et sont composées de milliers de racines latérales qui libèrent de larges quantités de carboxylates pour « miner » le P fixé aux particules de sol. Les carboxylates sont des petites molécules inorganiques chargées négativement et mobilisent le P du sol initialement immobile et indisponible pour les plantes. Les carboxylates mobilisent également d'autres éléments dont le manganèse (Mn). L'absorption du Mn qui s'en suit est peu régulée chez les végétaux, et l'élément s'accumule continuellement dans les feuilles des plantes. Ainsi la concentration en manganèse ([Mn]) dans les feuilles peut être utilisée comme indicateur de la concentration en carboxylates dans la rhizosphère, c'est-à-dire le sol proche et sous l'influence des racines. Cet indicateur est précieux car mesurer les concentrations en carboxylates dans la rhizosphère sur le terrain est un défi méthodologique de taille, malgré leur importance pour le maintien de la biodiversité dans les environnements extrêmement appauvris en nutriments. Les espèces mycorhiziennes, comme les Myrtacées et la plupart des Fabacées, acquièrent quant à elles le P grâce à leurs symbiotes « exploreurs », les champignons mycorhiziens (endo- ou ectomycorhizes). Les mycorhizes étendent grandement la surface de sol que la racine peut ainsi explorer. Bien que ces espèces mycorhiziennes soient généralement moins efficaces que les Protéacées non-mycorhiziennes pour acquérir le P dans ces sols où le P est immobile, elles coexistent néanmoins ensemble. Cela contribue ainsi à la remarquable diversité des espèces végétales dans les paysages sévèrement appauvris en P du Sud-Ouest australien.

Des adaptations pour pousser sur ces sols très pauvres en P ont également évolué au niveau des feuilles. Ces adaptations permettent aux espèces poussant dans des environnements pauvres en P de fonctionner avec de très faibles concentrations foliaires en P. Par exemple, pendant le développement des feuilles, les Protéacées remplacent les phospholipides par d'autres lipides qui ne contiennent pas de P, par exemple des sulfolipides ou galactolipides. Elles fonctionnent avec de faibles niveaux d'ARN ribosomal (des molécules très riches en P), et allouent préférentiellement le P aux cellules photosynthétiquement actives du mésophylle plutôt qu'aux cellules photosynthétiquement inactives de l'épiderme. À travers la modulation de l'allocation de P au sein de ces différents compartiments cellulaires et fractions biochimiques dans les feuilles, les Protéacées maintiennent des taux de photosynthèse élevés. Ainsi les Protéacées atteignent une très haute efficacité d'utilisation photosynthétique du P, c'est-à-dire le ratio d'assimilation de carbone par la photosynthèse rapporté à la concentration en P foliaire.

Dans cette thèse, j'ai cherché à comprendre les facteurs contribuant à l'importante diversité végétale des habitats extrêmement appauvris en P dans le Sud-Ouest australien. Pour cela, j'ai réalisé une série d'études sur le fonctionnement physiologique des racines et des feuilles d'espèces de Protéacées, particulièrement efficaces dans leur acquisition et utilisation du P, ainsi que d'espèces coexistantes appartenant aux Myrtacées.

Certaines espèces de *Hakea* (Protéacées) produisent des « racines *cluster* » et libèrent de larges quantités de carboxylates, mais ont une faible [Mn] foliaire. Cette observation remet ainsi en question l'hypothèse de l'indicateur mentionné ci-dessus. Dès lors, j'ai cherché dans une première étude à comprendre la relation entre l'accumulation de Mn dans les feuilles et le relargage de carboxylates chez trois espèces de *Hakea* qui possèdent des [Mn] contrastées. Mon évaluation physiologique a révélé que l'accumulation de Mn est étroitement associée à la capacité d'une espèce à libérer des protons (H^+) pour équilibrer les charges négatives des carboxylates libérés. Les espèces avec une forte [Mn] foliaire libéraient plus de protons que les espèces avec une faible [Mn]. Les protons libérés réduisent le pH du sol ce qui augmente la disponibilité en Mn, et compte-tenu de la faible régulation de l'assimilation du Mn par les racines, celui-ci s'accumule dans les feuilles. Au contraire, les espèces avec une faible [Mn] foliaire libéraient moins de protons, mais des quantités plus importantes de potassium et de magnésium sous forme de cations (K^+ et Mg^{2+}). La libération de ces cations autres que les protons ne diminue pas autant le pH du sol, rendant le Mn moins disponible. Il est possible que

ces cations augmentent le pH du sol. À travers cette expérience, je propose ainsi un modèle conceptuel alternatif complet reliant l'exsudation racinaire de carboxylates à l'accumulation de Mn dans les feuilles d'espèces de *Hakea*.

J'ai ensuite examiné l'interaction entre *Banksia menziesii*, une espèce non-mycorhizienne de Protéacées qui produit des « racines cluster », et *Eucalyptus todtiana*, une espèce mycorhizienne de Myrtacées, dans une expérience en serre. Comme attendu dans des environnements où la croissance est limitée par le P, la facilitation (c'est-à-dire une interaction positive entre deux individus) pour l'acquisition de P a joué un rôle clé dans le succès de ces deux espèces aux différentes stratégies d'acquisition des nutriments. Les « racines cluster » de *B. menziesii* qui exsudent des grandes quantités de carboxylates pour mobiliser le P ont amélioré l'acquisition du P d'*E. todtiana*. Cependant, ce processus de facilitation était accompagné d'une forte compétition de la part d'*E. todtiana*. En effet, la présence d'*E. todtiana* a eu un impact négatif sur la croissance de *B. menziesii*. Les deux espèces rivalisaient pour l'acquisition du P mobilisé et rendu disponible par les « racines cluster » de *B. menziesii*. L'ajout d'un champignon mycorhizien formant association avec son hôte *E. todtiana* a également induit une augmentation des concentrations de phytohormones, des molécules messagères, dans les racines de *B. menziesii* confrontées à des pathogènes indigènes du genre *Phytophthora*. Mes résultats suggèrent que l'espèce mycorhizienne *E. todtiana* et ses mycorhizes associées contribuent à stimuler les réactions de défense de *B. menziesii* contre les pathogènes oomycètes du sol. Cette étude met en avant les interactions complexes existantes entre des espèces non-mycorhiziennes, des espèces mycorhiziennes et leurs partenaires fongiques, et les pathogènes oomycètes. Pour la première fois, je démontre comment ces interactions façonnent la coexistence d'espèces qui possèdent des stratégies d'acquisition des nutriments contrastées (« racines cluster » vs. mycorhizes) dans un environnement extrêmement appauvri en P.

J'ai ensuite considéré les schémas d'allocation du P dans les feuilles de cinq espèces de *Banksia* et cinq espèces de *Hakea*, deux genres riches en espèces de la famille des Protéacées dans le Sud-Ouest australien. Au sein de chaque genre, l'efficacité d'utilisation photosynthétique du P (PPUE) était élevée en comparaison aux moyennes mondiales mais variait selon les espèces. Dans cette étude, j'ai cherché à comprendre si et comment les schémas d'allocation du P dans différentes fractions biochimiques expliquent la haute PPUE des espèces étudiées. Les espèces avec une PPUE plus élevée allouaient plus de P aux petits métabolites

(molécules impliquées dans le métabolisme, comme la photosynthèse ou la respiration) et moins de P aux lipides (composante structurelle majeure des membranes) que les espèces avec une PPUE plus basse. Les corrélations entre la PPUE et les concentrations en phosphate inorganique ou en P résiduel (probablement contenant des protéines phosphorylées) n'étaient néanmoins pas similaires pour les deux genres, mettant en évidence des différences majeures entre les espèces de *Banksia* et les espèces de *Hakea*. Pour les espèces de *Banksia* uniquement, la PPUE était positivement et négativement corrélée avec l'allocation de P aux petits métabolites et à la fraction résiduelle de P, respectivement. En conséquence, je suggère qu'il existe un compromis entre l'allocation de P aux substrats (petits métabolites utilisés par la machinerie photosynthétique) et à l'ARN ribosomal (produisant les protéines, c'est-à-dire la machinerie photosynthétique) pour atteindre une PPUE élevée.

En conclusion, l'étude du fonctionnement physiologique des racines et des feuilles d'espèces très efficaces pour l'acquisition et l'utilisation du P comme les Protéacées, et d'espèces qui coexistent, comme les Myrtacées, met en évidence une complémentarité de la diversité fonctionnelle. Cette diversité fonctionnelle, de l'acquisition du P et des interactions souterraines à la partition des ressources dans les feuilles, semble étayer la biodiversité exceptionnelle dans des environnements extrêmement appauvris en P, tel que le Sud-Ouest australien.

